frontiers | Research Topics

Cellular and systemic interplay of metabolism and inflammation in the pathogenesis of lung diseases

Edited by
Adan Chari Jirmo, Melanie Albrecht, Miguel Angel Alejandre Alcazar and Slaven Crnkovic

Published in
Frontiers in Immunology

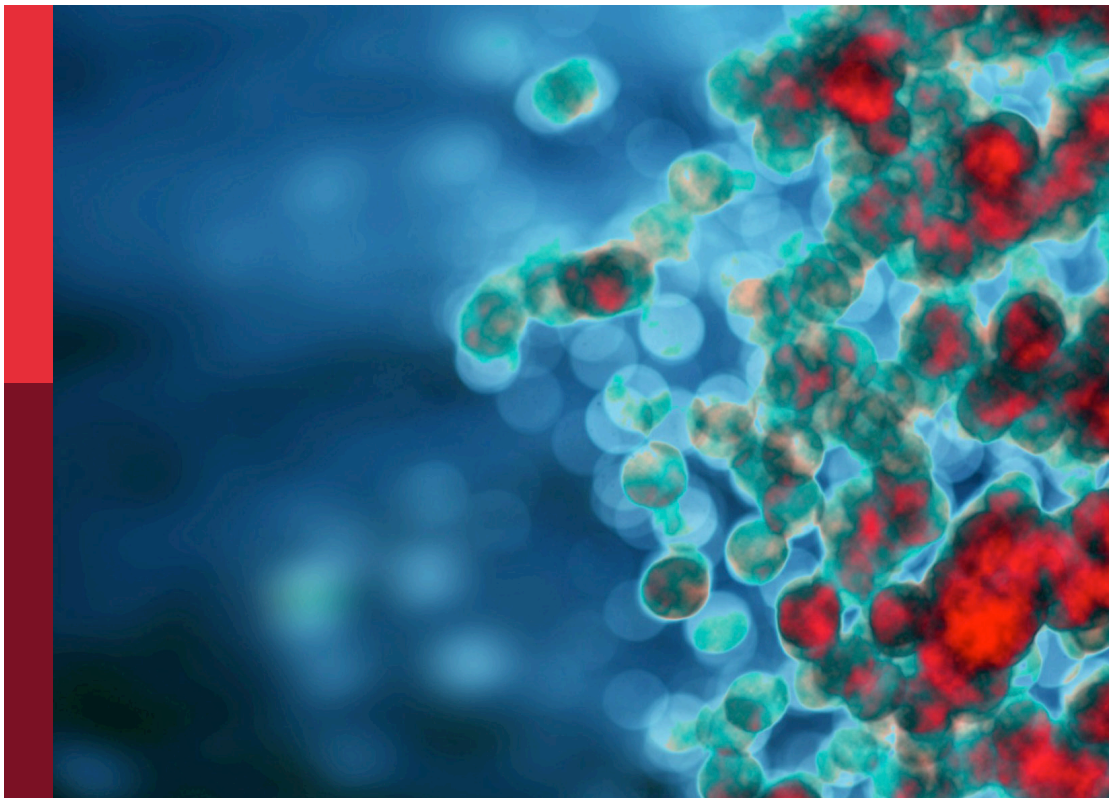

ISSN 1664-8714
ISBN 978-2-8325-4383-2
DOI 10.3389/978-2-8325-4383-2

About Frontiers

Frontiers is more than just an open access publisher of scholarly articles: it is a pioneering approach to the world of academia, radically improving the way scholarly research is managed. The grand vision of Frontiers is a world where all people have an equal opportunity to seek, share and generate knowledge. Frontiers provides immediate and permanent online open access to all its publications, but this alone is not enough to realize our grand goals.

Frontiers journal series

The Frontiers journal series is a multi-tier and interdisciplinary set of open-access, online journals, promising a paradigm shift from the current review, selection and dissemination processes in academic publishing. All Frontiers journals are driven by researchers for researchers; therefore, they constitute a service to the scholarly community. At the same time, the *Frontiers journal series* operates on a revolutionary invention, the tiered publishing system, initially addressing specific communities of scholars, and gradually climbing up to broader public understanding, thus serving the interests of the lay society, too.

Dedication to quality

Each Frontiers article is a landmark of the highest quality, thanks to genuinely collaborative interactions between authors and review editors, who include some of the world's best academicians. Research must be certified by peers before entering a stream of knowledge that may eventually reach the public - and shape society; therefore, Frontiers only applies the most rigorous and unbiased reviews. Frontiers revolutionizes research publishing by freely delivering the most outstanding research, evaluated with no bias from both the academic and social point of view. By applying the most advanced information technologies, Frontiers is catapulting scholarly publishing into a new generation.

What are Frontiers Research Topics?

Frontiers Research Topics are very popular trademarks of the *Frontiers journals series*: they are collections of at least ten articles, all centered on a particular subject. With their unique mix of varied contributions from Original Research to Review Articles, Frontiers Research Topics unify the most influential researchers, the latest key findings and historical advances in a hot research area.

Find out more on how to host your own Frontiers Research Topic or contribute to one as an author by contacting the Frontiers editorial office: frontiersin.org/about/contact

Cellular and systemic interplay of metabolism and inflammation in the pathogenesis of lung diseases

Topic editors

Adan Chari Jirmo — Biomedical Research in Endstage and Obstructive Lung Disease Hannover (BREATH), Germany

Melanie Albrecht — Paul-Ehrlich-Institut (PEI), Germany

Miguel Angel Alejandre Alcazar — University Hospital of Cologne, Germany

Slaven Crnkovic — Medical University of Graz, Austria

Citation

Jirmo, A. C., Albrecht, M., Alejandre Alcazar, M. A., Crnkovic, S., eds. (2024). *Cellular and systemic interplay of metabolism and inflammation in the pathogenesis of lung diseases*. Lausanne: Frontiers Media SA. doi: 10.3389/978-2-8325-4383-2

Table of contents

frontiers | Frontiers in Immunology

TYPE Editorial
PUBLISHED 17 January 2024
DOI 10.3389/fimmu.2023.1352304

OPEN ACCESS

EDITED AND REVIEWED BY
Pietro Ghezzi,
University of Urbino Carlo Bo, Italy

*CORRESPONDENCE
Adan Chari Jirmo
Jirmo.adan@mh-hannover.de
Melanie Albrecht
melanie.albrecht@pei.de
Slaven Crnkovic
Slaven.Crnkovic@lvr.lbg.ac.at
Miguel Angel Alejandre Alcazar
miguel.alejandre-alcazar@uk-koeln.de

RECEIVED 07 December 2023
ACCEPTED 13 December 2023
PUBLISHED 17 January 2024

CITATION
Jirmo AC, Albrecht M, Crnkovic S and Alejandre Alcazar MA (2024) Editorial: Cellular and systemic interplay of metabolism and inflammation in the pathogenesis of lung diseases.
Front. Immunol. 14:1352304.
doi: 10.3389/fimmu.2023.1352304

Editorial: Cellular and systemic interplay of metabolism and inflammation in the pathogenesis of lung diseases

Adan Chari Jirmo[1,2]*, Melanie Albrecht[3]*, Slaven Crnkovic[4]* and Miguel Angel Alejandre Alcazar[5,6,7]*

[1]Department of Pediatric Pneumology, Allergology and Neonatology, Hannover Medical School, Hannover, Germany, [2]German Center for Lung Research (DZL), Hannover, Germany, [3]Paul-Ehrlich Institute (PEI), Langen, Germany, [4]Ludwig Boltzmann Institute (LBI) for Lung and Vascular Research, Otto Loewi Research Center Medical University of Graz, Graz, Austria, [5]Department of Pediatric and Adolescent Medicine, Faculty of Medicine and University Hospital Cologne, University of Cologne, Cologne, Germany, [6]Cologne Excellence Cluster on Cellular Stress Responses in Aging-Associated Diseases (CECAD) and Center for Molecular Medicine Cologne (CMMC), Faculty of Medicine and University Hospital Cologne, University of Cologne, Cologne, Germany, [7]German Center for Lung Research (DZL), Institute for Lung Health (ILH), University of Giessen and Marburg Lung Center (UGMLC) and Cardiopulmonary Institute (CPI), Marburg, Germany

KEYWORDS

metabolism, metaflammation, inflammation, immuno-metabolism, lung pathologies

Editorial on the Research Topic
Cellular and systemic interplay of metabolism and inflammation in the pathogenesis of lung diseases

Research in the last couple of years has generated ample evidence showing that cellular alterations of the metabolic machinery could be the underlying factor in multiple human diseases. In this Research Topic, we have gathered scientific articles to underpin the interplay between perturbed metabolism/triggering of inflammation that contributes to pulmonary pathologies.

In this Research Topic, Wang et al., through a literature review, clearly illustrate the impact of various metabolic processes such as glycolysis, OXPHOS, FAO, and glutamine metabolism in modulating phenotypic and functional changes in macrophages and how these changes affect acute lung injury or acute respiratory distress syndrome. Moreover, through this review, Wang et al. reveal that metabolic reprogramming of macrophages is accompanied by dramatic shifts in cell metabolism and that functional state-associated unique metabolic signatures can be identified in various macrophage populations. Tang et al. have gone further in an original study to show that alveolar macrophages (AM) sensing of amino acid phenylalanine promotes pyroptosis, which causes the release of inflammatory mediators and, thereby, exacerbates lung inflammation and acute respiratory distress syndrome (ARDS) lethality in a murine model. This study is especially interesting since it not only elucidates the entire process of how phenylalanine initiates pyroptosis in AMs and the resulting inflammation but also elucidates the subsequent effects of the inhibition of this process on ARDS. The article clearly shows the significance of small-molecule metabolites in pulmonary inflammation and how they may be useful not only as

biomarkers but as potential therapeutic targets. In their work, Li et al. expand this Research Topic further by showing how sensitivity to ferroptosis influences the inflammatory and lung repair capabilities of macrophages. They demonstrate that in chronic obstructive pulmonary disease (COPD), lipid peroxidation favors the differentiation of AM toward ferroptosis-sensitive M2-like macrophages but not ferroptotic-resistant M1-like macrophages. The Ferroptotic M2-like AMs lose their anti-inflammatory and repair functions but continue invoking inflammatory responses in COPD. Due to persistent lipid peroxidation in a COPD lung, this polarization toward M2-like AMs is speculated to be the cause of consistent inflammation and tissue damage. Importantly, the study shows that this process is therapeutically targetable since the ferroptotic phenotype can be ameliorated with anti-ferroptotic compounds, iron chelators, and heme oxygenase (HO-1) inhibitors and thereby alleviate lung inflammation, destruction, and remodeling of COPD.

More evidence of the impact of metabolic distortion on cellular homeostasis and how it influences lung pathology was provided by Bauer et al. They report that in severe cases of coronavirus disease-2019 (COVID-19), hypoxia-sensitized toll-like receptor 4 (TLR4) signaling activates SARS-CoV-2 spike protein in monocytes, ultimately leading to systemic inflammation in severe cases of COVID-19 as a result of enhanced chemokine ISG expression in monocytes upon infection with SARS-CoV-2. The study by Bauer et al. shows the connection between hypoxia-evoked disturbances in cholesterol metabolism and altered interferon (IFN) responses in monocytes and how this concomitantly affects inflammatory responses in the lung. Furthermore, the study provides an explanation regarding the possible mechanism of systemic inflammation which has been observed in severe cases of COVID-19 infections. In addition, Hasankhani et al. show in their review that metabolic perturbances are an underlying factor in the induction of the SARS-CoV-2-associated cytokine storm which is the main COVID-associated immunopathology that is related to disease severity and mortality.

Finally, Lim and Templeton in their mini-review highlight the important immunomodulatory function of hormones on the example of Adipokines exemplified through Adiponectin (APN). They speculate possible roles and mechanisms of Adiponectin (APN) pathway-induced protection in lung diseases, including fungal, bacterial, and viral infection, which could result in novel therapies that protect against infection, excessive inflammation, and other lung pathologies. This closes the potential circle and provides "food for thought" on how potentially feeding behavior and accompanying disturbances in hormones that regulate metabolism might influence or be exploited in the management of lung inflammatory conditions. Thus, with this Research Topic on *Cellular and Systemic Interplay of Metabolism and Inflammation in the Pathogenesis of Lung Diseases*, we provide an overview though not exhaustive of how metaflammation influences pulmonary immunity and pathologies and the need for intensification of research in this area.

Author contributions

AJ: Conceptualization, Writing – original draft, Writing – review & editing. MA: Conceptualization, Writing – original draft, Writing – review & editing. SC: Conceptualization, Writing – original draft, Writing – review & editing. MA: Conceptualization, Writing – original draft, Writing – review & editing.

Conflict of interest

The authors declare that the research was conducted in the absence of any commercial or financial relationships that could be construed as a potential conflict of interest.

Publisher's note

frontiers | Frontiers in Immunology

TYPE Review
PUBLISHED 17 February 2023
DOI 10.3389/fimmu.2023.1127358

OPEN ACCESS

EDITED BY
Slaven Crnkovic,
Medical University of Graz, Austria

REVIEWED BY
Mohammad Asad,
Albert Einstein College of Medicine, United States
Alessandra Ammazzalorso,
University "G. d'Annunzio"of Chieti-Pescara, Italy

*CORRESPONDENCE
Aliakbar Hasankhani
A.hasankhani74@ut.ac.ir
Bahman Abedi Kiasari
abedikiasari.b@ut.ac.ir
Alireza Mohammadzadeh Shabestari
Drshabestari3@gmail.com

†These authors have contributed equally to this work and share first authorship

SPECIALTY SECTION
This article was submitted to Inflammation, a section of the journal Frontiers in Immunology

RECEIVED 19 December 2022
ACCEPTED 08 February 2023
PUBLISHED 17 February 2023

CITATION
Hasankhani A, Bahrami A, Tavakoli-Far B, Iranshahi S, Ghaemi F, Akbarizadeh MR, Amin AH, Abedi Kiasari B and Mohammadzadeh Shabestari A (2023) The role of peroxisome proliferator-activated receptors in the modulation of hyperinflammation induced by SARS-CoV-2 infection: A perspective for COVID-19 therapy. *Front. Immunol.* 14:1127358. doi: 10.3389/fimmu.2023.1127358

The role of peroxisome proliferator-activated receptors in the modulation of hyperinflammation induced by SARS-CoV-2 infection: A perspective for COVID-19 therapy

Aliakbar Hasankhani[1*†], Abolfazl Bahrami[1,2†], Bahareh Tavakoli-Far[3,4], Setare Iranshahi[5], Farnaz Ghaemi[6], Majid Reza Akbarizadeh[7], Ali H. Amin[8], Bahman Abedi Kiasari[9*] and Alireza Mohammadzadeh Shabestari[10,11*]

[1]Department of Animal Science, College of Agriculture and Natural Resources, University of Tehran, Karaj, Iran, [2]Biomedical Center for Systems Biology Science Munich, Ludwig-Maximilians-University, Munich, Germany, [3]Dietary Supplements and Probiotic Research Center, Alborz University of Medical Sciences, Karaj, Iran, [4]Department of Physiology and Pharmacology, School of Medicine, Alborz University of Medical Sciences, Karaj, Iran, [5]School of Pharmacy, Shahid Beheshty University of Medical Sciences, Tehran, Iran, [6]Department of Biochemistry, Faculty of Advanced Sciences and Technology, Tehran Medical Sciences, Islamic Azad University, Tehran, Iran, [7]Department of Pediatric, School of Medicine, Amir al momenin Hospital, Zabol University of Medical Sciences, Zabol, Iran, [8]Zoology Department, Faculty of Science, Mansoura University, Mansoura, Egypt, [9]Virology Department, Faculty of Veterinary Medicine, University of Tehran, Tehran, Iran, [10]Department of Dental Surgery, Mashhad University of Medical Sciences, Mashhad, Iran, [11]Khorasan Covid-19 Scientific Committee, Mashhad, Iran

Coronavirus disease 2019 (COVID-19) is a severe respiratory disease caused by infection with severe acute respiratory syndrome coronavirus 2 (SARS-CoV-2) that affects the lower and upper respiratory tract in humans. SARS-CoV-2 infection is associated with the induction of a cascade of uncontrolled inflammatory responses in the host, ultimately leading to hyperinflammation or cytokine storm. Indeed, cytokine storm is a hallmark of SARS-CoV-2 immunopathogenesis, directly related to the severity of the disease and mortality in COVID-19 patients. Considering the lack of any definitive treatment for COVID-19, targeting key inflammatory factors to regulate the inflammatory response in COVID-19 patients could be a fundamental step to developing effective therapeutic strategies against SARS-CoV-2 infection. Currently, in addition to well-defined metabolic actions, especially lipid metabolism and glucose utilization, there is growing evidence of a central role of the ligand-dependent nuclear receptors and peroxisome proliferator-activated receptors (PPARs) including PPARα, PPARβ/δ, and PPARγ in the control of inflammatory signals in various human inflammatory diseases. This makes them attractive targets for developing therapeutic approaches to control/suppress the hyperinflammatory response in patients with severe COVID-19. In

this review, we (1) investigate the anti-inflammatory mechanisms mediated by PPARs and their ligands during SARS-CoV-2 infection, and (2) on the basis of the recent literature, highlight the importance of PPAR subtypes for the development of promising therapeutic approaches against the cytokine storm in severe COVID-19 patients.

KEYWORDS

SARS-CoV-2, cytokine storm, PPARs, hyperinflammation, COVID-19 therapy,

1 Introduction

Coronavirus disease 2019 (COVID-19) is an infectious and severe respiratory disease caused by severe acute respiratory syndrome coronavirus 2 (SARS-CoV-2). SARS-CoV-2 is a positive sense single-stranded RNA beta-coronavirus that infects the lower and upper respiratory tract and has recently affected millions of people worldwide (1–3). Primary symptoms of COVID-19 include fever, cough, pneumonia, and shortness of breath, and histological pictures of this disease are characterized by mononuclear inflammatory cells, severe pneumocyte hyperplasia, interstitial thickening, hyaline membrane formation, and prominent alveolar damage with eosinophilic exudates (4, 5).

During COVID-19, a cascade of inflammatory pathways is activated, leading to massive cytokine release from the host immune system in response to SARS-CoV-2 infection (6, 7). In this regard, the vast increase in the secretion of circulating proinflammatory cytokines such as tumor necrosis factors (TNFs), interleukins (ILs), chemokines, and interferons (IFNs) leads to the exacerbation of the host inflammatory response to the pathogen. This exacerbation in the host's inflammatory response increases the severity of the disease (8–10). This hyperinflammation or imbalanced inflammation during SARS-CoV-2 infection is called "cytokine storm", which is one of the main hallmarks of the deterioration of the COVID-19 immunopathogenesis and triggers acute respiratory distress syndrome (ARDS), multi-organ failure (MOF), acute lung injury (ALI), decreased lung function, and finally, death of the host (11, 12). In this context, in recent years, various clinical and omics-based studies have investigated the molecular mechanisms behind the SARS-CoV-2 infection in different disease stages and different tissues (13–17). Surprisingly, most of these studies have observed the activation of inflammatory mechanisms and hyperinflammation in COVID-19 patients. Therefore, developing effective therapeutic strategies by targeting critical factors in regulating host inflammatory response can provide a potential and promising solution for the survival of COVID-19 patients, especially the prevention of cytokine storms (18–20). The peroxisome proliferator-activated receptors (PPARs) are a subgroup of ligand-activated transcription factors and members of the nuclear receptor superfamily that play a crucial role in regulating energy balance, carbohydrate and lipid metabolism, cell growth, and differentiation (21, 22). PPARs can regulate the transcriptional activity of target genes by two different mechanisms (1): binding to the promoter region of target genes with DNA sequences known as peroxisome proliferator response elements (PPREs) as a ligand-dependent transcription factor, and (2) controlling gene expression through association with PPRE-independent activator proteins (21, 23). Several previous reports highlighted the core role of PPARs in many human diseases, such as different types of cancer (24, 25), atherosclerosis (26), and type 2 diabetes (27, 28).

Interestingly, in addition to the central roles of PPARs in regulating energy homeostasis, such as fatty-acid metabolism and glucose utilization, growing evidence suggests that members of the nuclear receptor superfamily, such as PPARs, also have significant regulatory effects on inflammatory processes (29). Indeed, extensive research has proven that PPARs have potential anti-inflammatory effects during inflammation-related disease (30, 31). In this regard, previous literature, based on available evidence, has suggested that subtypes of PPARs exert their anti-inflammatory effects and subsequently control the host's inflammatory response through different mechanisms such as successful competition with other inflammatory transcription factors for the recruitment of essential and shared co-activator proteins, inhibition of binding of inflammatory transcription factors such as AP-1, nuclear factor-κB (NF-κB), NFAT, and STATs to their response elements through direct physical protein-protein interaction, blocking MAPK-induced signaling cascades, preventing the clearance of proinflammatory genes co-repressors, and upregulation in the

Abbreviations: ACE2, Angiotensin-converting enzyme 2; ALI, Acute lung injury; AP-1, Activator protein-1; ARDS, Acute respiratory distress syndrome; BALFs, bronchoalveolar lavage fluids; COVID-19, Coronavirus disease 2019; IBD, Inflammatory bowel disease; IFNs, Interferons; IκBs, Inhibitors of NF-κB; ILs, Interleukins; MOF, Multi-organ failure; NF-κB, Nuclear factor-κB; PAMPs, Pathogen associated molecular patterns; PBMCs, Peripheral blood mononuclear cells; PRRs, Pattern recognition receptors; PPARs, Peroxisome proliferator-activated receptors; PPI, Protein–protein interaction; PPREs, Peroxisome proliferator response elements; RXR, 9-cis-retinoic acid receptor; SARS-CoV-2, Severe acute respiratory syndrome corona virus 2; TNFs, Tumor necrose factors.

expression of anti-inflammatory genes (32). For example, it has been discussed that the activation of PPARs during inflammatory bowel disease (IBD) leads to the suppression of the main pathways of inflammation, such as NF-κB signaling. Subsequently, the activation of PPARs inhibits the production of proinflammatory cytokines such as TNF-α, IL6, and IL1B. Therefore, it was concluded that anti-inflammatory responses induced by the activation of PPARs might restore the physio-pathological imbalance associated with this disorder (21).

The interference of viral infections such as SARS-CoV-2 in the PPARs signaling is a completely new issue and interest in this area has been very motivated by the COVID-19 pandemic. Emerging studies show that SARS-CoV-2, by modulating PPAR subtypes, leads to metabolic changes (especially lipid metabolism) and exacerbation of pulmonary inflammation in lung epithelial cells of COVID-19 patients (33). Therefore, these findings have suggested that the use of agonists of PPARs with the aim of their activation may be a useful therapeutic strategy to reverse the inflammatory and metabolic changes caused by SARS-CoV-2 infection (34). In this regard, it has been reported that several natural ligands of PPARs, such as turmeric, docosahexaenoic acid (DHA), and eicosapentaenoic acid (EPA), lead to a decrease in the production of proinflammatory cytokines through interaction with PPARs and then induction of their activity (35, 36) For example, a very recent study has identified possible mechanisms by which the PPARα agonist palmitoylethanolamide (PEA) antagonizes the NF-κB signaling pathway and subsequently reduces the production of TNF-α, IL1B, and other inflammatory mediators such as inducible nitric oxide synthase (iNOS) and COX2 through selective activation of PPARα in cultured murine alveolar macrophages during SARS-CoV-2 infection (37). Moreover, it has been suggested that synthetic agonists of PPARγ, such as thiazolidinediones (TZDs), like pioglitazone, are anti-inflammatory drugs with ameliorative effects on severe viral pneumonia-like COVID-19 (38). On the other hand, by integrating different transcriptome datasets with computational network-based systems biology methods, promising therapeutic targets, including PPARα and PPARγ, have been identified for the modulation of inflammatory processes caused by COVID-19 (39, 40). Therefore, PPARs and their ligands have crucial therapeutic potential with key immunomodulatory effects on inflammatory mechanisms and cytokine/chemokine production during infectious and inflammation-related diseases such as the COVID-19 pandemic.

Nevertheless, considering the importance of immunopathology's role of the inflammatory response in COVID-19 patients and the role of PPARs in controlling inflammation, in this review, we (1) provide a summary of general information about PPARs such as subtypes, structure, tissue expression, and function (2), investigate the molecular mechanisms of the exacerbation of the host inflammatory response during COVID-19 (3), describe the anti-inflammatory mechanisms mediated by PPARs, and (4) discuss the anti-inflammatory roles of PPAR subtypes during COVID-19 pandemic on the basis of the recent clinical and omics-based literature.

2 PPARs: Subtypes, structure, tissue expression, and function

2.1 PPAR subtypes and structure

The PPARs are ligand-dependent/activated transcription factors, members of the nuclear- hormone-receptor superfamily (including the receptors for thyroid hormone, vitamin D, ecdysone, retinoic acids, and some orphan receptors) that transduce a wide range of signals, including environmental, nutritional, and inflammatory events, to a set of cellular responses at the transcriptional gene level; they were named due to their joint property in increasing the number and activity of peroxisomes (41–43). So far, three isoforms of PPARs, namely, PPARα (NR1C1), PPARβ/δ (NR1C2), and PPARγ (NR1C3), have been identified in vertebrates (including human, mouse, rat, hamster, and Xenopus), which are encoded by distinct genes on different chromosomes. They have shown a high degree of sequence and structural homology (Figure 1A) but different tissue distribution, ligand specificity, and regulatory activities (44–46).

2.2 Tissue distribution and function

In recent years, various *in vitro* and *in vivo* studies have reported that all isoforms of PPARs primarily regulate lipid and glucose metabolism and have additional regulatory roles in cell proliferation and differentiation, vascular homeostasis and atherosclerosis, cancer, and the immune system (38, 47). In addition to the mentioned activities, it is thought that the activation of PPAR subtypes reduces the expression of proinflammatory cytokines and inflammatory cell functions, exerting significant anti-inflammatory properties (48). PPARα is the first known PPAR that was initially cloned from a mouse liver complementary DNA library as a nuclear receptor that mediates the effects of an endogenous group and xenobiotic compounds known as peroxisome proliferators (PPs) (31, 49). This subtype of PPARs is highly expressed in metabolically active tissues such as the liver, heart, skeletal muscles, intestinal mucosa, and brown adipose tissue (50, 51). PPARα is mainly involved in the carbohydrate metabolism and catabolism of fatty acids and their oxidation, such that its activation reduces lipid levels (52–55). Additionally, it has been well highlighted that PPARα increases the expression of IκB, which is a factor that suppresses the nuclear translocation and transcriptional activity of NF-κB, thereby interfering with NF-κB signaling and the inflammatory response (48). Besides, increasing evidence has demonstrated that the anti-inflammatory properties of PPARα are manifested by a decrease in the secretion of several key downstream inflammatory factors such as NF-κB–driven cytokines (TNF-α, IL1B, and IL6), COX2, IL8, IL12, IL2, VCAM1, TLR4, MCP1, STAT3, AP-1, and IL18 (56, 57). Moreover, it has been reported that the activation of PPARα leads to the upregulation of important anti-inflammatory factors such as IL1 receptor antagonist (IL1ra) (58) and vanin-1 (59).

10.3389/fimmu.2023.1127358

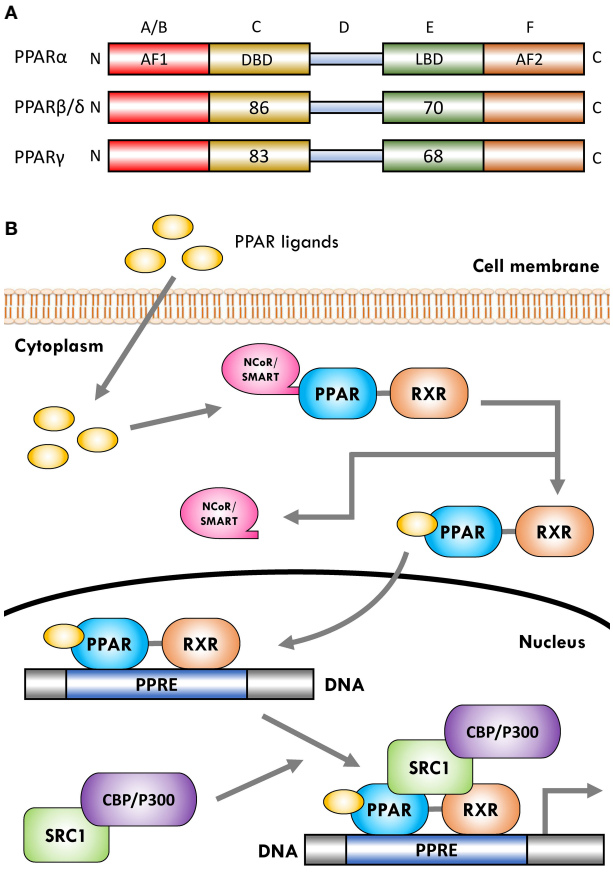

FIGURE 1
Schematic representation of peroxisome proliferator-activated receptor (PPAR) structure and ligand-induced activation. **(A)** The PPARs are composed of five distinct regions or domains (1): the ligand-independent activation domain of AF1 located in the N-terminus (amino-terminal A/B domain), which is responsible for receptor phosphorylation (2); the highly conserved DNA-binding domain **(DBD)** in the C region that contains two zinc finger motifs responsible for receptor binding to DNA targets on the peroxisome proliferator hormone response elements (PPREs) of PPARs target genes (3); a variable hinge region in the D domain that is the docking site for co-factors (4); a moderately conserved ligand-binding domain (LBD) in the E region that is responsible for the ligand specificity and activation, as well as for dimerization of the receptor with the 9-cis-retinoic acid receptor (RXR) (5); an AF2 ligand-dependent activation domain in the C-terminus (carboxyl-terminal in F domain) that is crucial for the recruitment of PPAR co-activators. Numbers shown in C and E regions indicate the percentage amino-acid identity of DBD and LBD of human PPARβ/δ and PPARγ compared to human PPARα. **(B)** Several co-activator or co-repressor factors affect the activity of PPARs, which can stimulate or inhibit the function of the receptor, respectively. When PPARs are in a non-ligand-bound state in solution (inactive mode), all three PPAR isoforms can bind transcription co-repressors in a DNA-independent manner. These co-repressors, such as nuclear receptor co-repressor/silencing mediators for retinoid and thyroid hormone receptors (NCoR/SMRT), suppress gene transcription by interacting with histone deacetylases (HDACs). The binding of ligands to the PPAR–RXR heterodimer causes the exchange of co-repressors with co-activators, thereby converting PPARs from an inactive state to an active state. Receptor activation generally occurs after agonist binding to the LBD. Following ligand binding and initiation of receptor phosphorylation, PPARs dissociate the co-repressor complex. Then, the ligand–heterodimer (ligand–PPAR–RXR) complex binds to the target DNA promoter through a PPRE. Next, in order to allow the transcriptional machinery to gain access to the promoter region, PPARs bind specific co-activator complexes, such as steroid receptor activator 1 (SRC1) and cAMP response element-binding (CREB)-binding protein (CBP)/p300, which have acetyltransferase activity. Subsequently, they regulate the transcription of various genes that play a key role in various physiological processes.

Furthermore, PPARα can interfere with angiogenic responses that are critical during chronic inflammation by targeting endothelial vascular endothelial growth factor receptor-2 (VEGFR-2) signaling, thereby controlling the inflammatory response (60).

PPARγ is the most widely studied PPAR isoform, which is expressed in white and brown adipose tissue, large intestine, and immune cells such as macrophages, the pancreas, and the spleen, and it plays a key role in a series of biochemical processes, including insulin sensitivity, inducing tumor cell differentiation and apoptosis, adipogenesis, lipoprotein metabolism, energy balance, reducing blood fat and blood pressure, and lipid biosynthesis (53, 61–63). Activation of PPARγ increases fat storage by increasing adipocyte differentiation and enhancing the transcription of genes important for lipogenesis (64, 65). Moreover, this subtype has been proposed as a potential therapeutic target for different types of cancer due to its various anti-tumor properties (66, 67). In terms of regulating inflammation, recent literature has reported that PPARγ prevent the inflammatory cascades caused by NF-κB activation and the production of proinflammatory cytokines such as TNF-α, IL1B, IFN-γ, IL2, iNOS, IL18, reactive oxygen species (ROS), and IL6 through the inhibition of NF-κB transactivation (38, 68–70). On the other hand, PPARγ exerts its protective effects by targeting major inflammatory factors such as STAT1, AP-1, PI3K, intercellular adhesion molecule (ICAM1), and matrix metallopeptidase 9

(MMP9) and inhibiting their activity to prevent destructive inflammatory damage (71). In addition, PPARγ regulates the expression of several essential inflammatory target genes such as MCP1/CCL2, endothelin-1, and adiponectin (APN) (72). Interestingly, a recent study well demonstrated that PPARγ inhibits dysregulated inflammatory responses by suppressing NLRP3 inflammasome activation as well as decreasing maturation of caspase-1 and IL1B (73).

The PPARβ/δ is the third subtype of PPARs, which has not been as intensely studied as PPARα and PPARγ; it consists of 441 amino acids with a molecular weight of 49.9 kDa. This isoform is expressed in almost all tissues. It is especially abundant in the liver, intestine, kidney, abdominal adipose tissue, and skeletal muscle, all of which are involved in lipid metabolism. Indeed, the PPARβ/δ isoform participates in fatty-acid oxidation, mainly in skeletal and cardiac muscles, and regulates blood cholesterol and glucose concentration (47, 74, 75). However, complete information on the exact role of PPARβ/δ in the regulation of inflammation is still not available, and more research is needed to deeply dissect the relationship between PPARβ/δ and inflammation or inflammatory response. In some contexts, PPARβ/δ has been shown to have anti-inflammatory functions. For example, it was demonstrated that activation of PPARβ/δ reduces the expression of inflammation-associated NF-κB and STAT1-targeted genes including TNF-α, MCP1, IL6, CXCL8, CCL2, CXCR2, and CXCL1 (76–79). Taken together, all three PPAR subtypes have distinct yet overlapping roles in regulating metabolic function and inflammation. Further details on the tissue distribution, function, and natural and synthetic ligands of PPARα, PPARβ/δ, and PPARγ are provided in Table 1.

2.3 Mechanism of PPAR activation

The activation of PPARs by ligands is associated with structural changes in the receptor, including dissociation from co-repressor complexes and association with appropriate transcriptional co-activators, binding to DNA, and acquiring transactivation/transrepression capabilities (31). Moreover, promotion of many biochemical mechanisms of PPARs requires that the receptor is part of a heterodimeric complex with another nuclear receptor, the 9-cis-retinoic acid receptor (RXR; NR2B) (21, 89). Therefore, after activation with ligands/agonists, the PPAR–RXR heterodimers are transported to the nucleus and bind to specific DNA sequences consisting of a direct repeat of DNA recognition motif AGGTCA separated by one or two nucleotides (DR-1 or DR-2 response elements), thereby stimulating/repressing the transcription of target genes (Figure 1B) (89, 90). This sequence is called the peroxisome proliferator response element (PPRE) and is located in the promoter regions of PPAR-regulated target genes (91). Furthermore, after binding the ligand-activated PPAR–RXR complex to the target DNA through PPARE, this complex binds to specific co-activator complexes such as CREB-binding protein (CBP)/p300 and steroid receptor co-activator 1 (SRC1), which have histone acetyltransferase activity and facilitate the remodeling of chromatin structure (92–95). In this regard, previous studies have reported that the binding of co-activator complexes to the ligand-activated, PPRE-associated PPAR–RXR complex can disrupt nucleosomes and induce transcriptional regulatory changes in the chromatin structure near the regulatory regions of PPAR target genes (Figure 1B) (57, 96, 97).

3 COVID-19 and cytokine storm

SARS-CoV-2, which affects the lower and upper respiratory tract, invades host cells through angiotensin-converting enzyme 2 (ACE2) receptors (98, 99) and causes a wide range of clinical manifestations from mild forms such as fever, cough, and myalgia to moderate forms with pneumonia and local inflammation symptoms requiring hospitalization, to severe/critical forms with

TABLE 1 The natural and synthetic ligands, tissue expression, and function of PPARs.

PPAR Subtypes	Main Ligands (Natural and Synthetic)	Function	Tissue Distribution	Reference
PPARα (NR1C1)	Unsaturated fatty acids, omega-3, leukotriene B4, 8-hydroxy-eicosatetraenoic acid, clofibrate, fenofibrate, gemfibrozil, bezafibrate, and ciprofibrate	Lipid catabolism and hemostasis by stimulating beta-oxidation of fatty acids, control of inflammatory processes and vascular integrity, and mediation of the hypolipidemic function of fibrates	Highly expressed in metabolically active tissues such as liver, heart, kidney, large intestine, skeletal muscle, intestinal mucosa, and brown adipose	(22, 47, 53, 54, 80)
PPARβ/δ (NR1C2)	Arachidonic acid, linoleic acid, PGI213s, 13S-HODE, carbaprostacyclin, components of VLDL, GW501516, GW0742, MBX-802, and L-165041	Responsible for glucose metabolism and homeostasis, vascular integrity, glycogen metabolism, and control of inflammation	Expressed ubiquitously in virtually all tissues, mostly expressed in the small intestine and large intestine, and highly expressed in skin, skeletal muscle, adipose tissue, inflammatory cells, and heart	(81–84)
PPARγ (NR1C3)	Unsaturated fatty acids, prostaglandin PGJ2, 15-hydroxy-eicosatetraenoic acid, 9- and 13-hydroxy-octadecadienoic acid, 15-deoxyΔ12,14-prostaglandin G2, prostaglandin PGJ2, ciglitazone, pioglitazone, rosiglitazone, troglitazone, farglitazar, S26948, and INT131	Lipid storage, glucose disposal, insulin sensitivity, cellular proliferation, differentiation, regulation of innate immune response and inflammation, and differentiation and maturation of adipocytes	Expressed at the highest level in adipose tissue (white and brown), as well as in epithelial surfaces, urinary tract, human placental trophoblast, immunologic system (bone marrow, lymphocytes, monocytes, and macrophages), and spleen	(61, 62, 85–88)

fatal outcomes (100). Upon cellular entry of SARS-CoV-2 *via* its ACE2 receptor, viral genomic single-stranded RNA or other RNA compositions (double-stranded RNA) can be recognized as pathogen-associated molecule patterns (PAMPs) by innate immune and epithelial cells through the activation of pattern recognition receptors (PRRs) such as Toll-like receptors (TLRs), retinoic acid-inducible gene-I (RIG-I)-like receptors (RLRs), and NOD-like receptors (NLRs) (101, 102). Following sensitization of PRRs, downstream key inflammation-related transcription factors such as NF-κB, activator protein-1 (AP-1), and IFN regulatory factors (IRFs) are activated and promote the transcription of proinflammatory cytokines, chemokines, and IFNs such as IL1β, IL18, IL6, IL12, TNF-α, IL8, IL2, IL7, IL17, CCL3, CCL5, CXCL8, CXCL10, and IFN-γ (103–108). Moreover, proinflammatory cytokines such as IL6, TNF-α, and IFN-γ, in turn, activate JAK/STAT, NF-κB, and mitogen-activated protein kinase (MAPK) signaling by binding to their receptors on immune cells to induce further production of proinflammatory cytokines and subsequently form positive feedback to initiate the cytokine storm (Figure 2) (102).

Exacerbation of the local inflammatory response and increased secretion of proinflammatory cytokines and chemokines by resident immune and respiratory epithelial cells leads to more recruitment of innate and adaptive immune cells such as macrophages, neutrophils, dendritic cells (DCs), natural killer (NK) cells, monocytes, and CD4+ and CD8+ T cells to the site of infection to produce more persistent inflammatory cytokines (102). Indeed, growing evidence suggests that the crosstalk between epithelial cells and immune cells in COVID-19 produces high levels of proinflammatory cytokines that trigger an uncontrollable inflammatory response, hyperinflammation, or imbalanced inflammation (known as "cytokine storm") with severe complications and poor outcomes (109, 110). In this regard, extensive studies have recently reported that high circulating levels of proinflammatory cytokines (IFN-α, IFN-γ, IL1β, IL6, IL12, IL18, IL33, TNF-α, TGF-β, IL1RA, IL7, IL8, IL9, VEGFA, etc.) and chemokines (CCL2, CCL3, CCL5, CXCL8, CXCL9, CXCL10, etc.) have been identified in patients with severe COVID-19 (105, 111–114). Furthermore, it has been highlighted that cytokine storm is one of the main features of ARDS, ALI, tissue damage, and MOF, which are the major causes of COVID-19 severity and death of patients (106, 111, 115). Therefore, we believe that any intervention approach to target the critical inflammatory factors during SARS-CoV-2 infection could be a fundamental step in developing therapeutic strategies to control hyperinflammation, combat the cytokine storm, and reduce COVID-19 severity.

4 Anti-inflammatory mechanisms mediated by PPARs

In the last decade, many studies have concluded that PPARs, in addition to being critical players in glucose and lipid metabolism, play an essential role in controlling various types of the inflammatory response (57, 116, 117). Indeed, the inflammatory role of PPARs was highlighted when a previous study showed that PPARα knockdown was directly associated with increased levels of

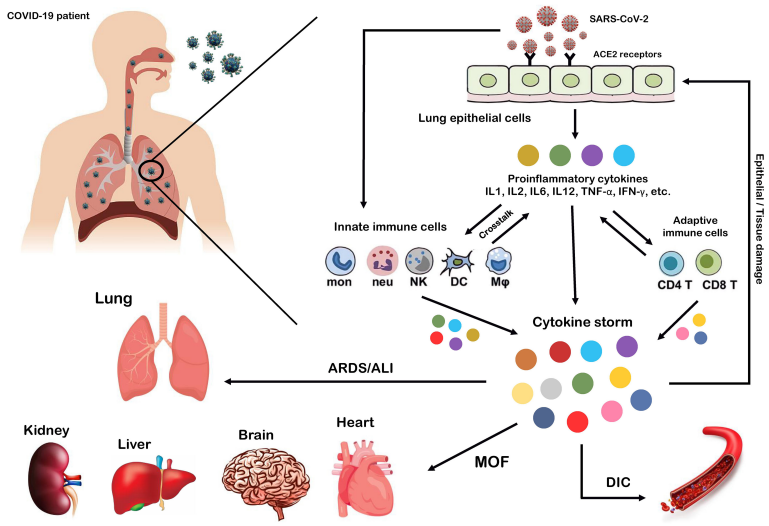

FIGURE 2
Cytokine storm as the hallmark of COVID-19 immunopathogenesis. Following the entry of SARS-CoV-2 into lung epithelial and immune cells *via* angiotensin-converting enzyme 2 (ACE2) receptors, a cascade of downstream signaling pathways is activated, ultimately leading to the massive release of proinflammatory cytokines and chemokines and tissue damage. Moreover, these proinflammatory cytokines lead to the recruitment of more innate immune cells, including neutrophils, macrophages, natural killer (NK) cells, monocytes, and dendritic cells (DCs) and active adaptive immune cells, including CD4+ and CD8+ T cells, to the site of infection, in order to induce the production of circulating cytokines. As a result, the crosstalk between epithelial and immune cells in vast cytokine release causes hyperinflammation and cytokine storm, which leads to a wide range of clinical manifestations from mild to severe/critical forms with a fatal outcome. Some of these fatal consequences include macrophage activation syndrome (MAS), hemophagocytic lymphohistiocytosis (HLH), capillary leak syndrome (CLS), thrombosis, disseminated intravascular coagulation (DIC), acute respiratory distress syndrome (ARDS), multi-organ failure (MOF), and acute lung injury (ALI).

proinflammatory cytokines (118). In agreement with this study, a recent study showed that, in addition to PPARα, the knockdown of PPARγ also leads to increased serum levels of IL6, IL1β, and TNF-α during lipopolysaccharide (LPS) stimulation (119). Furthermore, in an animal model, Huang et al. (120) showed that increased PPARγ expression levels prevented pulmonary inflammation and were directly associated with the recovery of influenza virus-infected animals (120). Moreover, several previous studies have shown that PPARα and PPARγ activation lead to reduced inflammation in polymicrobial sepsis (121) and HIV infection (122). In addition to these findings, in recent years, the central role of PPARs to control inflammation and reduce the levels of proinflammatory cytokines has been reviewed in many inflammatory disorders, including lung inflammatory diseases (32), IBD (21), and hepatic inflammation (116). These results indicate that PPARs suppress the transcription of main active inflammatory transcription factors, including NF-κB, AP-1, nuclear factor of activated T cells (NFAT), and signal transducers and activators of transcription (STATs), through an agonist-dependent mechanism (123). Among the various mechanisms PPARs use to repress many distinct transcriptions factor families, the most likely include four main mechanisms in which ligand-activated PPAR–RXR complexes suppress the activity of many inflammatory factors.

The first mechanism is the successful competition of PPARs to limit the amount of essential and shared co-activator proteins (such as CBP/P300) in a cell. As a result of this successful competition, these co-activators are not available for other transcription factors (31, 124). Therefore, the activities of other transcription factors (such as NF-κB) that use the same co-activators are repressed in these situations of co-activator competition. On the other hand, the second mechanism involves direct physical association between PPARs and other transcription factors without the mediation of co-activators. During the second mechanism, known as "cross-coupling" or "mutual receptor antagonism", ligand-activated PPAR–RXR heterodimers form a new complex with other transcription factors, such as AP-1, NF-κB, NFAT, and STATs through physical protein–protein interactions, thereby preventing transcription factor binding to its response element and also inhibiting their ability to induce the transcription of proinflammatory genes such as IL6, IL1β, and TNF-α (Figure 3) (46). For instance, agonist-activated PPARα and PPARγ negatively regulate the inflammatory gene response through bidirectionally blocking NF-κB and AP-1 signaling pathways *via* physical interaction with NF-κB p65 (38, 125). Moreover, PPARs can suppress the expression of NF-κB through the upregulation of inhibitors of NF-κB (IκBs) (126, 127). The third mechanism also involves blocking MAPK-inducted signaling cascades by ligand-activated PPAR–RXR heterodimers through inhibition of MAPK phosphorylation and activation (128, 129). Lastly, preventing the clearance of co-repressors whose removal is required for the transcriptional activation of AP-1 and NF-κB target proinflammatory genes is the fourth mechanism of inflammation suppression by PPARs (130, 131). Moreover, another anti-inflammatory effect of PPARs is their agonistic effect with other anti-inflammatory factors. Previous studies have shown that a significant increase in the expression level of PPARs is associated with an increase in the expression of anti-inflammatory factors such as IL10 (132–134). Several human and animal models have reported that PPARs and their ligands downregulate the expression of many chemokines such as CCL2, -4, -7, -12, -17, and -19, CXCL1, -9, and -10, and leukocyte adhesion molecules such as VCAM1, ICAM1, and endothelin-1. This downmodulation inhibits leukocyte

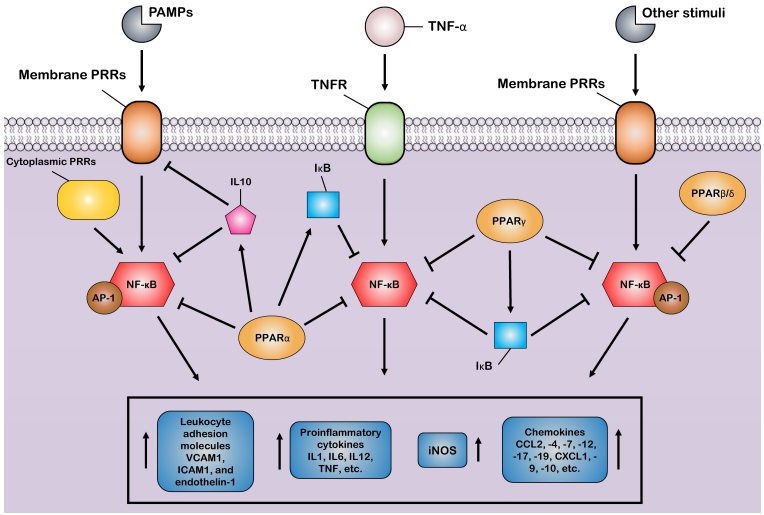

FIGURE 3
Control of the host inflammatory response mediated by PPARs. Most of the anti-inflammatory properties of PPARs are characterized by the suppression of key inflammatory transcription factors such as nuclear factor-κB (NF-κB) and activator protein-1 (AP-1) *via* different suppressive mechanisms, as induction of the production of anti-inflammatory cytokines. Through these mechanisms, PPARs block the expression of various inflammatory genes and, thus, reduce the production of many proinflammatory cytokines, chemokines, and other proinflammatory signal mediators, such as inducible nitric oxide synthase (iNOS). Additionally, the PPARs prevent the recruitment of leukocytes to the site of inflammation by inhibiting the production of cell adhesion molecules.

recruitment to the site of inflammation and reduces the crosstalk between immune cells and other resident cells for cytokine production (135–139).

5 Control of inflammation by PPARs during SARS-CoV-2 infection

The recent emergence of COVID-19 in the past years and its rapid worldwide spread have led to extensive clinical studies investigating the molecular regulatory mechanisms behind this severe disease. Intriguingly, at this time, many of these extensive clinical studies reported the influential role of PPAR subtypes, especially PPARγ and their ligands, in controlling the host inflammatory response during SARS-CoV-2 infection. Meanwhile, in previous clinical trials, a decrease in the expression of PPAR subtypes and an increase in the serum level of proinflammatory cytokines have been observed in inflammatory lungs of patients with severe COVID-19 (112, 113, 140). Additionally, in agreement with the results of clinical studies, several recent transcriptomics studies using microarray, RNA-sequencing (RNA-seq), and single-cell RNA-seq techniques have reported downregulation of PPARs in various tissues including whole blood, lung epithelial cells, bronchoalveolar lavage fluids (BALFs), and peripheral blood mononuclear cells (PBMCs) in the SARS-CoV-2-infected individuals (141–145). Following these findings, the results of previous proteomics and metabolomics studies also indicate the interference of SARS-CoV-2 infection in PPAR signaling (146, 147). Surprisingly, Keikha et al. (148) recently demonstrated that a set of miRNAs, including mir-27b, were upregulated during SARS-CoV-2 infection. They also reported that mir-27b has a significant negative correlation with its main target, i.e., PPARγ, and the increase in its expression during SARS-CoV-2 infection directly leads to the downregulation of PPARγ, thus playing a key role in the exacerbation of the inflammatory response in COVID-19 patients (148). One of the main immunopathogenesis strategies of SARS-CoV-2 infection has been suggested to interfere with PPAR signaling to exacerbate the inflammatory response (149). In other words, previous studies have reported that the decrease in the expression of PPARs including PPARγ, PPARα, and PPARβ/δ during SARS-CoV-2 infection is associated with the increased secretion of proinflammatory cytokines such as IL6, IL1β, and TNF-α, as well as cytokine storm; thus, it has a positive correlation with ARDS and ALI in COVID-19 patients (150, 151).

Moreover, a previous study concluded that SARS-CoV-2 suppresses PPAR expression in the lungs and abrogates one of the main anti-inflammatory cores for NF-κB activity, thereby exerting a hyperinflammatory response in patients with severe COVID-19 (152). Moreover, several recent studies also reported that the reduction in PPARγ and PPARα is directly related to acute pulmonary inflammation in COVID-19 and the shift of the disease from mild to severe and, finally, death (33, 153). Additionally, it has been highlighted that suppressing the expression of PPAR subtypes, especially PPARγ, leads to increased susceptibility to SARS-CoV-2 infection (154). Interestingly, the decrease in PPARγ expression during SARS-CoV-2 infection, in addition to being positively related to the occurrence of hyperinflammation, also leads to insulin resistance in COVID-19 patients (155). Besides, it has recently been reviewed that over-activation of the canonical WNT/β-catenin pathway in response to SARS-CoV-2 infection leads to inhibition of PPARγ expression in an opposing interplay (156). Furthermore, COVID-19 has more negative clinical consequences for obese people because clinical trials indicate that the serum levels of PPARγ are lower in obese people. Therefore, the probability of cytokine storm during SARS-CoV-2 infection is higher in these people (157). Furthermore, another study proved that alcohol consumption is directly related to systematic inflammation in COVID-19 patients because ethanol (EtOH) exacerbates the activation of proinflammatory cytokines, including IL6, IL1B, IFN, and TNF-α and inflammation-related transcription factors, including HIF1-α, JUN, NF-κB, and STATs *via* induction of PPAR–RXR inactivation (158).

Additionally, there is accumulating evidence that the T-helper 2 (Th2) inflammatory response phenotype can induce protective effects against the COVID-19 immunopathogenesis due to the increased secretion and release of Th2 anti-inflammatory cytokines such as IL10, IL4, and IL13 and recruitment of the eosinophils to the site of inflammation (159). Following these results, it has been well reviewed that cytokines associated with Th2 inflammatory response such as IL4 and IL13 inhibit the secretion of several proinflammatory cytokines such as IL6, IL1B, IL1α, IL12, and TNF-α, which play a central role in the pathogenesis of COVID-19 and hyperinflammation (160). Moreover, the anti-inflammatory M2 macrophages is activated by IL4 and IL13, which modulate inflammatory responses by producing anti-inflammatory cytokines, such as IL10 (161). Strikingly, recent results suggest that Th2 responses which driven by IL4, IL5, and IL13 dramatically reduce ACE2 in the respiratory tract and are associated with better clinical outcomes with COVID-19 (162, 163). Therefore, it has been hypothesized that the Th2 inflammatory response may exert potential protective effects against COVID-19 (164). Surprisingly, previous studies in several human inflammatory diseases indicate that both PPARα and PPARγ and their ligands increase the expression levels of anti-inflammatory markers associated with the Th2 inflammation such as IL13, IL4, IL10, and GATA3, thereby limiting the dysregulation of inflammation (165–167). Therefore, based on these findings, it can be concluded that PPARs can induce different anti-inflammatory mechanisms during SARS-CoV-2 infection through a synergistic effect with Th2 inflammatory responses.

Several reports suggest that PPARs play an important role in controlling the inflammatory response during COVID-19 by inducing the inactivation of the key inflammatory transcription factors, especially NF-κB (168). In this regard, it has been suggested that activation of PPARγ during COVID-19 can reduce the circulating levels of TNF-α, IL-1, and IL-6 in the innate immune cells such as macrophages and monocytes through interaction with NF-κB (169). Moreover, PPARγ acts as a negative regulator of cytotoxic T-cell activation and suppresses the production of cytokines by these adaptive immune cells (170). Following these studies, the recent emerging literature has also reported that activation of PPARα, PPARβ/δ, and PPARγ is inversely related to

pulmonary fibrosis caused by chronic inflammation in COVID-19 patients (147, 171–173). It has been also hypothesized that exercise may prevent untoward systemic consequences of SARS-CoV-2 infection including inflammation and metabolic dysfunctions such as lipotoxicity by having a positive effect on PPARα (33). The anti-inflammatory role of PPARβ/δ during COVID-19 has been less studied than the other two types of PPARs. However, a few reports have indicated that PPARβ/δ suppressing transcription factors involved in the inflammatory response, including NF-κB and AP-1 (31), reduce the expression levels of GDF-15 (one of the inflammatory biomarkers of COVID-19 severity) in a negative feedback manner (174).

Furthermore, PPARβ/δ and PPARγ have been shown to play a central role in the macrophage polarization toward an anti-inflammatory M2 phenotype during COVID-19 (175). On the other hand, the previous literature has shown that PPARα and PPARγ prevent the apoptosis of inflammatory cells by inducing anti-apoptotic factors of the BCL-2 family, thereby preventing the spread of cytokines and chemokines in the intercellular space (176). Notably, the decrease in the expression levels of PPARs in the early stages of SARS-CoV-2 infection and the increase in their expression during the treatment/recovery period indicate the opposite/inverse relationship of these receptors with the severity of the disease (38, 177).

Intriguingly, PPARα and PPARγ have been proposed as effective adjuvants for the development of COVID-19 vaccines because these receptors through an increase in the population of regulatory T-cells *via* upregulation in FOXP3 mRNA expression (a transcriptional factor for the function and differentiation of regulatory T-cells) (1): stimulate memory T-cells (2), upregulate the γδ type of T-cells, and (3) prolong B-cell memory and improve the secondary antibody response and thus can induce long-term memory (176, 178). However, the inverse relationship between regulatory T-cells and chronic inflammation has been revealed by previous research (175, 179), and the anti-inflammatory properties of these cells are well established (180, 181). Therefore, it can be predicted that the increase in the population of regulatory T-cells due to the activation of PPARs can play a potential dual-role by stimulating and strengthening long-term memory and exerting significant anti-inflammatory properties during SARS-CoV-2 infection.

Recent advances in high-throughput transcriptome-based technologies and the integration of these techniques with computational network-based algorithms of systems biology have provided an excellent opportunity to identify altered gene regulatory networks under infected conditions, activated pathways, potential therapeutic/diagnostic/prognostic targets, and understanding the complex molecular mechanisms underlying infectious disease at the systemic level (182). In our previous work, we integrated and analyzed the RNA-seq data from PBMCs of healthy individuals and COVID-19 patients with computational network-based methods of systems biology in order to identify potential therapeutic targets and candidate gene modules underlying COVID-19 and develop promising therapeutic strategies for COVID-19 (39). As a result, we identified nine candidate co-expressed gene modules and 290 hub-high traffic genes with the highest betweenness centrality (BC) score directly related to SARS-CoV-2 pathogenesis (39). Indeed, the genes with the highest BC score have the highest rate of "information transfer" in their respective modules with critical biological functions, which are known as "high traffic" genes and can be potential therapeutic, diagnostic, and prognostic targets for COVID-19 therapy (39). We observed that PPARα is among the hub-high traffic genes in one of the key modules with anti-inflammatory function, indicating the crucial anti-inflammatory role of this PPAR subtype during SARS-CoV-2 infection (39). In another study, Auwul et al. (40) integrated various transcriptomic data with computational systems biology and machine learning algorithms and identified 52 common drug targets, including PPARγ, for COVID-19 treatment (40).

Moreover, further studies using pharmacological network approaches have identified PPARα and PPARγ as promising drug/therapeutic targets to control inflammation caused by host–SARS-CoV-2 interactions (183, 184). On the other hand, recently, a study introduced glycyrrhetinic acid as an essential drug against cytokine storm in COVID-19 patients (185). During this study, using protein–protein interaction (PPI) network and molecular docking techniques, it was well established that glycyrrhetinic acid activates or represses 84 core genes to counter the cytokine storm during COVID-19 using multiple strategies (185). As an important result of this study, one of these glycyrrhetinic acid strategies to deal with the cytokine storm was to target PPARγ, PPARα, and PPARβ/δ for activation (185). Figure 4 shows that the PPI structure of the candidate modules identified by these studies that contained critical therapeutic targets, including PPARα, PPARβ/δ, and PPARγ for COVID-19 therapy.

Interestingly, the use of PPARs agonists to activate them to repress the inflammatory processes during COVID-19 has recently attracted much attention. In this regard, it has been demonstrated that PPAR activation through synthetic and nutritional compounds can be an efficient management program to overcome the cytokine storm and prevent the deleterious inflammatory effects after coronavirus infection (38, 186). Moreover, a recent study suggested using synthetic and natural ligands of PPARs in order to target NF-κB transcriptional activity and reduce inflammatory response as an attractive strategy for managing the nutrition of COVID-19 patients (187). Following these results, the recent literature also reported that several natural and synthetic PPARγ agonists suppress NF-κB activity through PPARγ activation, leading to reduced levels of proinflammatory cytokines such as IL1β, IL6, TNF-α, IL18, IFN-γ, IL8, and IL12 (38). It has been well established that PPARα activation using oleoylethanolamide, in addition to suppressing TLR4-mediated NF-κB signaling cascade and reducing proinflammatory cytokines such as COX2, IL6, CRP, IL1β, TNF-α, and iNOS, is also associated with increased levels of anti-inflammatory factors such as IL10 (56, 188–190). Additionally, it has recently been shown that fenofibrate is a PPARα agonist with anti-inflammatory, anti-oxidant, and anti-thrombotic properties that exerts broad anti-inflammatory effects such as inhibition of iNOS, repression of COX2 and MMP9, activation of inhibitory kappa B (IκB), and release of adiponectin through the activating of PPARα during SARS-CoV-2 infection (150). Furthermore, previous studies reported that fenofibrate inhibits viral replication in lung epithelial cells by reversing the metabolic changes caused by SARS-CoV-2 (175). On the other

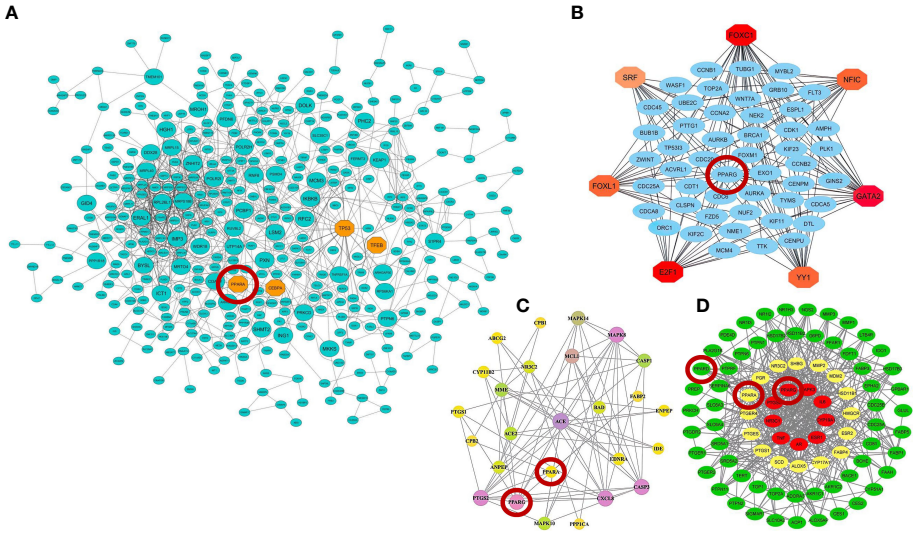

FIGURE 4
Protein–protein interaction (PPI) networks of therapeutic candidate modules for COVID-19 therapy obtained by **(A)** our group (39) **(B)** Auwul et al. (40), **(C)** Oh et al. (183), and **(D)** Li et al. (185). These modules had the most biological associations with the immunopathogenesis of COVID-19. Large circles represent hub-high traffic genes. PPAR genes as potential therapeutic targets for COVID-19 pandemic are highlighted by red circles in these PPI networks.

hand, natural astaxanthin (ASX), an important PPARγ agonist, has a clinically proven safety profile with anti-oxidant, anti-inflammatory, and immunomodulatory properties. Interestingly, mounting evidence from clinical studies suggests that this PPAR agonist prevents the ARDS/ALI in COVID-19 patients by downregulating NF-κB and JAK/STAT signaling and then reducing TNF-α, IL1β, and IL6 levels. Moreover, ASX caused a change in the inflammatory response of Th1 cells to Th2, leading to a shift from proinflammatory cytokine secretion to anti-inflammatory cytokine secretion (191). ASX also exerts an anti-oxidant effect and prevents oxidative damage through (1) inhibition of NLRP3 inflammasome and HIF1-α, and (2) suppression of plasma CRP, iNOS, COX2, PGE2, and ICAM1, respectively. Accordingly, ASX-mediated activation of PPARγ has been proposed as an effective therapeutic strategy to control host inflammatory and immune responses, antagonize the cytokine storm, and prevent deleterious inflammatory effects following COVID-19 (191). Moreover, troglitazone, an insulin-sensitizing drug that is prescribed for treating type 2 diabetes mellitus (192), is a synthetic PPARγ agonist that interferes with NF-κB activity and exerts its anti-inflammatory effects through the activation of PPARγ (38). Interestingly, this drug has been introduced as one of the most suitable options for applying anti-inflammatory effects for COVID-19-inducted hyperinflammation (38). In addition to troglitazone, pioglitazone (a synthetic agonist of PPARγ, see Table 1) is another member of the thiazolidinedione (TZD) family that has significant anti-inflammatory effects and has been suggested by Carboni et al. (193) as a support drug for the reduction in many inflammatory parameters in COVID-19 patients (193). Additionally, pioglitazone can reduce SARS-CoV-2 RNA synthesis and replication through potential inhibition of 3-chymotrypsin-like protease (3CL-Pro) (194). Moreover, it has recently been suggested that activation of PPARγ by agonists such as cannabidiol reduces cytokine secretion, pulmonary inflammation, and fibrosis in the lung of the patients during SARS-CoV-2 infection (195). Intriguingly, zinc supplementation has also been reported to have potential health benefits for managing inflammation in COVID-19 by suppressing the expression of many cytokines and adhesion molecules through increasing the expression of PPARα (196). Furthermore, natural compounds such as gamma-oryzanol (the main bioactive constituent from rice bran and germ) have been introduced as a possible adjunctive therapy to prevent the cytokine storm in COVID-19 patients, as this compound positively increases the expression of PPARγ in adipose tissue and as a result reduces the levels of inflammatory cytokines including TNF-α, IL6, and MCP1 (157). To the best of our knowledge, no information is yet available on the role of PPARβ/δ agonists during SARS-CoV-2 infection. Therefore, future research should investigate the anti-inflammatory effects of natural and synthetic agonists of PPARβ/δ during the COVID-19 pandemic. However, looking at the previous literature on similar inflammatory lung diseases in humans, it can be concluded that PPARβ/δ agonists have significant anti-inflammatory effects during lung infection (197). Conversely, using existing natural and synthetic ligands of PPARs may have limitations or challenges. For instance, recent data show that using natural and synthetic ligands of PPARs is highly dose-dependent and can interact with non-PPAR targets due to the complexities of the drug–target complex (94). Moreover, it has been reported that some ligands of PPARs can exert selective agonistic or antagonistic regulatory effects depending on the cell context (191, 198, 199). Additionally, it has been highlighted that using synthetic agonists of PPARs can lead to serious clinical complications, including bone fracture, heart failure, cardiovascular risk, liver failure, gastrointestinal bleeding, and liver and kidney toxicity (200).

These findings highlight the potential role of PPAR subtypes (particularly PPARγ) and their ligands with anti-inflammatory effects during the COVID-19 pandemic, which can be promising

candidates for inhibiting key inflammatory factors (especially NF-κB and AP-1), thus regulating inflammation during SARS-CoV-2 infection. Therefore, any intervention methods aimed at activating/upregulating/overexpressing of PPAR subtypes could be a promising therapeutic strategy to reduce the hyperinflammatory response in COVID-19 patients and prevent the cytokine storm.

6 Conclusions and future prospects

COVID-19 is an emerging global health threat caused by SARS-CoV-2 infection with severe inflammatory complications. Treatment of severely ill patients is an important healthcare issue. Despite developing various vaccines for disease prevention, there is still no definitive treatment solution for COVID-19 patients. The massive cytokine secretion caused by the exacerbation of the host inflammatory system in response to SARS-CoV-2 infection is known as a "cytokine storm", which is directly related to the progression of the disease from mild to severe. In recent years, among previous efforts, it has been suggested that one of the most effective strategies for improving the survival of COVID-19 patients and reducing the severity of the disease is to control the hyperinflammatory response and interfere with cytokine storm. Cytokine storm has been one of the main characteristics of disease severity, decreased lung function, ARDS, ALI, and MOF, and ultimately, the death of COVID-19 patients. Therefore, paying attention to anti-inflammatory factors and examining their response during SARS-CoV-2 infection can provide the basic solution to deal with COVID-19-inducted cytokine storm.

PPARs are ligand-dependent transcription factors belonging to the nuclear receptor superfamily, which are the main regulators of lipid and glucose metabolism. This transcription factor family consists of three subtypes: PPARα, PPARβ/δ, and PPARγ. In the last decade, it has been well established that these subtypes, in addition to their central role in metabolism and energy balance, play important roles in cell proliferation, differentiation, the immune cell system, and inflammation. Concerning inflammation and inflammation-related disease, PPARs play an important anti-inflammatory role as critical inhibitors of the host inflammatory response through adverse regulatory effects on active inflammatory transcription factors such as NF-κB, AP-1, NFAT, and STATs. Currently, extensive clinical and omics studies indicate downregulation in the expression of PPARs in response to SARS-CoV-2 infection, which has been proposed as one of the main causes of SARS-CoV-2 immunopathogenesis to exacerbate the host inflammatory response.

On the other hand, it has been highlighted that the activation of PPARs through natural and synthetic ligands is associated with the reduction of hyperinflammatory response, prevention of cytokine storm, and reduction in disease severity in COVID-19 patients. Therefore, this makes them attractive and practical targets for developing novel therapeutic strategies against COVID-19 and cytokine storm. However, the previous literature has indicated that using existing natural and synthetic ligands of PPARs may lead to severe clinical complications.

Therefore, considering the anti-inflammatory importance of PPARs to control the hyperinflammatory response during COVID-19, further research should deeply investigate the individual or collective effects of PPAR subtypes to inhibit cytokine storms during SARS-CoV-2 infection. Moreover, considering the side-effects and challenges of using existing natural and synthetic ligands to activate PPARs, further exploration of the underlying mechanisms is needed to establish new pathways of PPARs activation without causing severe clinical side-effects.

Author contributions

AH and AB conceived the ideas. AH, AB, AS, and BK designed the study. AH, AB, AS, BT-F, and SI determined the methodology. AH, AB, BK, FG, AS, AA, and MA validated and interpreted the results. AH, AB, BT-F, AS, MA, FG, and SI investigated and collected resources. AH, AB, and BK wrote and prepared the original draft. AH, AB, AS, AA, and BK reviewed and edited the manuscript. All authors contributed to the article and approved the submitted version.

Acknowledgments

The authors thank all the teams who contributed to and provided technical assistance during this study. We also thank the reviewers whose critical comments helped in improving the manuscript.

Conflict of interest

The authors declare that the research was conducted in the absence of any commercial or financial relationships that could be construed as a potential conflict of interest.

Publisher's note

References

1. Ahamad MM, Aktar S, Rashed-Al-Mahfuz M, Uddin S, Liò P, Xu H, et al. A machine learning model to identify early stage symptoms of sars-Cov-2 infected patients. *Expert Syst Appl* (2020) 160:113661. doi: 10.1016/j.eswa.2020.113661

2. Guan W-J, Ni Z-Y, Hu Y, Liang W-H, Ou C-Q, He J-X, et al. Clinical characteristics of coronavirus disease 2019 in China. *New Engl J Med* (2020) 382 (18):1708–20. doi: 10.1056/NEJMoa2002032

3. Sohrabi C, Alsafi Z, O'Neill N, Khan M, Kerwan A, Al-Jabir A, et al. World health organization declares global emergency: A review of the 2019 novel coronavirus (Covid-19). *Int J Surg* (2020) 76:71–6. doi: 10.1016/j.ijsu.2020.02.034

4. Tian S, Hu W, Niu L, Liu H, Xu H, Xiao S-Y. Pulmonary pathology of early-phase 2019 novel coronavirus (Covid-19) pneumonia in two patients with lung cancer. *J Thorac Oncol* (2020) 15(5):700–4. doi: 10.1016/j.jtho.2020.02.010

5. Chen N, Zhou M, Dong X, Qu J, Gong F, Han Y, et al. Epidemiological and clinical characteristics of 99 cases of 2019 novel coronavirus pneumonia in wuhan, China: A descriptive study. *Lancet* (2020) 395(10223):507–13. doi: 10.1016/S0140-6736(20)30211-7

6. McGonagle D, Sharif K, O'Regan A, Bridgewood C. The role of cytokines including interleukin-6 in covid-19 induced pneumonia and macrophage activation syndrome-like disease. *Autoimmun Rev* (2020) 19(6):102537. doi: 10.1016/j.autrev.2020.102537

7. Tay MZ, Poh CM, Rénia L, MacAry PA, Ng LFP. The trinity of covid-19: Immunity, inflammation and intervention. *Nat Rev Immunol* (2020) 20(6):363–74. doi: 10.1038/s41577-020-0311-8

8. Cao X. Covid-19: Immunopathology and its implications for therapy. *Nat Rev Immunol* (2020) 20(5):269–70. doi: 10.1038/s41577-020-0308-3

9. Merad M, Martin JC. Pathological inflammation in patients with covid-19: A key role for monocytes and macrophages. *Nat Rev Immunol* (2020) 20(6):355–62. doi: 10.1038/s41577-020-0331-4

10. Ragab D, Salah Eldin H, Taeimah M, Khattab R, Salem R. The covid-19 cytokine storm; what we know so far. *Front Immunol* (2020) 11:1446. doi: 10.3389/fimmu.2020.01446

11. Ahmed F. A network-based analysis reveals the mechanism underlying vitamin d in suppressing cytokine storm and virus in sars-Cov-2 infection. *Front Immunol* (2020) 11:590459. doi: 10.3389/fimmu.2020.590459

12. Rehan M, Ahmed F, Howladar SM, Refai MY, Baeissa HM, Zughaibi TA, et al. A computational approach identified andrographolide as a potential drug for suppressing covid-19-Induced cytokine storm. *Front Immunol* (2021) 12:648250. doi: 10.3389/fimmu.2021.648250

13. Xiong Y, Liu Y, Cao L, Wang D, Guo M, Jiang A, et al. Transcriptomic characteristics of bronchoalveolar lavage fluid and peripheral blood mononuclear cells in covid-19 patients. *Emerging Microbes Infections* (2020) 9(1):761–70. doi: 10.1080/22221751.2020.1747363

14. Ren X, Wen W, Fan X, Hou W, Su B, Cai P, et al. Covid-19 immune features revealed by a Large-scale single-cell transcriptome atlas. *Cell* (2021) 184(7):1895–913.e19. doi: 10.1016/j.cell.2021.01.053

15. Yang AC, Kern F, Losada PM, Agam MR, Maat CA, Schmartz GP, et al. Dysregulation of brain and choroid plexus cell types in severe covid-19. *Nature* (2021) 595(7868):565–71. doi: 10.1038/s41586-021-03710-0

16. McClain MT, Constantine FJ, Henao R, Liu Y, Tsalik EL, Burke TW, et al. Dysregulated transcriptional responses to sars-Cov-2 in the periphery. *Nat Commun* (2021) 12(1):1079. doi: 10.1038/s41467-021-21289-y

17. Arunachalam PS, Wimmers F, Mok CKP, Perera RAPM, Scott M, Hagan T, et al. Systems biological assessment of immunity to mild versus severe covid-19 infection in humans. *Science* (2020) 369(6508):1210–20. doi: 10.1126/science.abc6261

18. Hariharan A, Hakeem AR, Radhakrishnan S, Reddy MS, Rela M. The role and therapeutic potential of nf-Kappa-B pathway in severe covid-19 patients. *Inflammopharmacology* (2021) 29(1):91–100. doi: 10.1007/s10787-020-00773-9

19. Kircheis R, Haasbach E, Lueftenegger D, Heyken WT, Ocker M, Planz O. Nf-Kb pathway as a potential target for treatment of critical stage covid-19 patients. *Front Immunol* (2020) 11:598444. doi: 10.3389/fimmu.2020.598444

20. Sun X, Wang T, Cai D, Hu Z, Ja C, Liao H, et al. Cytokine storm intervention in the early stages of covid-19 pneumonia. *Cytokine Growth Factor Rev* (2020) 53:38–42. doi: 10.1016/j.cytogfr.2020.04.002

21. Decara J, Rivera P, López-Gambero AJ, Serrano A, Pavón FJ, Baixeras E, et al. Peroxisome proliferator-activated receptors: Experimental targeting for the treatment of inflammatory bowel diseases. *Front Pharmacol* (2020) 11:730. doi: 10.3389/fphar.2020.00730

22. Li J, Liu Y-P. The roles of ppars in human diseases. *Nucleosides Nucleotides Nucleic Acids* (2018) 37(7):361–82. doi: 10.1080/15257770.2018.1475673

23. Feige JN, Gelman L, Michalik L, Desvergne B, Wahli W. From molecular action to physiological outputs: Peroxisome proliferator-activated receptors are nuclear receptors at the crossroads of key cellular functions. *Prog Lipid Res* (2006) 45 (2):120–59. doi: 10.1016/j.plipres.2005.12.002

24. Gonzalez FJ, Shah YM. Pparα: Mechanism of species differences and hepatocarcinogenesis of peroxisome proliferators. *Toxicology* (2008) 246(1):2–8. doi: 10.1016/j.tox.2007.09.030

25. You M, Jin J, Liu Q, Xu Q, Shi J, Hou Y. Pparα promotes cancer cell Glut1 transcription repression. *J Cell Biochem* (2017) 118(6):1556–62. doi: 10.1002/jcb.25817

26. Hennuyer N, Duplan I, Paquet C, Vanhoutte J, Woitrain E, Touche V, et al. The novel selective pparα modulator (Spparmα) pemafibrate improves dyslipidemia, enhances reverse cholesterol transport and decreases inflammation and atherosclerosis. *Atherosclerosis* (2016) 249:200–8. doi: 10.1016/j.atherosclerosis.2016.03.003

27. Andrulionyte L, Kuulasmaa T, Chiasson J-L, Laakso MGroup ftS-NS. Single nucleotide polymorphisms of the peroxisome proliferator–activated receptor-A gene (Ppara) influence the conversion from impaired glucose tolerance to type 2 diabetes: The stop-niddm trial. *Diabetes* (2007) 56(4):1181–6. doi: 10.2337/db06-1110

28. Holness MJ, Samsuddin S, Sugden MC. The role of ppars in modulating cardiac metabolism in diabetes. *Pharmacol Res* (2009) 60(3):185–94. doi: 10.1016/j.phrs.2009.04.006

29. Ramon S, Bancos S, Thatcher TH, Murant TI, Moshkani S, Sahler JM, et al. Peroxisome proliferator-activated receptor Γ b Cell-Specific–deficient mice have an impaired antibody response. *J Immunol* (2012) 189(10):4740–7. doi: 10.4049/jimmunol.1200956

30. Choi J-M, Bothwell ALM. The nuclear receptor ppars as important regulators of T-cell functions and autoimmune diseases. *Molecules Cells* (2012) 33(3):217–22. doi: 10.1007/s10059-012-2297-y

31. Daynes RA, Jones DC. Emerging roles of ppars in inflammation and immunity. *Nat Rev Immunol* (2002) 2(10):748–59. doi: 10.1038/nri912

32. Becker J, Delayre-Orthez C, Frossard N, Pons F. Regulation of inflammation by ppars: A future approach to treat lung inflammatory diseases? *Fundam Clin Pharmacol* (2006) 20(5):429–47. doi: 10.1111/j.1472-8206.2006.00425.x

33. Heffernan KS, Ranadive SM, Jae SY. Exercise as medicine for covid-19: On ppar with emerging pharmacotherapy. *Med Hypotheses* (2020) 143:110197. doi: 10.1016/j.mehy.2020.110197

34. Fantacuzzi M, Amoroso R, Ammazzalorso A. Ppar ligands induce antiviral effects targeting perturbed lipid metabolism during sars-Cov-2, hcv, and hcmv infection. *Biology* (2022) 11(1):114. doi: 10.3390/biology11010114

35. Calder PC. N-3 fatty acids, inflammation and immunity: New mechanisms to explain old actions. *Proc Nutr Soc* (2013) 72(3):326–36. doi: 10.1017/S0029665113001031

36. Jacob A, Wu R, Zhou M, Wang P. Mechanism of the anti-inflammatory effect of curcumin: Ppar-Γ activation. *PPAR Res* (2007) 2007:089369. doi: 10.1155/2007/89369

37. Del Re A, Corpetti C, Pesce M, Seguella L, Steardo L, Palenca I, et al. Ultramicronized palmitoylethanolamide inhibits Nlrp3 inflammasome expression and pro-inflammatory response activated by sars-Cov-2 spike protein in cultured murine alveolar macrophages. *Metabolites* (2021) 11(9):592. doi: 10.3390/metabo11090592

38. Ciavarella C, Motta I, Valente S, Pasquinelli G. Pharmacological (or synthetic) and nutritional agonists of ppar-Γ as candidates for cytokine storm modulation in covid-19 disease. *Molecules* (2020) 25(9):2076. doi: 10.3390/molecules25092076

39. Hasankhani A, Bahrami A, Sheybani N, Aria B, Hemati B, Fatehi F, et al. Differential Co-expression network analysis reveals key hub-high traffic genes as potential therapeutic targets for covid-19 pandemic. *Front Immunol* (2021) 12:789317. doi: 10.3389/fimmu.2021.789317

40. Auwul MR, Rahman MR, Gov E, Shahjaman M, Moni MA. Bioinformatics and machine learning approach identifies potential drug targets and pathways in covid-19. *Briefings Bioinf* (2021) 22(5). doi: 10.1093/bib/bbab120

41. Hihi AK, Michalik L, Wahli W. Ppars: Transcriptional effectors of fatty acids and their derivatives. *Cell Mol Life Sci* (2002) 59(5):790–8. doi: 10.1007/s00018-002-8467-x

42. Kota BP, Huang TH-W, Roufogalis BD. An overview on biological mechanisms of ppars. *Pharmacol Res* (2005) 51(2):85–94. doi: 10.1016/j.phrs.2004.07.012

43. Wang Y-X. Ppars: Diverse regulators in energy metabolism and metabolic diseases. *Cell Res* (2010) 20(2):124–37. doi: 10.1038/cr.2010.13

44. Wagner N, Wagner K-D. Ppars and angiogenesis–implications in pathology. *Int J Mol Sci* (2020) 21(16):5723. doi: 10.3390/ijms21165723

45. Wahli W, Michalik L. Ppars at the crossroads of lipid signaling and inflammation. *Trends Endocrinol Metab* (2012) 23(7):351–63. doi: 10.1016/j.tem.2012.05.001

46. Ricote M, Glass CK. Ppars and molecular mechanisms of transrepression. *Biochim Biophys Acta (BBA) - Mol Cell Biol Lipids* (2007) 1771(8):926–35. doi: 10.1016/j.bbalip.2007.02.013

47. Grygiel-Górniak B. Peroxisome proliferator-activated receptors and their ligands: Nutritional and clinical implications - a review. *Nutr J* (2014) 13(1):17. doi: 10.1186/1475-2891-13-17

48. Crossland H, Constantin-Teodosiu D, Greenhaff PL. The regulatory roles of ppars in skeletal muscle fuel metabolism and inflammation: Impact of ppar agonism on muscle in chronic disease, contraction and sepsis. *Int J Mol Sci* (2021) 22(18):9775. doi: 10.3390/ijms22189775

49. Issemann I, Green S. Activation of a member of the steroid hormone receptor superfamily by peroxisome proliferators. *Nature* (1990) 347(6294):645–50. doi: 10.1038/347645a0

50. Yousefnia S, Momenzadeh S, Seyed Forootan F, Ghaedi K, Nasr Esfahani MH. The influence of peroxisome proliferator-activated receptor Γ (Pparγ) ligands on cancer cell tumorigenicity. *Gene* (2018) 649:14–22. doi: 10.1016/j.gene.2018.01.018

51. Basilotta R, Lanza M, Casili G, Chisari G, Munao S, Colarossi L, et al. Potential therapeutic effects of ppar ligands in glioblastoma. *Cells* (2022) 11(4):621. doi: 10.3390/cells11040621

52. Chinetti G, Fruchart JC, Staels B. Peroxisome proliferator-activated receptors (Ppars): Nuclear receptors at the crossroads between lipid metabolism and inflammation. *Inflammation Res* (2000) 49(10):497–505. doi: 10.1007/s000110050622

53. Kliewer SA, Sundseth SS, Jones SA, Brown PJ, Wisely GB, Koble CS, et al. Fatty acids and eicosanoids regulate gene expression through direct interactions with peroxisome proliferator-activated receptors A and Γ. *Proc Natl Acad Sci* (1997) 94 (9):4318–23. doi: 10.1073/pnas.94.9.4318

54. Neschen S, Morino K, Dong J, Wang-Fischer Y, Cline GW, Romanelli AJ, et al. N-3 fatty acids preserve insulin sensitivity in vivo in a peroxisome proliferator–activated Receptor-A–dependent manner. *Diabetes* (2007) 56(4):1034–41. doi: 10.2337/db06-1206

55. Tan Y, Wang M, Yang K, Chi T, Liao Z, Wei P. Ppar-A modulators as current and potential cancer treatments. *Front Oncol* (2021) 11:599995. doi: 10.3389/fonc.2021.599995

56. Yang L, Guo H, Li Y, Meng X, Yan L, Dan Z, et al. Oleoylethanolamide exerts anti-inflammatory effects on lps-induced thp-1 cells by enhancing pparα signaling and inhibiting the nf-Kb and Erk1/2/Ap-1/Stat3 pathways. *Sci Rep* (2016) 6(1):34611. doi: 10.1038/srep34611

57. Bougarne N, Weyers B, Desmet SJ, Deckers J, Ray DW, Staels B, et al. Molecular actions of pparα in lipid metabolism and inflammation. *Endocr Rev* (2018) 39(5):760–802. doi: 10.1210/er.2018-00064

58. Stienstra R, Mandard S, Tan NS, Wahli W, Trautwein C, Richardson TA, et al. The interleukin-1 receptor antagonist is a direct target gene of pparα in liver. *J Hepatol* (2007) 46(5):869–77. doi: 10.1016/j.jhep.2006.11.019

59. Mandard S, Müller M, Kersten S. Peroxisome proliferator-activated receptor A target genes. *Cell Mol Life Sci CMLS* (2004) 61(4):393–416. doi: 10.1007/s00018-003-3216-3

60. Meissner M, Stein M, Urbich C, Reisinger K, Suske G, Staels B, et al. Pparα activators inhibit vascular endothelial growth factor receptor-2 expression by repressing Sp1-dependent DNA binding and transactivation. *Circ Res* (2004) 94 (3):324–32. doi: 10.1161/01.RES.0000113781.08139.81

61. Medina-Gomez G, Gray SL, Yetukuri L, Shimomura K, Virtue S, Campbell M, et al. Ppar gamma 2 prevents lipotoxicity by controlling adipose tissue expandability and peripheral lipid metabolism. *PloS Genet* (2007) 3(4):e64. doi: 10.1371/journal.pgen.0030064

62. Lehrke M, Lazar MA. The many faces of pparγ. *Cell* (2005) 123(6):993–9. doi: 10.1016/j.cell.2005.11.026

63. Cataldi S, Costa V, Ciccodicola A, Aprile M. Pparγ and diabetes: Beyond the genome and towards personalized medicine. *Curr Diabetes Rep* (2021) 21(6):18. doi: 10.1007/s11892-021-01385-5

64. Desvergne B, Wahli W. Peroxisome proliferator-activated receptors: Nuclear control of metabolism. *Endocr Rev* (1999) 20(5):649–88. doi: 10.1210/edrv.20.5.0380

65. Jamwal S, Blackburn JK, Elsworth JD. Pparγ/Pgc1α signaling as a potential therapeutic target for mitochondrial biogenesis in neurodegenerative disorders. *Pharmacol Ther* (2021) 219:107705. doi: 10.1016/j.pharmthera.2020.107705

66. Xu WP, Zhang X, Xie WF. Differentiation therapy for solid tumors. *J Digestive Dis* (2014) 15(4):159–65. doi: 10.1111/1751-2980.12122

67. Cui L, Li Z, Xu F, Tian Y, Chen T, Li J, et al. Antitumor effects of astaxanthin on esophageal squamous cell carcinoma by up-regulation of pparγ. *Nutr Cancer Via* (2022) 74(4):1399–410. doi: 10.1080/01635581.2021.1952449

68. Wu L, Guo C, Wu J. Therapeutic potential of pparγ natural agonists in liver diseases. *J Cell Mol Med* (2020) 24(5):2736–48. doi: 10.1111/jcmm.15028

69. Choi M-J, Lee E-J, Park J-S, Kim S-N, Park E-M, Kim H-S. Anti-inflammatory mechanism of galangin in lipopolysaccharide-stimulated microglia: Critical role of ppar-Γ signaling pathway. *Biochem Pharmacol* (2017) 144:120–31. doi: 10.1016/j.bcp.2017.07.021

70. Luzi L, Radaelli MG. Influenza and obesity: Its odd relationship and the lessons for covid-19 pandemic. *Acta Diabetologica* (2020) 57(6):759–64. doi: 10.1007/s00592-020-01522-8

71. Caioni G, Viscido A, d'Angelo M, Panella G, Castelli V, Merola C, et al. Inflammatory bowel disease: New insights into the interplay between environmental factors and pparγ. *Int J Mol Sci* (2021) 22(3). doi: 10.3390/ijms22030985

72. Kökény G, Calvier L, Hansmann G. Pparγ and tgfβ–major regulators of metabolism, inflammation, and fibrosis in the lungs and kidneys. *Int J Mol Sci* (2021) 22(19):10431. doi: 10.3390/ijms221910431

73. Yang C-C, Wu C-H, Lin T-C, Cheng Y-N, Chang C-S, Lee K-T, et al. Inhibitory effect of pparγ on Nlrp3 inflammasome activation. *Theranostics* (2021) 11(5):2424. doi: 10.7150/thno.46873

74. Luquet S, Lopez-Soriano J, Holst D, Gaudel C, Jehl-Pietri C, Fredenrich A, et al. Roles of peroxisome proliferator-activated receptor delta (Pparδ) in the control of fatty acid catabolism. a new target for the treatment of metabolic syndrome. *Biochimie* (2004) 86(11):833–7. doi: 10.1016/j.biochi.2004.09.024

75. Stephen RL, Gustafsson MCU, Jarvis M, Tatoud R, Marshall BR, Knight D, et al. Activation of peroxisome proliferator-activated receptor Δ stimulates the proliferation of human breast and prostate cancer cell lines. *Cancer Res* (2004) 64(9):3162–70. doi: 10.1158/0008-5472.CAN-03-2760

76. Lee MY, Choi R, Kim HM, Cho EJ, Kim BH, Choi YS, et al. Peroxisome proliferator-activated receptor Δ agonist attenuates hepatic steatosis by anti-inflammatory mechanism. *Exp Mol Med* (2012) 44(10):578–85. doi: 10.3858/emm.2012.44.10.066

77. Liu Y, Colby JK, Zuo X, Jaoude J, Wei D, Shureiqi I. The role of ppar-Δ in metabolism, inflammation, and cancer: Many characters of a critical transcription factor. *Int J Mol Sci* (2018) 19(11):3339. doi: 10.3390/ijms19113339

78. Jung TW, Lee SH, Kim H-C, Bang JS, Abd El-Aty AM, Hacımüftüoğlu A, et al. Metrnl attenuates lipid-induced inflammation and insulin resistance *Via* ampk or pparδ-dependent pathways in skeletal muscle of mice. *Exp Mol Med* (2018) 50(9):1–11. doi: 10.1038/s12276-018-0147-5

79. Malm T, Mariani M, Donovan LJ, Neilson L, Landreth GE. Activation of the nuclear receptor pparδ is neuroprotective in a transgenic mouse model of alzheimer's disease through inhibition of inflammation. *J Neuroinflamm* (2015) 12(1):7. doi: 10.1186/s12974-014-0229-9

80. Delerive P, Furman C, Teissier E, Fruchart J-C, Duriez P, Staels B. Oxidized phospholipids activate pparα in a phospholipase A2-dependent manner. *FEBS Lett* (2000) 471(1):34–8. doi: 10.1016/S0014-5793(00)01364-8

81. Wagner K-D, Wagner N. Peroxisome proliferator-activated receptor Beta/Delta (Pparβ/Δ) acts as regulator of metabolism linked to multiple cellular functions. *Pharmacol Ther* (2010) 125(3):423–35. doi: 10.1016/j.pharmthera.2009.12.001

82. Chen W, Wang L-L, Liu H-Y, Long L, Li S. Peroxisome proliferator-activated receptor Δ-agonist, Gw501516, ameliorates insulin resistance, improves dyslipidaemia in monosodium l-glutamate metabolic syndrome mice. *Basic Clin Pharmacol Toxicol* (2008) 103(3):240–6. doi: 10.1111/j.1742-7843.2008.00268.x

83. Yu B-C, Chang C-K, Ou H-Y, Cheng K-C, Cheng J-T. Decrease of peroxisome proliferator-activated receptor delta expression in cardiomyopathy of streptozotocin-induced diabetic rats. *Cardiovasc Res* (2008) 80(1):78–87. doi: 10.1093/cvr/cvn172

84. Henke BR. Peroxisome proliferator-activated receptor A/Γ dual agonists for the treatment of type 2 diabetes. *J Medicinal Chem* (2004) 47(17):4118–27. doi: 10.1021/jm030631e

85. Egerod FL, Brünner N, Svendsen JE, Oleksiewicz MB. Pparα and pparγ are Co-expressed, functional and show positive interactions in the rat urinary bladder urothelium. *J Appl Toxicol* (2010) 30(2):151–62. doi: 10.1002/jat.1481

86. Schulman IG. Nuclear receptors as drug targets for metabolic disease. *Advanced Drug Delivery Rev* (2010) 62(13):1307–15. doi: 10.1016/j.addr.2010.07.002

87. Sheu S-H, Kaya T, Waxman DJ, Vajda S. Exploring the binding site structure of the pparγ ligand-binding domain by computational solvent mapping. *Biochemistry* (2005) 44(4):1193–209. doi: 10.1021/bi048032c

88. Sauer S. Ligands for the nuclear peroxisome proliferator-activated receptor gamma. *Trends Pharmacol Sci* (2015) 36(10):688–704. doi: 10.1016/j.tips.2015.06.010

89. Poulsen LLC, Siersbæk M, Mandrup S. Ppars: Fatty acid sensors controlling metabolism. *Semin Cell Dev Biol* (2012) 23(6):631–9. doi: 10.1016/j.semcdb.2012.01.003

90. Brunmeir R, Xu F. Functional regulation of ppars through post-translational modifications. *Int J Mol Sci* (2018) 19(6):1738. doi: 10.3390/ijms19061738

91. Tzeng J, Byun J, Park JY, Yamamoto T, Schesing K, Tian B, et al. An ideal ppar response element bound to and activated by pparα. *PloS One* (2015) 10(8):e0134996. doi: 10.1371/journal.pone.0134996

92. Ahmed W, Ziouzenkova O, Brown J, Devchand P, Francis S, Kadakia M, et al. Ppars and their metabolic modulation: New mechanisms for transcriptional regulation? *J Internal Med* (2007) 262(2):184–98. doi: 10.1111/j.1365-2796.2007.01825.x

93. Nolte RT, Wisely GB, Westin S, Cobb JE, Lambert MH, Kurokawa R, et al. Ligand binding and Co-activator assembly of the peroxisome proliferator-activated receptor-Γ. *Nature* (1998) 395(6698):137–43. doi: 10.1038/25931

94. Wright MB, Bortolini M, Tadayyon M, Bopst M. Minireview: Challenges and opportunities in development of ppar agonists. *Mol Endocrinol* (2014) 28(11):1756–68. doi: 10.1210/me.2013-1427

95. Zhang X, Young HA. Ppar and immune system–what do we know? *Int Immunopharmacol* (2002) 2(8):1029–44. doi: 10.1016/S1567-5769(02)00057-7

96. Berger JP, Akiyama TE, Meinke PT. Ppars: Therapeutic targets for metabolic disease. *Trends Pharmacol Sci* (2005) 26(5):244–51. doi: 10.1016/j.tips.2005.03.003

97. Xu L, Glass CK, Rosenfeld MG. Coactivator and corepressor complexes in nuclear receptor function. *Curr Opin Genet Dev* (1999) 9(2):140–7. doi: 10.1016/S0959-437X(99)80021-5

98. Wan Y, Shang J, Graham R, Baric Ralph S, Li F. Receptor recognition by the novel coronavirus from wuhan: An analysis based on decade-long structural studies of sars coronavirus. *J Virol* (2020) 94(7):e00127–20. doi: 10.1128/JVI.00127-20

99. Hamming I, Timens W, Bulthuis MLC, Lely AT, Navis GJ, van Goor H. Tissue distribution of Ace2 protein, the functional receptor for sars coronavirus. a first step in understanding sars pathogenesis. *J Pathol* (2004) 203(2):631–7. doi: 10.1002/path.1570

100. Fu L, Wang B, Yuan T, Chen X, Ao Y, Fitzpatrick T, et al. Clinical characteristics of coronavirus disease 2019 (Covid-19) in China: A systematic review and meta-analysis. *J Infection* (2020) 80(6):656–65. doi: 10.1016/j.jinf.2020.03.041

101. Jensen S, Thomsen Allan R. Sensing of rna viruses: A review of innate immune receptors involved in recognizing rna virus invasion. *J Virol* (2012) 86(6):2900–10. doi: 10.1128/JVI.05738-11

102. Yang L, Xie X, Tu Z, Fu J, Xu D, Zhou Y. The signal pathways and treatment of cytokine storm in covid-19. *Signal Transduction Targeted Ther* (2021) 6(1):255. doi: 10.1038/s41392-021-00679-0

103. Hadjadj J, Yatim N, Barnabei L, Corneau A, Boussier J, Smith N, et al. Impaired type I interferon activity and inflammatory responses in severe covid-19 patients. *Science* (2020) 369(6504):718–24. doi: 10.1126/science.abc6027

104. Ronit A, Berg RMG, Bay JT, Haugaard AK, Ahlström MG, Burgdorf KS, et al. Compartmental immunophenotyping in covid-19 Ards: A case series. *J Allergy Clin Immunol* (2021) 147(1):81–91. doi: 10.1016/j.jaci.2020.09.009

105. Nile SH, Nile A, Qiu J, Li L, Jia X, Kai G. Covid-19: Pathogenesis, cytokine storm and therapeutic potential of interferons. *Cytokine Growth Factor Rev* (2020) 53:66–70. doi: 10.1016/j.cytogfr.2020.05.002

106. Li X, Geng M, Peng Y, Meng L, Lu S. Molecular immune pathogenesis and diagnosis of covid-19. *J Pharm Anal* (2020) 10(2):102–8. doi: 10.1016/j.jpha.2020.03.001

107. Lucas C, Wong P, Klein J, Castro TBR, Silva J, Sundaram M, et al. Longitudinal analyses reveal immunological misfiring in severe covid-19. *Nature* (2020) 584 (7821):463–9. doi: 10.1038/s41586-020-2588-y

108. Azkur AK, Akdis M, Azkur D, Sokolowska M, van de Veen W, Brüggen M-C, et al. Immune response to sars-Cov-2 and mechanisms of immunopathological changes in covid-19. *Allergy* (2020) 75(7):1564–81. doi: 10.1111/all.14364

109. Mehta P, McAuley DF, Brown M, Sanchez E, Tattersall RS, Manson JJ. Covid-19: Consider cytokine storm syndromes and immunosuppression. *Lancet* (2020) 395 (10229):1033–4. doi: 10.1016/S0140-6736(20)30628-0

110. Henderson LA, Canna SW, Schulert GS, Volpi S, Lee PY, Kernan KF, et al. On the alert for cytokine storm: Immunopathology in covid-19. *Arthritis Rheumatol* (2020) 72(7):1059–63. doi: 10.1002/art.41285

111. Rothan HA, Byrareddy SN. The epidemiology and pathogenesis of coronavirus disease (Covid-19) outbreak. *J Autoimmun* (2020) 109:102433. doi: 10.1016/j.jaut.2020.102433

112. Han H, Ma Q, Li C, Liu R, Zhao L, Wang W, et al. Profiling serum cytokines in covid-19 patients reveals il-6 and il-10 are disease severity predictors. *Emerging Microbes Infections* (2020) 9(1):1123–30. doi: 10.1080/22221751.2020.1770129

113. Liu Y, Zhang C, Huang F, Yang Y, Wang F, Yuan J, et al. Elevated plasma levels of selective cytokines in covid-19 patients reflect viral load and lung injury. *Natl Sci Rev* (2020) 7(6):1003–11. doi: 10.1093/nsr/nwaa037

114. Xu Z-S, Shu T, Kang L, Wu D, Zhou X, Liao B-W, et al. Temporal profiling of plasma cytokines, chemokines and growth factors from mild, severe and fatal covid-19 patients. *Signal Transduction Targeted Ther* (2020) 5(1):100. doi: 10.1038/s41392-020-0211-1

115. Huang C, Wang Y, Li X, Ren L, Zhao J, Hu Y, et al. Clinical features of patients infected with 2019 novel coronavirus in wuhan, China. *Lancet* (2020) 395(10223):497–506. doi: 10.1016/S0140-6736(20)30183-5

116. Chinetti G, Fruchart JC, Staels B. Peroxisome proliferator-activated receptors and inflammation: From basic science to clinical applications. *Int J Obes* (2003) 27(3): S41–S5. doi: 10.1038/sj.ijo.0802499

117. Martin H. Role of ppar-gamma in inflammation. prospects for therapeutic intervention by food components. *Mutat Research/Fundamental Mol Mech Mutagenesis* (2009) 669(1):1–7. doi: 10.1016/j.mrfmmm.2009.06.009

118. Delayre-Orthez C, Becker J, Guenon I, Lagente V, Auwerx J, Frossard N, et al. Pparα downregulates airway inflammation induced by lipopolysaccharide in the mouse. *Respir Res* (2005) 6(1):91. doi: 10.1186/1465-9921-6-91

119. Heming M, Gran S, Jauch S-L, Fischer-Riepe L, Russo A, Klotz L, et al. Peroxisome proliferator-activated receptor-Γ modulates the response of macrophages to lipopolysaccharide and glucocorticoids. *Front Immunol* (2018) 9:893. doi: 10.3389/fimmu.2018.00893

120. Huang S, Goplen NP, Zhu B, Cheon IS, Son Y, Wang Z, et al. Macrophage ppar-Γ suppresses long-term lung fibrotic sequelae following acute influenza infection. *PloS One* (2019) 14(10):e0223430. doi: 10.1371/journal.pone.0223430

121. Kaplan J, Nowell M, Chima R, Zingarelli B. Pioglitazone reduces inflammation through inhibition of nf-Kb in polymicrobial sepsis. *Innate Immun* (2013) 20(5):519–28. doi: 10.1177/1753425913501565

122. Huang W, Rha GB, Han M-J, Eum SY, András IE, Zhong Y, et al. Pparα and pparγ effectively protect against hiv-induced inflammatory responses in brain endothelial cells. *J Neurochem* (2008) 107(2):497–509. doi: 10.1111/j.1471-4159.2008.05626.x

123. Neri T, Armani C, Pegoli A, Cordazzo C, Carmazzi Y, Brunelleschi S, et al. Role of nf-Kb and ppar-Γ in lung inflammation induced by monocyte-derived microparticles. *Eur Respir J* (2011) 37(6):1494–502. doi: 10.1183/09031936.00023310

124. Kamei Y, Xu L, Heinzel T, Torchia J, Kurokawa R, Gloss B, et al. A cbp integrator complex mediates transcriptional activation and ap-1 inhibition by nuclear receptors. *Cell* (1996) 85(3):403–14. doi: 10.1016/S0092-8674(00)81118-6

125. Delerive P, De Bosscher K, Besnard S, Vanden Berghe W, Peters JM, Gonzalez FJ, et al. Peroxisome proliferator-activated receptor A negatively regulates the vascular inflammatory gene response by negative cross-talk with transcription factors nf-Kb and ap-1. *J Biol Chem* (1999) 274(45):32048–54. doi: 10.1074/jbc.274.45.32048

126. Vanden Berghe W, Vermeulen L, Delerive P, De Bosscher K, Staels B, Haegeman G. A paradigm for gene regulation: Inflammation, nf-Kb and ppar. In: *Peroxisomal disorders and regulation of genes*. Boston, MA: Springer US (2003).

127. Kleemann R, Verschuren L, de Rooij B-J, Lindeman J, de Maat MM, Szalai AJ, et al. Evidence for anti-inflammatory activity of statins and pparα activators in human c-reactive protein transgenic mice in vivo and in cultured human hepatocytes in vitro. *Blood* (2004) 103(11):4188–94. doi: 10.1182/blood-2003-11-3791

128. Desreumaux P, Dubuquoy L, Nutten S, Peuchmaur M, Englaro W, Schoonjans K, et al. Attenuation of colon inflammation through activators of the retinoid X receptor (Rxr)/Peroxisome proliferator–activated receptor Γ (Pparγ) heterodimer: A basis for new therapeutic strategies. *J Exp Med* (2001) 193(7):827–38. doi: 10.1084/jem.193.7.827

129. Goetze S, Kintscher U, Kim S, Meehan WP, Kaneshiro K, Collins AR, et al. Peroxisome proliferator–activated receptor-Γ ligands inhibit nuclear but not cytosolic extracellular signal–regulated Kinase/Mitogen–activated protein kinase–regulated steps in vascular smooth muscle cell migration. *J Cardiovasc Pharmacol* (2001) 38(6):909–21. doi: 10.1097/00005344-200112000-00013

130. Ghisletti S, Huang W, Ogawa S, Pascual G, Lin M-E, Willson TM, et al. Parallel sumoylation-dependent pathways mediate gene- and signal-specific transrepression by lxrs and pparγ. *Mol Cell* (2007) 25(1):57–70. doi: 10.1016/j.molcel.2006.11.022

131. Pascual G, Fong AL, Ogawa S, Gamliel A, Li AC, Perissi V, et al. A sumoylation-dependent pathway mediates transrepression of inflammatory response genes by ppar-Γ. *Nature* (2005) 437(7059):759–63. doi: 10.1038/nature03988

132. Ferreira AE, Sisti F, Sônego F, Wang S, Filgueiras LR, Brandt S, et al. Ppar-Γ/Il-10 axis inhibits Myd88 expression and ameliorates murine polymicrobial sepsis. *J Immunol* (2014) 192(5):2357–65. doi: 10.4049/jimmunol.1302375

133. Xu Z, Wang G, Zhu Y, Liu R, Song J, Ni Y, et al. Ppar-Γ agonist ameliorates liver pathology accompanied by increasing regulatory b and T cells in high-Fat-Diet mice. *Obesity* (2017) 25(3):581–90. doi: 10.1002/oby.21769

134. Are A, Aronsson L, Wang S, Greicius G, Lee YK, Gustafsson J-Å, et al. Enterococcus faecalis from newborn babies regulate endogenous pparγ activity and il-10 levels in colonic epithelial cells. *Proc Natl Acad Sci* (2008) 105(6):1943–8. doi: 10.1073/pnas.0711734105

135. Marx N, Sukhova GK, Collins T, Libby P, Plutzky J. Pparα activators inhibit cytokine-induced vascular cell adhesion molecule-1 expression in human endothelial cells. *Circulation* (1999) 99(24):3125–31. doi: 10.1161/01.CIR.99.24.3125

136. Kurebayashi S, Xu X, Ishii S, Shiraishi M, Kouhara H, Kasayama S. A novel thiazolidinedione mcc-555 down-regulates tumor necrosis factor-A-Induced expression of vascular cell adhesion molecule-1 in vascular endothelial cells. *Atherosclerosis* (2005) 182(1):71–7. doi: 10.1016/j.atherosclerosis.2005.02.004

137. Ahmed W, Orasanu G, Nehra V, Asatryan L, Rader DJ, Ziouzenkova O, et al. High-density lipoprotein hydrolysis by endothelial lipase activates pparα. *Circ Res* (2006) 98(4):490–8. doi: 10.1161/01.RES.0000205846.46812.be

138. Ogawa S, Lozach J, Benner C, Pascual G, Tangirala RK, Westin S, et al. Molecular determinants of crosstalk between nuclear receptors and toll-like receptors. *Cell* (2005) 122(5):707–21. doi: 10.1016/j.cell.2005.06.029

139. Lee JW, Bajwa PJ, Carson MJ, Jeske DR, Cong Y, Elson CO, et al. Fenofibrate represses interleukin-17 and interferon-Γ expression and improves colitis in Interleukin-10–deficient mice. *Gastroenterology* (2007) 133(1):108–23. doi: 10.1053/j.gastro.2007.03.113

140. Prasad K, AlOmar SY, Almuqri EA, Rudayni HA, Kumar V. Genomics-guided identification of potential modulators of sars-Cov-2 entry proteases, Tmprss2 and cathepsins B/L. *PloS One* (2021) 16(8):e0256141. doi: 10.1371/journal.pone.0256141

141. Desterke C, Turhan AG, Bennaceur-Griscelli A, Griscelli F. Hla-dependent heterogeneity and macrophage immunoproteasome activation during lung covid-19 disease. *J Trans Med* (2021) 19(1):290. doi: 10.1186/s12967-021-02965-5

142. Jackson H, Rivero Calle I, Broderick C, Habgood-Coote D, D'Souza G, Nichols S, et al. Characterisation of the blood rna host response underpinning severity in covid-19 patients. *Sci Rep* (2022) 12(1):12216. doi: 10.1038/s41598-022-15547-2

143. Vlasov I, Panteleeva A, Usenko T, Nikolaev M, Izumchenko A, Gavrilova E, et al. Transcriptomic profiles reveal downregulation of low-density lipoprotein particle receptor pathway activity in patients surviving severe covid-19. *Cells* (2021) 10 (12):3495. doi: 10.3390/cells10123495

144. Nain Z, Barman SK, Sheam MM, Syed SB, Samad A, Quinn JMW, et al. Transcriptomic studies revealed pathophysiological impact of covid-19 to predominant health conditions. *Briefings Bioinf* (2021) 22(6):bbab197. doi: 10.1093/bib/bbab197

145. Desterke C, Turhan AG, Bennaceur-Griscelli A, Griscelli F. Pparγ cistrome repression during activation of lung monocyte-macrophages in severe covid-19. *iScience* (2020) 23(10):101611. doi: 10.1016/j.isci.2020.101611

146. Costanzo M, Caterino M, Fedele R, Cevenini A, Pontillo M, Barra L, et al. Covidomics: The proteomic and metabolomic signatures of covid-19. *Int J Mol Sci* (2022) 23(5):2414. doi: 10.3390/ijms23052414

147. Yang J, Chen C, Chen W, Huang L, Fu Z, Ye K, et al. Proteomics and metabonomics analyses of covid-19 complications in patients with pulmonary fibrosis. *Sci Rep* (2021) 11(1):14601. doi: 10.1038/s41598-021-94256-8

148. Keikha R, Hashemi-Shahri SM, Jebali A. The mirna neuroinflammatory biomarkers in covid-19 patients with different severity of illness. *Neurología* (2021). doi: 10.1016/j.nrl.2021.06.005

149. Batiha GE-S, Gari A, Elshony N, Shaheen HM, Abubakar MB, Adeyemi SB, et al. Hypertension and its management in covid-19 patients: The assorted view. *Int J Cardiol Cardiovasc Risk Prev* (2021) 11:200121. doi: 10.1016/j.ijcrp.2021.200121

150. Alkhayyat SS, Al-kuraishy HM, Al-Gareeb AI, El-Bouseary MM, AboKamer AM, Batiha GE-S, et al. Fenofibrate for covid-19 and related complications as an approach to improve treatment outcomes: The missed key for holy grail. *Inflammation Res* (2022) 71:1159–67. doi: 10.1007/s00011-022-01615-w

151. Jha NK, Sharma C, Hashiesh HM, Arunachalam S, Meeran MN, Javed H, et al. B-caryophyllene, a natural dietary Cb2 receptor selective cannabinoid can be a candidate to target the trinity of infection, immunity, and inflammation in covid-19. *Front Pharmacol* (2021) 12:590201. doi: 10.3389/fphar.2021.590201

152. O'Carroll SM, O'Neill LAJ. Targeting immunometabolism to treat covid-19. *Immunother Adv* (2021) 1(1). doi: 10.1093/immadv/ltab013

153. Ghasemnejad-Berenji M. Immunomodulatory and anti-inflammatory potential of crocin in covid-19 treatment. *J Food Biochem* (2021) 45(5):e13718. doi: 10.1111/jfbc.13718

154. Ayres JS. A metabolic handbook for the covid-19 pandemic. *Nat Metab* (2020) 2(7):572–85. doi: 10.1038/s42255-020-0237-2

155. Mahmudpour M, Vahdat K, Keshavarz M, Nabipour I. The covid-19-Diabetes mellitus molecular tetrahedron. *Mol Biol Rep* (2022) 49(5):4013–24. doi: 10.1007/s11033-021-07109-y

156. Vallée A, Lecarpentier Y, Vallée J-N. Interplay of opposing effects of the Wnt/B;-catenin pathway and pparγ and implications for sars-Cov2 treatment. *Front Immunol* (2021) 12:666693. doi: 10.3389/fimmu.2021.666693

157. Francisqueti-Ferron FV, Garcia JL, Ferron AJT, Nakandakare- Maia ET, Gregolin CS, JPdC S, et al. Gamma-oryzanol as a potential modulator of oxidative stress and inflammation *Via* ppar-y in adipose tissue: A hypothetical therapeutic for cytokine storm in covid-19? *Mol Cell Endocrinol* (2021) 520:111095. doi: 10.1016/j.mce.2020.111095

158. Huang W, Zhou H, Hodgkinson C, Montero A, Goldman D, Chang SL. Network meta-analysis on the mechanisms underlying alcohol augmentation of covid-19 pathologies. *Alcohol Clin Exp Res* (2021) 45(4):675–88. doi: 10.1111/acer.14573

159. Adir Y, Saliba W, Beurnier A, Humbert M. Asthma and covid-19: An update. *Eur Respir Rev* (2021) 30(162):210152. doi: 10.1183/16000617.0152-2021

160. Ramakrishnan RK, Al Heialy S, Hamid Q. Implications of preexisting asthma on covid-19 pathogenesis. *Am J Physiol-Lung Cell Mol Physiol* (2021) 320(5):L880–L91. doi: 10.1152/ajplung.00547.2020

161. Farruggia C, Kim M-B, Bae M, Lee Y, Pham TX, Yang Y, et al. Astaxanthin exerts anti-inflammatory and antioxidant effects in macrophages in Nrf2-dependent and independent manners. *J Nutr Biochem* (2018) 62:202–9. doi: 10.1016/j.jnutbio.2018.09.005

162. Steinman JB, Lum FM, Ho PP-K, Kaminski N, Steinman L. Reduced development of covid-19 in children reveals molecular checkpoints gating pathogenesis illuminating potential therapeutics. *Proc Natl Acad Sci* (2020) 117 (40):24620–6. doi: 10.1073/pnas.2012358117

163. Ferastraoaru D, Hudes G, Jerschow E, Jariwala S, Karagic M, de Vos G, et al. Eosinophilia in asthma patients is protective against severe covid-19 illness. *J Allergy Clin Immunol: In Pract* (2021) 9(3):1152–62.e3. doi: 10.1016/j.jaip.2020.12.045

164. Franceschini L, Macchiarelli R, Rentini S, Biviano I, Farsi A. Eosinophilic esophagitis: Is the Th2 inflammation protective against the severe form of covid-19? *Eur J Gastroenterol Hepatol* (2020) 32(12):1583. doi: 10.1097/meg.0000000000001909

165. Kostadinova R, Wahli W, Michalik L. Ppars in diseases: Control mechanisms of inflammation. *Curr Medicinal Chem* (2005) 12(25):2995–3009. doi: 10.2174/092986705774462905

166. Saubermann LJ, Nakajima A, Wada K, Zhao S, Terauchi Y, Kadowaki T, et al. Peroxisome proliferator-activated receptor gamma agonist ligands stimulate a Th2 cytokine response and prevent acute colitis. *Inflammatory Bowel Dis* (2002) 8(5):330–9. doi: 10.1097/00054725-200209000-00004

167. Chen T, Tibbitt CA, Feng X, Stark JM, Rohrbeck L, Rausch L, et al. Ppar-Γ promotes type 2 immune responses in allergy and nematode infection. *Sci Immunol* (2017) 2(9):eaal5196. doi: 10.1126/sciimmunol.aal5196

168. Jiang Y, Zhao T, Zhou X, Xiang Y, Gutierrez-Castrellon P, Ma X. Inflammatory pathways in covid-19: Mechanism and therapeutic interventions. *MedComm* (2022) 3 (3):e154. doi: 10.1002/mco2.154

169. Mukherjee JJ, Gangopadhyay KK, Ray S. Management of diabetes in patients with covid-19. *Lancet Diabetes Endocrinol* (2020) 8(8):666. doi: 10.1016/S2213-8587(20)30226-6

170. Shirazi J, Donzanti MJ, Nelson KM, Zurakowski R, Fromen CA, Gleghorn JP. Significant unresolved questions and opportunities for bioengineering in understanding and treating covid-19 disease progression. *Cell Mol Bioengineering* (2020) 13(4):259–84. doi: 10.1007/s12195-020-00637-w

171. Kheirollahi V, Wasnick RM, Biasin V, Vazquez-Armendariz AI, Chu X, Moiseenko A, et al. Metformin induces lipogenic differentiation in myofibroblasts to reverse lung fibrosis. *Nat Commun* (2019) 10(1):2987. doi: 10.1038/s41467-019-10839-0

172. Bargagli E, Refini RM, d'Alessandro M, Bergantini L, Cameli P, Vantaggiato L, et al. Metabolic dysregulation in idiopathic pulmonary fibrosis. *Int J Mol Sci* (2020) 21 (16):5663. doi: 10.3390/ijms21165663

173. Landi C, Bargagli E, Carleo A, Bianchi L, Gagliardi A, Prasse A, et al. A system biology study of balf from patients affected by idiopathic pulmonary fibrosis (Ipf) and healthy controls. *Proteomics – Clin Appl* (2014) 8(11-12):932–50. doi: 10.1002/prca.201400001

174. Ahmed DS, Isnard S, Berini C, Lin J, Routy J-P, Royston L. Coping with stress: The mitokine gdf-15 as a biomarker of covid-19 severity. *Front Immunol* (2022) 13:820350. doi: 10.3389/fimmu.2022.820350

175. Batabyal R, Freishtat N, Hill E, Rehman M, Freishtat R, Koutroulis I. Metabolic dysfunction and immunometabolism in covid-19 pathophysiology and therapeutics. *Int J Obes* (2021) 45(6):1163–9. doi: 10.1038/s41366-021-00804-7

176. AbdelMassih AF, Menshawey R, Ismail JH, Husseiny RJ, Husseiny YM, Yacoub S, et al. Ppar agonists as effective adjuvants for covid-19 vaccines, by modifying immunogenetics: A review of literature. *J Genet Eng Biotechnol* (2021) 19 (1):82. doi: 10.1186/s43141-021-00179-2

177. Li Z, Peng M, Chen P, Liu C, Hu A, Zhang Y, et al. Imatinib and methazolamide ameliorate covid-19-Induced metabolic complications *Via* elevating Ace2 enzymatic activity and inhibiting viral entry. *Cell Metab* (2022) 34(3):424–40.e7. doi: 10.1016/j.cmet.2022.01.008

178. AbdelMassih A, El Shershaby M, Gaber H, Habib M, Gamal N, Husseiny R, et al. Should we vaccinate the better seroconverters or the most vulnerable? game changing insights for covid-19 vaccine prioritization policies. *Egyptian Pediatr Assoc Gazette* (2021) 69(1):39. doi: 10.1186/s43054-021-00086-8

179. Lumeng CN, Liu J, Geletka L, Delaney C, Delproposto J, Desai A, et al. Aging is associated with an increase in T cells and inflammatory macrophages in visceral adipose tissue. *J Immunol* (2011) 187(12):6208–16. doi: 10.4049/jimmunol.1102188

180. Caza T, Landas S. Functional and phenotypic plasticity of Cd4+ T cell subsets. *BioMed Res Int* (2015) 2015:521957. doi: 10.1155/2015/521957

181. Meftahi GH, Jangravi Z, Sahraei H, Bahari Z. The possible pathophysiology mechanism of cytokine storm in elderly adults with covid-19 infection: The contribution of "Inflame-aging". *Inflammation Res* (2020) 69(9):825–39. doi: 10.1007/s00011-020-01372-8

182. Durmuş S, Çakır T, Özgür A, Guthke R. A review on computational systems biology of pathogen–host interactions. *Front Microbiol* (2015) 6:235. doi: 10.3389/fmicb.2015.00235

183. Oh KK, Adnan M, Cho DH. Network pharmacology approach to decipher signaling pathways associated with target proteins of nsaids against covid-19. *Sci Rep* (2021) 11(1):9606. doi: 10.1038/s41598-021-88313-5

184. Afroz S, Fairuz S, Joty JA, Uddin MN, Rahman MA. Virtual screening of functional foods and dissecting their roles in modulating gene functions to support post covid-19 complications. *J Food Biochem* (2021) 45(12):e13961. doi: 10.1111/jfbc.13961

185. Li H, You J, Yang X, Wei Y, Zheng L, Zhao Y, et al. Glycyrrhetinic acid: A potential drug for the treatment of covid-19 cytokine storm. *Phytomedicine* (2022) 102:154153. doi: 10.1016/j.phymed.2022.154153

186. Shirazi FM, Banerji S, Nakhaee S, Mehrpour O. Effect of angiotensin ii blockers on the prognosis of covid-19: A toxicological view. *Eur J Clin Microbiol Infect Dis* (2020) 39(10):2001–2. doi: 10.1007/s10096-020-03932-6

187. Fernández-Quintela A, Milton-Laskibar I, Trepiana J, Gómez-Zorita S, Kajarabille N, Léniz A, et al. Key aspects in nutritional management of covid-19 patients. *J Clin Med* (2020) 9(8):2589. doi: 10.3390/jcm9082589

188. Di Renzo L, Gualtieri P, Pivari F, Soldati L, Attinà A, Leggeri C, et al. Covid-19: Is there a role for immunonutrition in obese patient? *J Trans Med* (2020) 18(1):415. doi: 10.1186/s12967-020-02594-4

189. Ghaffari S, Roshanravan N, Tutunchi H, Ostadrahimi A, Pouraghaei M, Kafil B. Oleoylethanolamide, a bioactive lipid amide, as a promising treatment strategy for Coronavirus/Covid-19. *Arch Med Res* (2020) 51(5):464–7. doi: 10.1016/j.arcmed.2020.04.006

190. Akbari N, Ostadrahimi A, Tutunchi H, Pourmoradian S, Farrin N, Najafipour F, et al. Possible therapeutic effects of boron citrate and oleoylethanolamide supplementation in patients with covid-19: A pilot randomized, double-blind, clinical trial. *J Trace Elements Med Biol* (2022) 71:126945. doi: 10.1016/j.jtemb.2022.126945

191. Talukdar J, Bhadra B, Dattaroy T, Nagle V, Dasgupta S. Potential of natural astaxanthin in alleviating the risk of cytokine storm in covid-19. *Biomed Pharmacother* (2020) 132:110886. doi: 10.1016/j.biopha.2020.110886

192. Petersen KF, Krssak M, Inzucchi S, Cline GW, Dufour S, Shulman GI. Mechanism of troglitazone action in type 2 diabetes. *Diabetes* (2000) 49(5):827–31. doi: 10.2337/diabetes.49.5.827

193. Carboni E, Carta AR, Carboni E. Can pioglitazone be potentially useful therapeutically in treating patients with covid-19? *Med Hypotheses* (2020) 140:109776. doi: 10.1016/j.mehy.2020.109776

194. Wu C, Liu Y, Yang Y, Zhang P, Zhong W, Wang Y, et al. Analysis of therapeutic targets for sars-Cov-2 and discovery of potential drugs by computational methods. *Acta Pharm Sin B* (2020) 10(5):766–88. doi: 10.1016/j.apsb.2020.02.008

195. Esposito G, Pesce M, Seguella L, Sanseverino W, Lu J, Corpetti C, et al. The potential of cannabidiol in the covid-19 pandemic. *Br J Pharmacol* (2020) 177 (21):4967–70. doi: 10.1111/bph.15157

196. Oyagbemi AA, Ajibade TO, Aboua YG, Gbadamosi IT, Adedapo ADA, Aro AO, et al. Potential health benefits of zinc supplementation for the management of covid-19 pandemic. *J Food Biochem* (2021) 45(2):e13604. doi: 10.1111/jfbc.13604

197. Belvisi MG, Mitchell JA. Targeting ppar receptors in the airway for the treatment of inflammatory lung disease. *Br J Pharmacol* (2009) 158(4):994–1003. doi: 10.1111/j.1476-5381.2009.00373.x

198. Choi C-I. Astaxanthin as a peroxisome proliferator-activated receptor (Ppar) modulator: Its therapeutic implications. *Mar Drugs* (2019) 17(4):242. doi: 10.3390/md17040242

199. Inoue M, Tanabe H, Matsumoto A, Takagi M, Umegaki K, Amagaya S, et al. Astaxanthin functions differently as a selective peroxisome proliferator-activated receptor Γ modulator in adipocytes and macrophages. *Biochem Pharmacol* (2012) 84 (5):692–700. doi: 10.1016/j.bcp.2012.05.021

200. Cheang WS, Tian XY, Wong WT, Huang Y. The peroxisome proliferator-activated receptors in cardiovascular diseases: Experimental benefits and clinical challenges. *Br J Pharmacol* (2015) 172(23):5512–22. doi: 10.1111/bph.13029

frontiers | Frontiers in Immunology

TYPE Review
PUBLISHED 20 March 2023
DOI 10.3389/fimmu.2023.1117548

OPEN ACCESS

EDITED BY
Melanie Albrecht,
Paul-Ehrlich-Institut (PEI), Germany

REVIEWED BY
Sonja Rittchen,
Medical University of Graz, Austria
Thomas Bärnthaler,
Medical University of Graz, Austria

*CORRESPONDENCE
Hong Fan
fanhongfan@qq.com
Xiang Tong
tongxiangscu@sina.com

†These authors have contributed equally to this work and share first authorship

SPECIALTY SECTION
This article was submitted to Inflammation, a section of the journal Frontiers in Immunology

RECEIVED 06 December 2022
ACCEPTED 03 March 2023
PUBLISHED 20 March 2023

CITATION
Wang L, Wang D, Zhang T, Ma Y, Tong X and Fan H (2023) The role of immunometabolism in macrophage polarization and its impact on acute lung injury/acute respiratory distress syndrome. *Front. Immunol.* 14:1117548. doi: 10.3389/fimmu.2023.1117548

The role of immunometabolism in macrophage polarization and its impact on acute lung injury/acute respiratory distress syndrome

Lian Wang[1†], Dongguang Wang[1†], Tianli Zhang[1], Yao Ma[2], Xiang Tong[1*] and Hong Fan[1*]

[1]Department of Respiratory and Critical Care Medicine, West China Hospital, Sichuan University, Chengdu, China, [2]Department of Geriatrics and National Clinical Research Center for Geriatrics, West China Hospital, Sichuan University, Chengdu, China

Lung macrophages constitute the first line of defense against airborne particles and microbes and are key to maintaining pulmonary immune homeostasis. There is increasing evidence suggesting that macrophages also participate in the pathogenesis of acute lung injury (ALI)/acute respiratory distress syndrome (ARDS), including the modulation of inflammatory responses and the repair of damaged lung tissues. The diversity of their functions may be attributed to their polarized states. Classically activated or inflammatory (M1) macrophages and alternatively activated or anti-inflammatory (M2) macrophages are the two main polarized macrophage phenotypes. The precise regulatory mechanism of macrophage polarization is a complex process that is not completely understood. A growing body of literature on immunometabolism has demonstrated the essential role of immunometabolism and its metabolic intermediates in macrophage polarization. In this review, we summarize macrophage polarization phenotypes, the role of immunometabolism, and its metabolic intermediates in macrophage polarization and ALI/ARDS, which may represent a new target and therapeutic direction.

KEYWORDS

macrophage polarization, polarization regulation, immunometabolism, metabolic reprogramming, acute lung injury, acute respiratory distress syndrome

1 Introduction

Acute lung injury (ALI) is a common and critical disease caused by a variety of direct or indirect factors, including severe infection, pancreatitis, shock, trauma, major surgery, and ischemia–reperfusion (1–3). ALI usually leads to acute respiratory distress syndrome (ARDS), a more severe clinical manifestation, and the terminal pathophysiological characteristics are remarkably similar. ALI/ARDS is characterized by excessive and

uncontrolled inflammatory responses to lung injury, leading to generalized epithelial and endothelial barrier injury, alveolar-capillary membrane dysfunction, increased vascular permeability, alveolar hemorrhage, and diffuse alveolar damage (3–7). The clinical manifestations include severe hypoxemia, diffuse bilateral pulmonary infiltration, and pulmonary edema (8). ALI is associated with high morbidity and poor prognosis, with an age-adjusted incidence of 86.2/100,000, a mortality rate of 38.5%, and persistent pulmonary dysfunction in 50% of survivors (9, 10). Currently, there is no effective therapy to reduce mortality or improve the prognosis of patients with ALI/ARDS. Hence, researching the pathogenesis and identifying the signaling pathways of ALI/ARDS could help provide novel targets for therapeutic intervention.

Macrophages play a significant role in innate immunity by serving as heterologous phagocytes and by expressing pattern recognition receptors (11). Lung macrophages constitute the first line of defense against airborne particles and microbes and are key to maintaining pulmonary immune homeostasis (11). There is increasing evidence suggesting that macrophages also participate in the pathogenesis of ALI/ARDS, including the modulation of inflammatory responses and the repair of damaged lung tissues (12, 13). During the development of the inflammatory response, macrophages exert a pro-inflammatory effect in the early stages and play an anti-inflammatory role in the later stages. The diversity of their functions may be attributed to their polarized phenotypes; however, the precise regulatory mechanisms of macrophage polarization remain incompletely understood and involve a range of signaling pathways and transcriptional and post-transcriptional regulatory networks (13–16). Phenotypic and functional changes in macrophages are accompanied by dramatic shifts in cell metabolism, an emerging research field termed immunometabolism, also known as metabolic reprogramming. Pro-inflammatory polarization of macrophages is associated with increased glycolysis and a shift toward the pentose phosphate pathway (PPP) and fatty acid synthesis (17–19). However, anti-inflammatory macrophages primarily use oxidative phosphorylation (OXPHOS), glutamine metabolism, and fatty acid oxidation (FAO) (19, 20). Moreover, pro- and anti-inflammatory macrophages are characterized by specific pathways that regulate lipid and amino acid metabolism and affect their responses (18). These metabolic adaptations are necessary to support macrophage activity and maintain polarization in specific contexts. The regulation of immune metabolism to affect macrophage polarization may be a novel direction for the treatment of ALI. In this review, we summarize macrophage polarization phenotypes, the role of immunometabolism in macrophage polarization, and its impact on ALI/ARDS.

2 Macrophage subsets

Macrophages are a major group of innate immune cells, which exist in various tissues with significant heterogeneity and phenotypic specialization (21). They are regulated in a tissue-specific manner and play a significant role in phagocytosis and digestion of pathogens and infected and apoptotic cells and can recruit and regulate other immune cells and inflammatory responses and assist in tissue repair (22). Pulmonary macrophages contain two different macrophage subsets based on anatomical location: alveolar macrophages (AMs) and interstitial macrophages (IMs). AMs are the most abundant population in pulmonary macrophages, which exist in the alveolar cavity and are directly exposed to the air and the environment and constitute the first line of defense against airborne particles and microbes (22, 23). AMs include tissue-resident alveolar macrophages (TR-AMs) and monocyte-derived alveolar macrophages (Mo-AMs). TR-AMs are derived from yolk sac-derived erythromyeloid progenitors and fetal liver monocytes, which can proliferate at a steady state to maintain self-renewal, and GM-CSF and TGF-β play an important role in this process (24–27). However, more macrophages are needed in acute inflammatory responses. When infection or injury occurs, monocytes are rapidly recruited into the alveolar cavity and develop into Mo-AMs to promote the inflammatory response and eliminate pathogens (28–30). Mo-AMs exhibit strong accumulation during early inflammation, followed by a gradual decline in their numbers, which undergo Fas-mediated cell death and local phagocytic clearance (28). A small fraction of Mo-AMs persist after infection and become phenotypically and functionally similar to TR-AMs. However, TR-AMs still survive and persist during the resolution of inflammation (28). IMs are located in the parenchyma between the microvascular endothelium and alveolar epithelium and comprise 30%-40% of lung macrophages (22, 31). IMs are initially derived from yolk sac macrophages and fetal liver monocytes and then replenished by circulating progenitor cells for their maintenance in adults (22, 32). IMs are involved in tissue remodeling and maintenance of lung homeostasis and antigen presentation as well as affect dendritic cell function to prevent airway allergy (33–35).

3 Polarization phenotype and polarization regulation

3.1 Polarization phenotype and plasticity

Macrophage polarization refers to the activation of macrophages under the stimulation of a variety of factors and their differentiation into different phenotypes according to the state and changes in the microenvironment (14, 36). AMs have two main macrophage phenotypes: classically activated or inflammatory (M1) macrophages and alternatively activated or anti-inflammatory (M2) macrophages (37, 38). The regulatory mechanisms and functional characteristics of M1/M2 macrophages are shown in Figure 1. M1 macrophages constitute the first line of defense against intracellular pathogens (36). Currently, it is believed that M1 macrophages are mainly induced by lipopolysaccharide (LPS), interferon-γ (IFN-γ), and granulocyte–macrophage colony-stimulating factor (GM-CSF) (38, 39). M1 macrophages can guide acute inflammatory responses and produce a large number of pro-inflammatory cytokines such as IL-1β, inducible nitric oxide synthase (iNOS), tumor necrosis factor-α (TNF-α), IL-1, IL-6, IL-12, CCL8, IL-23, CXCL1-3, CXCL-5, CXCL8-10, monocyte chemotactic protein-1 (MCP-1),

10.3389/fimmu.2023.1117548

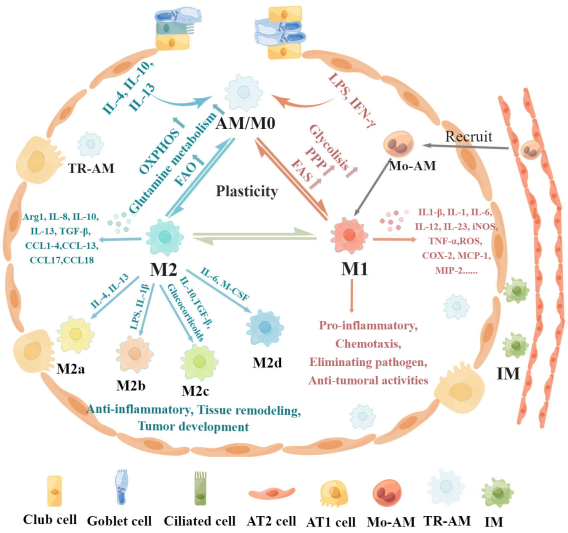

FIGURE 1
Regulatory mechanisms and functional characteristics of macrophage polarization. Non-polarized M0 macrophages can be polarized into M1 macrophages stimulated by LPS, IFN-γ, and GM-CSF, which are associated with increased glycolysis, PPP, and FAS. In addition, M0 macrophages can be polarized into M2 macrophages in the presence of IL-4, IL-13, IL-10, and M-CSF, which is related to increased OXPHOS, FAO, and glutamine metabolism. Furthermore, these polarized macrophages exhibit plasticity, as they can depolarize to M0 macrophages or exhibit the opposite phenotype through repolarization, which depends on the specific microenvironment. M1 macrophages produce pro-inflammatory cytokines such as IL-1β, iNOS, TNF-α, IL-1, IL-6, IL-12, IL-23, CCL8, CXCL1-3, CXCL-5, CXCL8-10, MCP-1, MIP-2, ROS, and COX-2, leading to pro-inflammatory responses, chemotaxis, pathogenic microorganism elimination, and antitumoral activities. M2 macrophages can be further divided into four subsets, M2a, M2b, M2c, and M2d, according to the different activating stimuli received. M2 macrophages secrete anti-inflammatory cytokines such as IL-8, IL-10, IL-13, CCL1, CCL2, CCL3, CCL4, CCL13, CCL14, CCL17, CCL18, CCL22, CCL23, CCL24, and CCL26 to exert anti-inflammatory effects, promote tissue remodeling, facilitate tumor development, and remove parasites.

macrophage inflammatory protein 2 (MIP-2), reactive oxygen species (ROS), and cyclooxygenase 2 (COX-2) (16, 38, 40–42). M1 macrophages mainly induce Th1 response activation, exert antigen-presenting functions, and engage in pro-inflammatory responses, chemotaxis, radical formation, elimination of pathogenic microorganisms, and antitumoral activities (37, 43).

Conversely, M2 macrophages are induced in response to Th2 cytokines such as macrophage colony-stimulating factor (M-CSF), IL-4, IL-13, and IL-10 (43–45). M2 macrophages mainly express CD64 and CD209 and produce anti-inflammatory cytokines such as IL-8, IL-10, IL-13, CCL1, CCL2, CCL3, CCL4, CCL13, CCL14, CCL17, CCL18, CCL22, CCL23, CCL24, and CCL26 to exert anti-inflammatory effects, promote tissue remodeling, facilitate tumor development, and remove parasites (14, 43, 46–48). M2 macrophages can be further divided into four subsets, M2a, M2b, M2c, and M2d, according to the different activating stimuli received (41, 49). The M2a subset of macrophages can be stimulated by IL-4 or IL-13 to produce IL-10, CCL13, CCL17, and CCL22 (36, 49). These chemokines are associated with Th2 cell activation and can promote eosinophil recruitment to the lungs (50, 51). The M2b subset can be stimulated by LPS or IL-1β and produce pro-inflammatory cytokines (36, 49). The M2c subset is induced by IL-10, TGF-β, and glucocorticoids and releases high amounts of IL-10, CCL18, and CCL16 to exhibit anti-inflammatory activities (49, 52, 53). The M2d subset is induced by IL-6 and M-CSF and secretes high IL-10 and low IL-12 and TGF-β cytokine production and CXCL10, CXCL16, and CCL5 chemokines to promote angiogenesis and tumor metastasis (54, 55).

These polarized macrophages exhibit plasticity, as they can depolarize to M0 macrophages or exhibit the opposite phenotype through repolarization, which depends on the specific microenvironment (4, 43). For instance, a high αKG/succinate ratio further promotes the anti-inflammatory phenotype in M2 macrophages, whereas a low ratio enhances the pro-inflammatory phenotype in M1 macrophages (56). Specific microRNAs induced by different microenvironmental signals can regulate different patterns of macrophage polarization states by regulating transcriptional output. For instance, miR-155 promotes M1 polarization by directly inhibiting expression of BCL6, and overexpression of miR-155 can reprogram M2 macrophages into M1 macrophages (57, 58). The plasticity of epigenetic modification is an essential factor in macrophage identity and heterogeneity, which is remodeled in response to acute and polarizing stimulation (59). Histone deacetylases (HDACs) are strongly involved in M1 activation and play a prominent role in inflammatory responses (60). HDAC6 and HDAC7 are involved in the expression of pro-inflammatory genes in macrophages stimulated by LPS, and inhibition of their activity significantly limits M1 activation and the production of pro-inflammatory cytokines (61, 62). Overexpression of DNA methyltransferase 3B (DNMT3B) or loss of HDAC3 renders macrophages hyperresponsive to IL-4, skewing differentiation toward the M2 phenotype (59).

However, not all macrophages fit the classical paradigm of M1 and M2 macrophages. Tumor-associated macrophages (TAMs), one of the main types of tumor-infiltrating immune cells, are

generally characterized as M2 macrophages, which are found to promote angiogenesis and invasion and tumor progression (63, 64). TCR+ macrophages, expressing the CD3/T-cell receptor (TCR)αβ complex, exist in tuberculous granulomas, atherosclerosis, and several types of cancer, which enhance phagocytosis and secrete IFN-γ, TNF, MIP-1β, and CCL2 to exhibit a specific pro-inflammatory profile (65–68).

3.2 Polarization regulation

Macrophage polarization is a complex process modulated by multiple factors, such as microRNAs (miR), proteins, glucocorticoids, and immunometabolism, involving numerous signaling pathways and transcriptional and post-transcriptional regulatory networks (14, 15, 42, 69). The precise regulatory mechanisms of macrophage polarization are still not completely understood and require further investigation. The phenotypic and functional changes in macrophages are accompanied by dramatic shifts in cell metabolism, with unique metabolic signatures related to their functional state, which is termed metabolic reprogramming (70–72). Recent studies have shown that specific metabolic pathways in macrophages are closely related to their phenotype and function, including glycolysis, tricarboxylic acid (TCA) cycle, PPP, arginine metabolism, glutamine metabolism, and fatty acid metabolism. The metabolic pathways of macrophages are shown in Figure 2. Some metabolic intermediates can regulate macrophage activation and effector function through various mechanisms (72).

4 Immunometabolism in macrophage polarization

4.1 Glycolysis

Glycolysis is a metabolic pathway that converts glucose to pyruvate, which plays a key role in energy metabolism, especially in the production of ATP in cells under hypoxia and other conditions. Tumor cells preferentially utilize glycolysis to produce lactic acid under normoxic conditions, known as "aerobic glycolysis." Subsequently, several studies have observed that aerobic glycolysis is increased in pro-inflammatory macrophages (73). Although glycolysis produces far less ATP than mitochondrial OXPHOS (2 ATP *vs.* 36 ATP), glycolysis can be activated faster to match the immune response of macrophages (74–76). Multiple studies have shown that classically activated M1 macrophages in mice and humans are highly dependent on glycolysis. Van den Bossche et al. used extracellular flux analysis to demonstrate that M1 macrophages display enhanced glycolytic metabolism and reduced mitochondrial OXPHOS; conversely, M2 macrophages display enhanced mitochondrial OXPHOS (77). Rodríguez-Prados et al. showed that activation of murine peritoneal macrophages *via* the Toll-like receptor (TLR) pathway results in a hyperglycolytic phenotype, and classic activation favors the upregulation of gene expression from the glycolytic pathway and the repression of genes encoding proteins that participate in OXPHOS (73). IL-10, an anti-inflammatory cytokine that induces M2 macrophages, inhibits LPS-induced glucose uptake and glycolysis and promotes OXPHOS to oppose the switch to the

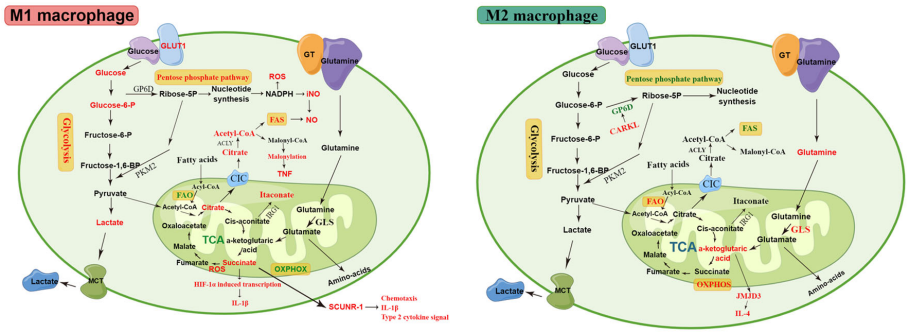

FIGURE 2
The metabolic pathways of M1 and M2 macrophages. M1 macrophages are associated with increased glycolysis, PPP, and FAS. The disturbed TCA cycle results in the accumulation of citrate and succinate. The accumulated citrate in the mitochondria of M1 macrophages is exported into the cytoplasm *via* the CIC and converted into acetyl-coenzyme A by ACLY. The downstream metabolic intermediate, acetyl-CoA, is necessary for TNF-α or IFN-γ to induce pro-inflammatory cytokines, such as NO and prostaglandin production. The malonylation response relies on citrate-derived metabolite malonyl-CoA production, which is an essential pro-inflammatory signal that promotes TNF translation and secretion by regulating glyceraldehyde 3-phosphate dehydrogenase (GAPDH). Succinate is a critical regulator of the pro-inflammatory response and regulates the expression of IL-1β via the the stabilization of hypoxia-inducible factor 1-alpha (HIF-1α)., thereby promoting LPS-induced expression of IL-1β. SDH mediates succinate oxidation and reverses electron transport, which together drive mitochondrial ROS production and induce a pro-inflammatory gene expression profile. Extracellular succinate binds to SUCNR1 and increases IL-1β production, which in turn increases SUCNR1 levels, fueling this cycle of cytokine production and perpetuating inflammation. M2 macrophages rely more heavily on OXPHOS, glutamine metabolism, and FAO than M1 macrophages. The enhancement of OXPHOS in M2 macrophages results in the continued production of ATP, leading to the upregulation of genes associated with tissue repair. The downregulated enzyme carbohydrate kinase-like protein (CARKL) causes glycolysis to feed the PPP, thereby generating nucleotides, amino acids, and NADPH, leading to an increase in ROS. αKG produced by glutamine hydrolysis promoted M2 activation through Jmjd3-dependent metabolic and epigenetic reprogramming, and a high αKG/succinate ratio further promoted the anti-inflammatory phenotype in M2 macrophages, whereas a low ratio enhances the pro-inflammatory phenotype in M1 macrophages. Elevated metabolites and processes are highlighted in red, and suppressed processes are highlighted in green.

metabolic program induced by inflammatory stimuli in macrophages (78).

After LPS stimulation of macrophages, transcription of the glucose transporter (GLUT1) is induced, leading to increased glucose uptake and aerobic glycolysis (79, 80). LPS specifically induces dimeric pyruvate kinase M2 (PKM2) protein expression and phosphorylation, and dimeric PKM2 interacts with HIF-1α, which is a transcription factor that contributes to both glycolysis and the induction of inflammatory genes and is critical for macrophage activation (81). HIF-1α can directly bind to the IL-1β promoter, an event that is inhibited by the activation of tetrameric PKM2 (82, 83). Activation of tetrameric PKM2 inhibits LPS-induced IL-1β production while promoting IL-10 production, thereby attenuating LPS-induced pro-inflammatory M1 macrophages and promoting the typical characteristics of M2 macrophages (82). Thus, PKM2 is a key determinant of LPS-activated macrophages that promote inflammatory responses (82). Another study demonstrated that PKM2-mediated glycolysis promotes NLRP3 and AIM2 inflammasome activation by modulating EIF2AK2 phosphorylation in LPS-primed mouse bone marrow-derived macrophages (BMDMs), consequently promoting the release of IL-1β and IL-18 and high-mobility group box 1 (HMGB1) (84). PFKFB3 is another LPS-regulated target involved in glycolytic conversion (73). PFKFB3 encodes u-PFK2, a subtype of 6-phosphofructo-2-kinase/fructose-2,6-bisphosphatase (PFK-2), which increases flux through the glycolytic pathway. PFKFB3 is a target gene of HIF-1α in response to hypoxia in human glioblastoma cell lines and mouse embryonic fibroblasts, thereby providing another mechanism by which HIF-1α promotes glycolysis (85).

Previous studies have suggested that M2 macrophages do not exhibit increased glycolysis and that aerobic glycolysis is predominantly associated with M1 macrophages. However, recent studies have shown that M2 macrophages also display an upregulated rate of glycolysis in addition to augmented mitochondrial metabolism (71). The glycolysis inhibitor 2-deoxyglucose (2-DG) (1 mM) attenuated enhanced mitochondrial respiration, significantly reduced 13C-labeled Krebs cycle metabolite levels and intracellular ATP levels, impaired IL-4-stimulated activation of early BMDMs, and reduced the expression of M2 phenotypic markers, such as Arg1, YM-1, FIZZ-1, and MRC1 (86–88). M-CSF associated with M2 polarization was found to induce similar glucose transporter expression, oxidative metabolism, mitochondrial biogenesis, and increased expression of glycolytic enzymes in macrophages compared with GM-CSF associated with the M1 phenotype (89). Glycolysis may play a more important role in M2 macrophages than previously thought, and further studies are needed.

4.2 Pentose phosphate pathway

PPP is an essential step in glucose metabolism, which is required for maintaining the cellular redox state and carbon homeostasis and provides precursors for nucleotide and amino acid biosynthesis. PPP can be divided into an initial oxidative phase that converts glucose 6-phosphate into carbon dioxide, ribulose 5-phosphate, and NADPH and a later non-oxidative phase that produces ribose 5-phosphate for nucleic acid synthesis and phosphate sugar precursors for amino acid synthesis (75, 90).

PPP is a major source of NADPH, which is a cofactor for NADPH-oxidase (Nox2)-dependent ROS production and is required for the generation of the antioxidant glutathione (75). The regulation of ROS levels was mediated in M1 macrophages by Cybb-encoded Nox2, which was transcriptionally upregulated in M1 macrophages and downregulated in M2 cells. Moreover, both the total pool of pentose-5-phosphates and their labeled fraction increased significantly in M1 macrophages (91). CARKL, a sedoheptulose kinase, also known as sedoheptulokinase (SHPK), catalyzes sedoheptulose to sedoheptulose-7-phosphate (S7P), which is a PPP intermediate and PPP flux restraint (92). The downregulated enzyme CARKL causes glycolysis to feed the PPP, thereby generating nucleotides, amino acids, and NADPH, leading to an increase in ROS. The CARKL expression level was rapidly downregulated in mice and humans *in vitro* and *in vivo* upon stimulation by LPS; conversely, it was upregulated in response to IL-4, leading to PPP inhibition in M2 macrophages (80). PPP was upregulated in M1 macrophages but downregulated in M2 macrophages.

4.3 Krebs cycle (tricarboxylic acid cycle)

The Krebs cycle, also known as the TCA cycle, is the final common pathway for the oxidation of carbohydrates, fatty acids, and amino acids and is also a source of precursors for many other biological molecules, such as non-essential amino acids, nucleotide bases, and porphyrin (93, 94). Therefore, the Krebs cycle is an important hub for cellular anabolism (gluconeogenesis and lipid synthesis) and catabolism (glycolysis).

In recent years, several studies have shown that the TCA cycle of M1 macrophages is disrupted at various points, and OXPHOS is inhibited, leading to the accumulation of citrate, itaconate, and succinate (91, 95, 96). Conversely, M2 macrophages maintain robust oxidative Krebs cycle activity, while increasing OXPHOS and ATP levels (88, 91).

4.3.1 Citrate

Previous studies have demonstrated that the disruption of the TCA cycle and accumulation of citrate in M1 macrophages may be related to the transcriptional downregulation of isocitrate dehydrogenase (IDH), which catalyzes the conversion of isocitrate to α-ketoglutarate (α-KG) (91). However, Palmieri et al. showed that NO-mediated suppression of mitochondrial aconitase (ACO2), rather than IDH1, might be the TCA breakpoint in M1 macrophages, which is responsible for an increase in citrate levels and a reduction in α-KG levels (97). The mRNA and protein levels of the mitochondrial citrate carrier (CIC/SLC25a1) are markedly increased in LPS-activated macrophages (98). Inhibition of SLC25a1 in activated macrophages by genetic silencing leads to a significant reduction in ROS, NO, and prostaglandin, suggesting

that the effluence of citrate from the mitochondria is an essential pro-inflammatory signal in M1 macrophage activation (98). The accumulated citrate in the mitochondria of M1 macrophages is exported into the cytoplasm *via* the CIC and converted into acetyl-coenzyme A by ATP citrate lyase (ACLY) (98). The downstream metabolic intermediate, acetyl-CoA, is necessary for TNF-α or IFN-γ to induce pro-inflammatory cytokines, such as nitric oxide (NO) and prostaglandin production (99). Inhibition of either CIC or ACLY markedly reduced prostaglandin E2 (PGE2), NO, and ROS levels (98–100). The mRNA expression of the anti-inflammatory cytokine IL-10 and IL-1 receptor antagonists in LPS-stimulated macrophages increased after ACLY inhibition (101). Another study found that the IL-4 signaling pathway cooperates with the Akt–mTORC1 pathway to regulate ACLY, resulting in increased histone acetylation and M2 gene induction (102). Furthermore, the malonylation response relies on citrate-derived metabolite malonyl-CoA production, which is an essential pro-inflammatory signal that promotes TNF translation and secretion by regulating glyceraldehyde 3-phosphate dehydrogenase (GAPDH) in response to inflammation induced by LPS (103). Furthermore, extracellular citrate may serve as a damage-associated molecular pattern (DAMP) and aggravate LPS-induced ALI by overactivating the NACHT, LRR, and PYD domain-containing protein 3 (NLRP3) inflammasome (104). Citrate and its metabolic intermediates play an important role in the M1 macrophage response, and their role in M2 macrophages needs to be further explored.

4.3.2 Itaconate

Aconitase 2 catalyzes citrate to form cis-aconitate, which is decarboxylated by cis-aconitate decarboxylase, also known as immunoresponsive gene 1 (IRG1), leading to itaconate production (105, 106). Pro-inflammatory conditions can induce IRG1 expression and itaconic acid synthesis. The overexpression of IRG1 significantly inhibits LPS-induced production of TNF-α, IL-6, and IFN-β in mouse macrophages (107). In contrast, IRG1 knockout aggravates the inflammatory response in LPS-stimulated murine BMDMs and myeloid cells infected with *Mycobacterium tuberculosis* (108, 109). Itaconate has recently emerged as a regulator of macrophage functions. Itaconate reduced the production of pro-inflammatory mediators in LPS-treated macrophages, and the mechanism of this anti-inflammatory effect may be related to the inhibition of succinate dehydrogenase, blocking of IκBζ translation, and activation of Nrf2. Lampropoulou et al. reported that inhibition of itaconate-mediated succinate dehydrogenase (SDH) activity blocks mitochondrial ROS generation, inhibits NLRP3 inflammasome activation, and reduces pro-inflammatory mediator release from mouse BMDMs (108). Mills et al. demonstrated that itaconate is required for LPS-induced activation of the anti-inflammatory transcription factor Nrf2 in mouse and human macrophages (110). Itaconate directly modifies the protein KEAP1 through alkylation of cysteine residues, enabling Nrf2 to increase the expression of downstream genes with antioxidant and anti-inflammatory capacities, thereby limiting inflammatory responses and regulating type I interferons (110). Bambouskova et al. showed that itaconate and its membrane-permeable derivative dimethyl itaconate induce electrophilic stress, react with glutathione, and subsequently induce both Nrf2-dependent and Nrf2-independent responses, selectively regulating secondary transcriptional responses to TLR stimulation *via* inhibition of IκBζ protein induction (111). However, a recent study demonstrated that itaconate and itaconate derivatives (4-octyl itaconate) target JAK1 to suppress M2 macrophage polarization (112).

4.3.3 Succinate

Succinate is a pro-inflammatory metabolite that accumulates during macrophage activation. Activation of macrophages using LPS leads to the accumulation of intracellular succinate through glutamine-dependent proliferation and γ-aminobutyric acid (GABA) shunt pathways (95). Increased succinate is a critical regulator of the pro-inflammatory response to LPS, both through the generation of ROS following oxidation by the electron transport chain (ETC) and *via* the stabilization of HIF-1α, a key transcription factor in the expression of pro-inflammatory genes, which in turn specifically regulates the expression of IL-1β and other HIF-1α-dependent genes and causes protein succinylation, such as malate dehydrogenase, GAPDH, glutamate carrier 1, and lactate dehydrogenase (95). Increased mitochondrial oxidation of succinate through SDH and elevation of mitochondrial membrane potential combine to drive mitochondrial ROS production and induce a pro-inflammatory gene expression profile (113). Inhibition of SDH causes succinate to accumulate and prevents the induction of a range of pro-inflammatory factors typified by IL-1β while enhancing a range of anti-inflammatory factors typified by IL-1RA and IL-10 (113). Thus, SDH enhances the oxidation of succinate, is required for the induction of pro-inflammatory genes, and simultaneously limits the induction of anti-inflammatory genes. The succinate receptor SUCNR1/GPR91 is a G protein-coupled cell surface sensor for extracellular succinate. Littlewood-Evans et al. proposed a mechanism for SUCNR1-driven autocrine and paracrine enhancement of IL-1β release from activated macrophages (114, 115). Endogenous TLR ligands activate macrophages locally, resulting in enhanced glycolysis and increased intracellular succinate levels. Simultaneously, succinate is released into the extracellular milieu, where it binds to SUCNR1 and increases IL-1β production from the same or adjacent SUCNR1-expressing cells, which in turn increases SUCNR1 levels, fueling this cycle of cytokine production and perpetuating inflammation (115). Gut microbiota-derived succinate exacerbates intestinal ischemia/reperfusion-induced ALI through SUCNR1-dependent M1 polarization, and plasma succinate levels are significantly correlated with ALI (116). Succinate and its receptors play an important role in macrophage metabolism and may serve as important targets for inflammatory diseases in the future.

4.4 Glutamine metabolism

Glutamine, serving as a carbon and nitrogen source for metabolic reprogramming of M1 macrophages, can be broken

down to produce glutamate and α-KG, the latter of which enters the TCA cycle to provide energy. Furthermore, glutamine metabolism represents an important metabolic module governing the alternative activation of macrophages in response to IL-4 (91). Palmieri et al. reported that inhibition of glutamine synthetase skewed M2-polarized macrophages toward the M1-like phenotype, characterized by decreased intracellular glutamine and increased succinate with enhanced glucose flux through glycolysis, showing an enhanced capacity to induce T-cell recruitment and reduced T-cell suppressive potential, which could be partly related to the activation of HIF-1α (117). Production of αKG by glutamine hydrolysis is important for the alternative activation of macrophages (56). αKG promotes M2 activation through Jmjd3-dependent metabolic and epigenetic reprogramming, and a high αKG/succinate ratio further promotes the anti-inflammatory phenotype in M2 macrophages, whereas a low ratio enhances the pro-inflammatory phenotype in M1 macrophages (56). Moreover, αKG inhibits the nuclear factor-κB (NF-κB) pathway through prolyl hydroxylase (PHD)-dependent proline hydroxylation of protein kinase IKKβ, thereby impairing the pro-inflammatory response of M1 macrophages (56). The peroxisome proliferator-activated receptor γ (PPARγ) is involved in the alternative activation of macrophages (56, 118, 119). PPARγ is required for IL-4-induced M2 macrophage respiration, and the absence of PPARγ dramatically affects glutamine oxidation (120). Unstimulated macrophages lacking PPARγ contain elevated levels of the inflammation-associated metabolite itaconate and express a pro-inflammatory transcriptome (120).

4.5 Arginine metabolism

Arginine metabolism is a complex process characterized differently in M1 and M2 macrophages. M1 macrophages express NO synthase, which metabolizes arginine to NO and citrulline, and citrulline can be reused for efficient NO synthesis *via* the citrulline–NO cycle (121). M2 macrophages are characterized by the expression of arginase, which hydrolyzes arginine to generate ornithine and urea, a precursor of l-proline and polyamines involved in tissue repair and wound healing (122). There are two isozymes of arginase: arginase I and arginase II. The hepatic urea cycle arginase I is expressed as a cytosolic enzyme, while human granulocyte arginase I is found in the granular compartment and arginase II is found as a mitochondrial enzyme (123). Arg1 inhibits NO-mediated inflammatory pathways by competing with iNOS for L-arginine. A recent study demonstrated that renal tubular cells apically exposed to dead cell debris induce reparative macrophage activation, expressing Arg1, which is required for the S3 tubular cell proliferative response that promotes renal repair after ischemia–reperfusion injury (124). Moreover, Zhang et al. found that polarization of M2a macrophages promotes the expression of Arg1, which restores axonal regeneration and promotes the structural and functional recovery of the contused spinal cord (125). Hardbower et al. reported that Arg2 deletion leads to enhanced M1 macrophage activation, pro-inflammatory cytokine expression, and immune cell-derived chemokine production (126). Arg2 is essential for the IL-10-mediated increase in mitochondrial oxidative metabolism and succinate dehydrogenase/complex II activity and the decrease in the inflammatory mediators succinate, HIF-1α, and IL-1β (127). Therefore, arginine metabolism plays an important role in the anti-inflammatory effects and tissue repair of macrophages.

4.6 Fatty acid metabolism

The TCA cycle of M1 macrophages is disrupted, causing the accumulation of citrate, which is exported from the mitochondria to the cytoplasm to generate acetyl-CoA *via* ACLY, which fuels the *de-novo* synthesis of cholesterol and FA (128). These steps involve ACLY, acetyl-CoA carboxylase (ACC), fatty acid synthase (FASN), desaturases, and elongation proteins. Fatty acids tightly couple glucose and lipid metabolism *via* the *de-novo* FA synthesis pathway, supporting cell adaptation to environmental changes. The FAO pathway produces acetyl-CoA, NADH, and FADH2, which are further used in the TCA cycle and ETC to generate large amounts of ATP, which is thought to promote M2 polarization. This process is coordinated by multiple enzymes such as fatty acyl CoA synthetase, carnitine palmitoyltransferase I (CPT1), and carnitine palmitoyltransferase II (CPT2).

4.6.1 Fatty acid synthesis

Fatty acid synthesis is closely related to the pro-inflammatory function of macrophages. Several studies have suggested that cellular fatty acid synthesis (e.g., synthesis of triglycerides and cholesteryl esters) is activated during inflammation (129–131). Saturated fatty acids (SFAs) can induce inflammation either extracellularly by activating TLR signaling or intracellularly *via* products of SFA metabolism, thereby inducing NF-κB activation and the expression of COX-2 and other inflammatory markers (132). Moon et al. demonstrated that mitochondrial uncoupling protein-2 regulates the NLRP3 inflammasome by inducing the lipid synthesis pathway during macrophage activation (133). The NLRP3 inflammasome finely regulates the activation of caspase-1 and the production and secretion of potent pro-inflammatory cytokines such as IL-1β and IL-18 (134). The fatty acid metabolism-immunity nexus (FAMIN; LACC1, C13orf31) forms a complex with FASN on peroxisomes to concomitantly drive high levels of FAO and glycolysis, controlled inflammasome activation, mitochondrial and NADPH-oxidase-dependent production of ROS, TLR-dependent signaling, cytokine secretion, and the bactericidal activity of macrophages (135). Impaired FAMIN compromises both classically activated M1 macrophages and alternatively activated M2 macrophages (135–137).

4.6.2 FAO

LPS-treated macrophages stimulated fatty acid uptake into the cell, which was accompanied by a marked increase in the expression of CD36, a protein that transports fatty acids (131). The ability of LPS-treated macrophages to oxidize fatty acids to CO_2 was greatly reduced, which was associated with reduced expression of CPT1α

and CPT1β proteins that promote fatty acid entry into the mitochondria for oxidation (131). Lv et al. demonstrated that didymin, a flavonoid constituent, strengthened FAO rather than glycolysis by inducing Hadhb expression, resulting in the conversion of M1-like macrophages toward M2-like macrophages and eventually alleviating colitis (138). Hohensinner et al. showed that the pharmacological inhibition of FAO in macrophages reduced NLRP3 activation, leading to reduced levels of the pro-inflammatory cytokine IL-1β in macrophages, thereby suppressing the inflammatory response (139). Namgaladze et al. showed that IL-4-induced M2 polarization of murine macrophages in response to IL-4 is associated with the increase in mitochondrial oxidative metabolism and FAO (140). However, in human macrophages, IL-4 causes only moderate changes in mitochondrial oxidative metabolism and FAO; attenuating FAO had no effect on IL-4-induced polarization-associated gene expression (140). FAO is not essential for M2 activation, and further research is needed to clarify the underlying mechanism.

5 Macrophage polarization and ALI/ARDS

Macrophages participate in the pathogenesis of ALI/ARDS, including the regulation of inflammatory responses and the repair of damaged lung tissues (12, 13). M1 macrophages are involved in the acute inflammatory response and exudative phase of ALI/ARDS by secreting various pro-inflammatory cytokines and recruiting neutrophils from the circulation into the lungs and alveoli, leading to the progression of inflammation and enhanced lung injury (4, 16). However, M2 macrophages are mainly associated with the resolution of inflammation and the recovery phase in ALI/ARDS by producing anti-inflammatory cytokines and limiting the levels of pro-inflammatory cytokines to alleviate the inflammation response and promote lung tissue repair (4, 16). Excessive M2 polarization may result in a pathological fibroproliferative response and pulmonary fibrosis (4). Macrophage polarization can be modulated by multiple factors, and immunometabolism and its metabolic intermediates are one of the most important factors. Altering the direction of macrophage polarization and limiting excessive pro-inflammatory responses by modulating immunometabolism and its metabolic intermediates may greatly affect the prognosis of ALI/ARDS.

Recent studies have shown that several compounds affect macrophage polarization by modulating immunometabolism and its metabolic intermediates. N-phenethyl-5-phenylpicolinamide (N5P) is a newly synthesized HIF-1α inhibitor. Du et al. showed that N5P effectively reduced HIF-1α, GLUT1, HK2, ASIC1a, IL-1β, and IL-6 expression levels in LPS-induced ALI, which may alleviate inflammation in ALI through the HIF-1α/glycolysis/ASIC1a signaling pathway (141). Zhong et al. demonstrated that inhibition of glycolysis by 2-DG pronouncedly attenuated lung tissue pathological injury, oxidative stress, and the expression of pro-inflammatory factors in ALI mice induced by LPS (142). Tanshinone IIA (Tan-IIA), a major constituent of *Salvia miltiorrhiza* Bunge, significantly decreased succinate-boosted IL-1β and IL-6 production, accompanied by upregulation of IL-1RA and IL-10 release *via* inhibition of SDH and reduced mitochondrial ROS production, leading to remarkably attenuated LPS-induced acute inflammatory responses (143). Dimethyl malonate (DMM), which is rapidly hydrolyzed in cells to form malonate, is a competitive inhibitor of succinate oxidation by SDH (113). Mills et al. found that inhibition of SDH with DMM was effective in an LPS-induced sepsis mouse model, where it decreased the serum levels of IL-1β and boosted IL-10, but had no significant effect on TNF-α (113). In a mouse model of LPS-induced peritonitis, Lauterbach et al. revealed decreased protein levels of IL-6 and IL-12 in the peritoneum and serum by inhibiting ACLY using BMS 303141, suggesting that ACLY inhibition was able to alter the local and systemic inflammatory profiles (144). Inhibition of SLC25a1 in activated macrophages with the inhibitor 1,2,3-benzentricarboxylic acid (BTA) or through genetic silencing reduced accumulated citrate output from the mitochondria to the cytoplasm *via* SLC25a1, leading to a marked reduction in ROS, NO, and prostaglandin production (98). Production of αKG by glutamine hydrolysis is important for the alternative activation of macrophages. Liu et al. found that α-KG pretreatment diminished the lung damage score, inhibited the secretion of inflammatory cytokines in sera, suppressed M1 marker gene expression (IL-1β, IL-6, and TNF-α) and enhanced M2 marker gene expression (Arg1) to attenuate LPS-induced ALI/ARDS in a mouse model (145). Furthermore, in other diseases mediated by inflammatory responses, it is also promising to reduce the severity of disease by regulating the polarization of macrophages through immunometabolism. Didymin, a flavonoid constituent, strengthens FAO rather than glycolysis, resulting in the conversion of M1- toward M2-like macrophages, but does not alter the polarization of M2-like macrophages and remarkably alleviates the clinical symptoms of acute and chronic colitis in mice (138). Targeting immunometabolism to regulate macrophage polarization for ALI/ARDS treatment has been proven effective and promising in many studies. However, the current relevant studies are insufficient, and almost all of them are cell experiments or animal experiments. Further studies are needed to elucidate the role of immunometabolism and its metabolic intermediates in macrophage polarization and ALI/ARDS, which may represent new targets and therapeutic directions.

6 Conclusion

In the pathogenesis of ALI/ARDS, M1 macrophages engage in pro-inflammatory responses, chemotaxis, radical formation, and elimination of pathogenic microorganisms, while M2 macrophages exert anti-inflammatory effects and promote tissue remodeling and lung repair. Polarized macrophages exhibit plasticity; thus, targeting macrophage polarization has potential benefits for alleviating inflammation and promoting lung repair in ALI/ARDS. Immunometabolism is a significant and complex process involving multiple metabolic pathways and metabolic intermediates, such as glycolysis, the Krebs cycle, the pentose

phosphate pathway, amino acid metabolism, and fatty acid metabolism. A growing body of literature on immunometabolism has demonstrated the essential role of immunometabolism and its metabolic intermediates in macrophage polarization. Therefore, the regulation of macrophage immunometabolism to alter macrophage polarization may be a new direction for the treatment of ALI/ARDS.

Author contributions

Conceptualization: LW and DW Investigation: XT and HF. Resources: TZ and YM. Writing—original draft preparation: LW and DW. Writing—review and editing: XT and HF. Supervision: HF All authors contributed to the article and approved the submitted version.

Funding

This research was funded by the Sichuan Science and Technology Program (2022YFS0261 and 2020YFS0148).

Acknowledgments

Figures 1 and 2 are made by Figdraw.

Conflict of interest

The authors declare that the research was conducted in the absence of any commercial or financial relationships that could be construed as a potential conflict of interest.

Publisher's note

References

1. Matthay MA, Zemans RL, Zimmerman GA, Arabi YM, Beitler JR, Mercat A, et al. Acute respiratory distress syndrome. *Nat Rev Dis Primers* (2019) 5(1):18. doi: 10.1038/s41572-019-0069-0

2. Butt Y, Kurdowska A, Allen TC. Acute lung injury: A clinical and molecular review. *Arch Pathol Lab Med* (2016) 140(4):345–50. doi: 10.5858/arpa.2015-0519-RA

3. Matuschak GM, Lechner AJ. Acute lung injury and the acute respiratory distress syndrome: pathophysiology and treatment. *Mo Med* (2010) 107(4):252–8.

4. Cheng P, Li S, Chen H. Macrophages in lung injury, repair, and fibrosis. *Cells* (2021) 10(2):436. doi: 10.3390/cells10020436

5. Manicone AM. Role of the pulmonary epithelium and inflammatory signals in acute lung injury. *Expert Rev Clin Immunol* (2009) 5(1):63–75. doi: 10.1586/1744666X.5.1.63

6. Meyer NJ, Gattinoni L, Calfee CS. Acute respiratory distress syndrome. *Lancet* (2021) 398(10300):622–37. doi: 10.1016/S0140-6736(21)00439-6

7. Thompson BT, Chambers RC, Liu KD. Acute respiratory distress syndrome. *N Engl J Med* (2017) 377(6):562–72. doi: 10.1056/NEJMra1608077

8. Wheeler AP, Bernard GR. Acute lung injury and the acute respiratory distress syndrome: a clinical review. *Lancet* (2007) 369(9572):1553–64. doi: 10.1016/S0140-6736(07)60604-7

9. Xin Y, Peng J, Hong YY, Chao QC, Na S, Pan S, et al. Advances in research on the effects of platelet activation in acute lung injury (Review). *BioMed Rep* (2022) 16(3):17. doi: 10.3892/br.2022.1500

10. Rubenfeld GD, Caldwell E, Peabody E, Weaver J, Martin DP, Neff M, et al. Incidence and outcomes of acute lung injury. *N Engl J Med* (2005) 353(16):1685–93. doi: 10.1056/NEJMoa050333

11. Kumar V. Pulmonary innate immune response determines the outcome of inflammation during pneumonia and sepsis-associated acute lung injury. *Front Immunol* (2020) 11:1722. doi: 10.3389/fimmu.2020.01722

12. Huang X, Xiu H, Zhang S, Zhang G. The role of macrophages in the pathogenesis of ALI/ARDS. *Mediators Inflammation* (2018) 2018:1264913. doi: 10.1155/2018/1264913

13. Johnston LK, Rims CR, Gill SE, McGuire JK, Manicone AM. Pulmonary macrophage subpopulations in the induction and resolution of acute lung injury. *Am J Respir Cell Mol Biol* (2012) 47(4):417–26. doi: 10.1165/rcmb.2012-0090OC

14. Wang N, Liang H, Zen K. Molecular mechanisms that influence the macrophage m1-m2 polarization balance. *Front Immunol* (2014) 5:614. doi: 10.3389/fimmu.2014.00614

15. Lawrence T, Natoli G. Transcriptional regulation of macrophage polarization: enabling diversity with identity. *Nat Rev Immunol* (2011) 11(11):750–61. doi: 10.1038/nri3088

16. Chen X, Tang J, Shuai W, Meng J, Feng J, Han Z. Macrophage polarization and its role in the pathogenesis of acute lung injury/acute respiratory distress syndrome. *Inflammation Res* (2020) 69(9):883–95. doi: 10.1007/s00011-020-01378-2

17. Zuo H, Wan Y. Metabolic reprogramming in mitochondria of myeloid cells. *Cells* (2019) 9(1):5. doi: 10.3390/cells9010005

18. Viola A, Munari F, Sánchez-Rodríguez R, Scolaro T, Castegna A.. The metabolic signature of macrophage responses. *Front Immunol* (2019) 10:1462. doi: 10.3389/fimmu.2019.01462

19. Mills EL, O'Neill LA. Reprogramming mitochondrial metabolism in macrophages as an anti-inflammatory signal. *Eur J Immunol* (2016) 46(1):883–95. doi: 10.1007/s00011-020-01378-2

20. Michaeloudes C, Bhavsar PK, Mumby S, Xu B, Hui CKM, Chung KF, et al. Role of metabolic reprogramming in pulmonary innate immunity and its impact on lung diseases. *J Innate Immun* (2020) 12(1):31–46. doi: 10.1159/000504344

21. Hu G, Christman JW. Editorial: Alveolar macrophages in lung inflammation and resolution. *Front Immunol* (2019) 10:2275. doi: 10.3389/fimmu.2019.02275

22. Tan SY, Krasnow MA. Developmental origin of lung macrophage diversity. *Development* (2016) 143(8):1318–27. doi: 10.1242/dev.129122

23. Ginhoux F, Guilliams M. Tissue-resident macrophage ontogeny and homeostasis. *Immunity* (2016) 44(3):439–49. doi: 10.1016/j.immuni.2016.02.024

24. Gomez Perdiguero E, Klapproth K, Schulz C, Busch K, Azzoni E, Crozet L, et al. Tissue-resident macrophages originate from yolk-sac-derived erythro-myeloid progenitors. *Nature* (2015) 518(7540):547–51. doi: 10.1038/nature13989

25. Hoeffel G, Chen J, Lavin Y, Low D, Almeida FF, See P, et al. C-myb(+) erythro-myeloid progenitor-derived fetal monocytes give rise to adult tissue-resident macrophages. *Immunity* (2015) 42(4):665–78. doi: 10.1016/j.immuni.2015.03.011

26. Yu X, Buttgereit A, Lelios I, Utz SG, Cansever D, Becher B, et al. The cytokine TGF-β promotes the development and homeostasis of alveolar macrophages. *Immunity* (2017) 47(5):903–912.e4. doi: 10.1016/j.immuni.2017.10.007

27. Schneider C, Nobs SP, Kurrer M, Rehrauer H, Thiele C, Kopf M. Induction of the nuclear receptor PPAR-γ by the cytokine GM-CSF is critical for the differentiation of fetal monocytes into alveolar macrophages. *Nat Immunol* (2014) 15(11):1026–37. doi: 10.1038/ni.3005

28. Janssen WJ, Barthel L, Muldrow A, Oberley-Deegan RE, Kearns MT, Jakubzick C, et al. Fas determines differential fates of resident and recruited macrophages during resolution of acute lung injury. *Am J Respir Crit Care Med* (2011) 184(5):547–60. doi: 10.1164/rccm.201011-1891OC

29. Goritzka M, Makris S, Kausar F, Durant LR, Pereira C, Kumagai Y, et al. Alveolar macrophage-derived type I interferons orchestrate innate immunity to RSV

through recruitment of antiviral monocytes. *J Exp Med* (2015) 212(5):699–714. doi: 10.1084/jem.20140825

30. Zasłona Z, Przybranowski S, Wilke C, van Rooijen N, Teitz-Tennenbaum S, Osterholzer JJ, et al. Resident alveolar macrophages suppress, whereas recruited monocytes promote, allergic lung inflammation in murine models of asthma. *J Immunol* (2014) 193(8):4245–53. doi: 10.4049/jimmunol.1400580

31. Bedoret D, Wallemacq H, Marichal T, Desmet C, Quesada Calvo F, Henry E, et al. Lung interstitial macrophages alter dendritic cell functions to prevent airway allergy in mice. *J Clin Invest* (2009) 119(12):3723–38. doi: 10.1172/JCI39717

32. Dang W, Tao Y, Xu X, Zhao H, Zou L, Li Y. The role of lung macrophages in acute respiratory distress syndrome. *Inflammation Res* (2022) 71(12):1417–32. doi: 10.1007/s00011-022-01645-4

33. Schyns J, Bureau F, Marichal T. Lung interstitial macrophages: Past, present, and future. *J Immunol Res* (2018) 2018:5160794. doi: 10.1155/2018/5160794

34. Hoppstädter J, Diesel B, Zarbock R, Breinig T, Monz D, Koch M, et al. Differential cell reaction upon toll-like receptor 4 and 9 activation in human alveolar and lung interstitial macrophages. *Respir Res* (2010) 11(1):124. doi: 10.1186/1465-9921-11-124

35. Draijer C, Boorsma CE, Robbe P, Timens W, Hylkema MN, Ten Hacken NH, et al. Human asthma is characterized by more IRF5+ M1 and CD206+ M2 macrophages and less IL-10+ M2-like macrophages around airways compared with healthy airways. *J Allergy Clin Immunol* (2017) 140(1):280–283.e3. doi: 10.1016/j.jaci.2016.11.020

36. Atri C, Guerfali FZ, Laouini D. Role of human macrophage polarization in inflammation during infectious diseases. *Int J Mol Sci* (2018) 19(6):1801. doi: 10.3390/ijms19061801

37. Yunna C, Mengru H, Lei W, Weidong C. Macrophage M1/M2 polarization. *Eur J Pharmacol* (2020) 877:173090. doi: 10.1016/j.ejphar.2020.173090

38. Shapouri-Moghaddam A, Mohammadian S, Vazini H, Taghadosi M, Esmaeili SA, Mardani F, et al. Macrophage plasticity, polarization, and function in health and disease. *J Cell Physiol* (2018) 233(9):6425–40. doi: 10.1002/jcp.26429

39. Mosser DM, Edwards JP. Exploring the full spectrum of macrophage activation. *Nat Rev Immunol* (2008) 8(12):958–69. doi: 10.1038/nri2448

40. Gordon S, Taylor PR. Monocyte and macrophage heterogeneity. *Nat Rev Immunol* (2005) 5(12):953–64. doi: 10.1038/nri1733

41. Vogel DY, Glim JE, Stavenuiter AW, Breur M, Heijnen P, Amor S, et al. Human macrophage polarization in vitro: maturation and activation methods compared. *Immunobiology* (2014) 219(9):695–703. doi: 10.1016/j.imbio.2014.05.002

42. Sica A, Mantovani A. Macrophage plasticity and polarization: in vivo veritas. *J Clin Invest* (2012) 122(3):787–95. doi: 10.1172/JCI59643

43. Tarique AA, Logan J, Thomas E, Holt PG, Sly PD, Fantino E. Phenotypic, functional, and plasticity features of classical and alternatively activated human macrophages. *Am J Respir Cell Mol Biol* (2015) 53(5):676–88. doi: 10.1165/rcmb.2015-0012OC

44. Xu W, Zhao X, Daha MR, van Kooten C. Reversible differentiation of pro- and anti-inflammatory macrophages. *Mol Immunol* (2013) 53(3):179–86. doi: 10.1016/j.molimm.2012.07.005

45. Verreck FA, de Boer T, Langenberg DM, van der Zanden L, Ottenhoff TH. Phenotypic and functional profiling of human proinflammatory type-1 and anti-inflammatory type-2 macrophages in response to microbial antigens and IFN-gamma- and CD40L-mediated costimulation. *J Leukoc Biol* (2006) 79(2):285–93. doi: 10.1189/jlb.0105015

46. Martinez FO, Gordon S, Locati M, Mantovani A. Transcriptional profiling of the human monocyte-to-macrophage differentiation and polarization: new molecules and patterns of gene expression. *J Immunol* (2006) 177(10):7303–11. doi: 10.4049/jimmunol.177.10.7303

47. Gordon S, Martinez FO. Alternative activation of macrophages: mechanism and functions. *Immunity* (2010) 32(5):593–604. doi: 10.1016/j.immuni.2010.05.007

48. Mantovani A, Germano G, Marchesi F, Locatelli M, Biswas SK. Cancer-promoting tumor-associated macrophages: new vistas and open questions. *Eur J Immunol* (2011) 41(9):2522–5. doi: 10.1002/eji.201141894

49. Martinez FO, Sica A, Mantovani A, Locati M. Macrophage activation and polarization. *Front Biosci* (2008) 13:453–61. doi: 10.2741/2692

50. Byers DE, Holtzman MJ. Alternatively activated macrophages and airway disease. *Chest* (2011) 140(3):768–74. doi: 10.1378/chest.10-2132

51. Siddiqui S, Secor ERJr., Silbart LK. Broncho-alveolar macrophages express chemokines associated with leukocyte migration in a mouse model of asthma. *Cell Immunol* (2013) 281(2):159–69. doi: 10.1016/j.cellimm.2013.03.001

52. Zizzo G, Hilliard BA, Monestier M, Cohen PL. Efficient clearance of early apoptotic cells by human macrophages requires M2c polarization and MerTK induction. *J Immunol* (2012) 189(7):3508–20. doi: 10.4049/jimmunol.1200662

53. Lu J, Cao Q, Zheng D, Sun Y, Wang C, Yu X, et al. Discrete functions of M2a and M2c macrophage subsets determine their relative efficacy in treating chronic kidney disease. *Kidney Int* (2013) 84(4):745–55. doi: 10.1038/ki.2013.135

54. Duluc D, Delneste Y, Tan F, Moles MP, Grimaud L, Lenoir J, et al. Tumor-associated leukemia inhibitory factor and IL-6 skew monocyte differentiation into tumor-associated macrophage-like cells. *Blood* (2007) 110(13):4319–30. doi: 10.1182/blood-2007-02-072587

55. Wu H, Xu JB, He YL, Peng JJ, Zhang XH, Chen CQ, et al. Tumor-associated macrophages promote angiogenesis and lymphangiogenesis of gastric cancer. *J Surg Oncol* (2012) 106(4):462–8. doi: 10.1002/jso.23110

56. Liu PS, Wang H, Li X, Chao T, Teav T, Christen S, et al. α-ketoglutarate orchestrates macrophage activation through metabolic and epigenetic reprogramming. *Nat Immunol* (2017) 18(9):985–94. doi: 10.1038/ni.3796

57. Nazari-Jahantigh M, Wei Y, Noels H, Akhtar S, Zhou Z, Koenen RR, et al. MicroRNA-155 promotes atherosclerosis by repressing Bcl6 in macrophages. *J Clin Invest* (2012) 122(11):4190–202. doi: 10.1172/JCI61716

58. Cai X, Yin Y, Li N, Zhu D, Zhang J, Zhang CY, et al. Re-polarization of tumor-associated macrophages to pro-inflammatory M1 macrophages by microRNA-155. *J Mol Cell Biol* (2012) 4(5):341–3. doi: 10.1093/jmcb/mjs044

59. Locati M, Curtale G, Mantovani A. Diversity, mechanisms, and significance of macrophage plasticity. *Annu Rev Pathol* (2020) 15:123–47. doi: 10.1146/annurev-pathmechdis-012418-012718

60. Chen S, Yang J, Wei Y, Wei X. Epigenetic regulation of macrophages: from homeostasis maintenance to host defense. *Cell Mol Immunol* (2020) 17(1):36–49. doi: 10.1038/s41423-019-0315-0

61. Yan B, Xie S, Liu Z, Ran J, Li Y, Wang J, et al. HDAC6 deacetylase activity is critical for lipopolysaccharide-induced activation of macrophages. *PloS One* (2014) 9(10):e110718. doi: 10.1371/journal.pone.0110718

62. Shakespear MR, Hohenhaus DM, Kelly GM, Kamal NA, Gupta P, Labzin LI, et al. Histone deacetylase 7 promotes toll-like receptor 4-dependent proinflammatory gene expression in macrophages. *J Biol Chem* (2013) 288(35):25362–74. doi: 10.1074/jbc.M113.496281

63. Pan Y, Yu Y, Wang X, Zhang T. Tumor-associated macrophages in tumor immunity. *Front Immunol* (2020) 11:583084. doi: 10.3389/fimmu.2020.583084

64. Myers KV, Amend SR, Pienta KJ. Targeting Tyro3, axl and MerTK (TAM receptors): implications for macrophages in the tumor microenvironment. *Mol Cancer* (2019) 18(1):94. doi: 10.1186/s12943-019-1022-2

65. Rodriguez-Cruz A, Vesin D, Ramon-Luing L, Zuñiga J, Quesniaux VFJ, Ryffel B, et al. CD3(+) macrophages deliver proinflammatory cytokines by a CD3- and transmembrane TNF-dependent pathway and are increased at the BCG-infection site. *Front Immunol* (2019) 10:2550. doi: 10.3389/fimmu.2019.02550

66. Fuchs T, Hahn M, Riabov V, Yin S, Kzhyshkowska J, Busch S, et al. A combinatorial αβ T cell receptor expressed by macrophages in the tumor microenvironment. *Immunobiology* (2017) 222(1):39–44. doi: 10.1016/j.imbio.2015.09.022

67. Zhang N, Gao X, Zhang W, Xiong J, Cao X, Fu ZF, et al. JEV infection induces m-MDSC differentiation into CD3(+) macrophages in the brain. *Front Immunol* (2022) 13:838990. doi: 10.3389/fimmu.2022.838990

68. Jiang Y, Zhang S, Tang L, Li R, Zhai J, Luo S, et al. Single-cell RNA sequencing reveals TCR(+) macrophages in HPV-related head and neck squamous cell carcinoma. *Front Immunol* (2022) 13:1030222. doi: 10.3389/fimmu.2022.1030222

69. Hoeksema MA, Stöger JL, de Winther MP. Molecular pathways regulating macrophage polarization: implications for atherosclerosis. *Curr Atheroscler Rep* (2012) 14(3):254–63. doi: 10.1007/s11883-012-0240-5

70. Artyomov MN, Sergushichev A, Schilling JD. Integrating immunometabolism and macrophage diversity. *Semin Immunol* (2016) 28(5):417–24. doi: 10.1016/j.smim.2016.10.004

71. Diskin C, Pålsson-McDermott EM. Metabolic modulation in macrophage effector function. *Front Immunol* (2018) 9:270. doi: 10.3389/fimmu.2018.00270

72. He W, He D, Gong L, Wang W, Yang L, Zhang Z, et al. Complexity of macrophage metabolism in infection. *Curr Opin Biotechnol* (2021) 68:231–9. doi: 10.1016/j.copbio.2021.01.020

73. Rodríguez-Prados JC, Través PG, Cuenca J, Rico D, Aragonés J, Martín-Sanz P, et al. Substrate fate in activated macrophages: a comparison between innate, classic, and alternative activation. *J Immunol* (2010) 185(1):605–14. doi: 10.4049/jimmunol.0901698

74. O'Neill LA, Kishton RJ, Rathmell J. A guide to immunometabolism for immunologists. *Nat Rev Immunol* (2016) 16(9):553–65. doi: 10.1038/nri.2016.70

75. Nagy C, Haschemi A. Time and demand are two critical dimensions of immunometabolism: The process of macrophage activation and the pentose phosphate pathway. *Front Immunol* (2015) 6:164. doi: 10.3389/fimmu.2015.00164

76. Liu Y, Xu R, Gu H, Zhang E, Qu J, Cao W, et al. Metabolic reprogramming in macrophage responses. *biomark Res* (2021) 9(1):1. doi: 10.1186/s40364-020-00251-y

77. Van den Bossche J, Baardman J, de Winther MP. Metabolic characterization of polarized M1 and M2 bone marrow-derived macrophages using real-time extracellular flux analysis. *J Vis Exp* (2015) 105:53424. doi: 10.3791/53424

78. Ip WKE, Hoshi N, Shouval DS, Snapper S, Medzhitov R. Anti-inflammatory effect of IL-10 mediated by metabolic reprogramming of macrophages. *Science* (2017) 356(6337):513–9. doi: 10.1126/science.aal3535

79. Freemerman AJ, Johnson AR, Sacks GN, Milner JJ, Kirk EL, Troester MA, et al. Metabolic reprogramming of macrophages: glucose transporter 1 (GLUT1)-mediated

glucose metabolism drives a proinflammatory phenotype. *J Biol Chem* (2014) 289 (11):7884–96. doi: 10.1074/jbc.M113.522037

80. Haschemi A, Kosma P, Gille L, Evans CR, Burant CF, Starkl P, et al. The sedoheptulose kinase CARKL directs macrophage polarization through control of glucose metabolism. *Cell Metab* (2012) 15(6):813–26. doi: 10.1016/j.cmet.2012.04.023

81. Palsson-McDermott EM, Curtis AM, Goel G, Lauterbach MA, Sheedy FJ, Gleeson LE, et al. Pyruvate kinase M2 regulates hif-1α activity and IL-1β induction and is a critical determinant of the warburg effect in LPS-activated macrophages. *Cell Metab* (2015) 21(1):65–80. doi: 10.1016/j.cmet.2014.12.005

82. Palsson-McDermott EM, Curtis AM, Goel G, Lauterbach MA, Sheedy FJ, Gleeson LE, et al. Pyruvate kinase M2 regulates hif-1α activity and IL-1β induction and is a critical determinant of the warburg effect in LPS-activated macrophages. *Cell Metab* (2015) 21(2):347. doi: 10.1016/j.cmet.2015.01.017

83. Luo W, Hu H, Chang R, Zhong J, Knabel M, O'Meally R, et al. Pyruvate kinase M2 is a PHD3-stimulated coactivator for hypoxia-inducible factor 1. *Cell* (2011) 145 (5):732–44. doi: 10.1016/j.cell.2011.03.054

84. Xie M, Yu Y, Kang R, Zhu S, Yang L, Zeng L, et al. PKM2-dependent glycolysis promotes NLRP3 and AIM2 inflammasome activation. *Nat Commun* (2016) 7:13280. doi: 10.1038/ncomms13280

85. Obach M, Navarro-Sabaté A, Caro J, Kong X, Duran J, Gómez M, et al. 6-Phosphofructo-2-kinase (pfkfb3) gene promoter contains hypoxia-inducible factor-1 binding sites necessary for transactivation in response to hypoxia. *J Biol Chem* (2004) 279(51):53562–70. doi: 10.1074/jbc.M406096200

86. Tan Z, Xie N, Cui H, Moellering DR, Abraham E, Thannickal VJ, et al. Pyruvate dehydrogenase kinase 1 participates in macrophage polarization via regulating glucose metabolism. *J Immunol* (2015) 194(12):6082–9. doi: 10.4049/jimmunol.1402469

87. Van den Bossche J, Baardman J, Otto NA, van der Velden S, Neele AE, van den Berg SM, et al. Mitochondrial dysfunction prevents repolarization of inflammatory macrophages. *Cell Rep* (2016) 17(3):684–96. doi: 10.1016/j.celrep.2016.09.008

88. Wang F, Zhang S, Vuckovic I, Jeon R, Lerman A, Folmes CD, et al. Glycolytic stimulation is not a requirement for M2 macrophage differentiation. *Cell Metab* (2018) 28(3):463–475.e4. doi: 10.1016/j.cmet.2018.08.012

89. Tavakoli S, Short JD, Downs K, Nguyen HN, Lai Y, Zhang W, et al. Differential regulation of macrophage glucose metabolism by macrophage colony-stimulating factor and granulocyte-macrophage colony-stimulating factor: Implications for (18)F FDG PET imaging of vessel wall inflammation. *Radiology* (2017) 283(1):87–97. doi: 10.1148/radiol.2016160839

90. Stincone A, Prigione A, Cramer T, Wamelink MM, Campbell K, Cheung E, et al. The return of metabolism: biochemistry and physiology of the pentose phosphate pathway. *Biol Rev Camb Philos Soc* (2015) 90(3):927–63. doi: 10.1111/brv.12140

91. Jha AK, Huang SC, Sergushichev A, Lampropoulou V, Ivanova Y, Loginicheva E, et al. Network integration of parallel metabolic and transcriptional data reveals metabolic modules that regulate macrophage polarization. *Immunity* (2015) 42(3):419–30. doi: 10.1016/j.immuni.2015.02.005

92. Blagih J, Jones RG. Polarizing macrophages through reprogramming of glucose metabolism. *Cell Metab* (2012) 15(6):793–5. doi: 10.1016/j.cmet.2012.05.008

93. Owen OE, Kalhan SC, Hanson RW. The key role of anaplerosis and cataplerosis for citric acid cycle function. *J Biol Chem* (2002) 277(34):30409–12. doi: 10.1074/jbc.R200006200

94. Ryan DG, O'Neill LAJ. Krebs Cycle reborn in macrophage immunometabolism. *Annu Rev Immunol* (2020) 38:289–313. doi: 10.1146/annurev-immunol-081619-104850

95. Tannahill GM, Curtis AM, Adamik J, Palsson-McDermott EM, McGettrick AF, Goel G, et al. Succinate is an inflammatory signal that induces IL-1β through HIF-1α. *Nature* (2013) 496(7444):238–42. doi: 10.1038/nature11986

96. O'Neill LA. A broken krebs cycle in macrophages. *Immunity* (2015) 42(3):393–4. doi: 10.1016/j.immuni.2015.02.017

97. Palmieri EM, Gonzalez-Cotto M, Baseler WA, Davies LC, Ghesquière B, Maio N, et al. Nitric oxide orchestrates metabolic rewiring in M1 macrophages by targeting aconitase 2 and pyruvate dehydrogenase. *Nat Commun* (2020) 11(1):698. doi: 10.1038/s41467-020-14433-7

98. Infantino V, Convertini P, Cucci L, Panaro MA, Di Noia MA, Calvello R, et al. The mitochondrial citrate carrier: a new player in inflammation. *Biochem J* (2011) 438 (3):433–6. doi: 10.1042/BJ20111275

99. Infantino V, Iacobazzi V, Menga A, Avantaggiati ML, Palmieri F. A key role of the mitochondrial citrate carrier (SLC25A1) in TNFα- and IFNγ-triggered inflammation. *Biochim Biophys Acta* (2014) 1839(11):1217–25. doi: 10.1016/j.bbagrm.2014.07.013

100. Infantino V, Iacobazzi V, Palmieri F, Menga A. ATP-citrate lyase is essential for macrophage inflammatory response. *Biochem Biophys Res Commun* (2013) 440 (1):105–11. doi: 10.1016/j.bbrc.2013.09.037

101. Dominguez M, Brüne B, Namgaladze D. Exploring the role of ATP-citrate lyase in the immune system. *Front Immunol* (2021) 12:632526. doi: 10.3389/fimmu.2021.632526

102. Covarrubias AJ, Aksoylar HI, Yu J, Snyder NW, Worth AJ, Iyer SS, et al. Akt-mTORC1 signaling regulates acly to integrate metabolic input to control of macrophage activation. *Elife* (2016) 5:e11612. doi: 10.7554/eLife.11612

103. Galván-Peña S, Carroll RG, Newman C, Hinchy EC, Palsson-McDermott E, Robinson EK, et al. Malonylation of GAPDH is an inflammatory signal in macrophages. *Nat Commun* (2019) 10(1):338. doi: 10.1038/s41467-018-08187-6

104. Duan JX, Jiang HL, Guan XX, Zhang CY, Zhong WJ, Zu C, et al. Extracellular citrate serves as a DAMP to activate macrophages and promote LPS-induced lung injury in mice. *Int Immunopharmacol* (2021) 101(Pt B):108372. doi: 10.1016/j.intimp.2021.108372

105. Luan HH, Medzhitov R. Food fight: Role of itaconate and other metabolites in antimicrobial defense. *Cell Metab* (2016) 24(3):379–87. doi: 10.1016/j.cmet.2016.08.013

106. Yu XH, Zhang DW, Zheng XL, Tang CK. Itaconate: an emerging determinant of inflammation in activated macrophages. *Immunol Cell Biol* (2019) 97(2):134–41. doi: 10.1111/imcb.12218

107. Li Y, Zhang P, Wang C, Han C, Meng J, Liu X, et al. Immune responsive gene 1 (IRG1) promotes endotoxin tolerance by increasing A20 expression in macrophages through reactive oxygen species. *J Biol Chem* (2013) 288(23):16225–34. doi: 10.1074/jbc.M113.454538

108. Lampropoulou V, Sergushichev A, Bambouskova M, Nair S, Vincent EE, Loginicheva E, et al. Itaconate links inhibition of succinate dehydrogenase with macrophage metabolic remodeling and regulation of inflammation. *Cell Metab* (2016) 24(1):158–66. doi: 10.1016/j.cmet.2016.06.004

109. Nair S, Huynh JP, Lampropoulou V, Loginicheva E, Esaulova E, Gounder AP, et al. Irg1 expression in myeloid cells prevents immunopathology during m. tuberculosis infection. *J Exp Med* (2018) 215(4):1035–45. doi: 10.1084/jem.20180118

110. Mills EL, Ryan DG, Prag HA, Dikovskaya D, Menon D, Zaslona Z, et al. Itaconate is an anti-inflammatory metabolite that activates Nrf2 via alkylation of KEAP1. *Nature* (2018) 556(7699):113–7. doi: 10.1038/nature25986

111. Bambouskova M, Gorvel L, Lampropoulou V, Sergushichev A, Loginicheva E, Johnson K, et al. Electrophilic properties of itaconate and derivatives regulate the IκBζ-ATF3 inflammatory axis. *Nature* (2018) 556(7702):501–4. doi: 10.1038/s41586-018-0052-z

112. Runtsch MC, Angiari S, Hooftman A, Wadhwa R, Zhang Y, Zheng Y, et al. Itaconate and itaconate derivatives target JAK1 to suppress alternative activation of macrophages. *Cell Metab* (2022) 34(3):487–501.e8. doi: 10.1016/j.cmet.2022.02.002

113. Mills EL, Kelly B, Logan A, Costa ASH, Varma M, Bryant CE, et al. Succinate dehydrogenase supports metabolic repurposing of mitochondria to drive inflammatory macrophages. *Cell* (2016) 167(2):457–470.e13. doi: 10.1016/j.cell.2016.08.064

114. He W, Miao FJ, Lin DC, Schwandner RT, Wang Z, Gao J, et al. Citric acid cycle intermediates as ligands for orphan G-protein-coupled receptors. *Nature* (2004) 429 (6988):188–93. doi: 10.1038/nature02488

115. Littlewood-Evans A, Sarret S, Apfel V, Loesle P, Dawson J, Zhang J, et al. GPR91 senses extracellular succinate released from inflammatory macrophages and exacerbates rheumatoid arthritis. *J Exp Med* (2016) 213(9):1655–62. doi: 10.1084/jem.20160061

116. Wang YH, Yan ZZ, Luo SD, Hu JJ, Wu M, Zhao J, et al. Gut microbiota-derived succinate aggravates acute lung injury after intestinal ischemia/reperfusion in mice. *Eur Respir J* (2022) 61(2):2200840. doi: 10.1183/13993003.00840-2022

117. Palmieri EM, Menga A, Martín-Pérez R, Quinto A, Riera-Domingo C, De Tullio , et al. Pharmacologic or genetic targeting of glutamine synthetase skews macrophages toward an M1-like phenotype and inhibits tumor metastasis. *Cell Rep* (2017) 20(7):1654–66. doi: 10.1016/j.celrep.2017.07.054

118. Odegaard JI, Ricardo-Gonzalez RR, Goforth MH, Morel CR, Subramanian V, Mukundan L, et al. Macrophage-specific PPARgamma controls alternative activation and improves insulin resistance. *Nature* (2007) 447(7148):1116–20. doi: 10.1038/nature05894

119. Davies LC, Rice CM, Palmieri EM, Taylor PR, Kuhns DB, McVicar DW, et al. Peritoneal tissue-resident macrophages are metabolically poised to engage microbes using tissue-niche fuels. *Nat Commun* (2017) 8(1):2074. doi: 10.1038/s41467-017-02092-0

120. Nelson VL, Nguyen HCB, Garcìa-Cañaveras JC, Briggs ER, Ho WY, DiSpirito JR, et al. PPARγ is a nexus controlling alternative activation of macrophages via glutamine metabolism. *Genes Dev* (2018) 32(15-16):1035–44. doi: 10.1101/gad.312355.118

121. Rath M, Müller I, Kropf P, Closs EI, Munder M. Metabolism via arginase or nitric oxide synthase: Two competing arginine pathways in macrophages. *Front Immunol* (2014) 5:532. doi: 10.3389/fimmu.2014.00532

122. Pourcet B, Pineda-Torra I. Transcriptional regulation of macrophage arginase 1 expression and its role in atherosclerosis. *Trends Cardiovasc Med* (2013) 23(5):143–52. doi: 10.1016/j.tcm.2012.10.003

123. Munder M. Arginase: an emerging key player in the mammalian immune system. *Br J Pharmacol* (2009) 158(3):638–51. doi: 10.1111/j.1476-5381.2009.00291.x

124. Shin NS, Marlier A, Xu L, Doilicho N, Linberg D, Guo J, et al. Arginase-1 is required for macrophage-mediated renal tubule regeneration. *J Am Soc Nephrol* (2022) 33(6):1077–86. doi: 10.1681/ASN.2021121548

125. Zhang J, Li Y, Duan Z, Kang J, Chen K, Li G, et al. The effects of the M2a macrophage-induced axonal regeneration of neurons by arginase 1. *Biosci Rep* (2020) 40(2):BSR20193031. doi: 10.1042/BSR20193031

126. Hardbower DM, Asim M, Murray-Stewart T, Casero RA, Jr. , Verriere T, Lewis ND, et al, et al. Arginase 2 deletion leads to enhanced M1 macrophage activation and upregulated polyamine metabolism in response to helicobacter pylori infection. *Amino Acids* (2016) 48(10):2375–88. doi: 10.1007/s00726-016-2231-2

127. Dowling JK, Afzal R, Gearing LJ, Cervantes-Silva MP, Annett S, Davis GM, et al. Mitochondrial arginase-2 is essential for IL-10 metabolic reprogramming of inflammatory macrophages. *Nat Commun* (2021) 12(1):1460. doi: 10.1038/s41467-021-21617-2

128. Laval T, Chaumont L, Demangel C. Not too fat to fight: The emerging role of macrophage fatty acid metabolism in immunity to mycobacterium tuberculosis. *Immunol Rev* (2021) 301(1):84–97. doi: 10.1111/imr.12952

129. Posokhova EN, Khoshchenko OM, Chasovskikh MI, Pivovarova EN, Dushkin MI. Lipid synthesis in macrophages during inflammation in vivo: effect of agonists of peroxisome proliferator activated receptors alpha and gamma and of retinoid X receptors. *Biochem (Mosc)* (2008) 73(3):296–304. doi: 10.1134/S0006297908030097

130. Khovidhunkit W, Kim MS, Memon RA, Shigenaga JK, Moser AH, Feingold KR, et al. Effects of infection and inflammation on lipid and lipoprotein metabolism: mechanisms and consequences to the host. *J Lipid Res* (2004) 45(7):1169–96. doi: 10.1194/jlr.R300019-JLR200

131. Feingold KR, Shigenaga JK, Kazemi MR, McDonald CM, Patzek SM, Cross AS, et al. Mechanisms of triglyceride accumulation in activated macrophages. *J Leukoc Biol* (2012) 92(4):829–39. doi: 10.1189/jlb.1111537

132. Lee JY, Sohn KH, Rhee SH, Hwang D. Saturated fatty acids, but not unsaturated fatty acids, induce the expression of cyclooxygenase-2 mediated through toll-like receptor 4. *J Biol Chem* (2001) 276(20):16683–9. doi: 10.1074/jbc.M011695200

133. Moon JS, Lee S, Park MA, Siempos II, Haslip M, Lee PJ, et al. UCP2-induced fatty acid synthase promotes NLRP3 inflammasome activation during sepsis. *J Clin Invest* (2015) 125(2):665–80. doi: 10.1172/JCI78253

134. Danielski LG, Giustina AD, Bonfante S, Barichello T, Petronilho F. The NLRP3 inflammasome and its role in sepsis development. *Inflammation* (2020) 43(1):24–31. doi: 10.1007/s10753-019-01124-9

135. Cader MZ, Boroviak K, Zhang Q, Assadi G, Kempster SL, Sewell GW, et al. C13orf31 (FAMIN) is a central regulator of immunometabolic function. *Nat Immunol* (2016) 17(9):1046–56. doi: 10.1038/ni.3532

136. Cader MZ, de Almeida Rodrigues RP, West JA, Sewell GW, Md-Ibrahim MN, Reikine S, et al. FAMIN is a multifunctional purine enzyme enabling the purine nucleotide cycle. *Cell* (2020) 180(2):278–295.e23. doi: 10.1016/j.cell.2019.12.017

137. Lahiri A, Hedl M, Yan J, Abraham C. Human LACC1 increases innate receptor-induced responses and a LACC1 disease-risk variant modulates these outcomes. *Nat Commun* (2017) 8:15614. doi: 10.1038/ncomms15614

138. Lv Q, Xing Y, Liu Y, Chen Q, Xu J, Hu L, et al. Didymin switches M1-like toward M2-like macrophage to ameliorate ulcerative colitis via fatty acid oxidation. *Pharmacol Res* (2021) 169:105613. doi: 10.1016/j.phrs.2021.105613

139. Hohensinner PJ, Lenz M, Haider P, Mayer J, Richter M, Kaun C, et al. Pharmacological inhibition of fatty acid oxidation reduces atherosclerosis progression by suppression of macrophage NLRP3 inflammasome activation. *Biochem Pharmacol* (2021) 190:114634. doi: 10.1016/j.bcp.2021.114634

140. Namgaladze D, Brüne B. Fatty acid oxidation is dispensable for human macrophage IL-4-induced polarization. *Biochim Biophys Acta* (2014) 1841(9):1329–35. doi: 10.1016/j.bbalip.2014.06.007

141. Du N, Lin H, Zhang A, Cao C, Hu X, Zhang J, et al. N-phenethyl-5-phenylpicolinamide alleviates inflammation in acute lung injury by inhibiting HIF-1α/glycolysis/ASIC1a pathway. *Life Sci* (2022) 309:120987. doi: 10.1016/j.lfs.2022.120987

142. Zhong WJ, Yang HH, Guan XX, Xiong JB, Sun CC, Zhang CY, et al. Inhibition of glycolysis alleviates lipopolysaccharide-induced acute lung injury in a mouse model. *J Cell Physiol* (2019) 234(4):4641–54. doi: 10.1002/jcp.27261

143. Liu QY, Zhuang Y, Song XR, Niu Q, Sun QS, Li XN, et al. Tanshinone IIA prevents LPS-induced inflammatory responses in mice via inactivation of succinate dehydrogenase in macrophages. *Acta Pharmacol Sin* (2021) 42(6):987–97. doi: 10.1038/s41401-020-00535-x

144. Lauterbach MA, Hanke JE, Serefidou M, Mangan MSJ, Kolbe CC, Hess T, et al. Toll-like receptor signaling rewires macrophage metabolism and promotes histone acetylation via ATP-citrate lyase. *Immunity* (2019) 51(6):997–1011.e7. doi: 10.1016/j.immuni.2019.11.009

145. Liu M, Chen Y, Wang S, Zhou H, Feng D, Wei J, et al. α-ketoglutarate modulates macrophage polarization through regulation of PPARγ transcription and mTORC1/p70S6K pathway to ameliorate ALI/ARDS. *Shock* (2020) 53(1):103–13. doi: 10.1097/SHK.0000000000001333

frontiers | Frontiers in Immunology

TYPE Original Research
PUBLISHED 30 March 2023
DOI 10.3389/fimmu.2023.1121237

OPEN ACCESS

EDITED BY
Miguel Angel Alejandre Alcazar,
University Hospital of Cologne, Germany

REVIEWED BY
Kathleen Bartemes,
Mayo Clinic, United States
Rohit Saluja,
AIIMS Bibinagar, India

*CORRESPONDENCE
Corrado Pelaia
pelaia.corrado@gmail.com

SPECIALTY SECTION
This article was submitted to Inflammation, a section of the journal Frontiers in Immunology

RECEIVED 11 December 2022
ACCEPTED 20 March 2023
PUBLISHED 30 March 2023

CITATION
Pelaia C, Benfante A, Busceti MT, Caiaffa MF, Campisi R, Carpagnano GE, Crimi N, D'Amato M, Foschino Barbaro MP, Maglio A, Minenna E, Nolasco S, Paglino G, Papia F, Pelaia G, Portacci A, Ricciardi L, Scichilone N, Scioscia G, Triggiani M, Valenti G, Vatrella A and Crimi C (2023) Real-life effects of dupilumab in patients with severe type 2 asthma, according to atopic trait and presence of chronic rhinosinusitis with nasal polyps. *Front. Immunol.* 14:1121237. doi: 10.3389/fimmu.2023.1121237

Real-life effects of dupilumab in patients with severe type 2 asthma, according to atopic trait and presence of chronic rhinosinusitis with nasal polyps

Corrado Pelaia[1*], Alida Benfante[2], Maria Teresa Busceti[1], Maria Filomena Caiaffa[3], Raffaele Campisi[4], Giovanna Elisiana Carpagnano[5], Nunzio Crimi[4], Maria D'Amato[6], Maria Pia Foschino Barbaro[3], Angelantonio Maglio[7], Elena Minenna[3], Santi Nolasco[4], Giuseppe Paglino[8], Francesco Papia[8], Girolamo Pelaia[1], Andrea Portacci[5], Luisa Ricciardi[9], Nicola Scichilone[2], Giulia Scioscia[3], Massimo Triggiani[7], Giuseppe Valenti[8], Alessandro Vatrella[7] and Claudia Crimi[4]

[1]Department of Health Sciences, University "Magna Graecia" of Catanzaro, Catanzaro, Italy, [2]Dipartimento di Promozione della Salute, Materno Infantile, Medicina Interna e Specialistica di Eccellenza (PROMISE), University of Palermo, Palermo, Italy, [3]Department of Medical and Surgical Sciences, University of Foggia, Foggia, Italy, [4]Department of Clinical and Experimental Medicine, University of Catania, Catania, Italy, [5]Department of Basic Medical Science, Neuroscience and Sense Organs, University "Aldo Moro", Bari, Italy, [6]Department of Respiratory Medicine, University "Federico II" of Naples, Naples, Italy, [7]Department of Medicine, Surgery and Dentistry, University of Salerno, Salerno, Italy, [8]Allergology and Pulmonology Unit, Provincial Outpatient Center of Palermo, Palermo, Italy, [9]Department of Clinical and Experimental Medicine, University of Messina, Messina, Italy

Background: The efficacy of dupilumab as biological treatment of severe asthma and chronic rhinosinusitis with nasal polyps (CRSwNP) depends on its ability to inhibit the pathophysiologic mechanisms involved in type 2 inflammation.

Objective: To assess in a large sample of subjects with severe asthma, the therapeutic impact of dupilumab in real-life, with regard to positive or negative skin prick test (SPT) and CRSwNP presence or absence.

Methods: Clinical, functional, and laboratory parameters were measured at baseline and 24 weeks after the first dupilumab administration. Moreover, a comparative evaluation was carried out in relation to the presence or absence of SPT positivity and CRSwNP.

Results: Among the 127 recruited patients with severe asthma, 90 had positive SPT, while 78 reported CRSwNP. Compared with the 6 months preceding the first dupilumab injection, asthma exacerbations decreased from 4.0 (2.0-5.0) to 0.0 (0.0-0.0) ($p < 0.0001$), as well as the daily prednisone intake fell from 12.50 mg (0.00-25.00) to 0.00 mg (0.00-0.00) ($p < 0.0001$). In the same period, asthma control test (ACT) score increased from 14 (10-18) to 22 (20-24) ($p < 0.0001$), and sino-nasal outcome test (SNOT-22) score dropped from 55.84 ±

10.3389/fimmu.2023.1121237

20.32 to 19.76 ± 12.76 ($p < 0.0001$). Moreover, we observed relevant increases in forced expiratory volume in one second (FEV1) from the baseline value of 2.13 L (1.62-2.81) to 2.39 L (1.89-3.06) ($p < 0.0001$). Fractional exhaled nitric oxide (FeNO) values decreased from 27.0 ppb (18.0-37.5) to 13.0 ppb (5.0-20.0) ($p < 0.0001$). These improvements were quite similar in subgroups of patients characterized by SPT negativity or positivity, and CRSwNP absence or presence. No statistically significant correlations were detected between serum IgE levels, baseline blood eosinophils or FeNO levels and dupilumab-induced changes, with the exception of FEV1 increase, which was shown to be positively correlated with FeNO values ($r = 0.3147$; $p < 0.01$).

Conclusion: Our results consolidate the strategic position of dupilumab in its role as an excellent therapeutic option currently available within the context of modern biological treatments of severe asthma and CRSwNP, frequently driven by type 2 airway inflammation.

KEYWORDS

severe asthma, nasal polyps, interleukin 4, interleukin 13, dupilumab, clinical remission

Introduction

Dupilumab is a completely human monoclonal antibody, belonging to the IgG4 immunoglobulin class, whose mechanism of action consists of the dual antagonism of the interleukin 4 (IL-4) and 13 (IL-13) receptors (1). In addition to the treatment of severe asthma and atopic dermatitis, dupilumab is also indicated for the biological therapy of nasal polyposis, which is a frequent comorbidity of severe asthma (2).

IL-4 and IL-13 play critical roles in the pathogenesis of severe type 2 asthma (3). In particular, IL-4 is crucial in the development and maintenance of the acquired immune response mediated by T helper 2 (Th2) lymphocytes. At the level of B lymphocytes of allergic patients, IL-4 and IL-13 induce the so-called isotypic switch, responsible for the synthesis of immunoglobulins E (IgE), which degranulate mast cells and basophils, facilitate the presentation of allergens by dendritic cells to T lymphocytes, and inhibit eosinophil apoptosis (4). IL-4 and IL-13 promote the trafficking of eosinophils to inflammatory sites and impair the integrity of the airway epithelial barrier. Furthermore, IL-13 stimulates mucus secretion and goblet cell hyperplasia, and also up-regulates the expression of the inducible form of the enzyme nitric oxide (NO) synthase (iNOS), which increases NO production within the airways (5, 6). Chronic rhinosinusitis with nasal polyps (CRSwNP) is a frequent comorbidity of severe asthma, and type 2 inflammation very often contributes significantly to the pathogenesis of nasal polyposis. Indeed, at the level of upper airways IL-4 and IL-13 play a key role in both inflammatory and structural changes (tissue remodelling) that underlie the formation of nasal polyps (7).

The efficacy of dupilumab as biological treatment of severe asthma and nasal polyposis depends on its remarkable ability to inhibit the pathophysiologic mechanisms involved in type 2 inflammation. In fact, dupilumab is an efficient dual antagonist of both IL-4 and IL-13 receptors 13 (3). Specifically, dupilumab binds with high affinity to the IL-4 receptor α subunit (IL-4Rα). This receptor subunit is a key component of the type I receptor, consisting of the IL-4Rα/γC dimer, which is activated by IL-4 (8). The type II receptor is instead constituted by the IL-4Rα subunit and the α1 chain of the IL-13 receptor (IL-4Rα/IL-13Rα1 dimer), and can therefore be stimulated by IL-4 and IL-13. The type I receptor is predominantly expressed by immune-inflammatory cells such as T and B lymphocytes, dendritic cells, monocytes/macrophages, mast cells, basophils and eosinophils. The type II receptor is also present on airway structural cells such as goblet cells, fibroblasts and smooth muscle cells (9). Upon pharmacological blockade of both type I and type II receptors, dupilumab neutralizes the biological effects of IL-4 and IL-13.

Due to this powerful mechanism of action, within the context of add-on biological treatment of severe asthma and nasal polyposis dupilumab exerts remarkable therapeutic effects, well documented by several randomized controlled trials (RCTs) (10). In particular, the "LIBERTY ASTHMA QUEST" study demonstrated that dupilumab was capable of significantly reducing the annual rate of severe asthma exacerbations and improving lung function (11). Furthermore, the "LIBERTY ASTHMA VENTURE" trial highlighted the ability of dupilumab to significantly decrease the consumption of oral corticosteroids (OCS) (12). These results were recently confirmed by the open-label extension study LIBERTY ASTHMA TRAVERSE, which further monitored for additional 96 weeks many patients previously enrolled in the LIBERTY ASTHMA

Abbreviations: SPT, skin prick test; CRSwNP, chronic rhinosinusitis with nasal polyps; IQR, interquartile range; SD, standard deviation; BMI, body mass index; ACT, asthma control test; FEV_1, forced expiratory volume in one second; FeNO, fractional exhaled nitric oxide.

QUEST and LIBERTY ASTHMA VENTURE (13). As regards the adjunctive biological therapy of nasal polyposis, the studies "LIBERTY NP SINUS-24" and "LIBERTY NP SINUS-52" documented the efficacy of dupilumab by evaluating the improvement of many relevant parameters (14).

However, only a few real-world studies referring to a quite low number of patients have been published so far (15–19). Hence, the aim of our present real-life observational investigation was to evaluate, in a larger sample of subjects with severe asthma, also including many patients with nasal polyposis, the therapeutic impact of dupilumab on upper and lower airway symptoms, severe asthma exacerbations, OCS intake and lung function, as well as on the overall clinical expression of nasal polyposis.

Patients and methods

Study design and patient enrollment

In the present retrospective multicenter observational study, we recruited adult outpatients (>18 years) with severe type 2 asthma treated with dupilumab. Subjects were enrolled at the following asthma centers: Respiratory Medicine Section, University "Aldo Moro", Bari, Italy; Allergy and Respiratory Medicine, University of Catania, Italy; Respiratory Disease Unit, University "Magna Graecia" of Catanzaro, Italy; Allergology and Clinical Immunology Unit, University of Foggia, Italy; Respiratory Disease Unit, University of Foggia, Italy; Allergy and Clinical Immunology Unit, University of Messina; Pulmonology Unit, "Monaldi" University Hospital, Naples, Italy; Pulmonology Unit, University of Palermo, Italy; Allergology and Pulmonology Unit, Provincial Outpatient Center of Palermo, Italy; Respiratory Disease Unit, University of Salerno, Italy; Division of Allergy and Clinical Immunology, University of Salerno.

Patients reported persistent asthmatic symptoms and required high doses of the inhaled therapeutic combinations ICS (inhaled corticosteroids)/LABA (long-acting β_2-adrenergic agonists), associated with a LAMA (long-acting muscarinic receptor antagonist). Enrollment took place consecutively, and the only inclusion criteria were those needed for prescription of dupilumab. All recruited patients met the European Respiratory Society (ERS)/American Thoracic Society (ATS) criteria defining severe uncontrolled asthma (20). Blood counts of eosinophils, basophils and neutrophils were obtained using automated hematology analyzers (21, 22). At baseline, all participants had an eosinophilic blood count of at least 150 cells/μL and/or fractional exhaled nitric oxide (FeNO) levels greater than 25 parts per billion (ppb), and/or they were treated with lifelong or near-continuous OCS therapies.

The aforementioned centers participating in the study used a shared database to acquire clinical, functional and biological data. Smoking habit and comorbidities such as gastroesophageal reflux disease (GERD), nasal polyposis, bronchiectasis, osteoporosis, anxiety, atopic dermatitis and obstructive sleep apnea syndrome (OSAS) were evaluated. Symptom control was assessed by administering to all recruited patients the asthma control test (ACT). The latter includes 5 key questions referring to the frequency of asthma symptoms and to the need of inhaled rescue medication during the previous 4 weeks (23). Each question scores from 1 to 5; therefore, ACT score ranges from 5 (worse control) to 25 points (complete control). Spirometry was performed following ATS/ERS guidelines (24). FeNO levels were measured in accordance with ATS/ERS recommendations (25, 26). Treatment with dupilumab was prescribed according to current eligibility guidelines, and the drug was administered subcutaneously using an initial dose of 600 mg (two 300 mg injections at different skin sites), followed by a maintenance dose of 300 mg every 2 weeks (27, 28).

This observational study met the standards of Good Clinical Practice (GCP) and the principles of the Declaration of Helsinki. All recruited patients signed a written informed consent. Our study was also conducted in accordance with the provisions of the local Ethics Committee of Calabria Region, Italy (Catanzaro, Italy; document n. 182 – 20 May 2021).

Outcomes and measurements

The main purpose of this real-life study was to evaluate the efficacy of dupilumab in daily clinical practice. The number of asthma exacerbations, emergency department visits and daily inhalations of short-acting β_2-adrenergic agonists (SABA), as well as prednisone intake, ACT score, sino-nasal outcome test questionnaire (SNOT-22), the number of relapses of nasal polyposis, forced expiratory volume in one second (FEV_1), forced vital capacity (FVC), mean forced expiratory flow between 25% and 75% of FVC (FEF_{25-75}), FeNO levels, as well as blood eosinophil, basophil, and neutrophil counts were assessed at baseline and 24 weeks after the first dupilumab administration.

A secondary objective was to retrospectively verify the therapeutic responses of our patients to dupilumab, in relation to SPT positivity or negativity, as well as with regard to the presence or absence of CRSwNP. The diagnosis of CRSwNP was formulated on the basis of symptoms, nasal endoscopy and computed tomography (CT) (29, 30). Skin prick test (SPT) was performed by placing a drop of each allergen on the forearm evidenced with a skin marker, and each drop was pricked by a sterile lancet; skin sensitivity was determined by comparing any wheal with that one caused by histamine (31).

Furthermore, after 6 months of adjunctive therapy with dupilumab we analyzed the possible correlations existing between the baseline concentrations of serum IgE, FeNO and blood eosinophils, and the observed changes regarding asthma exacerbations, daily consumption of prednisone and SABA, ACT score, SNOT-22 score, FEV_1, FVC, and FEF_{25-75} values.

In addition, the occurrence of unwanted side effects was investigated on the basis of available information stored in clinical records.

Statistical analysis

All data are expressed as mean ± standard deviation (SD) if normally distributed, otherwise as median values with the interquartile range (IQR). The normality of data distribution was checked using Anderson-Darling and Kolmogorov-Smirnov tests. Paired t-test and Mann-Whitney's U-test for paired data were used to compare variables when appropriate. The latter statistical test was also used for the secondary objective of the study, i.e. the comparative evaluation of dupilumab efficacy in patients with positive or negative SPT, and with regard to the presence or absence of CRSwNP. Fisher's test was applied to compare categorical variables. The association between baseline concentrations of type 2 inflammation biomarkers (serum IgE, blood eosinophils, and FeNO) and changes in clinical and functional parameters was assessed using linear regression analysis. In particular, the correlation index R for Spearman's ranks was evaluated. A p-value less than 0.05 (two-tailed) was considered as statistically significant. Statistical analyses and figures were performed using Prism Version 9.4.0 software (GraphPad Software Inc., San Diego, California, USA).

Results

Efficacy of dupilumab in the whole population

A total of 127 participants were recruited, including 63 (49.6%) women and 64 (50.4%) men, with a median age of 56.0 years (45.0-64.0), and a median body mass index (BMI) value of 26.0 Kg/m^2 (23.0-30.0). Mean baseline FEV_1 was 76.56 ± 20.03% of predicted value. Among the enrolled patients, 90 (70.9%) had positive SPT for perennial and/or seasonal allergens, while 78 (61.4%) reported CRSwNP. Baseline patient characteristics are summarized in Table 1.

Compared with the 6-month pre-treatment period (before the first injection of dupilumab), the median number of asthma

TABLE 1 Baseline patient characteristics, stratified according SPT negativity or positivity and CRSwNP absence or presence.

Characteristic	Overall N = 127	SPT - N = 37	SPT + N = 90	p	CRSwNP - N = 49	CRSwNP + N = 78	p
Female gender, N (%)	63 (49.6)	13 (35.1)	50 (55.6)	< 0.05	27 (55.1)	36 (46.2)	0.3651
Male gender, N (%)	64 (50.4)	24 (64.9)	40 (44.4)	< 0.05	22 (44.9)	42 (53.8)	0.3651
Age, median values (IQR), years	56.0 (45.0-64.0)	59.0 (54.0-69.0)	55.0 (43.0-63.3)	< 0.05	54.0 (45.0-63.0)	56.5 (45.0-65.3)	0.6326
Age of asthma onset, median values (IQR), years	30.0 (20.0-44.0)	44.0 (31.5-58.0)	25.5 (18.0-40.0)	< 0.0001	35.0 (20.0-48.5)	30.0 (19.8-42.0)	0.5924
Duration of asthma, median values (IQR), years	17.0 (10.0-30.0)	10.0 (8.0-20.0)	20.0 (14.0-33.0)	< 0.01	10.0 (6.0-21.0)	20.0 (14.0-33.3)	< 0.001
BMI, median values (IQR), Kg/m^2	26.0 (23.0-30.0)	25.6 (23.3-27.0)	27.0 (23.2-30.1)	0.2436	27.0 (25.0-31.1)	25.2 (23.0-28.4)	0.1730
Exacerbations, median values (IQR), N	4.0 (2.0-5.0)	3.5 (2.0-5.0)	4.0 (2.0-5.0)	0.6830	3.0 (2.0-5.0)	4.0 (2.0-5.0)	0.1124
Prednisone, median values (IQR), mg/day	12.50 (0.00-25.00)	6.75 (0.00-12.50)	12.50 (0.00-25.00)	0.0899	5.00 (0.00-12.50)	12.50 (3.75-25.00)	< 0.01
ACT score, median values (IQR)	14 (10-18)	16 (14-18)	13 (9-17)	< 0.01	15 (11-18)	14 (10-17)	0.2057
FEV_1, mean values (SD), % predicted	76.56 (20.03)	77.75 (17.64)	76.07 (21.01)	0.6730	76.28 (17.41)	76.73 (21.58)	0.9038
FeNO, median values, (IQR), ppb	27.0 (18.0-37.5)	20.0 (9.5-33.0)	29.0 (20.0-40.0)	0.0675	29.0 (19.0-44.0)	25.0 (16.0-35.0)	0.3369
Blood eosinophils, median values, (IQR), cells/μL	400.0 (210.0-680.0)	410.0 (177.5-780.0)	399.0 (230.0-610.0)	0.9638	415.0 (222.3-734.8)	399.0 (200.0-640.0)	0.6567
Gastro-esophageal reflux disease, N (%)	56 (44.1)	15 (40.5)	41 (45.6)	0.6954	19 (38.8)	37 (47.4)	0.3640
Atopy, N (%)	90 (70.9)	0 (0.00)	90 (100)	< 0.0001	35 (71.4)	55 (70.5)	> 0.9999
CRSwNP, N (%)	78 (61.4)	23 (62.2)	55 (61.1)	> 0.9999	0 (0.00)	78 (100)	< 0.0001
Bronchiectasis, N (%)	22 (17.3)	7 (18.9)	15 (16.7)	0.7987	4 (8.2)	18 (23.1)	< 0.05
Osteoporosis, N (%)	25 (19.7)	7 (18.9)	18 (20.0)	0.6410	5 (10.2)	20 (25.6)	< 0.05
Anxiety, N (%)	32 (25.2)	7 (18.9)	25 (27.8)	0.3713	5 (10.2)	27 (34.6)	< 0.01
Dermatitis, N (%)	14 (11.0)	0 (0.00)	14 (15.6)	< 0.05	6 (12.2)	8 (10.3)	0.7755
Obstructive sleep apnea syndrome, N (%)	13 (10.2)	0 (0.00)	13 (14.4)	< 0.05	6 (12.2)	7 (8.9)	0.5618

SPT, skin prick test; CRSwNP, chronic rhinosinusitis with nasal polyps; IQR, interquartile range; SD, standard deviation; BMI, body mass index; ACT, asthma control test; FEV1, forced expiratory volume in one second; FeNO, fractional exhaled nitric oxide.

exacerbations dramatically decreased from 4.0 (2.0-5.0) to 0.0 (0.0-0.0) ($p < 0.0001$) after 6 months of anti-IL4R/IL-13R therapy (Figure 1A). Furthermore, in the same period the mean number of emergency department (ED) visits (0.40 ± 0.75 vs. 0.0 ± 0.0; $p < 0.0001$) (Figure 1B) and daily SABA inhalations (1.67 ± 1.59 vs. 0.09 ± 0.39; $p < 0.0001$) also significantly fell down (Figure 1C). These therapeutic effects allowed a reduction of the daily prednisone intake from 12.50 mg (0.00-25.00) to 0.00 mg (0.00-0.00) ($p < 0.0001$) (Figure 1D). In addition, the percentage of patients taking daily OCS decreased from 66.9% (before starting dupilumab treatment) to 5.5% after six months of therapy. After 24 weeks of treatment with dupilumab, ACT score increased significantly from a baseline value of 14 (10-18) to 22 (20-24) ($p < 0.0001$) (Figure 1E), and SNOT-22 score dropped from 55.84 ± 20.32 to 19.76 ± 12.76 ($p < 0.0001$) (Figure 1F) in subjects also suffering from nasal polyposis. Furthermore, in this subset of patients the number of recurrences of nasal polyposis decreased from 2 (1-2.5) to 0 (0-0) ($p < 0.0001$) after initiation of dupilumab therapy (Figure 1G). In addition to the above clinical results, we also observed a significant improvement in respiratory function, documented by increases in FEV_1 from the baseline value of 2.13 L (1.62-2.81) to 2.39 L (1.89-3.06) ($p < 0.0001$) (Figure 1H), in FVC from 3.16 L (2.43-3.84) to 3.36 L (2.68-3.92) ($p < 0.0001$) (Figure 1I), and in FEF_{25-75} from 46.50% (30.75-69.00) to 63.50% (44.75-81.25) ($p < 0.0001$) of predicted values (Figure 1J). Furthermore, serum IgE levels lowered from 238.0 IU/mL (81.0-499.0) to 160.0 IU/mL (49.0-450.0) ($p < 0.0001$) (Figure 1K). In the same observation period FeNO values decreased from 27.0 ppb (18.0-37.5) to 13.0 ppb (5.0-20.0) ($p < 0.0001$) (Figure 1L). Regarding the possible hematological effects of dupilumab, after six months of additional treatment, the blood eosinophil count did not undergo substantial variations, thus changing from 400.0 cells/μL (222.5-677.5) to 395.0 cells/μL (181.5-565.0) ($p = 0.427$) (Figure 1M). Similarly, blood basophil and neutrophil values did not change significantly, going from 40.0 cells/μL (30.0-60.0) to 37.5 cells/μL (20.0-60.0) ($p = 0.068$) (Figure 1N), and from 4705.0 cells/μL (3635.0-5423.0) to 4500.0 cells/μL (4000.0-5250.0) ($p = 0.396$) (Figure 1O), respectively.

Moreover, after a six-month treatment with dupilumab, when considering the key variables of clinical remission that include evaluation of asthma symptoms (ACT score ≥20), optimization of lung function (FEV_1 ≥80% of predicted value), zeroing of exacerbations and OCS (zero exacerbations and zero OCS use) (32, 33), 47.24% of enrolled patients satisfied these criteria.

Efficacy of dupilumab in different type 2 asthma phenotypes

Improvements in clinical, functional, and hematological parameters after six months of dupilumab treatment were quite similar in subgroups of patients characterized by SPT negativity or positivity, respectively. Specifically, the decrease in the number of asthma exacerbations was -3.00 (from -4.00 to -0.50) in patients with negative SPT and -4.00 (from -5.00 to -2.00) in subjects with positive SPT, respectively ($p = 0.158$) (Figure 2A). The daily dose of prednisone decreased by -5.00 mg (from -12.50 to 0.00) in patients

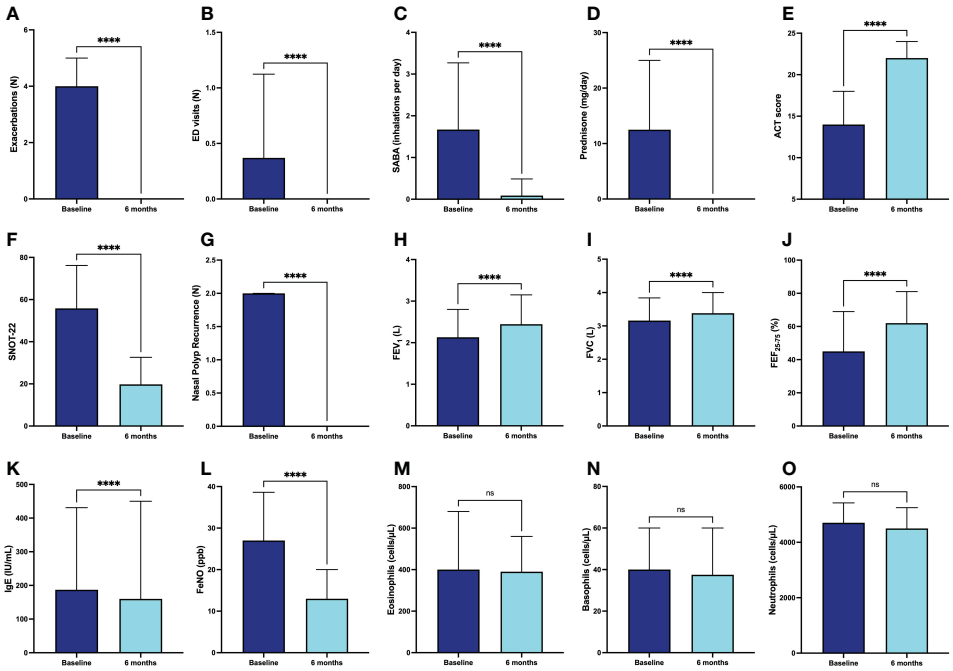

FIGURE 1
Efficacy of dupilumab in the whole population of patients with severe asthma, with regard to asthma exacerbations **(A)**, ED visits **(B)**, daily SABA inhalations **(C)**, prednisone intake **(D)**, ACT score **(E)**, SNOT-22 **(F)**, nasal polyp recurrence **(G)**, FEV1 **(H)**, FVC **(I)**, FEF25-75 **(J)**, IgE **(K)**, FeNO **(L)**, blood eosinophils **(M)**, blood basophils **(N)**, and blood neutrophils **(O)**. Values of ED visits, daily SABA inhalations and SNOT-22 are expressed as mean (± SD). All other parameters are expressed as median values (IQR). **** $p < 0.0001$; ns, not significant.

with negative SPT and -12.5 mg (from -25.00 to 0.00) in subjects with positive SPT, respectively (p = 0.136) (Figure 2B). The median changes in ACT score were 7 points (5-10) and 7 points (4-12) in patients with negative and positive SPT, respectively (p = 0.690) (Figure 2C). The mean increase in FEV_1 was 0.20 L (0.00-0.48) in patients with negative SPT and 0.20 L (0.01-0.62) in subjects with positive SPT; this difference was not statistically significant (p = 0.409) (Figure 2D). Six months after the first dupilumab injection, the increase in FEF_{25-75} was 12.00% (3.75-19.50) in patients with negative SPT and 11.00% (0.00-29.00) in subjects with positive SPT, respectively (p = 0.827) (Figure 2E). Furthermore, the reduction of FeNO levels was -8.00 ppb (from -16.17 to -1.75) in patients with negative SPT and -19.00 ppb (from -29.25 to -9.00) in subjects with positive SPT, but in this case the difference overcame the threshold of statistical significance (p < 0.01) (Figure 2F).

No statistically significant correlations were detected between either serum IgE levels or baseline blood eosinophils, and dupilumab-induced changes in the following parameters: reduction in asthma exacerbations (Figures 3A, 4A), decrease in daily prednisone dose (Figures 3B, 4B), increases in ACT score (Figures 3C, 4C), FEV_1 (Figures 3D, 4D), FVC (Figures 3E, 4E), and FEF_{25-75} (Figures 3F, 4F).

In addition, when considering the above parameters, no correlations were also found between baseline FeNO levels and dupilumab-induced changes (Figures 5A–C, E, F), with the exception of FEV_1 increases, which were shown to be positively correlated with FeNO values (r = 0.3147; p < 0.01) (Figure 5D).

Efficacy of dupilumab in patients with or without CRSwNP

The improvements in clinical and functional parameters observed after six months of treatment with dupilumab were quite similar in the subgroups of patients characterized by the absence or presence of CRSwNP, respectively. In particular, the decrease in the number of asthma exacerbations was -3.00 (-5.00 to -1.50) in patients without CRSwNP and -4.00 (-5.00 to -2.00) in subjects with CRSwNP, respectively (p = 0.413) (Figure 6A). The daily dose of prednisone decreased by -5.00 mg (from -12.50 to 0.00) in patients without CRSwNP and -12.5 mg (from -25.00 to 0.00) in subjects with CRSwNP, respectively (p < 0.05) (Figure 6B). The increase in ACT score was 7 points (4-10) and 7 points (4-11) in patients without or with CRSwNP, respectively (p = 0.422) (Figure 6C). The mean increase in FEV_1 was 0.15 L (-0.01-0.49) in patients without CRSwNP, and 0.24 L (0.01-0.69) in subjects with CRSwNP; this difference was not statistically significant (p = 0.138) (Figure 6D). Six months after the first dupilumab injection, the increase in FEF_{25-75} was 11.00% (2.00-21.00) in patients without CRSwNP and 12.00% (1.25-29.75) in subjects with CRSwNP, respectively (p = 0.479) (Figure 6E). Furthermore, the reduction in FeNO levels was -10.51 ppb (-23.50 to -1.00) in patients without CRSwNP and -17.00 ppb (-28.00 to -7.50) in subjects with CRSwNP, respectively, but in this case the difference reached the threshold of statistical significance (p < 0.05) (Figure 6F).

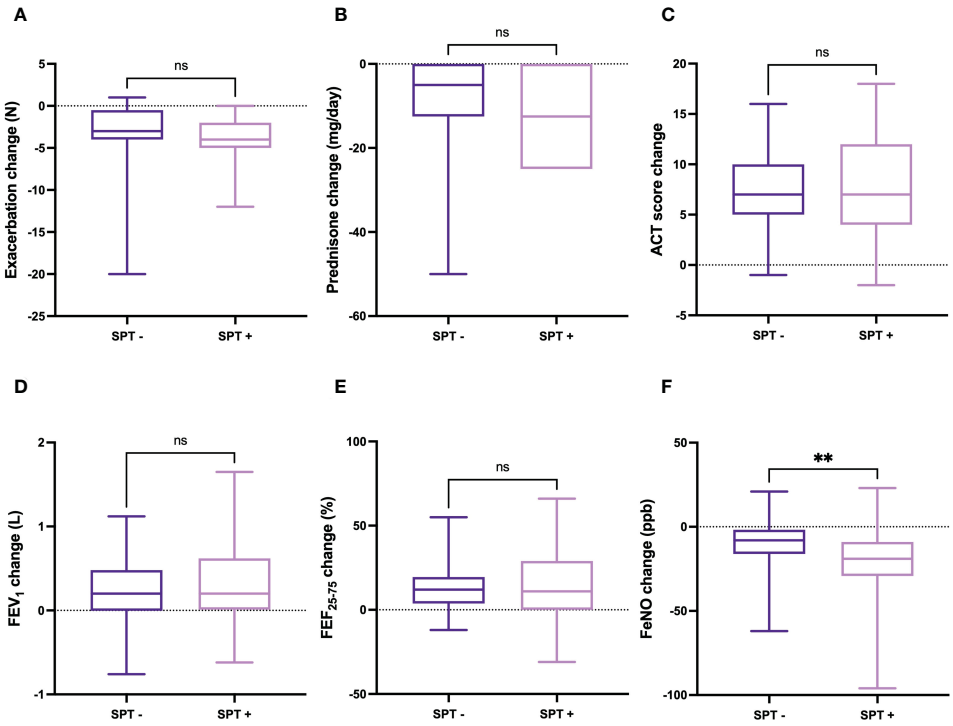

FIGURE 2
Comparative evaluation of dupilumab effects in relation to SPT negativity or positivity, with regard to asthma exacerbations **(A)**, prednisone intake **(B)**, ACT score **(C)**, FEV1 **(D)**, FEF25-75 **(E)**, and FeNO levels **(F)**. Boxes display median values and IQR, and whiskers define maximum and minimum. ns, not significant; ** p < 0.01.

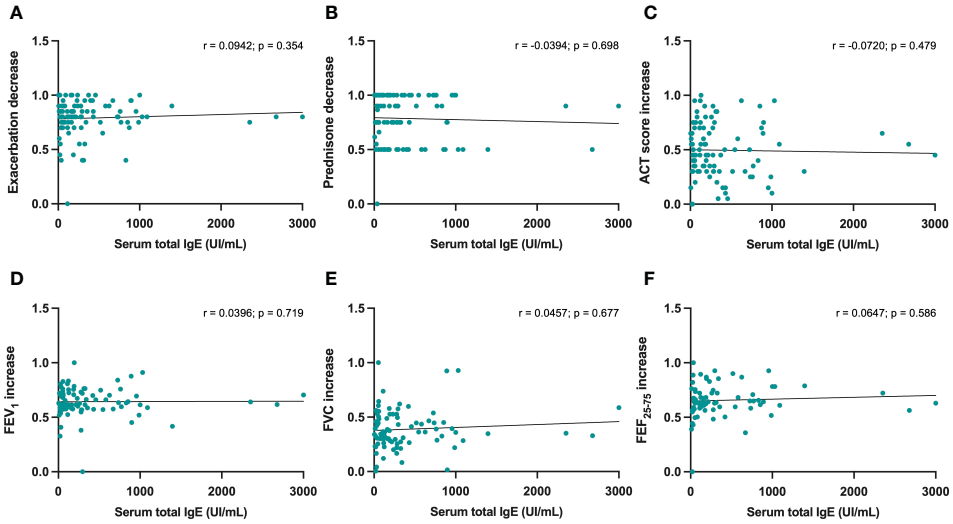

FIGURE 3
Correlations between serum IgE concentrations and 6-month changes induced by dupilumab, with regard to asthma exacerbations **(A)**, prednisone intake **(B)**, ACT score **(C)**, FEV1 **(D)**, FVC **(E)**, and FEF25-75 **(F)**.

Safety and tolerability profile of dupilumab

Add-on biological treatment with dupilumab was well tolerated, and no serious adverse reactions were observed during this real-world investigation. With regard to mild and transient side effects, increases in blood eosinophil counts with no symptoms were found in 5 (3.94%) subjects, 4 (3.15%) cases of conjunctivitis were reported, 2 (1.57%) injection site reactions were detected, and 1 (0.79%) patient experienced headache. All these mild side effects remitted spontaneously and did not require any specific treatment.

Discussion

Taken together, the results of the present multicenter real-life study, performed in patients with severe asthma and frequent nasal polyposis, show that dupilumab induced relevant therapeutic effects. Firstly, six months of treatment with this biologic drug cleared asthma exacerbations. This made it possible to effectively prevent any access to the emergency room, the use of short-acting bronchodilators as needed, and the intake of OCS. The latter aspect is of considerable importance as it further exceeds the efficacy data

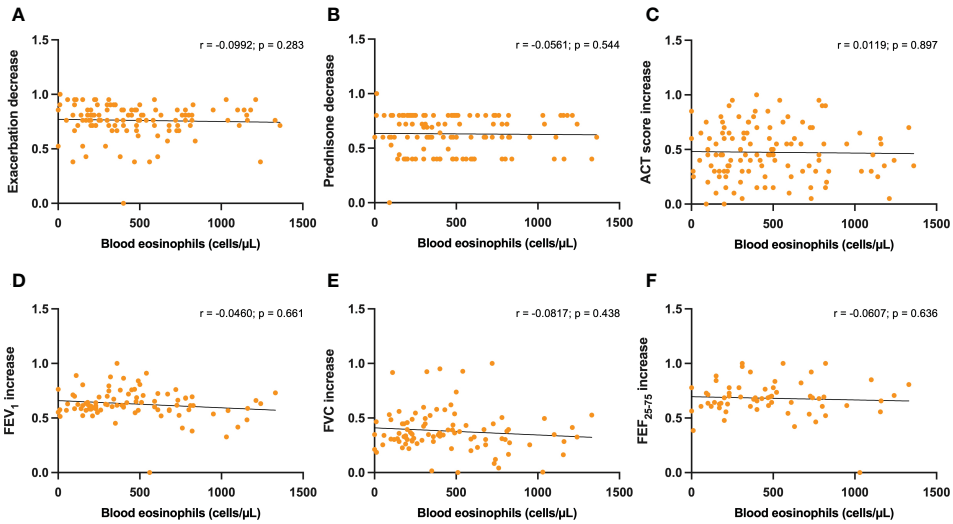

FIGURE 4
Correlations between blood eosinophils and 6-month changes induced by dupilumab, with regard to asthma exacerbations **(A)**, prednisone intake **(B)**, ACT score **(C)**, FEV1 **(D)**, FVC **(E)**, and FEF25-75 **(F)**.

10.3389/fimmu.2023.1121237

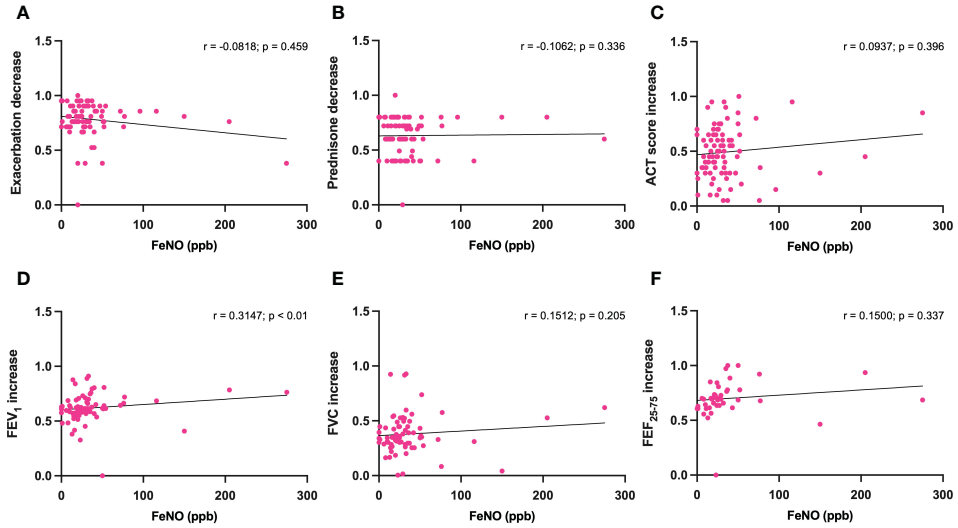

FIGURE 5
Correlations between FeNO levels and 6-month changes induced by dupilumab, with regard to asthma exacerbations **(A)**, prednisone intake **(B)**, ACT score **(C)**, FEV1 **(D)**, FVC **(E)**, and FEF25-75 **(F)**.

reported by the Liberty Asthma VENTURE trial (12). Indeed, VENTURE authors reported that 52.4% of patients interrupted OCS after 24 weeks of treatment with dupilumab, whereas after the same period of time OCS withdrawal was achieved by 92.9% of our steroid-dependent patients. The relevance of zeroing the use of OCS is closely related to the possibility of abrogating the well-known side effects of oral corticosteroid therapy, including adrenal insufficiency, respiratory infections, diabetes mellitus, arterial hypertension, osteoporosis, glaucoma and cataract (34, 35).

When compared to QUEST (Q) and VENTURE (V) trials, other important differences with our real-life study regard the baseline characteristics of recruited patients. In particular, we

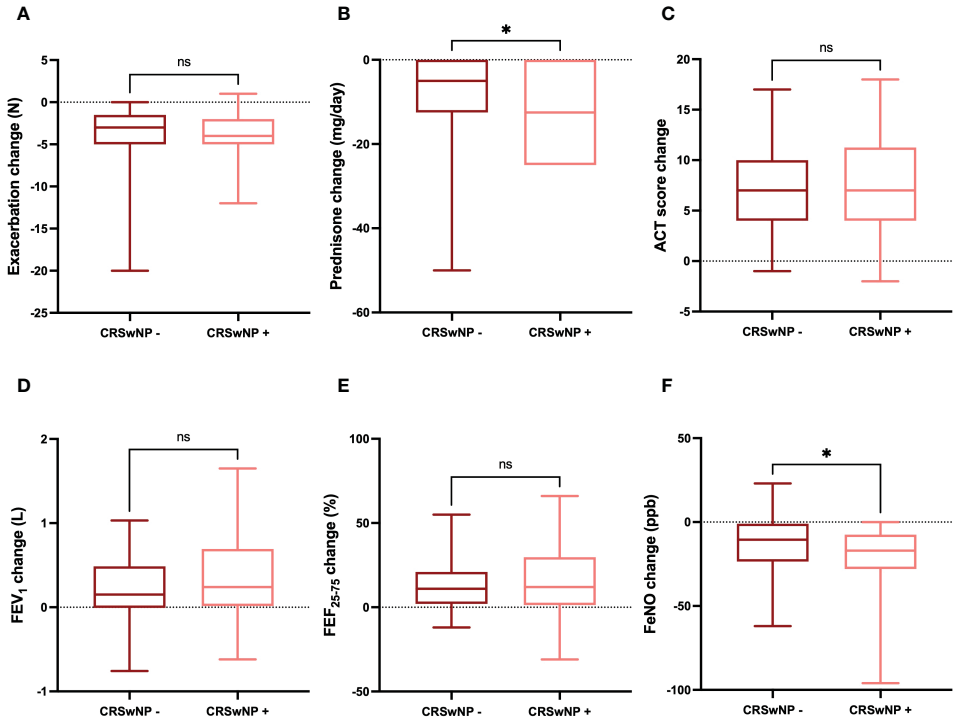

FIGURE 6
Comparative evaluation of dupilumab effects in relation to CRSwNP absence or presence, with regard to asthma exacerbations **(A)**, prednisone intake **(B)**, ACT score **(C)**, FEV1 **(D)**, FEF25-75 **(E)**, and FeNO levels **(F)**. Boxes display median values and IQR, and whiskers define maximum and minimum. ns, not significant; * $p < 0.05$.

enrolled a population of asthmatic subjects with a greater percentage of male patients (50.4% vs. Q 37.8% and V 39.8%, respectively), a higher number of asthma exacerbations (4.00 vs. Q 2.02 and V 2.01, respectively), a greater blood eosinophil count (400.0 cells/μL vs. Q 250 cells/μL and V 280 cells/μL, respectively), and especially a much higher percentage of patients presented with CRSwNP (61.4% vs. Q 22.9% and V 32.0%, respectively).

Dupilumab significantly reduced asthma symptoms, as demonstrated by the significant increase in ACT score, which after 24 weeks of biological therapy reached and exceeded the threshold of 20, which expresses a satisfactory control of asthma symptoms, despite the baseline pre-treatment score stood at a rather low value of 14. This result confirms, in a real-life context, the data reported by the Liberty Asthma QUEST trial, in which the ACQ (Asthma Control Questionnaire) was utilized. However, compared to the ACQ test, the ACT questionnaire administered by us seems to be more appropriate to respond to the needs of practicality and easiness of completion wished by patients who refer to our severe asthma assessment centers. In fact, ACT is clearly preferred to ACQ in the few real-life studies that have recently evaluated the efficacy of dupilumab in the biological therapy of severe asthma (15–19).

In patients with both asthma and nasal polyposis, dupilumab elicited a significant improvement in the score of SNOT-22 questionnaire. In such a group of subjects, this result was associated with a complete prevention of the relapses of nasal polyposis. These findings corroborate in a real-life setting the efficacy of dupilumab in the treatment of CRSwNP, previously demonstrated by the Liberty NP trials SINUS-24 and SINUS-52 (14).

In addition to the clinical effects, the results of our study regarding the respiratory function are also of marked relevance. Indeed, after 6 months of therapy dupilumab significantly increased FEV_1, and also incremented FVC and FEF_{25-75}. These findings indicate that dupilumab can improve lung function by increasing airway patency from the central proximal sector to the distal periphery of the respiratory tree. The clinical and functional results of the present observational study strongly suggest that clinical remission was achieved by a relevant number of our patients. Although this very important therapeutic target should be evaluated after 12 months of continuous treatment, already after 6 months we noticed that 47.24% of our patients reached the criteria of clinical remission, including significant improvements in asthma exacerbations, OCS intake, symptom control and lung function (32, 33). Such a real-life observation further confirms that dupilumab is characterized by a very fast onset of its therapeutic action, as already shown by previous data referring to the short-term clinical, functional and biological effects of this monoclonal antibody (18, 36). However, a few weeks of observation do not allow to assess the effects of dupilumab on severe asthma exacerbations. Thus, we decided to prolong up to 6 months the last time point for evaluation of dupilumab efficacy. Indeed, this approach made it possible to appreciate the impressive reduction of asthma exacerbations induced by dupilumab.

With regard to the biomarkers of type 2 inflammation, dupilumab dramatically reduced the concentration of FeNO. This outcome is closely linked to the ability of dupilumab to antagonize at the receptor level the biological activities of IL-4 and IL-13, the latter being responsible for the induction of iNOS expression in the bronchial epithelium (37, 38). Indeed, it is reasonable that inhibition of iNOS-dependent FeNO production, induced by dupilumab in airway epithelial cells, leads to relevant decrements of FeNO levels. FeNO is a reliable indicator of type 2 inflammation, and FeNO levels correlate with asthma severity, deterioration of respiratory function, and risk of asthma exacerbations (39). Furthermore, FeNO represents a valuable aid in guiding the choice and monitoring of biological treatments for severe asthma, within the context of a personalized therapeutic approach, based on the treatable traits pertinent to specific inflammatory pheno-endotypes (40).

Hence, the efficacy of dupilumab in inhibiting the pathobiologic mechanisms underlying type 2 inflammation, strongly dependent on IL-4 and IL-13 actions, explains the extension of the therapeutic effects of this monoclonal antibody to both asthma and nasal polyposis in our patients. In fact, asthma and CRSwNP share common cellular and molecular pathogenic substrates (41), which outline a very good responsiveness to dupilumab. In our observational investigation, the add-on biological therapy with dupilumab provided similar patterns of efficacy in allergic and non-allergic patients, suffering from severe asthma and possibly also from nasal polyposis. Indeed, dupilumab induced overlapping clinical and functional effects in subjects characterized by positive or negative skin prick tests. This is probably due to the specific properties of the mechanism of action of dupilumab, which by blocking IL-4 and IL-13 receptors effectively intercepts the pathogenic pathways responsible for type 2 inflammation sustained by either allergic or non-allergic traits. In particular, by neutralizing the biological activities of IL-4 and IL-13, dupilumab inhibits the functions of the main cells producing these cytokines, including Th2 lymphocytes and type 2 innate lymphoid cells (ILC2) (42). In this way dupilumab interrupts the close interactions between innate immunity and acquired adaptive immunity, mediated by the intercellular crosstalk between ILC2 and Th2 cells, which underlies the development and progression of type 2 inflammation characterizing many cases of severe asthma and nasal polyposis, driven by either allergic or non-allergic events (41, 43, 44).

Another interesting aspect of our real-life study concerns the finding of a greater decrease in FeNO values detected in allergic patients, compared to non-allergic ones. This result suggests that patients characterized by a higher expression of multiple endotypic traits referable to type 2 inflammation, respond to dupilumab treatment by experiencing a greater decrement in FeNO levels. On the other hand, IL-4 and IL-13 are intensely involved in the cellular pathophysiology of type 2 inflammation, which could imply an enhanced predisposition of allergic patients to dupilumab-induced FeNO reduction. Furthermore, we did not detect significant correlations between serum IgE levels and the clinical and functional effects of dupilumab, whose therapeutic activity does not appear to be affected by the presence or absence of an atopic state. In our case series, the clinical and functional effects of dupilumab also occurred without substantial differences among severe asthmatic patients who presented or did not manifest the

comorbidity of nasal polyposis. However, compared to patients without nasal polyps, we observed a greater reduction in FeNO values in subjects with severe asthma and concomitant nasal polyposis. This suggests that patients characterized by type 2 inflammation involving both upper and lower airways are more susceptible to the therapeutic action of dupilumab. Therefore, it is plausible to speculate that the coexistence of severe asthma and nasal polyposis could be associated with a higher expression of IL-4 and IL-13 in the airways of patients reporting both these diseases, who would therefore respond to dupilumab with a more relevant decrease in FeNO levels. Finally, our real-life evaluation shows an excellent tolerability and safety profile of dupilumab, which did not induce significant adverse events. Differently from what occurred in some individuals recruited in the Liberty Asthma QUEST and Liberty Asthma VENTURE trials, though not confirmed by the open label extension TRAVERSE study, no increases in blood levels of eosinophils were found in our patients. Based on the specific mechanism of action of dupilumab, it is thus possible to explain the lack of effects of this drug on the number of blood eosinophils, as we report. In fact, dupilumab acts as a highly efficient dual receptor antagonist of IL-4 and IL-13, but does not interfere with the biological activity of IL-5, which is the main cytokine responsible for the maturation, activation, proliferation and survival of eosinophils (45).

In conclusion, the present observational study confirms and expands, in the real-life of pulmonary clinical practice, the data reported by randomized controlled trials investigating the efficacy of dupilumab in the treatment of severe asthma. In particular, we herein show that after 6 months of treatment this biological therapy had a very positive impact on asthma exacerbations, OCS consumption, symptom control in both asthma and nasal polyposis, respiratory function and FeNO levels. Such findings have been recently extended up to one year by the results of other real-world clinical investigations (46–48). In addition, we also detected these therapeutic benefits in both allergic and non-allergic patients, as well as in asthmatics with or without nasal polyposis. Therefore, our results further consolidate the strategic position of dupilumab in its role as an excellent therapeutic option currently available within the context of modern biological treatments of severe asthma and CRSwNP, frequently driven by type 2 airway inflammation.

Data availability statement

The raw data supporting the conclusions of this article will be made available by the authors, without undue reservation.

Ethics statement

The studies involving human participants were reviewed and approved by Local Ethics Committee of Calabria Region, Italy (Catanzaro, Italy; document n. 182 – 20 May 2021). The patients/participants provided their written informed consent to participate in this study.

Author contributions

All authors contributed to data analysis, drafting or revising the article, have agreed on the journal to which the article will be submitted, gave final approval of the version to be published, and agree to be accountable for all aspects of the work.

Acknowledgments

Collaborators: Enrico Buonamico: Department of Basic Medical Science, Neuroscience and Sense Organs, University “Aldo Moro”, Bari, Italy; Vitaliano Quaranta: Department of Basic Medical Science, Neuroscience and Sense Organs, University “Aldo Moro”, Bari, Italy; Pietro Impellizzeri: Department of Clinical and Experimental Medicine, University of Catania, Catania, Italy; Serena Brancato: Department of Clinical and Experimental Medicine, University of Catania, Catania, Italy; Morena Porto: Department of Clinical and Experimental Medicine, University of Catania, Catania, Italy; Rossella Intravaia: Department of Clinical and Experimental Medicine, University of Catania, Catania, Italy; Nicola Lombardo: Department of Medical and Surgical Sciences, University “Magna Graecia” of Catanzaro, Catanzaro, Italy; Giovanna Lucia Piazzetta: Department of Medical and Surgical Sciences, University “Magna Graecia” of Catanzaro, Catanzaro, Italy; Stefania Caccavelli: Department of Medical and Surgical Sciences, University of Foggia, Foggia, Italy; Luciana D’Elia: Department of Medical and Surgical Sciences, University of Foggia, Foggia, Italy; Luca Gammeri: Department of Clinical and Experimental Medicine, University of Messina, Messina, Italy; Claudio Candia: Department of Respiratory Medicine, University “Federico II” of Naples, Naples, Italy; Eliana Sferra: Department of Respiratory Medicine, University “Federico II” of Naples, Naples, Italy; Claudia Gagliani: Allergology and Pulmonology Unit, Provincial Outpatient Center of Palermo, Palermo, Italy; Maria Noemi Cicero: PROMISE Department, University of Palermo, Palermo, Italy; Alessandra Tomasello: PROMISE Department, University of Palermo, Palermo, Italy; Isabella Carrieri: Department of Medicine, Surgery and Dentistry, University of Salerno, Salerno, Italy; Luigi Ciampo: Department of Medicine, Surgery and Dentistry, University of Salerno, Salerno, Italy; Carolina Vitale: Department of Medicine, Surgery and Dentistry, University of Salerno, Salerno, Italy.

Conflict of interest

The authors declare that the research was conducted in the absence of any commercial or financial relationships that could be construed as a potential conflict of interest.

Publisher's note

References

1. Pelaia C, Pelaia G, Crimi C, Maglio A, Stanziola AA, Calabrese C, et al. Novel biological therapies for severe asthma endotypes. *Biomedicines* (2022) 10(5):1064. doi: 10.3390/biomedicines10051064

2. Global Initiative for Asthma. *GINA report: Global strategy for asthma management and prevention* (2022). Available at: https://ginasthma.org/gina-reports (Accessed November 14, 2022).

3. Pelaia C, Vatrella A, Gallelli L, Terracciano R, Navalesi P, Maselli R, et al. Dupilumab for the treatment of asthma. *Expert Opin Biol Ther* (2017) 17:1565–72. doi: 10.1080/14712598.2017.1387245

4. Ricciardolo FLM, Bertolini F, Carriero V. The role of dupilumab in severe asthma. *Biomedicines* (2021) 9:1096. doi: 10.3390/biomedicines9091096

5. Corren J. Role of interleukin-13 in asthma. *Curr Allergy Asthma Rep* (2013) 13:415–20. doi: 10.1007/s11882-013-0373-9

6. Firszt R, Francisco D, Church TD, Thomas JM, Ingram JL, Kraft M. Interleukin-13 induces collagen type-1 expression through matrix metalloproteinase-2 and transforming growth factor-β_1 in airway fibroblasts in asthma. *Eur Respir J* (2014) 43:464–73. doi: 10.1183/09031936.00068712

7. Gandhi NA, Bennett BL, Graham NM, Pirozzi G, Stahl N, Yancopoulos GD. Targeting key proximal drivers of type 2 inflammation in disease. *Nat Rev Drug Discovery* (2016) 15:35–50. doi: 10.1038/nrd4624

8. Wills-Karp M, Finkelman FD. Untangling the complex web of IL-4- and IL-13-mediated signaling pathways. *Sci Signal* (2008) 1:pe55. doi: 10.1126/scisignal.1.51.pe55

9. Kelly-Welch AE, Hanson EM, Boothby MR, Keegan AD. Interleukin-4 and interleukin-13 signaling connections maps. *Science* (2003) 300:1527–8. doi: 10.1126/science.1085458

10. Pelaia C, Heffler E, Crimi C, Maglio A, Vatrella A, Pelaia G, et al. Interleukins 4 and 13 in asthma: Key pathophysiologic cytokines and druggable molecular targets. *Front Pharmacol* (2022) 13:851940. doi: 10.3389/fphar.2022.851940

11. Castro M, Corren J, Pavord ID, Maspero J, Wenzel S, Rabe KF, et al. Dupilumab efficacy and safety in moderate-to-severe uncontrolled asthma. *N Engl J Med* (2018) 378:2486–96. doi: 10.1056/NEJMoa1804092

12. Rabe KF, Nair P, Brusselle G, Maspero JF, Castro M, Sher L, et al. Efficacy and safety of dupilumab in glucocorticoid-dependent severe asthma. *N Engl J Med* (2018) 378:2475–85. doi: 10.1056/NEJMoa1804093

13. Wechsler ME, Ford LB, Maspero JF, Pavord ID, Papi A, Bourdin A, et al. Long-term safety and efficacy of dupilumab in patients with moderate-to-severe asthma (TRAVERSE): an open-label extension study. *Lancet Respir Med* (2022) 10:11–25. doi: 10.1016/S2213-2600(21)00322-2

14. Bachert C, Han JK, Desrosiers M, Hellings PW, Amin N, Lee SE, et al. Efficacy and safety of dupilumab in patients with severe chronic rhinosinusitis with nasal polyps (LIBERTY NP SINUS-24 and LIBERTY NP SINUS-52): Results from two multicentre, randomised, double-blind, placebo-controlled, parallel-group phase 3 trials. *Lancet* (2019) 394:1638–50. doi: 10.1016/S0140-6736(19)31881-1

15. Dupin C, Belhadi D, Guilleminault L, Gamez AS, Berger P, De Blay F, et al. Effectiveness and safety of dupilumab for the treatment of severe asthma in a real-life French multi-centre adult cohort. *Clin Exp Allergy* (2020) 50:789–98. doi: 10.1111/cea.13614

16. Nettis E, Patella V, Lombardo C, Detoraki A, Macchia L, Di Leo E, et al. Efficacy of dupilumab in atopic comorbidities associated with moderate-to-severe adult atopic dermatitis. *Allergy* (2020) 10:2653–61. doi: 10.1111/all.14338

17. Campisi R, Crimi C, Nolasco S, Beghè B, Antonicelli L, Guarnieri G, et al. Real-world experience with dupilumab in severe asthma: one-year data from an Italian named patient program. *J Asthma Allergy* (2021) 14:575–83. doi: 10.2147/JAA.S312123

18. Pelaia C, Lombardo N, Busceti MT, Piazzetta G, Crimi C, Calabrese C, et al. Short-term evaluation of dupilumab effects in patients with severe asthma and nasal polyposis. *J Asthma Allergy* (2021) 14:1165–72. doi: 10.2147/JAA.S328988

19. Numata T, Araya J, Miyagawa H, Okuda K, Takekoshi D, Hashimoto M, et al. Real-world effectiveness of dupilumab for patients with severe asthma: A retrospective study. *J Asthma Allergy* (2022) 15:395–405. doi: 10.2147/JAA.S357548

20. Chung KF, Wenzel SE, Brozek JL, Bush A, Castro M, Sterk PJ, et al. International ERS/ATS guidelines on definition, evaluation and treatment of severe asthma. *Eur Respir J* (2014) 43:343–73. doi: 10.1183/09031936.00202013

21. Laufer P, Chryssanthopoulos C, Laufer R, Hause LL. The determination of the eosinophil count: comparison of two techniques. *J Allergy Clin Immunol* (1987) 79:438–41. doi: 10.1016/0091-6749(87)90360-5

22. Borzova E, Dahinden CA. The absolute basophil count. *Methods Mol Biol* (2014) 1192:87–100. doi: 10.1007/978-1-4939-1173-8_7

23. Nathan RA, Sorkness CA, Kosinski M, Schatz M, Li JT, Marcus P, et al. Development of the asthma control test: A survey for assessing asthma control. *J Allergy Clin Immunol* (2004) 113(1):59–65. doi: 10.1016/j.jaci.2003.09.008

24. Graham BL, Steenbruggen I, Miller MR, Barjaktarevic IZ, Cooper BG, Hall GL, et al. Standardization of spirometry 2019 update. an official American thoracic society and European respiratory society technical statement. *Am J Respir Crit Care Med* (2019) 200:e70–88. doi: 10.1164/rccm.201908-1590ST

25. American Thoracic Society and European Respiratory Society. ATS/ERS recommendations for standardized procedures for the online and offline measurement of exhaled lower respiratory nitric oxide and nasal nitric oxide, 2005. *Am J Respir Crit Care Med* (2005) 171:912–30. doi: 10.1164/rccm.200406-710ST

26. Horváth I, Barnes PJ, Loukides S, Sterk PJ, Högman M, Olin AC, et al. A European respiratory society technical standard: Exhaled biomarkers in lung disease. *Eur Respir J* (2017) 49:1600965. doi: 10.1183/13993003.00965-2016

27. Wenzel S, Castro M, Corren J, Maspero J, Wang L, Zhang B, et al. Dupilumab efficacy and safety in adults with uncontrolled persistent asthma despite use of medium-to-high-dose inhaled corticosteroids plus a long-acting β_2 agonist: a randomised double-blind placebo-controlled pivotal phase 2b dose-ranging trial. *Lancet* (2016) 388:31–44. doi: 10.1016/S0140-6736(16)30307-5

28. Muñoz-Bellido FJ, Moreno E, Dávila I. Dupilumab: A review of present indications and off-label uses. *J Investig Allergol Clin Immunol* (2022) 32(2):97–115. doi: 10.18176/jiaci.0682

29. Fokkens WJ, Lund VJ, Mullol J, Bachert C, Alobid I, Baroody F, et al. EPOS 2012: European position paper on rhinosinusitis and nasal polyps 2012. A summary for otorhinolaryngologists. *Rhinology* (2012) 50:1–12. doi: 10.4193/Rhino12.000

30. Lombardo N, Pelaia C, Ciriolo M, Della Corte M, Piazzetta G, Lobello N, et al. Real-life of benralizumab on allergic chronic rhinosinusitis and nasal polyposis associated with severe asthma. *Int J Immunopathol Pharmacol* (2020) 34:2058738420950851. doi: 10.1177/2058738420950851

31. Malling HJ. Skin prick testing and the use of histamine references. *Allergy* (1984) 39:596–601. doi: 10.1111/j.1398-9995.1984.tb01979.x

32. Menzies-Gow A, Bafadhel M, Busse WW, Casale TB, Kocks JWH, Pavord ID, et al. An expert consensus framework for asthma remission as a treatment goal. *J Allergy Clin Immunol* (2020) 145(3):757–65. doi: 10.1016/j.jaci.2019.12.006

33. Thomas D, McDonald VM, Pavord ID, Gibson PG. Asthma remission: what is it and how can it be achieved? *Eur Respir J* (2022) 60(5):2102583. doi: 10.1183/13993003.02583-2021

34. Heffler E, Blasi F, Latorre M, Menzella F, Paggiaro P, Pelaia G, et al. The severe asthma network in Italy: findings and perspectives. *J Allergy Clin Immunol Pract* (2019) 7:1462–8. doi: 10.1016/j.jaip.2018.10.016

35. Canonica GW, Colombo GL, Bruno GM, Di Matteo S, Martinotti C, Blasi F, et al. Shadow cost of oral corticosteroids-related adverse events: A pharmacoeconomic evaluation applied to real-life data from the severe asthma network in Italy (SANI) registry. *World Allergy Organ J* (2019) 12:100007. doi: 10.1016/j.waojou.2018.12.001

36. Canonica GW, Bourdin A, Peters AT, Desrosiers M, Bachert C, Weidinger S, et al. Dupilumab demonstrates rapid onset of response across three type 2 inflammatory diseases. *J Allergy Clin Immunol Pract* (2022) 10(6):1515–26. doi: 10.1016/j.jaip.2022.02.026

37. Busse WW, Kraft M, Rabe KF, Deniz Y, Rowe PJ, Ruddy M, et al. Understanding the key issues in the treatment of uncontrolled persistent asthma with type 2 inflammation. *Eur Respir J* (2021) 58:2003393. doi: 10.1183/13993003.03393-2020

38. Carr TF, Kraft M. Use of biomarkers to identify phenotypes and endotypes of severe asthma. *Ann Allergy Asthma Immunol* (2018) 121:414–20. doi: 10.1016/j.anai.2018.07.029

39. Ulrik CS, Lange P, Hilberg O. Fractional exhaled nitric oxide as a determinant for the clinical course of asthma: A systematic review. *Eur Clin Respir J* (2021) 8:1891725. doi: 10.1080/20018525.2021.1891725

40. Rolla G, Heffler E, Pizzimenti S. An emerging role for exhaled nitric oxide in guiding biological treatment in severe asthma. *Curr Med Chem* (2020) 27:7159–67. doi: 10.2174/0929867327666200713184659

41. Scadding GK, Scadding GW. Innate and adaptive immunity: ILC2 and Th2 cells in upper and lower airway allergic diseases. *J Allergy Clin Immunol Pract* (2021) 9:1851–7. doi: 10.1016/j.jaip.2021.02.013

42. Hammad H, Lambrecht BN. The basic immunology of asthma. *Cell* (2021) 184:1469–85. doi: 10.1016/j.cell.2021.02.016

43. Rodriguez-Rodriguez N, Gogoi M, McKenzie ANJ. Group 2 innate lymphoid cells: team players in regulating asthma. *Annu Rev Immunol* (2021) 39:167–98. doi: 10.1146/annurev-immunol-110119-091711

44. Matucci A, Bormioli S, Nencini F, Maggi E, Vultaggio A. The emerging role of type 2 inflammation in asthma. *Expert Rev Clin Immunol* (2021) 17:63–71. doi: 10.1080/1744666X.2020.1860755

45. Pelaia C, Paoletti G, Puggioni F, Racca F, Pelaia G, Canonica GW, et al. Interleukin-5 in the pathophysiology of severe asthma. *Front Physiol* (2019) 10:1514. doi: 10.3389/fphys.2019.01514

46. Thelen JC, van Zelst CM, van Brummelen SE, Rauh S, In 't Veen JCCM, Kappen JH, et al. Efficacy and safety of dupilumab as add-on therapy for patients with severe asthma: A real-world Dutch cohort study. *Respir Med* (2023) 206:107058. doi: 10.1016/j.rmed.2022.107058

47. Ottaviano G, Saccardo T, Roccuzzo G, Bernardi R, Chicco AD, Pendolino AL, et al. Effectiveness of dupilumab in the treatment of patients with uncontrolled severe CRSwNP: A "Real-life" observational study in naïve and post-surgical patients. *J Pers Med* (2022) 12(9):1526. doi: 10.3390/jpm12091526

48. De Corso E, Settimi S, Montuori C, Corbò M, Passali GC, Porru DP, et al. Effectiveness of dupilumab in the treatment of patients with severe uncontrolled CRSwNP: A "Real-life" observational study in the first year of treatment. *J Clin Med* (2022) 11(10):2684. doi: 10.3390/jcm11102684

frontiers | Frontiers in Immunology

TYPE Original Research
PUBLISHED 05 May 2023
DOI 10.3389/fimmu.2023.1162087

OPEN ACCESS

EDITED BY
Adan Chari Jirmo,
Hannover Medical School, Germany

REVIEWED BY
Yves Laumonnier,
University of Lübeck, Germany
Antje Munder,
Hannover Medical School, Germany

*CORRESPONDENCE
Yi Li
peach_adore@hotmail.com;
liyi@wchscu.cn
Weimin Li
weimi003@scu.edu.cn

RECEIVED 09 February 2023
ACCEPTED 19 April 2023
PUBLISHED 05 May 2023

CITATION
Li Y, Yang Y, Guo T, Weng C, Yang Y, Wang Z, Zhang L and Li W (2023) Heme oxygenase-1 determines the cell fate of ferroptotic death of alveolar macrophages in COPD. *Front. Immunol.* 14:1162087. doi: 10.3389/fimmu.2023.1162087

Heme oxygenase-1 determines the cell fate of ferroptotic death of alveolar macrophages in COPD

Yi Li[1]*, Ying Yang[1], Tingting Guo[1], Chengxin Weng[2], Yongfeng Yang[1], Zhoufeng Wang[1], Li Zhang[1] and Weimin Li[1]*

[1]Department of Respiratory and Critical Care Medicine, Institute of Respiratory Health, Precision Medicine Key Laboratory, West China Hospital, Sichuan University, Chengdu, China, [2]Department of Vascular Surgery, West China Hospital, Sichuan University, Chengdu, China

Background: Despite an increasing understanding of chronic obstructive pulmonary disease (COPD) pathogenesis, the mechanisms of diverse cell populations in the human lung remain unknown. Using single-cell RNA sequencing (scRNA-Seq), we can reveal changes within individual cell populations in COPD that are important for disease pathogenesis and characteristics.

Methods: We performed scRNA-Seq on lung tissue obtained from donors with non-COPD and mild-to-moderate COPD to identify disease-related genes within different cell types. We testified the findings using qRT–PCR, immunohistochemistry, immunofluorescence and Western blotting from 25 additional subjects and RAW 264.7 macrophages. Targeting ferroptosis with the ferroptosis inhibitor ferrostatin-1, iron chelator deferoxamine or HO-1 inhibitor zinc protoporphyrin was administered in the experimental cigarette smoke COPD mouse model.

Results: We identified two populations of alveolar macrophages (AMs) in the human lung that were dysregulated in COPD patients. We discovered that M2-like AMs modulate susceptibility to ferroptosis by disrupting lipid and iron homeostasis both in vivo and in vitro. The discrepancy in sensitivity to ferroptosis can be determined and regulated by HO-1. In contrast, M1-like AMs showed the ability to attenuate oxidative stress and exert resistance to ferroptosis. In addition, the expression of genes within M2-like AMs is also involved in defects in phagocytosis and lysosome distortion. This ferroptotic phenotype was ameliorated by antiferroptotic compounds, iron chelators and HO-1 inhibitors. During COPD, the accumulation of lipid peroxidation drives ferroptosis-sensitive M2-like AMs, while M1-like AMs show characteristics of ferroptosis resistance. Ferroptotic M2 AMs lose their anti-inflammatory and repair functions but provoke inflammatory responses, resulting in consistent inflammation and tissue damage in the presence of M1 AMs in COPD.

Conclusion: Appropriate interventions in ferroptosis can reduce the occurrence of infections and acute onset, and delay the COPD process.

KEYWORDS

chronic obstructive pulmonary disease (COPD), RNA sequencing, alveolar macrophages (AMs), ferroptosis, immune response

Introduction

Iron-dependent cell death known as ferroptosis was initially detected in cancer cells in 2012 by Dixon et al. (1). In the absence of apoptotic hallmarks, this mode of cell death induced by erastin and RSL3 was found to be nonapoptotic and termed. It is characterized by (phospho)lipid peroxidation caused by reactive oxygen species (ROS) during iron-mediated Fenton reactions. Ferroptosis is regulated by glutathione peroxidase 4 (GPX4) by directly converting lipid hydroperoxides (L-OOH) to nontoxic lipid alcohols (L-OH) (2). Aberrant regulation of ferroptosis has been implicated in disease pathogenesis and development in the kidney (3), brain (4, 5), liver (6) and lung (7). Recently, protection by ferroptosis inhibitors such as ferrostatin-1 (fer-1) and liproxstatin-1 was also proposed for use in neurodegenerative disease (8–10).

Chronic obstructive pulmonary disease (COPD) is currently the fourth leading cause of morbidity and mortality in the world and is predicted to be the third leading cause of death. It is characterized by chronic airway inflammation, lung destruction and remodeling, resulting in irreversible airflow obstruction (11). Cigarette smoke (CS) exposure is the main risk factor for COPD due to its high concentration of ROS. The consequent cellular oxidative stress provokes inflammation, cell senescence and death. However, although cigarette and other tobacco smoking is the leading environmental risk factor, less than 50% of heavy smokers develop COPD during their lifetime (12, 13). Early studies have demonstrated that accumulated iron and ferritin and increased serum ferritin and nonheme iron were observed in lung epithelial cells and alveolar macrophages during exposure to CS. Recently, a report demonstrated CS-induced ferroptosis in human lung epithelial cells *in vitro* and *in vivo* (14). The experiments revealed the phenomenon of an inverse relationship between ferritin and nuclear receptor coactivator 4 (NCOA4), as well as the negative regulation of GPX4 in epithelial cells. However, the contribution of ferroptosis in other cell types remains unknown. Notably, alveolar macrophages (AMs), which act as innate immune modulators, display a crucial switch in inflammation, cell death and aging, tissue proliferation and repair in COPD pathogenesis. For instance, triggered macrophages amplify the inflammatory process by secreting cytokines and mediators and cause tissue damage by generating and releasing ROS (15, 16). One of the most striking features of AMs in COPD patients is the complexity of the polarization and coexpression of M1 (activated state) and M2 (alternatively activated state) markers (17, 18). In the aspect of functionality, AMs from patients with COPD showed disability in clearing apoptotic cells or bacteria (19, 20), but the nature of this defect in phagocytosis is currently not fully understood. While CS-induced inflammation initiated by the accumulation of lipids in AMs after pulmonary damage has been previously reported (21), a system-wide approach to evaluate AMs in COPD remains to be performed.

The heme oxygenase 1 (HO-1) protein, which is encoded by the *Hmox-1* gene, is known to be an inducible cytoprotective enzyme that copes with oxidative stress. HO-1 catalyzes the first and rate-limiting step in the oxidative degradation of heme to generate biliverdin IXα, carbon monoxide (CO), and ferrous iron (22). Numerous studies have demonstrated that HO-1 and its reaction products can display antioxidant, antiapoptotic, and immunomodulatory effects (23–25). The protective role of HO-1 and CO on inflammation occurs in diseases such as neurodegenerative diseases (26, 27), high-fat induced liver injury and ethanol-induced liver (28, 29), obesity and cardiovascular disease (30), and endothelial injury (31, 32). Deficiency of *Bach1*, a repressor of *Hmox-1*, protected mice from hyperoxic lung injury (33, 34). Studies have reported that the expression of HO-1 is induced in mild COPD compared to smokers without COPD and explained by its potential protective role against ROS-mediated cell senescence and mitochondrial dysfunction. However, this hypothesis has been challenged and not clearly demonstrated. Researchers recently found that HO-1 acts as a critical mediator in ferroptosis induction and plays a causative role in the progression of several diseases; for example, in renal epithelial cells and proximal tubule cells, HO-1 downregulation was associated with ferroptosis, while HO-1 overexpression inhibited ferroptosis (35). On the other hand, overactivation of HO-1 may become detrimental and cytotoxic due to increased intracellular iron, which also induces ferroptosis. The two-sided effect implicates HO-1 in conferring protection or enhancing vulnerability. The complex role of HO-1 in ferroptosis is controversial due to its antiferroptotic or ferroptotic effects *in vitro* and *in vivo*.

In recent years, investigators have used single-cell RNA sequencing technology (scRNA-Seq) to develop an organ-based transcriptomic map of the human body linked to cell populations. The advent of scRNA-Seq allows for the identification of novel and rare cell populations (36, 37) and provides the opportunity to assess the heterogeneity of gene expression in individual cell populations during health and disease (38). Here, in the present study, we report the extensive profiling of whole cells in the lungs by scRNA-Seq of 34572 cells in smokers without COPD and mild-to-moderate COPD patients. We observed a variety of cell types and discovered discrepancies in lipid accumulation and loss of iron homeostasis, leading to peroxidation and ferroptosis in AMs in patients with COPD. We also revealed defects in phagocytosis and lysosome distortion in these cells by analysis of genetic interactions. Our findings reveal an important role of alveolar macrophages in COPD and may guide the design of new strategies for clinical therapeutics aimed at restoring homeostasis.

Materials and methods

Human lung tissue collection

Lung resection specimens were obtained from patients who underwent surgery for solitary pulmonary tumors in West China Hospital. Lung tissue was collected at the maximum distance of the tumor. COPD was diagnosed according to the Global Initiative for Chronic Obstructive Lung Disease (GOLD) guidelines before surgery. The patients were divided into three subgroups: 1. Smokers without COPD (n=4), 2. Mild COPD patients (GOLD stage I) (n=4), and 3. Moderate COPD patients (GOLD stage II) (n=4). Clinical information on the patients is shown in Table S1. All

subjects were enrolled with informed consent from West China Hospital of Sichuan University, China. All patients received surgical treatment, and none of them underwent neoadjuvant therapy before surgery. Cancer clinical stage was matched according to the 8th edition of the American Joint Committee on Cancer (AJCC) TNM staging system. This study was approved by the Ethics Committee of West China Hospital, Sichuan University (project identification code: 2018.270).

Lung tissue dissociation and single-cell sorting

Lung tissue was transported in Hank's balanced salt solution (HBSS, Life Technologies) on ice immediately after surgery. Half of the tissue was embedded, and the rest was cut into 1-mm^3 pieces and digested with collagenase I (2 mg/mL) and IV; (1 mg/mL) in a 15 mL conical tube (BD Falcon) at 37°C for 30 min on a tube revolver (Thermo) with frequent agitation. All samples were then filtered through 70 µm and 40 µm nylon mesh filters (BD Biosciences) and centrifuged at 4°C at 400 x g for 5 min. The cell pellet was suspended in red blood cell lysis buffer, centrifuged and resuspended in PBS with 0.04% FBS. Following dissociation, single-cell suspensions were stained with 7-aminoactinomycin D (7-AAD) in a dark room for 15 min before being analyzed by flow cytometry for live-cell sorting with a MoFloAstrios EQ (Beckman Coulter). Cell suspensions were added to the Master Mix to achieve a final number of 8000 cells per reaction for scRNA-seq.

ScRNA-Seq library preparation and sequencing

For scRNA-seq, single-cell suspensions were converted to barcoded scRNA-seq libraries using the Chromium Single Cell 3' Library, Gel Bead & Multiplex Kit and Chip Kit (10x Genomics) following the manufacturer's instructions. In brief, dissociated single cells were coencapsulated into 3-4 nl droplets together with hydrogel beads carrying barcoding reverse transcription primers. Following reverse transcription, the droplets were taken through the following steps: i) second strand synthesis; ii) linear amplification by *in vitro* transcription (IVT); iii) amplified RNA fragmentation; iv) reverse transcription; and v) PCR. The resulting libraries were sequenced on an Illumina NovaSeq-6000 system and mapped to the human genome using CellRanger (10x Genomics).

ScRNA-Seq analysis

Raw gene expression matrices generated per sample using CellRanger (version 3.0.0) were combined in R (version 3.6.3) and converted to a Seurat object using the Seurat R package (version 3.0.3.9028). After filtering, the gene expression matrices were normalized to the total cellular read count, original sample identity, and mitochondrial read count using linear regression. To identify marker genes of cell clusters, gene expression was required to be >2.5-fold higher than that in the other clusters. The gene ontology (GO) terms were mapped, and sequences were annotated using the software program Blast2GO. The GO annotation results were plotted by R scripts. Following annotation steps, the studied proteins were blasted against the online Kyoto Encyclopedia of Genes and Genomes (KEGG) database (http://geneontology.org/) to retrieve their KEGG orthology identifications and were subsequently mapped to pathways in KEGG. The protein–protein interaction (PPI) data were retrieved from the IntAct molecular interaction database. The network was then visualized using Cytoscape software (version 3.8.0) (https://cytoscape.org/). The degree of each protein was calculated to evaluate the importance of the protein in the PPI network. The abovementioned analysis was performed by Novogene Bioinformatics Technology Co., Ltd. (Beijing, China).

For validation data, public genomics data in the Gene Expression Omnibus (GEO) database were downloaded. Three datasets (GSE47460-GPL14550, GSE37768 and GSE52509) were used, and differential expression was assessed.

Histology analysis

Human lung samples were fixed in 4% paraformaldehyde at room temperature for 48 hours. They were dehydrated using a graded ethanol series, immersed in xylene and embedded in paraffin. The samples were cut into 4 µm sections and stained with hematoxylin and eosin (H&E), Masson's trichrome or Perls' blue. For immunochemistry and immunofluorescence staining, the sections were blocked with normal goat serum and stained using primary antibodies at 4°C overnight in a wet box. Primary antibodies against the following proteins were used: HO-1 (Abcam, ab52947, 1:200), CD68 (Abcam, ab955, 1:200), FTL (Abcam, ab110017, 1:200), SOD2 (Abcam, ab68155, 1:200), FTH1 (Abcam, ab76972, 1:200), and GPX4 (Abcam, ab125066, 1:100). An Envision kit (DAKO) was used for immunohistochemistry. Secondary antibodies were used for immunofluorescence at room temperature for 1 hour in the dark and counterstained with DAPI (Vector Labs). The images were captured on the respective microscope and evaluated. Immunofluorescence images were captured using an N-SIM-S Super Resolution Microscope (Nikon, Tokyo, Japan). Other images were captured on a NanoZoomer Digital Pathology (NDP) scanning system (Hamamatsu, Hamamatsu City, Japan).

Flow cytometry analysis

Alveolar macrophages (M1 or M2) were isolated from human lung samples using the markers mentioned above and described elsewhere. Briefly, after cell dissociation, fluorescence staining was performed using the following antibodies: anti-human CD45-FITC (MHCD4501, 1:100, eBiosciences), anti-human CD206-PE (12-2069-42, 1:100, Invitrogen), anti-human CD1c-APC (17-0015-42, 1:100, Invitrogen), anti-human CD11b-PerCP/Cy5.5 (301327, 1:100, Biolegend), and anti-human CD163-PE-CY7 (25-1639-42, 1:100, Invitrogen). Cells were analyzed in flow cytometers, and data were analyzed using FlowJo Software version 10.8.1 (FlowJo, LLC).

Quantitative reverse transcription polymerase chain reaction

RNA was prepared using TRIzol reagent (Invitrogen, CA, USA) and reverse transcribed to cDNA using an iScript cDNA synthesis kit (Bio-Rad, CA, USA). qRT-PCRs were carried out using the SYBR Green Master mix kit (Bio-Rad) according to the instructions. The housekeeping gene *β-Actin* or *Gapdh* was used as an endogenous internal control, and the results were normalized to those of smokers without COPD. The primer sequences are listed in the Table S2.

Western blot analysis

For Western blot analysis, collected lung tissue was washed in cold PBS, ground and lysed by an electric grinder in RIPA Lysis Buffer (P0013B, Beyotime, Haimen, China) with PMSF (ST506, Beyotime). The protein-transferred polyvinylidene difluoride (PVDF) membrane was probed with the respective antibodies. The immunoreactive protein was detected by a ChemiDoc MP Imaging System (Bio-Rad Laboratories, Hercules, CA, USA). Autoradiographs were quantified using ImageJ software (National Institutes of Health, Bethesda, MD, USA).

Preparation of cigarette smoke extract

Approximately 30–50 mL of cigarette smoke was drawn into the syringe and bubbled into sterile PBS in 15 mL centrifuge tubes (Thermo Fisher) to prepare cigarette smoke (CS) extract. We used one cigarette for the preparation of 10 mL of solution. To remove insoluble particles, the CS extract solution was filtered (0.22 μm; Merck Millipore) and stored for further use.

Cell culture

RAW 264.7 macrophages were obtained and cultured at 37°C and 5% CO_2 in DMEM supplemented with 10% heat-inactivated fetal bovine serum (FBS, HyClone) and 10% penicillin –streptomycin (HyClone). The macrophages were polarized in DMEM containing interferon-γ (IFN-γ, 100 ng/mL, Sigma –Aldrich) for the M1 state or interleukin-4 (IL-4, 20 ng/mL, Sigma–Aldrich) for the M2 state for 48 hours as reported and then used for experiments. Cells were plated in 24-well plates and incubated with CS extract with or without the HO-1 agonist cobalt protoporphyrin (CoPP, 100 mM, Sigma–Aldrich) and the HO-1 antagonist zinc protoporphyrin (ZnPP, 5 mM) for 48 hours. The final DMSO concentration for agent dissolution was less than 0.1%. Cells were stained with Fluoroquench fluorescence stain to assess the live versus dead status of cells. Cell death was monitored by LDH release assay. Quantifications of HO-1, CO, Fe, iNOS and NO production in cells or supernatants were performed using ELISA or biochemistry analysis.

Mouse cigarette smoke exposure and interventions

Male C57BL/6NCrl mice aged 10 weeks were purchased from Vitalriver Biotechnology (Pinghu, China). All experimental protocols were approved by the Institutional Animal Care and Use Committee (IACUC) and Animal Experiment Center of Sichuan University. All animals were cared for in accordance with the requirements of the Laboratory Animal Welfare Act and amendments thereof. Briefly, mice were exposed twice daily for 1 hour, 5 days a week, to the mainstream smoke of 12 cigarettes using a whole-body exposure system for 4 months. Total particulate matter ranged from 700-900 mg/m^3. The cotinine and carboxyhaemoglobin levels in cigarette smoke-exposed mice are comparable to those observed in human smokers. Age-matched, air-exposed mice served as nonsmoking controls.

The ferroptosis inducer erastin (MCE, 10 mg/kg), ferroptosis inhibitor ferrostatin-1 (MCE, 5 mg/kg), HO-1 inhibitor ZnPP (MCE, 25 mg/kg), and iron chelator deferoxamine (Sigma –Aldrich, 100 mg/kg) were administered intraperitoneally in 125 μL of corn oil once a week. The final DMSO concentration for agent dissolution was less than 0.1%. Sham mice received corn oil with 0.1% DMSO solution only. Mice were sacrificed after the last administration.

For bronchoalveolar lavage (BAL) acquirement, the mouse tracheae were cannulated and lavaged three times with 500 μL of cold PBS after anesthetization. Cells were pelleted, and the cell-free BAL fluid (BALF) was collected and detected.

Lung function measurements

Mice were anesthetized, tracheostomized and ventilated using a flexiVent system running Flexiware v.7.6.4 software to measure respiratory functions such as forced vital capacities (FVC), forced expiratory volume (FEV), and inspiratory capacity (IC). The FEV/FVC was calculated.

C11-BODIPY staining

Lungs were harvested, digested and cultured for 2 days to isolate alveolar macrophages to quantify lipid peroxidation. Cells were stained using a solution of C11-BODIPY 581/591 (1 μM; Thermo Fisher) in PBS (Invitrogen, 10 μM) for 1 hour at 37 °C in a tissue culture incubator. After two PBS washes, representative samples were imaged by confocal microscopy (Nikon).

Mitochondrial membrane potential detection

The cells were digested, resuspended and stained with JC-1 working solution (Beyotime, 10 μg/mL). After mixing, the cells were incubated at 37 °C for 20 minutes. After incubation, the cells were

centrifuged, washed, resuspended in JC-1 staining buffer, and then analyzed by flow cytometry. The ratio of the mean fluorescence intensity (MFI) of FL2 (J-aggregates, red)/FL1 (monomer, green) fluorescence was calculated for each sample.

Statistical analysis

All data were analyzed using SPSS 25.0 and organized using GraphPad Prism 9. Data are presented as the means ± standard errors of the means (SEM). One-way analysis of variance (ANOVA) was used for multiple comparisons, and Dunnett's test was used for each two-group comparison. At least three parallel experiments were conducted using different samples. A level of $p<0.05$ was accepted as significant.

Results

A comprehensive map of the cell types in the lungs of smokers without COPD and individuals with mild-to-moderate COPD

To understand the alteration of immune and nonimmune cell types and states for mild-to-moderate COPD compared to disease-free patients, we collected single-cell profiles from 12 samples according to the grading of illness to construct the lung cellular map (non-COPD; mild-COPD; moderate-COPD: n=4 each) (Figures 1A–C, Supplementary Table S1). The composition of cells undergoes dramatic alteration along with the inflammatory process and tissue destruction. The pulmonary profile was composed of 56.3%, 71.3% and 65.6% CD45+ immune cells in smokers without COPD and in those with mild and moderate COPD, respectively. Among the immune cells, the percentages of dendritic cells (DCs), B cells and specific subtypes of natural killer (NK) cells declined. Meanwhile, the composition of AMs showed a steady increase in the myeloid cell compartment, which was 3.0% in the non-COPD samples and reached up to 3.8% and 6.4% in mild and moderate COPD, respectively (Figures 1D, E). In the CD45+ immune compartment, lymphoid lineages were detected, including T cells (characterized by high expression of *Cd3d*), NK cells (*Fgfbp2*), and B cells (*Ms4a1*), while myeloid cells were separated into neutrophils (*S100a12*), macrophages (*Cd68*), DCs (*Cd1c*), and mast cells (*Tpsab1*). In the nonimmune compartment, alveolar cells type I and II (AT I and II) (*Aqp5* and *Sftpd*), epithelium (*Caps*), club cells (*Scgb3a2*), fibroblasts (*Col1a1*), and basal cells (*Krt5*) were recognized (Figure 1F). A two-dimensional representation of immune and nonimmune single cells revealed the separation of cells into diverse lineages (Figure 1G).

Distinct intergroup genes are localized in alveolar macrophages

We analyzed the differentially expressed genes among groups. Transcriptionally, the COPD samples expressed high or elevated levels of *Fabp4*, *Ccl18*, *C1qa*, *C1qb, C1qc, Lmna, Lgals3, Ctsd, Ftl Apoc1, and Glul*, especially in moderate patients. In contrast, the expression levels of *Igkc*, *Klrb1*, *Gnly*, *Gzmh*, *Gzmb*, *Cst7*, *Nkg7*, and *Prf1* were significantly downregulated compared to those in non-COPDs. The profiles demonstrated that the downregulation of key genes in B cells and NKs of COPD patients may be related to susceptibility to infection (Figure 2A). Notably, differentially expressed genes were uniquely or partially localized in cells expressing the macrophage hallmarks *Cd68*, *Fcgr3a, Mrc-1* (*Cd206*), Msr-1 and *Marco*. AM-CLST13 cells expressing higher levels of *Ccl18*, *C1qb* and *Apoc1* were classified as M2 alternatively activated macrophages with anti-inflammatory effects, while AM-CLST14 cells expressing higher levels of *Il-18*, *Hla-dqb1* and *Ccl20* were classified as M1 classically activated macrophages with proinflammatory effects (Figure 2B, Supplementary Table S3). AM-CLST13 increased in the COPD samples; in contrast, AM-CLST14 originated largely from the lungs of patients without or with mild COPD (Figure 2C). Our analysis showed 445 identical genes shared in the two AM clusters, as well as 127 and 99 specific genes in each cluster (Figure 2D). AM-CLST13 was characterized by high expression of complement factors (*C1qa*, *C1qb* and *C1qc*), genes associated with cathepsin *(Ctsd*, *Ctsl*, *Ctsz)*, ferroptosis (*Ftl*, *Glul*, *Homx-1*) and lipid metabolism (*Apoc1*, *Fabp5*), while AM-CLST14 was characterized by the expression of MHC class II molecules (*Hla-dr*, *Hla-dq* and *Hla-dp*), antigen processing and presentation (*Cd74*) and antioxidant metabolism (*Sod2*) (Figure 2E). We performed pseudotime analysis and tracked the gene expression changes along the trajectory of two alveolar macrophage clusters from smokers without COPD and patients with mild and moderate COPD. AM-CLST13 was positioned at the opposite end of AM-CLST14, especially in moderate cases (Figures 2F, S1). We then identified genes expressed in prebranch, cell fate 1 and cell fate 2 and classified differentially expressed genes into six subsets. The expression profile of subset 1 showed high levels of chemokines, while subset 2 expressed the S100 family of proteins, indicating activation and chemotaxis of the immune system. Subset 3 showed expression of metallothionein, which was consistent with a recent report (39). Subset 4 expressed immunoregulatory genes associated with the complement system, whereas subset 5 was involved in cell cycle regulation and was downregulated in mild and moderate COPD patients. Subset 6, on the other hand, was involved in the regulation of cytosolic ion concentration and stress-induced cell death (Figures 2G, S1).

Different cell fates of ferroptotic death of alveolar macrophages

The coexpressed ferroptotic-specific genes were selected and compared between the two alveolar macrophage clusters. Noticeably, the genetic phenotypes of *Emp1*, *Fth1*, *Ftl, Hmox-1*, *Slc11a1*, *Tfrc* and *Prdx1* were different (Figure 3A). In addition, the ferroptosis-mediated genes *Acsl1*, *Scd1* and *Por* were uniquely expressed in AM-CLST13 cells (Table S3). Meanwhile, the ferroptotic-associated transcription factor expression levels were also distinct, including those of Ahr, Atf3, Cebpb, Egr1, Nr4a1, and Pparg (Figure 3B). We then performed

10.3389/fimmu.2023.1162087

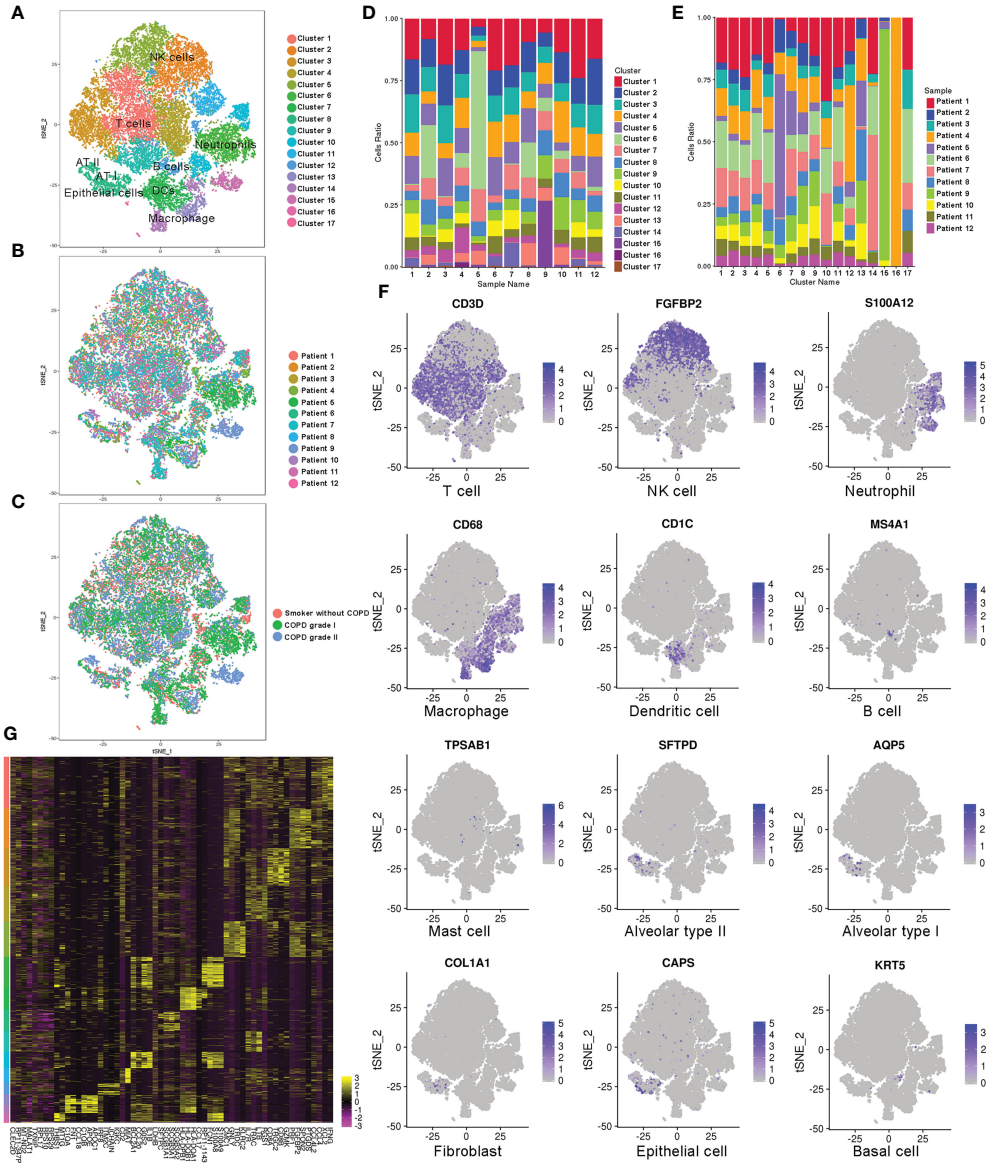

FIGURE 1
Single-cell RNA-Seq analysis of patients with COPD identifies diverse lung cell populations. **(A)** Cellular populations were identified and visualized using a t-distributed Stochastic Neighbor Embedding (tSNE) plot. **(B)** Each population included cells from smokers without COPD and patients with COPD. **(C)** Cells were grouped as originating from smokers without COPD, mild COPD (COPD grade I) and moderate COPD (COPD grade II). **(D)** Cell type distribution in each sample. **(E)** Cell source in each cluster. **(F)** Classic cell markers were used to label clusters by cell identity as represented in the tSNE plot. **(G)** Heatmap representing gene signatures in each cellular population.

GO, KEGG and Reactome analyses. Reactome analysis revealed that AM-CLST13 is involved in the distinctive metabolic networks of plasma lipoprotein and LDL clearance, generation of second messenger molecules, trafficking and processing of endosomal TLRs and scavenging by class A receptors, while AM-CLST14 is involved in IL-10 signaling, RHO GTPases activation of NADPH oxidases, regulation of actin dynamics for phagocytic cup formation, clathrin-derived vesicle budding, and FCGR-dependent phagocytosis (Figure 3C). Similarly, KEGG pathways identified that the expression of AM-CLST13 was distinctly enriched in antigen processing and presentation, the PPAR signaling pathway and ferroptosis (Figure 3D). Through PPI analysis, the expression profiles of alveolar macrophage clusters and their networks were revealed. Specifically, expressed genes, such as *Decr1*, *Cd36* and *Slc3a2* in AM-CLST13, while *Sod2*, *Gpx3* and *Cat* in AM-CLST14, were also involved in ferroptotic death and resistance, aside from the others we mentioned above. Moreover, most of them were regulated by Hmox-1 (Figure 3E).

Characterization and identification of alveolar macrophages across different stages

Heatmaps for representative differentially expressed genes involved in iron transport and metabolism, lipid metabolism, and biosynthetic and catabolic processes from observed alveolar macrophage

10.3389/fimmu.2023.1162087

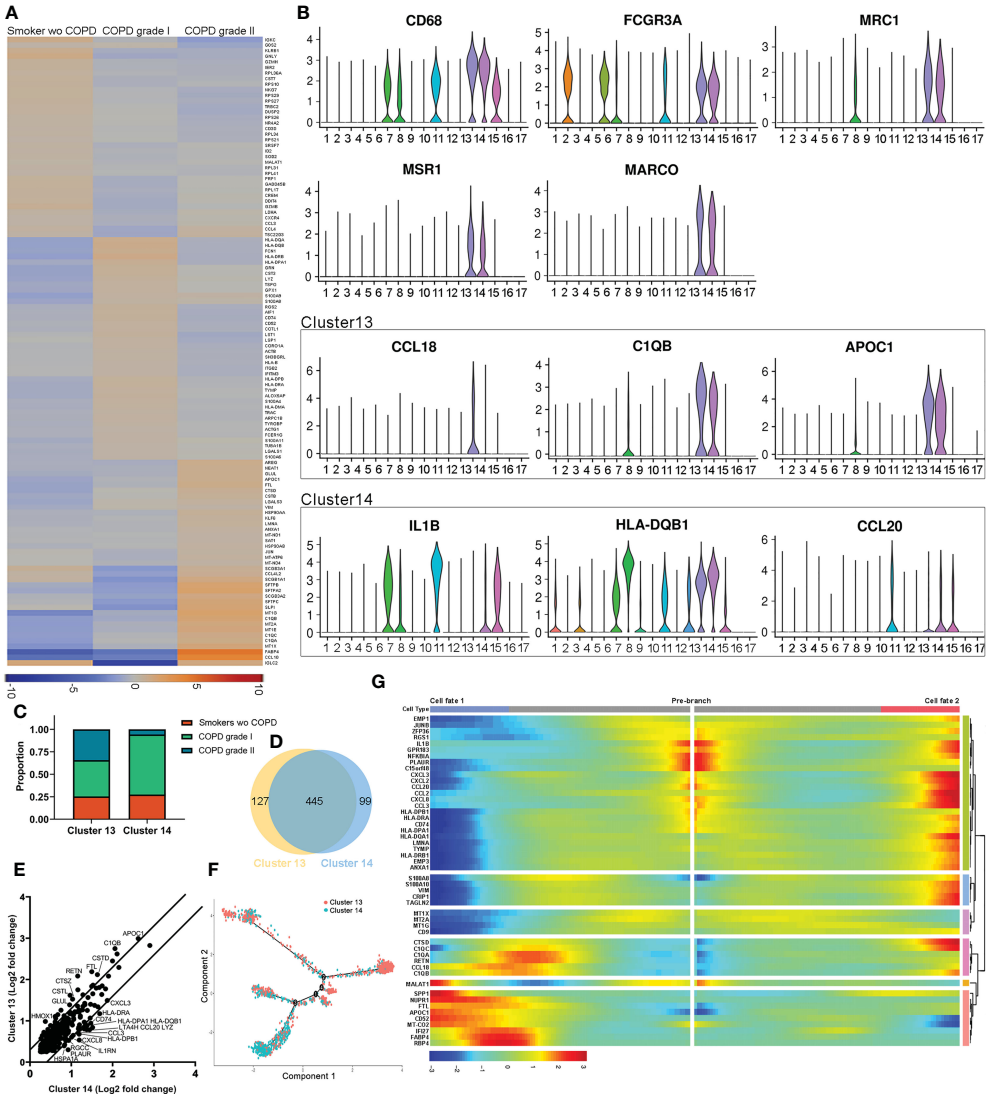

FIGURE 2
Distinct populations of alveolar macrophages in healthy smoker and COPD lungs. **(A)** Heatmap of significantly differentially expressed genes between smokers without COPD, mild COPD patients and moderate COPD patients. **(B)** Expression of markers and significant differentially expressed genes associated with activated M1 and alternatively activated M2 alveolar macrophages. **(C)** Relative cell contributions from healthy and COPD lungs to each alveolar macrophage cluster. **(D)** Venn diagram of all detected genes in each alveolar macrophage cluster. **(E)** Differential expression of shared genes in each alveolar macrophage cluster. **(F)** Trajectory analysis of the alveolar macrophage state transition in two-dimensional state-space. **(G)** Heatmap showing differentially expressed genes arranged in pseudotemporal patterns.

populations in the three groups are shown and dysregulated (Figure 4A). Through Gene Ontology (GO) analysis, the identified transcripts were found to be involved in iron homeostasis, lipid metabolism, some biosynthetic and catabolic processes and endocytosis. Upregulated terms such as “iron ion transport”, “transferrin transport”, “regulation of sterol transport”, “cholesterol efflux” and “triglyceride metabolic process” and downregulated terms such as “lipase inhibitor activity”, “plasma lipoprotein clearance”, and “negative regulation of endocytosis” were observed in M2 alveolar macrophages in COPD lungs (Figure 4B). We then examined paraffin-embedded lung tissues from patients. Histologic examination of H&E and Masson’s trichrome staining revealed destruction of alveolar walls with diminished alveolar capillaries, leading to enlarged air spaces. Ongoing inflammation and black pigment are present in advanced disease (Figures 4C, D). Perls’ staining revealed that AMs and alveolar epithelial cells in COPD patients had higher levels of free iron accumulation than those in smokers without COPD (Figure 4E). The expression of HO-1 (encoded by the *Hmox-1* gene) was decreased in mild and moderate COPD compared to healthy smoker lungs using immunohistochemistry staining (Figure 4F). Analysis of an RNA sequencing (RNA-seq) dataset from the public GEO database showed upregulation of *Hmox-1* in COPD compared to healthy controls (Figures 4G, S2) but slight downregulation compared to smokers without COPD (Figures 4H, S2). Similarly, analysis based on mice revealed that *Hmox-1* was much more highly expressed in lung tissues from mice treated with CS than in normal tissues from mice treated with filtered air (Figures 4I, S2). Meanwhile, upregulation of *Ftl* in COPD compared to healthy controls and smokers without

10.3389/fimmu.2023.1162087

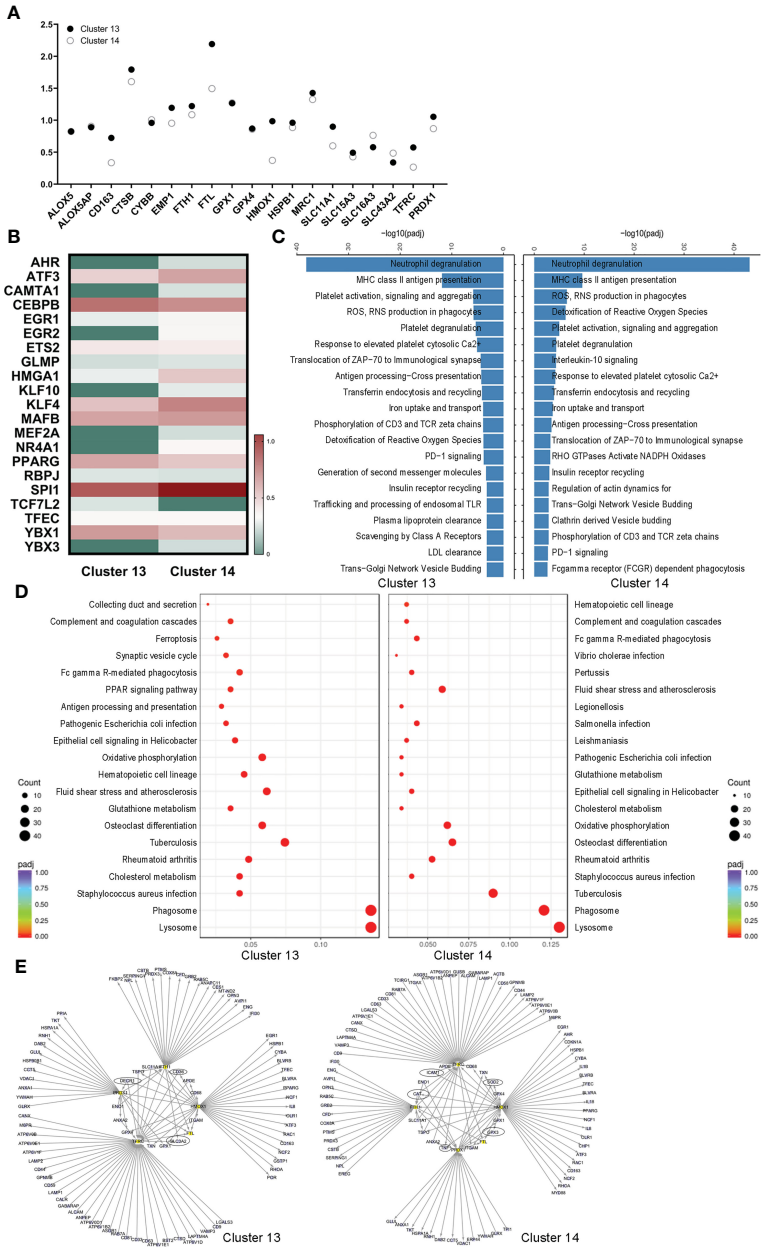

FIGURE 3
Different cell fates of ferroptotic death of alveolar macrophages. **(A)** Selected ferroptotic genes, **(B)** differential expression of transcription factors, **(C)** Reactome analysis, **(D)** Kyoto Encyclopedia of Genes and Genomes (KEGG) pathway analysis, and **(E)** protein–protein interaction (PPI) networks revealed different cell fates for ferroptotic death between activated M1 and alternatively activated M2 alveolar macrophages in the lungs.

COPD was observed in humans and was more highly expressed in lung tissues from mice treated with CS, but the difference was not statistically significant (Figures 4G–I). We further explored *Hmox-1* and *Ftl* expression in our clinical samples and found that they were consistent with the data (Figure 4J). We then performed coimmunofluorescence staining for macrophages (CD68) and divided them into AM-CLST13 (FTL) and AM-CLST14 (SOD2) based on their expression in tissues from COPD patients and smokers without COPD (Figure 4K). According to the cell count, the CD68+ populations increased as COPD progressed. The number and percentage of FTL+ populations increased, while the percentage of SOD2+ populations decreased (Figure 4L).

Profiling of alternatively activated (M2) macrophages in lungs

The leukocytes ($CD45^+$) were gated with $CD206^+$, $CD1c^-$ and $CD11b^+$ and then segregated into $CD163^{high}$ (R8, AM-CLST13) and $CD163^{intermediate}$ (R9, AM-CLST14) by flow cytometry. Consistent with the results, the number and percentage of M2 macrophages increased from 5.87% in smokers without COPD to 8.76% and 11.22% in mild and moderate COPD, respectively. Meanwhile, the percentage of M1 macrophages fluctuated as 75.57%, 79.21% and 64.87% in smokers without COPD and mild and moderate COPD, respectively (Figure 5A). Increases in intracellular ferritin (*Fth1*, *Ftl*)

10.3389/fimmu.2023.1162087

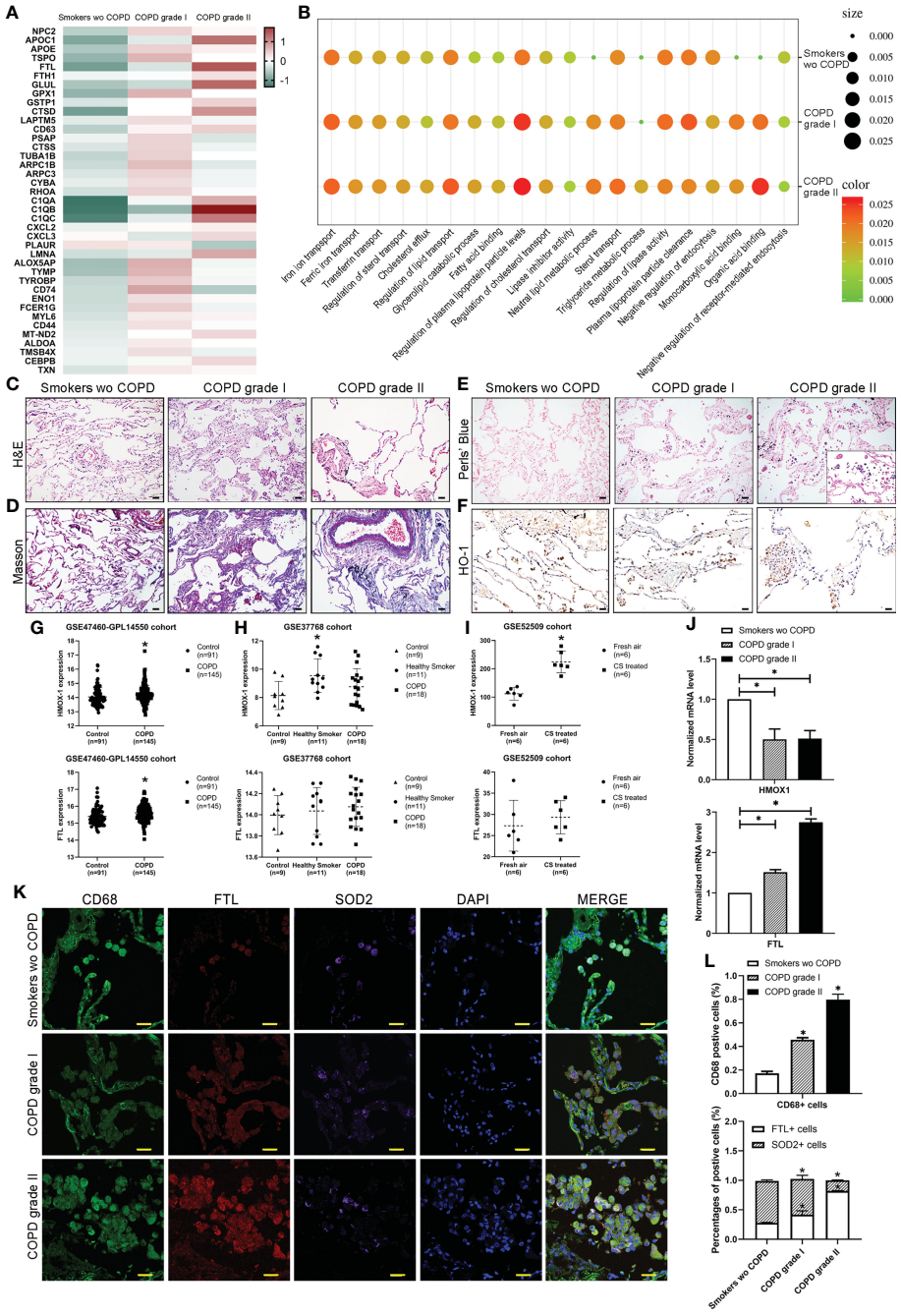

FIGURE 4
Characterization of macrophages across different stages. **(A)** The expression of selected significant differentially expressed genes across different stages. **(B)** Gene Ontology (GO) enrichment plot of iron and lipid metabolism in COPD. **(C)** H&E and **(D)** Masson's trichrome staining revealed the morphology of COPD lungs. **(E)** Perls' staining revealed free iron accumulation in additional COPD samples. **(F)** Immunohistochemical staining for HO-1 showed the expression of HO-1 in COPD patients compared to smokers without COPD. **(G)** The mRNA expression levels of HMOX-1 and FTL in publicly available array data from lung tissue (GSE47460-GPL14550) of healthy subjects (n = 91) versus patients with COPD (n = 145) **(H)** versus lung tissue (GSE37768) of healthy subjects (n = 9) versus heathy smokers (n=11) and patients with COPD (n = 18) **(I)** in whole lung from B6 mice exposed to filtered air (n = 6) or cigarette smoke (n = 8). **(J)** The mRNA expression levels of HMOX-1 and FTL determined by qPCR in whole lungs from our samples. **(K)** Coimmunofluorescence staining for macrophages (CD68, green), activated M1 (FTL, red) and alternatively activated M2 (SOD2, purple) across lung tissues. **(L)** The number and percentage of positive cells. *p<0.05 versus the control group. Scale bar=50 μm.

and *Cybb*, as well as decreases in *Acsl1*, *Slc3a2* and *Gpx4*, were observed in AM-CLST13 cells (R8) sorted by FACS from mild-moderate COPD patients compared to smokers without COPD, indicating that M2 alveolar macrophages had marked changes in ferroptosis (Figure 5B). The cell death TUNEL assay revealed that positive alveolar macrophages were increased in COPD lungs (Figure 5C). Immunofluorescence staining showed enhanced FTL and FTH1 expression and reduced expression of GPX4 in alveolar macrophages corresponding to patients' pathological status (Figures 4K, 5D, E). A protein–protein interaction (PPI) network

10.3389/fimmu.2023.1162087

was constructed, and a specific network was visualized by Cytoscape. The AM-CLST13 networks interacted with phagosome, lysosome, fat and cholesterol metabolism and ferroptosis proteins (Figure 5F). Western blotting confirmed these results and revealed the promotion of ferroptosis in AM-CLST13 cells from patients with mild and moderate COPD (Figure 5G).

Heme oxygenase 1 determines sensitivity to ferroptosis in macrophages

To investigate the regulatory mechanism of HO-1 and different cell fates in ferroptosis in alveolar macrophages, we established an exposure protocol for RAW 264.7 macrophages to CS extract and nontoxic concentrations of the HO-1 agonist CoPP or antagonist ZnPP. The experiments revealed that M1 classically activated macrophages exerted high resistance to CS-induced ferroptosis, whereas M2 alternatively activated macrophages were vulnerable. The contents of HO-1, CO and Fe were higher in the M2 versus M1 state (Figures 6A–C) and consistently responded with cell death estimated by LDH release (Figure 6D). This was effectively preventable by ZnPP. Considering the contribution of iNOS/NO previously reported, our results showed that iNOS/NO was enriched in M1 macrophages, but the changes in iNOS/NO were not significantly different in parallel macrophages (Figures 6E, F). We found that the number of M1 macrophages was lower than the

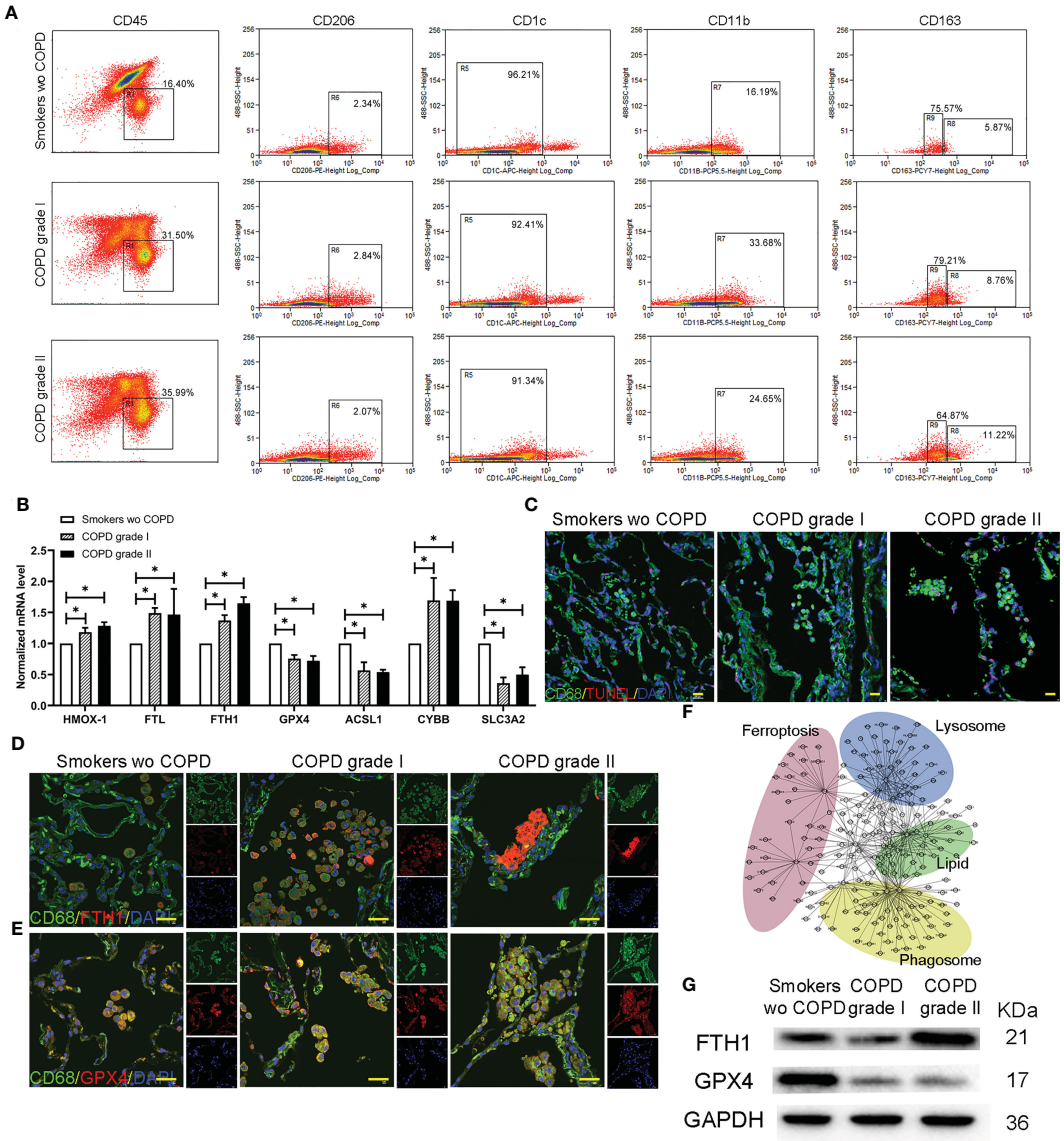

FIGURE 5
Profiling of alternatively activated (M2) macrophages in lungs. **(A)** Flow cytometry analysis of single-cell suspensions for myeloid cells from whole lungs in smokers without COPD and COPD patients. **(B)** The mRNA levels of ferroptotic genes expressed in separated alternatively activated (M2) macrophages across groups determined by qPCR. **(C)** TUNEL-positive alveolar macrophages indicated that cell death was increased in COPD lungs. Immunofluorescence staining for **(D)** FTH and **(E)** GPX4 in alternatively activated (M2) macrophages in the lungs. **(F)** Gene–gene interaction maps of alveolar macrophages involved in phagosome, lysosome, fat and cholesterol metabolism and ferroptosis are shown. **(G)** Western blotting of FTH and GPX4 was performed to examine alternatively activated (M2) macrophages. *p<0.05 versus the control group. Scale bar=50 μm.

number of M2 macrophages, and cells treated with CS extract exhibited higher levels of death in M2 macrophages. Cells treated with CoPP showed increased cell death, whereas ZnPP abolished CS extract-mediated death (Figure 6G). There was also a positive correlation between HO-1, CO, and Fe concentrations and LDH levels (Pearson<0.0001,<0.001,<0.0001, respectively) (Figure 6H).

Ferroptosis as a target for protection of lung function in cigarette smoke-induced COPD mice

We examined whether the administration of ferroptosis attenuated lung inflammation, destruction and remodeling in COPD mice by utilizing the ferroptosis inducer erastin, ferroptosis inhibitor Fer-1, HO-1 inhibitor ZnPP, and iron chelator DFO (Figure 7A). We observed that the cellular profile and appearance of AMs from the lungs of administered mice were similar to those in humans, and alveolar space enlargement, AM recruitment and iron accumulation in the airway were observed by Perl's staining (Figure 7B). Lung function measurements of mice demonstrated a decreased FEV/FVC ratio, indicating deteriorated expiratory flow and lung compliance (Figure 7C). C11-BODIPY581/591 staining showed that lipid peroxidation in isolated alveolar macrophages from mice was attenuated by the administration of Fer-1, ZnPP and DFO (Figure 7D). Fe(II) concentrations in bronchoalveolar lavage fluid and ferritin concentrations released from separated alveolar macrophages from mouse lungs were also decreased at different levels (Figures 7E, F). Significant increases in mitochondrial membrane potential (measured by JC-1 fluorescence) were observed after treatment with Fer-1, ZnPP and DFO in mouse alveolar macrophages (Figure 7G). Immunofluorescence analyses of FTL and GPX4 and CD68 double-positive alveolar macrophages in mice were in accordance with the pathological characteristics of ferroptosis (Figures 7H, I). Taken together, these data showed that disruptions in lipid peroxidation and iron homeostasis in alveolar macrophages drive ferroptosis, which is involved in lung inflammation, destruction and remodeling in COPD and can be regulated as a potential target.

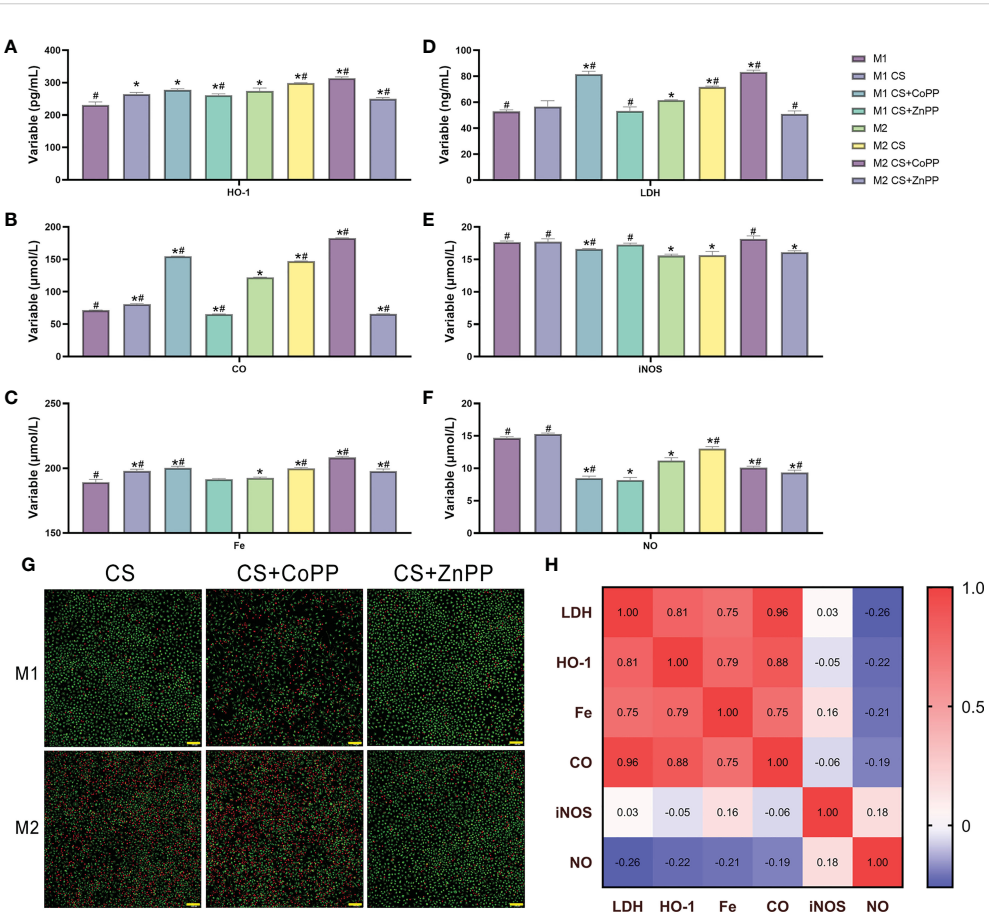

FIGURE 6
HO-1 determines sensitivity to ferroptosis in RAW 264.7 macrophages. Activated (M1) macrophages display resistance to cigarette smoke-induced ferroptosis compared to alternatively activated (M2) macrophages. RAW 264.7 macrophages were treated with cigarette smoke in the presence or absence of the HO-1 agonist CoPP and antagonist ZnPP. **(A)** Heme oxygenase-1 (HO-1), **(B)** carbon monoxide (CO), **(C)** Fe(II), **(D)** lactate dehydrogenase (LDH), **(E)** inducible nitric oxide synthase (iNOS), and **(F)** nitric oxide (NO) concentrations were examined. **(G)** Apoptosis assay of macrophages using acridine orange/ethidium bromide (AO/EB) staining. **(H)** Correlation coefficient of gene expression levels between HO-1/CO/Fe (II) and iNOS/NO in macrophages. *p<0.05 versus the M1 group; # p<0.05 versus the M2 group. Scale bar=100 μm.

10.3389/fimmu.2023.1162087

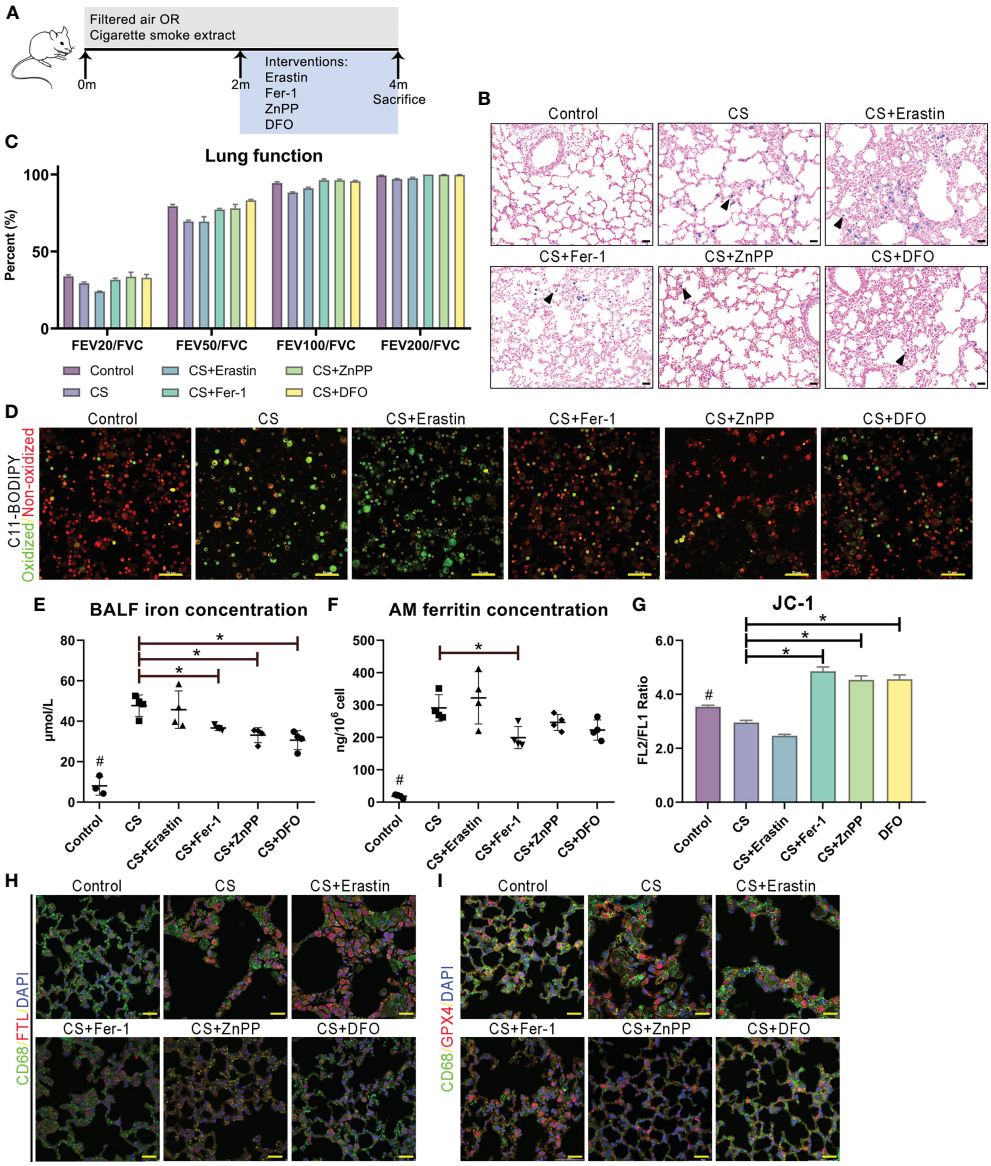

FIGURE 7
Ferroptosis as a target for protection for lung function in cigarette smoke induced COPD. **(A)** Schematic representation of the ferroptosis treatment protocol in cigarette smoke-treated mice. **(B)** Representative images of lung sections stained with Perls' stain. **(C)** Lung function data from mice exposed to filtered air or cigarette smoke and treated with erastin (ferroptosis agonist), Fer-1 (ferroptosis antagonist), ZnPP (HO-1 antagonist) and DFO (iron chelator). **(D)** C11-BODIPY581/591 staining showed lipid peroxidation and antioxidant efficacy in membrane systems in alveolar macrophages. **(E)** Fe(II) concentrations in bronchoalveolar lavage fluid. **(F)** Ferritin concentrations released from separated alveolar macrophages. **(G)** Representative images of JC-1 fluorescence in cells exposed to filtered air or cigarette smoke and treated with erastin, Fer-1, ZnPP and DFO. Immunofluorescence analyses of **(H)** FTL and **(I)** GPX4 and CD68 double-positive alveolar macrophages in model mice. *p<0.05 versus the control group. Scale bar=50 μm. # p<0.05 all groups versus the control group.

Discussion

In this study, we demonstrated that ferroptosis was involved in inflammation in alveolar macrophages in COPD. In alveolar macrophages, there were discrepancies in sensitivity to ferroptosis, which can be determined and regulated by HO-1. During COPD, the accumulation of lipid peroxidation drives ferroptosis-sensitive M2-like AMs, while M1-like AMs show characteristics of ferroptosis resistance. Differential HO-1 expression in alveolar macrophages modulates susceptibility to ferroptosis. This ferroptotic phenotype was ameliorated by anti-ferroptotic compounds, iron chelators, and HO-1 inhibitors, which alleviated lung inflammation and the destruction and remodeling of COPD, representing a potential target (Figure 8).

Chronic airway inflammation and lung destruction are critical components of COPD pathogenesis (16). Ferroptosis was identified as a type of necrotic regulated cell death characterized by free iron-dependent phospholipid peroxidation of cell membranes, which is negatively regulated by the selenoprotein GPx4 (40, 41). A recent study demonstrated that epithelial cell ferroptosis was involved in the pathogenesis of cigarette smoke-induced COPD (14, 42). Increased iron burden as evidence of increased concentrations of

iron and ferritin in BAL in smoker lungs has been reported (14). Mitochondrial dysfunction and endoplasmic reticulum stress are usually observed in the cytoplasm, and ferroptosis occurs in bronchial epithelial cells (43). The increased ferritinophagy mediated by nuclear receptor coactivator 4 (NCOA4) and reduction of glutathione peroxidase 4 (GPX4) led to the accumulation of free iron and lipid peroxidation during CS exposure. Moreover, GPX4+/− mice showed significantly higher degrees of lipid peroxidation and an enhanced COPD phenotype than wild-type mice, whereas these phenotypes could be attenuated in GPX-transgenic mice (14, 44). PM2.5 is another risk factor for COPD. Increased cellular iron content and ROS production in human endothelial cells were observed after inhaling PM2.5 particles, while the levels of glutathione (GSH) and nicotinamide adenine dinucleotide phosphate (NADPH) decreased. Iron overload and redox imbalance caused by TFRC and ferritin dysregulation are the major inducers of ferroptosis (45). The abovementioned investigations indicated that ferroptosis is involved and plays a crucial damaging role in COPD (40), and searching for an accurate inhibitor of ferroptosis to delay the progression and prevent the occurrence of COPD is pivotal to forthcoming research. Experimental interventions, such as the iron chelator deferoxamine, the ferroptosis inhibitor ferrostatin-1, and suppression of lipid peroxidation by GPX4, could effectively reduce lipid peroxidation, upregulate GSH and NADPH levels, and inhibit ferroptosis (14, 41, 46, 47). Moreover, recent reports revealed that antioxidants, such as N-acetyl-l-cysteine (NAC) and curcumin, could improve the reduction of GSH and reduce lipid peroxidation (46), while dihydroquercetin could inhibit ferroptosis in lung epithelial cells by activating the Nrf2-mediated pathway (48).

Macrophages can be divided into two main phenotypes: M1 and M2. In response to inflammatory signals, such as IFN-γ, LPS and GM-CSF, macrophages polarize into activated M1 macrophages with characteristic transcriptional and secretory profiles, including strong upregulation of iNOS and proinflammatory signals, such as IL-12, IL-1β, and TNF-α. In contrast, alternatively activated M2 macrophages are polarized by anti-inflammatory signals such as IL-4, IL-13 and M-CSF, upregulate genes such as *Arg1*, *Mrc-1* (*Cd206*) and *Cd163*, and release IL-10 (49, 50). Similarly, M1 AMs can produce high levels of proinflammatory and cytotoxic mediators that hinder lung repair, while M2 AMs generate protective factors and orchestrate restorative processes that are beneficial for tissue recovery after injury (51). It has been reported that iNOS-derived

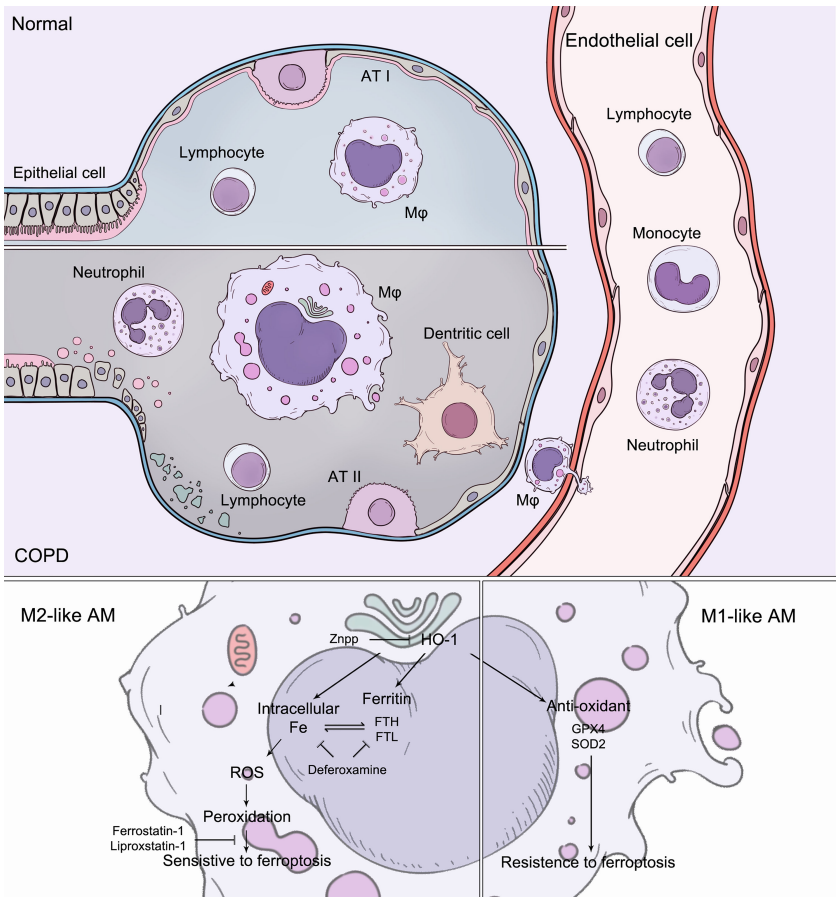

FIGURE 8
During COPD, the accumulation of lipid peroxidation drives ferroptosis-sensitive M2-like AMs, while M1-like AMs show characteristics of ferroptosis resistance. Increased HO-1 expression in alveolar macrophages modulates susceptibility to ferroptosis. The ferroptotic phenotypes were regulated by anti-ferroptotic compounds, iron chelators, and HO-1 inhibitors.

NO• can interact with 15-LOX-generated lipid intermediates and is thus a regulator of ferroptotic death in macrophages and microglia *in vitro* (52). In our study, M2 macrophages displayed high sensitivity to ferroptosis, which can be explained by the lack of *Stat-1* and *Stat-2*. Lipid peroxidation has been recognized as a fundamental part of ferroptosis, and it can be divided between two major Fe-dependent pathways: a. nonenzymatic random free-radical chemical reactions (53) and b. a highly selective and specific enzymatic LOX-controlled process (54). The accumulation of lipids and free iron can increase lipid peroxidation in both ways. Given the high expression of ALOX5, enzymatic LOX-controlled reactions are, in our view, most likely prominent in this process.

AM-CLST14-IL1β was characterized by high expression of MHC class II molecules (*Hla-dr*, *Hla-dq* and *Hla-dp*) and antigen processing and presentation (*Cd74*). They also specifically expressed *Il-1β*, *Il-18* and *Tnf*, which are usually recognized as hallmarks of M1 macrophages; however, they also express *Mrc-1* (*Cd206*) and the intermediate *Cd163*. We hypothesized that this cluster of macrophages underwent proinflammatory M1-like polarization. Notably, this cluster expressed high levels of superoxide dismutase (*Sod2*) and glutathione peroxidases (*Gpx1* and *Gpx4*). The *Sod2* gene encodes the mitochondrial antioxidant manganese superoxide dismutase (Mn-SOD), which converts toxic superoxide radicals into less damaging hydrogen peroxide. In previous findings, we observed a clear reduction in *Sod2* between COPD and non-COPD, presumably reflecting increased oxidative stress consumption during disease (55). Glutathione peroxidases (Gpxs) can catalyze the reduction of hydrogen peroxides and lipid hydroperoxides by glutathione to prevent oxidative stress (2). The development and progression of COPD has been strongly associated not only with enhanced ROS production but also with reduced antioxidant capacity. In addition, they expressed intermediate levels of *Ftl*, *Fth1* and *Trfc*, with low levels of *Acsl1* and *Slc3a2*, implying that M1-like AMs were less susceptible to ferroptosis than M2-like AMs.

The presence of foamy AMs (foam cells) is frequently observed in patients with COPD and smokers. Studies have reported that accumulated lipids in AMs are associated with driving lung inflammation (21). It is widely accepted that foam cells derived from lipid-accumulating macrophages drive inflammatory processes in plaques in atherosclerosis (56). Our observations confirmed that the initiation and progression associated with COPD and atherosclerosis (AS) may share similar inflammatory molecular mechanisms. Lung-resident AMs were laden with abundant intracellular lipids, especially very low-density and low-density lipoproteins (VLDL/LDL), and were incapable of dealing with them. This could be explained by the dysregulation of transport proteins (Figure S3). This type of AM also expressed high levels of genes mediating innate immune responses, indicating that they initiate an inflammatory cascade resulting in the recruitment of immune inflammatory cells. Lipid-loaded AMs may drive inflammatory processes, similar to pathogenic macrophages in plaques in AS. The source of lipids that accumulate in macrophages is currently not explicit. Given the abundance of phospholipids in surfactant due to hyperresponsiveness in COPD and the critical role that alveolar macrophages play in surfactant regulation, damaged surfactant is the most likely source.

According to reports, alveolar macrophages from patients with COPD show reduced phagocytic uptake of bacteria, such as *Haemophilus influenzae* or *Streptococcus pneumoniae* (57). A high prevalence of bacterial colonization in the lower airways, accounting for over 50% of patients with COPD, can predispose patients to increased infection, inflammatory response and acute exacerbation. Macrophages from patients with COPD are also defective in taking up apoptotic cells, which might contribute to constant inflammation in patients. The mechanism of the defect in phagocytosis appears to be due to defects in scavenger receptors and cytoskeleton organization, which are required for phagocytosis. Another major function of AMs is digesting particles, including exogenous or autologous bacteria, lipids and proteins, via lysosomes. The AMs from COPD patients showed abnormal lysosomes. This does not appear to be a generalized defect, and it may account for decreased lysosomal membrane proteins and some H^+-transporting ATPases. The cathepsins, on the other hand, were released from AMs to destroy parenchymal construction and drive the immune response (Figure S4).

To determine the feasibility of transcriptomic profiling in scRNA-Seq, we examined lung tissue samples obtained from patients with severe COPD (GOLD stage III). We identified a higher proportion of M2-like AMs containing free iron and expressing increased FTH1 and reduced GPX4. In addition, these cells also expressed APOC1, APOE and OLR1. This illustrated that lipid and iron homeostasis are correlated with the disease status of COPD. The patient also had complications of left coronary atherosclerosis and type 2 diabetes mellitus, reflecting the concurrence of diabetes and cardiovascular disease in patients with airway obstruction, which may be related to the deterioration of homeostasis. In another case we included, the patient was identified as having a prominent M2-like AM population but was graded as having moderate COPD. Such patients, in our view, should be followed up more often in cases of acute exacerbation and rapid progression. Thus, the analysis of AMs is promising from a clinical perspective. Although peripheral blood cells are safe and easy to collect and monitor, they have not generated accurate transcriptomic information on disease development and outcome, particularly at the early stage. Alveolar macrophages can be identified using scRNA-Seq or histology analysis to predict and manage the disease; however, repeatedly acquired from bronchoscopic alveolar lavage or biopsy is invasive and intolerable. Sputum specimens containing alveolar macrophages may appear to be an ideal noninvasive way to acquire specimens in practice.

The HO-1 reaction may either exhibit cytoprotection by converting prooxidant hemoproteins and heme to the antioxidants bilirubin and biliverdin or, conversely, exacerbate oxidative stress by releasing ferrous iron and CO. Suppression of HO-1 is related to diseases including obesity, metabolic syndrome and vascular disease (30, 58–60). However, several recent reports have revealed that the role of Nrf2/HO-1 in ferroptosis is controversial due to its antiferroptotic/protective or ferroptotic

role in various *in vitro* models, such as *in vivo* and *in vitro* models (35, 61). Using the HO-1 inhibitor ZnPP has been shown to significantly rescue ferroptotic dysfunction of alveolar macrophages and subsequently prevent airway inflammation. The classification of AMs provides clues for developing novel immunotherapy drugs based on the cell populations and their effects. Inhibitors aimed at intracellular free iron (deferoxamine, DFO), lipid peroxidation and ferroptosis (ferrostatin-1 (Fer-1) and liproxstatin-1) and HO-1 may be employed to attenuate the disease. In addition, by examining genes, we found not only currently pursued immunotherapy targets (such as PPARG or PCG-1 activators, e.g., rosiglitazone and pioglitazone) (62) but also other distinct expressions that may serve as targets in the same categories in our dataset. For instance, statins, including simvastatin and rosuvastatin, work by lowering the production of cholesterol and low-density lipoprotein, as well as triglycerides. It can block the metabolic pathway of mevalonate by competitive inhibition of the endogenous rate-limiting enzyme HMG CoA reductase to reduce the synthesis of cholesterol in cells. Statins also stimulate the uptake of apoptotic cells by AMs via inhibition of the prenylation and activation of RhoA (63), which were weakened in M2-like AMs in our data (Figure S3). Furthermore, antioxidants such as vitamin E (α-tocopherol), a specific inhibitor of LOX enzyme activity, can increase GSH levels and reduce lipid peroxidation (64–66). Meanwhile, the treatment of comorbidities should be evaluated carefully. For example, studies have shown that anemia was observed in 15-30% of COPD patients, particularly in patients with severe disease, and may be an independent predictor of mortality (67, 68). Sarcopenia/skeletal muscle dysfunction is also an important comorbidity in patients with COPD and is associated with poor quality of life and reduced survival. The prevalence of skeletal muscle dysfunction in patients with stable COPD ranged from 14.5% to 55%. However, iron supplements, nutritional supplements or iron-rich diets should be utilized with caution because they are likely to be detrimental, as iron may increase ROS and ferroptosis. In particular, ferroptosis has been demonstrated to be involved in the pathogenesis of COPD-related skeletal muscle dysfunction (69). Iron levels of COPD patients should be determined, and according to their levels, patients should be supplemented with iron as appropriate. Soluble transferrin receptor (sTfr) reflects iron utilization in the body and can better describe functional or absolute iron deficiency in the body than ferritin and transferrin saturation in clinical practice. High-dose and systemic administration of medications may have adverse effects; thus, it is wise to deliver drugs by the inhaled route.

Taken together, these findings suggest that alterations in iron homeostasis in AMs and discrepancies in sensitivity to ferroptosis play newly discovered roles in COPD pathogenesis. Ferroptotic M2 AMs lose their anti-inflammatory and repair functions but provoke inflammatory responses, resulting in consistent inflammation and tissue damage in the presence of M1 AMs in COPD. We have also demonstrated that the applications of ferroptosis inhibitor, HO-1 inhibitor and iron chelator prevent airway inflammation and lung destruction in COPD. The mechanisms of these inhibitors should be deeply investigated in the future, and further experimental studies and clinical trials may be warranted to test the efficacy of these compounds. Appropriate therapeutic strategies specifically targeting ferroptosis can reduce the occurrence of infections and acute onset and delay the COPD process.

Data availability statement

The datasets presented in this study can be found in online repositories. The names of the repository/repositories and accession number(s) can be found below: GSE227691 (GEO).

Ethics statement

The studies involving human participants were reviewed and approved by Ethics Committee of West China Hospital of Sichuan University. The patients/participants provided their written informed consent to participate in this study. The animal study was reviewed and approved by Institutional Animal Care and Use Committee (IACUC) and Animal Experiment Center of Sichuan University.

Author contributions

YL assisted in conducting experiments, collecting data and writing the manuscript. YY and TG assisted in conducting the experiments. CW assisted in making illustrations. YFY assisted in sample collection. ZW and LZ assisted in designing the study design, conducting experiments, and collecting and analyzing the data. WL designed the study design and supervised and assisted in writing the manuscript. All authors contributed to the article and approved the submitted version.

Funding

The research leading to these results has received funding from the National Natural Science Foundation of China (No. 92159302, WL), Science and Technology Project of Sichuan (2022ZDZX0018, WL), 1.3.5 project for disciplines of excellence, West China Hospital, Sichuan University (ZYGD22009, WL), and Sichuan University Full-time Postdoctoral Research and Development Fund (2020SCU12023, YL).

Acknowledgments

The authors are grateful to Qiqi Zhou and Chunjuan Bao for their valuable assistance in conducting experiments.

Conflict of interest

The authors declare that the research was conducted in the absence of any commercial or financial relationships that could be construed as a potential conflict of interest.

Publisher's note

All claims expressed in this article are solely those of the authors and do not necessarily represent those of their affiliated organizations, or those of the publisher, the editors and the reviewers. Any product that may be evaluated in this article, or claim that may be made by its manufacturer, is not guaranteed or endorsed by the publisher.

Supplementary material

The Supplementary Material for this article can be found online at: https://www.frontiersin.org/articles/10.3389/fimmu.2023.1162087/full#supplementary-material

References

1. Dixon SJ, Lemberg KM, Lamprecht MR, Skouta R, Zaitsev EM, Gleason CE, et al. Stockwell BR. ferroptosis: an iron-dependent form of nonapoptotic cell death. *Cell* (2012) 149:1060–72. doi: 10.1016/j.cell.2012.03.042

2. Forcina GC, Dixon SJ. GPX4 at the crossroads of lipid homeostasis and ferroptosis. *Proteomics* (2019) 19:e1800311. doi: 10.1002/pmic.201800311

3. Muller T, Dewitz C, Schmitz J, Schroder AS, Brasen JH, Stockwell BR, et al. Necroptosis and ferroptosis are alternative cell death pathways that operate in acute kidney failure. *Cell Mol Life Sci* (2017) 74:3631–45. doi: 10.1007/s00018-017-2547-4

4. Zhang YH, Wang DW, Xu SF, Zhang S, Fan YG, Yang YY, et al. Alpha-lipoic acid improves abnormal behavior by mitigation of oxidative stress, inflammation, ferroptosis, and tauopathy in P301S tau transgenic mice. *Redox Biol* (2018) 14:535–48. doi: 10.1016/j.redox.2017.11.001

5. Tuo QZ, Lei P, Jackman KA, Li XL, Xiong H, Li XL, et al. Tau-mediated iron export prevents ferroptotic damage after ischemic stroke. *Mol Psychiatry* (2017) 22:1520–30. doi: 10.1038/mp.2017.171

6. Wang H, An P, Xie E, Wu Q, Fang X, Gao H, et al. Characterization of ferroptosis in murine models of hemochromatosis. *Hepatology* (2017) 66:449–65. doi: 10.1002/hep.29117

7. Alvarez SW, Sviderskiy VO, Terzi EM, Papagiannakopoulos T, Moreira AL, Adams S, et al. NFS1 undergoes positive selection in lung tumours and protects cells from ferroptosis. *Nature* (2017) 551:639–43. doi: 10.1038/nature24637

8. Li Q, Han X, Lan X, Gao Y, Wan J, Durham F, et al. Inhibition of neuronal ferroptosis protects hemorrhagic brain. *JCI Insight* (2017) 2:e90777. doi: 10.1172/jci.insight.90777

9. Zilka O, Shah R, Li B, Friedmann Angeli JP, Griesser M, Conrad M, et al. On the mechanism of cytoprotection by ferrostatin-1 and liproxstatin-1 and the role of lipid peroxidation in ferroptotic cell death. *ACS Cent Sci* (2017) 3:232–43. doi: 10.1021/acscentsci.7b00028

10. Ito K, Eguchi Y, Imagawa Y, Akai S, Mochizuki H, Tsujimoto Y. MPP+ induces necrostatin-1- and ferrostatin-1-sensitive necrotic death of neuronal SH-SY5Y cells. *Cell Death Discovery* (2017) 3:17013. doi: 10.1038/cddiscovery.2017.13

11. Barnes PJ, Burney PG, Silverman EK, Celli BR, Vestbo J, Wedzicha JA, et al. Chronic obstructive pulmonary disease. *Nat Rev Dis Primers* (2015) 1:15076. doi: 10.1038/nrdp.2015.76

12. Lancet T. COPD-more than just tobacco smoke. *Lancet* (2009) 374:663. doi: 10.1016/S0140-6736(09)61535-X

13. Salvi SS, Barnes PJ. Chronic obstructive pulmonary disease in non-smokers. *Lancet* (2009) 374(9691):733–43. doi: 10.1016/S0140-6736(09)61303-9

14. Yoshida M, Minagawa S, Araya J, Sakamoto T, Hara H, Tsubouchi K, et al. Involvement of cigarette smoke-induced epithelial cell ferroptosis in COPD pathogenesis. *Nat Commun* (2019) 10:3145. doi: 10.1038/s41467-019-10991-7

15. Barnes PJ. Inflammatory endotypes in COPD. *Allergy* (2019) 74:1249–56. doi: 10.1111/all.13760

16. Barnes PJ. Cellular and molecular mechanisms of asthma and COPD. *Clin Sci (Lond)* (2017) 131:1541–58. doi: 10.1042/CS20160487

17. Hiemstra PS. Altered macrophage function in chronic obstructive pulmonary disease. *Ann Am Thorac Soc* (2013) 10:S180–5. doi: 10.1513/AnnalsATS.201305-123AW

18. Chana KK, Fenwick PS, Nicholson AG, Barnes PJ, Donnelly LE. Identification of a distinct glucocorticosteroid-insensitive pulmonary macrophage phenotype in patients with chronic obstructive pulmonary disease. *J Allergy Clin Immunol* (2014) 133:207–216 e201-211. doi: 10.1016/j.jaci.2013.08.044

19. Belchamber KBR, Singh R, Batista CM, Whyte MK, Dockrell DH, Kilty I, et al. Defective bacterial phagocytosis is associated with dysfunctional mitochondria in COPD macrophages. *Eur Respir J* (2019) 54(4):1802244. doi: 10.1183/13993003.02244-2018

20. Bewley MA, Preston JA, Mohasin M, Marriott HM, Budd RC, Swales J, et al. Impaired mitochondrial microbicidal responses in chronic obstructive pulmonary disease macrophages. *Am J Respir Crit Care Med* (2017) 196:845–55. doi: 10.1164/rccm.201608-1714OC

21. Morissette MC, Shen P, Thayaparan D, Stampfli MR. Disruption of pulmonary lipid homeostasis drives cigarette smoke-induced lung inflammation in mice. *Eur Respir J* (2015) 46:1451–60. doi: 10.1183/09031936.00216914

22. Poss KD, Tonegawa S. Reduced stress defense in heme oxygenase 1-deficient cells. *Proc Natl Acad Sci USA* (1997) 94:10925–30. doi: 10.1073/pnas.94.20.10925

23. Maamoun H, Zachariah M, McVey JH, Green FR, Agouni A. Heme oxygenase (HO)-1 induction prevents endoplasmic reticulum stress-mediated endothelial cell death and impaired angiogenic capacity. *Biochem Pharmacol* (2017) 127:46–59. doi: 10.1016/j.bcp.2016.12.009

24. Zhu C, Jiang W, Cheng Q, Hu Z, Hao J. Hemeoxygenase-1 suppresses IL-1β-Induced apoptosis through the NF-κB pathway in human degenerative nucleus pulposus cells. *Cell Physiol Biochem* (2018) 46:644–53. doi: 10.1159/000488632

25. Waza AA, Hamid Z, Ali S, Bhat SA, Bhat MA. A review on heme oxygenase-1 induction: is it a necessary evil. *Inflamm Res* (2018) 67:579–88. doi: 10.1007/s00011-018-1151-x

26. Neis VB, Rosa PB, Moretti M, Rodrigues ALS. Involvement of heme oxygenase-1 in neuropsychiatric and neurodegenerative diseases. *Curr Pharm Des* (2018) 24:2283–302. doi: 10.2174/1381612824666180717160623

27. Cuadrado A, Rojo AI. Heme oxygenase-1 as a therapeutic target in neurodegenerative diseases and brain infections. *Curr Pharm Des* (2008) 14:429–42. doi: 10.2174/138161208783597407

28. Liu X, Gao Y, Li M, Geng C, Xu H, Yang Y, et al. Sirt1 mediates the effect of the heme oxygenase inducer, cobalt protoporphyrin, on ameliorating liver metabolic damage caused by a high-fat diet. *J Hepatol* (2015) 63:713–21. doi: 10.1016/j.jhep.2015.05.018

29. Bakhautdin B, Das D, Mandal P, Roychowdhury S, Danner J, Bush K, et al. Protective role of HO-1 and carbon monoxide in ethanol-induced hepatocyte cell death and liver injury in mice. *J Hepatol* (2014) 61:1029–37. doi: 10.1016/j.jhep.2014.06.007

30. Abraham NG, Junge JM, Drummond GS. Translational significance of heme oxygenase in obesity and metabolic syndrome. *Trends Pharmacol Sci* (2016) 37:17–36. doi: 10.1016/j.tips.2015.09.003

31. Cheng Y, Rong J. Therapeutic potential of heme oxygenase-1/carbon monoxide system against ischemia-reperfusion injury. *Curr Pharm Des* (2017) 23:3884–98. doi: 10.2174/1381612823666170413122439

32. Motterlini R, Foresti R, Bassi R, Green CJ. Curcumin, an antioxidant and anti-inflammatory agent, induces heme oxygenase-1 and protects endothelial cells against oxidative stress. *Free Radical Biol Med* (2000) 28:1303–12. doi: 10.1016/S0891-5849(00)00294-X

33. Tanimoto T, Hattori N, Senoo T, Furonaka M, Ishikawa N, Fujitaka K, et al. Genetic ablation of the Bach1 gene reduces hyperoxic lung injury in mice: role of IL-6. *Free Radic Biol Med* (2009) 46:1119–26. doi: 10.1016/j.freeradbiomed.2009.01.017

34. Go H, La P, Namba F, Ito M, Yang G, Brydun A, et al. MiR-196a regulates heme oxygenase-1 by silencing Bach1 in the neonatal mouse lung. *Am J Physiology-Lung Cell Mol Physiol* (2016) 311:L400–11. doi: 10.1152/ajplung.00428.2015

35. Adedoyin O, Boddu R, Traylor A, Lever JM, Bolisetty S, George JF, et al. Heme oxygenase-1 mitigates ferroptosis in renal proximal tubule cells. *Am J Physiol Renal Physiol* (2018) 314:F702–14. doi: 10.1152/ajprenal.00044.2017

36. Montoro DT, Haber AL, Biton M, Vinarsky V, Lin B, Birket SE, et al. A revised airway epithelial hierarchy includes CFTR-expressing ionocytes. *Nature* (2018) 560:319–24. doi: 10.1038/s41586-018-0393-7

37. Plasschaert LW, Zilionis R, Choo-Wing R, Savova V, Knehr J, Roma G, et al. A single-cell atlas of the airway epithelium reveals the CFTR-rich pulmonary ionocyte. *Nature* (2018) 560:377–81. doi: 10.1038/s41586-018-0394-6

38. Reyfman PA, Walter JM, Joshi N, Anekalla KR, McQuattie-Pimentel AC, Chiu S, et al. Single-cell transcriptomic analysis of human lung provides insights into the pathobiology of pulmonary fibrosis. *Am J Respir Crit Care Med* (2019) 199:1517–36. doi: 10.1164/rccm.201712-2410OC

39. Sauler M, McDonough JE, Adams TS, Kothapalli N, Barnthaler T, Werder RB, et al. Characterization of the COPD alveolar niche using single-cell RNA sequencing. *Nat Commun* (2022) 13:494. doi: 10.1038/s41467-022-28062-9

40. Mizumura K, Gon Y. Iron-regulated reactive oxygen species production and programmed cell death in chronic obstructive pulmonary disease. *Antioxidants (Basel)* (2021) 10(10):1569. doi: 10.3390/antiox10101569

41. Ghio AJ, Hilborn ED, Stonehuerner JG, Dailey LA, Carter JD, Richards JH, et al. Pinkerton KE. particulate matter in cigarette smoke alters iron homeostasis to produce a biological effect. *Am J Respir Crit Care Med* (2008) 178:1130–8. doi: 10.1164/rccm.200802-334OC

42. Li Y, Yang Y, Yang Y. Multifaceted roles of ferroptosis in lung diseases. *Front Mol Biosci* (2022) 9:919187. doi: 10.3389/fmolb.2022.919187

43. Park EJ, Park YJ, Lee SJ, Lee K, Yoon C. Whole cigarette smoke condensates induce ferroptosis in human bronchial epithelial cells. *Toxicol Lett* (2019) 303:55–66. doi: 10.1016/j.toxlet.2018.12.007

44. Dowdle WE, Nyfeler B, Nagel J, Elling RA, Liu S, Triantafellow E, et al. Selective VPS34 inhibitor blocks autophagy and uncovers a role for NCOA4 in ferritin degradation and iron homeostasis *in vivo*. *Nat Cell Biol* (2014) 16:1069–79. doi: 10.1038/ncb3053

45. Wang Y, Tang M. PM2.5 induces ferroptosis in human endothelial cells through iron overload and redox imbalance. *Environ pollut* (2019) 254:112937. doi: 10.1016/j.envpol.2019.07.105

46. Tang X, Li Z, Yu Z, Li J, Zhang J, Wan N, et al. Effect of curcumin on lung epithelial injury and ferroptosis induced by cigarette smoke. *Hum Exp Toxicol* (2021) 40:S753–62. doi: 10.1177/09603271211059497

47. Lian N, Zhang Q, Chen J, Chen M, Huang J, Lin Q. The role of ferroptosis in bronchoalveolar epithelial cell injury induced by cigarette smoke extract. *Front Physiol* (2021) 12:751206. doi: 10.3389/fphys.2021.751206

48. Liu X, Ma Y, Luo L, Zong D, Li H, Zeng Z, et al. Dihydroquercetin suppresses cigarette smoke induced ferroptosis in the pathogenesis of chronic obstructive pulmonary disease by activating Nrf2-mediated pathway. *Phytomedicine* (2022) 96:153894. doi: 10.1016/j.phymed.2021.153894

49. Mills CD, Kincaid K, Alt JM, Heilman MJ, Hill AM. M-1/M-2 macrophages and the Th1/Th2 paradigm. *J Immunol* (2000) 164:6166–73. doi: 10.4049/jimmunol.164.12.6166

50. Chavez-Galan L, Olleros ML, Vesin D, Garcia I. Much more than M1 and M2 macrophages, there are also CD169(+) and TCR(+) macrophages. *Front Immunol* (2015) 6:263. doi: 10.3389/fimmu.2015.00263

51. Arora S, Dev K, Agarwal B, Das P, Syed MA. Macrophages: their role, activation and polarization in pulmonary diseases. *Immunobiology* (2018) 223:383–96. doi: 10.1016/j.imbio.2017.11.001

52. Kapralov AA, Yang Q, Dar HH, Tyurina YY, Anthonymuthu TS, Kim R, et al. Redox lipid reprogramming commands susceptibility of macrophages and microglia to ferroptotic death. *Nat Chem Biol* (2020) 16:278–90. doi: 10.1038/s41589-019-0462-8

53. Yin H, Xu L, Porter NA. Free radical lipid peroxidation: mechanisms and analysis. *Chem Rev* (2011) 111:5944–72. doi: 10.1021/cr200084z

54. Haeggstrom JZ, Funk CD. Lipoxygenase and leukotriene pathways: biochemistry, biology, and roles in disease. *Chem Rev* (2011) 111:5866–98. doi: 10.1021/cr200246d

55. Mak JC, Ho SP, Yu WC, Choo KL, Chu CM, Yew WW, et al. Polymorphisms and functional activity in superoxide dismutase and catalase genes in smokers with COPD. *Eur Respir J* (2007) 30:684–90. doi: 10.1183/09031936.00015207

56. Yan ZQ, Hansson GK. Innate immunity, macrophage activation, and atherosclerosis. *Immunol Rev* (2007) 219:187–203. doi: 10.1111/j.1600-065X.2007.00554.x

57. Berenson CS, Kruzel RL, Eberhardt E, Dolnick R, Minderman H, Wallace PK, et al. Impaired innate immune alveolar macrophage response and the predilection for COPD exacerbations. *Thorax* (2014) 69:811–8. doi: 10.1136/thoraxjnl-2013-203669

58. Abraham NG, Tsenovoy PL, McClung J, Drummond GS. Heme oxygenase: a target gene for anti-diabetic and obesity. *Curr Pharm Des* (2008) 14:412–21. doi: 10.2174/138161208783597371

59. Chung HT, Pae HO, Cha YN. Role of heme oxygenase-1 in vascular disease. *Curr Pharm Des* (2008) 14:422–8. doi: 10.2174/138161208783597335

60. Kishimoto Y, Kondo K, Momiyama Y. The protective role of heme oxygenase-1 in atherosclerotic diseases. *Int J Mol Sci* (2019) 20(15):3628. doi: 10.3390/ijms20153628

61. Fang X, Wang H, Han D, Xie E, Yang X, Wei J, et al. Ferroptosis as a target for protection against cardiomyopathy. *Proc Natl Acad Sci USA* (2019) 116:2672–80. doi: 10.1073/pnas.1821022116

62. Lakshmi SP, Reddy AT, Reddy RC. Emerging pharmaceutical therapies for COPD. *Int J Chron Obstruct Pulmon Dis* (2017) 12:2141–56. doi: 10.2147/COPD.S121416

63. Morimoto K, Janssen WJ, Fessler MB, McPhillips KA, Borges VM, Bowler RP, et al. Lovastatin enhances clearance of apoptotic cells (efferocytosis) with implications for chronic obstructive pulmonary disease. *J Immunol* (2006) 176:7657–65. doi: 10.4049/jimmunol.176.12.7657

64. Khanna S, Roy S, Ryu H, Bahadduri P, Swaan PW, Ratan RR, et al. Molecular basis of vitamin e action. *J Biol Chem* (2003) 278:43508–15. doi: 10.1074/jbc.M307075200

65. Kagan VE, Mao G, Qu F, Angeli JP, Doll S, Croix CS, et al. Oxidized arachidonic and adrenic PEs navigate cells to ferroptosis. *Nat Chem Biol* (2017) 13:81–90. doi: 10.1038/nchembio.2238

66. Hinman A, Holst CR, Latham JC, Bruegger JJ, Ulas G, McCusker KP, et al. Vitamin e hydroquinone is an endogenous regulator of ferroptosis via redox control of 15-lipoxygenase. *PloS One* (2018) 13:e0201369. doi: 10.1371/journal.pone.0201369

67. Similowski T, Agusti A, MacNee W, Schonhofer B. The potential impact of anaemia of chronic disease in COPD. *Eur Respir J* (2006) 27:390–6. doi: 10.1183/09031936.06.00143704

68. Cote C, Zilberberg MD, Mody SH, Dordelly LJ, Celli B. Haemoglobin level and its clinical impact in a cohort of patients with COPD. *Eur Respir J* (2007) 29:923–9. doi: 10.1183/09031936.00137106

69. Zhang L, Li D, Chang C, Sun Y. Myostatin/HIF2α-mediated ferroptosis is involved in skeletal muscle dysfunction in chronic obstructive pulmonary disease. *Int J Chron Obstruct Pulmon Dis* (2022) 17:2383–99. doi: 10.2147/COPD.S377226

frontiers | Frontiers in Immunology

TYPE Review
PUBLISHED 12 May 2023
DOI 10.3389/fimmu.2023.1175387

OPEN ACCESS

EDITED BY
Miguel Angel Alejandre Alcazar,
University Hospital of Cologne, Germany

REVIEWED BY
Yue Li,
First Affiliated Hospital of Zhengzhou University, China
John W. Semple,
Lund University, Sweden

*CORRESPONDENCE
Zhengqiu Lian
2237932531@qq.com

RECEIVED 27 February 2023
ACCEPTED 27 April 2023
PUBLISHED 12 May 2023

CITATION
Yu Y and Lian Z (2023) Update on transfusion-related acute lung injury: an overview of its pathogenesis and management.
Front. Immunol. 14:1175387.
doi: 10.3389/fimmu.2023.1175387

Update on transfusion-related acute lung injury: an overview of its pathogenesis and management

Yunhong Yu and Zhengqiu Lian*

Department of Blood Transfusion, The Third People's Hospital of Chengdu, Affiliated Hospital of Southwest Jiaotong University, Chengdu, China

Transfusion-related acute lung injury (TRALI) is a severe adverse event and a leading cause of transfusion-associated death. Its poor associated prognosis is due, in large part, to the current dearth of effective therapeutic strategies. Hence, an urgent need exists for effective management strategies for the prevention and treatment of associated lung edema. Recently, various preclinical and clinical studies have advanced the current knowledge regarding TRALI pathogenesis. In fact, the application of this knowledge to patient management has successfully decreased TRALI-associated morbidity. This article reviews the most relevant data and recent progress related to TRALI pathogenesis. Based on the existing two-hit theory, a novel three-step pathogenesis model composed of a priming step, pulmonary reaction, and effector phase is postulated to explain the process of TRALI. TRALI pathogenesis stage-specific management strategies based on clinical studies and preclinical models are summarized with an explication of their models of prevention and experimental drugs. The primary aim of this review is to provide useful insights regarding the underlying pathogenesis of TRALI to inform the development of preventive or therapeutic alternatives.

KEYWORDS

transfusion-related acute lung injury (TRALI), pathogenesis, priming step, pulmonary reaction, effector phase, management

1 Introduction

Transfusion of blood components is a widely employed life-saving treatment in clinical settings; however, it can result in potentially life-threatening adverse reactions (1). For example, transfusion-related acute lung injury (TRALI) is a rare but severe adverse event that occurs during—or within—6 hours of blood transfusion and is characterized by hypoxia and non-cardiogenic pulmonary edema, known as respiratory distress (2). In 2019, a new diagnostic criteria was established using the Delphi approach, effectively subdividing TRALI into Type I and II, which occur in the absence or presence of acute respiratory distress syndrome (ARDS) risk factors, respectively (3). Although TRALI represents a main cause of transfusion-associated mortality in developed countries (4), it is likely

underdiagnosed, particularly in intensive care patients, owing to the synergetic action of multiple factors (5, 6). Although estimates of TRALI mortality vary markedly between 5% and 25% (7, 8), they can reach 47% in intensive care and surgical patients (9). Even so, specific therapeutics remain unavailable.

When TRALI was first reported in 1957, it was thought to be related to the passive transfer of high-titer leucoagglutinins (10). It was not until 1983 that TRALI was formally identified as a distinctive clinical syndrome caused by transfused anti-human leukocyte antigen (HLA) antibodies (11). However, in addition to the transfer of anti-HLA antibodies, anti-human neutrophil antigen (HNA) antibodies also contribute to TRALI induction. In fact, antibody-dependent mechanisms are estimated to be responsible for 50–80% of TRALI cases (12); however, because of the inaccuracy of current laboratory testing techniques, their contribution has likely been underestimated (13). Moreover, TRALI cases that meet the diagnostic criteria have been reported in patients who received transfused products without antibodies (14). More specifically, approximately 10–15% of TRALI cases are associated with biological response modifiers (BRMs), such as soluble CD40 ligand (sCD40L) or lyso-phosphatidylcholines (lyso-PCs), which originate from the storage of blood components. Thus, non-antibody-mediated TRALI has also been proposed. Although significant progress has been made in the field, the complex pathogenesis of TRALI has not yet been fully characterized.

In this review, we highlight the recent advances in the field regarding TRALI pathogenesis and management based on clinical studies and preclinical models. The findings of these studies provide a clearer understanding of the underlying pathogenesis, which will assist in developing effective prevention or therapeutic strategies.

2 Pathogenesis

The pathogenesis of TRALI has been described as a two-hit theory, in which recipient predisposition, together with the presence of detrimental factors in blood components, play significant roles (15). That is, the first hit focusing on recipient predisposition, in which pulmonary endothelial cells (ECs) are activated and polymorphonuclear neutrophils (PMNs) are primed. The second hit comprises mediators in transfused stored units, which trigger the primed PMNs and other cells including ECs,monocytes, macrophages, and platelets to release pathogenetic factors and induce coagulopathy, ultimately resulting in fluid intrapulmonary infiltration. The second hit can be classified into antibody-dependent and -independent TRALI based on the detection of differential pathogenic mediators in the blood components. While the two-hit hypothesis clearly explains TRALI pathogenic factors, the disease pathogenesis can be further characterized as three overlapping phases (Figure 1), i.e., the priming step, pulmonary reaction, and effector phase. During the priming step, recipient-related risk factors mainly lead to endothelial activation and PMN priming via the EC-PMN interaction. Subsequently, in the pulmonary reaction, antibodies or BRMs bind to target cells, such as ECs, PMNs, or mononuclear cells, thereby inducing a host response. In the final effector phase, the pulmonary vascular endothelial barrier may become damaged by the release of neutrophil extracellular traps (NETs) and reactive oxygen species (ROS); the resulting coagulopathy might aggravate lung injury. The diverse phase characteristics of the three-step pathogenesis model will be described in detail to provide a better understanding of TRALI pathogenesis.

2.1 Priming step

As early as 1997, the results of a retrospective study in combination with an *in vivo* rat lung model suggested that stronger PMN-priming activity occurred in patients with TRALI and underlying clinical conditions than in those not diagnosed with TRALI (16). A prospective study revealed that patients diagnosed with hematologic malignance or cardiac disease are at increased risk for developing TRALI (15). Subsequent studies have identified myriad complications that function as first hits, including hypertension, end-stage liver disease, chronic alcohol abuse, surgery, mechanical ventilation, trauma, massive transfusion, and

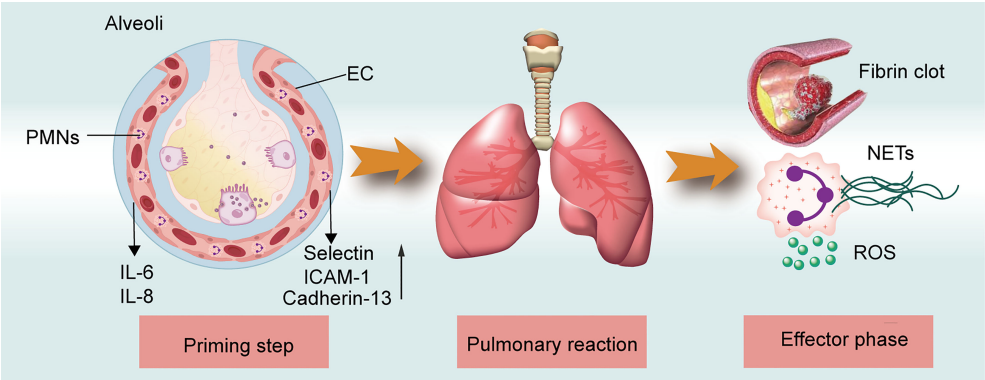

FIGURE 1
TRALI pathogenesis model. The three-step of TRALI pathogenesis: prime step, pulmonary reaction, and effector step. The pathogenesis of each step is described.

systemic inflammation (13, 17). Based on retrospective cohort studies, pulmonary diseases, including pulmonary fibrosis, interstitial lung disease, and tobacco abuse, are identified as potential high-risk factors for TRALI occurrence (18, 19). Moreover, critical patients with these underlying diseases conveyed a serious first hit, requiring only a minor second hit to trigger TRALI (20). Patients with TRALI in an intensive care unit (ICU) exhibited 70% mortality compared with typical 5–25% rates (20, 21). Thus, underlying clinical events play a pivotal pathogenic role in TRALI onset; screening these events in transfusion recipients might improve clinical outcomes.

In the initial TRALI mouse model, transfusion of major histocompatibility complex (MHC) I antibodies 1 to BALB/c mice resulted in TRALI induction (22). In a subsequent study, housing the mice in a specific pathogen-free barrier facility prevented the same lung injury, unless the mice were primed by treatment with lipopolysaccharide (LPS) (23). The difference in results according to housing conditions may be explained by gut flora (24). Therefore, gut flora can be considered a pivotal factor in the priming of TRALI. However, the impact of gut flora on TRALI pathogenesis requires further study.

The role of risk factors of recipients in TRALI pathogenesis has been investigated in preclinical studies, employing low-dose LPS or C-reactive protein (CRP) as the first hit in two-hit TRALI models to represent systemic inflammation in transfusion recipients (25, 26). However, the nature of TRALI first hits, e.g., LPS, is different from CRP. For instance, LPS activates cells by triggering a toll-like receptor four-signal pathway (27). Alternatively, CRP can represent the first hit by benefiting PMN sequestration in the lungs and activating ECs (27). Collectively, these first hits facilitate the activation of pulmonary ECs and macrophage to release interleukin (IL)-6, macrophage inflammatory protein-2 (MIP-2), the murine homolog of human IL-8, and osteopontin (OPN) and increase the expression of adhesion molecules and cadherin-13 due to endothelial activation (14, 26, 28, 29) (Figure 2). Circulating PMNs retained within the lung microvasculature constitute a lung-marginated pool that maintains a dynamic equilibrium with the circulating pool (30). These elevated molecules attract PMNs from the circulating pool to travel to the injured lung and firmly adhere to ECs, creating a predisposition for developing TRALI (Figure 2). These mechanisms might account, in part, for why patients with underlying clinical conditions, such as systemic inflammation, are at a high risk of developing TRALI. However, multiple underlying conditions that are not associated with systemic inflammation, such as chronic alcohol abuse and hypertension, among others, also represent high-risk factors for TRALI onset. In particular, reduced production of nitric oxide, an endothelial anti-adhesive molecule, strengthens endothelial intercellular cell adhesion molecule-1-dependent PMN adhesion, thus providing an alternate mechanism for PMN priming in the absence of systemic inflammation (31).

Taken together, these data indicate that endothelial activation and pulmonary sequestration are key process in the priming step, where direct activation of pulmonary ECs leading to PMN priming initiates the first phase of TRALI development.

2.2 Pulmonary reaction

Following pulmonary endothelial activation and PMN priming caused by underlying diseases, donor-derived risk factors, including pathogenic antibodies and BRMs, target different cell populations, such as hematopoietic and non-hematopoietic cells. Thus, these risk factors make specific contributions to the host response and

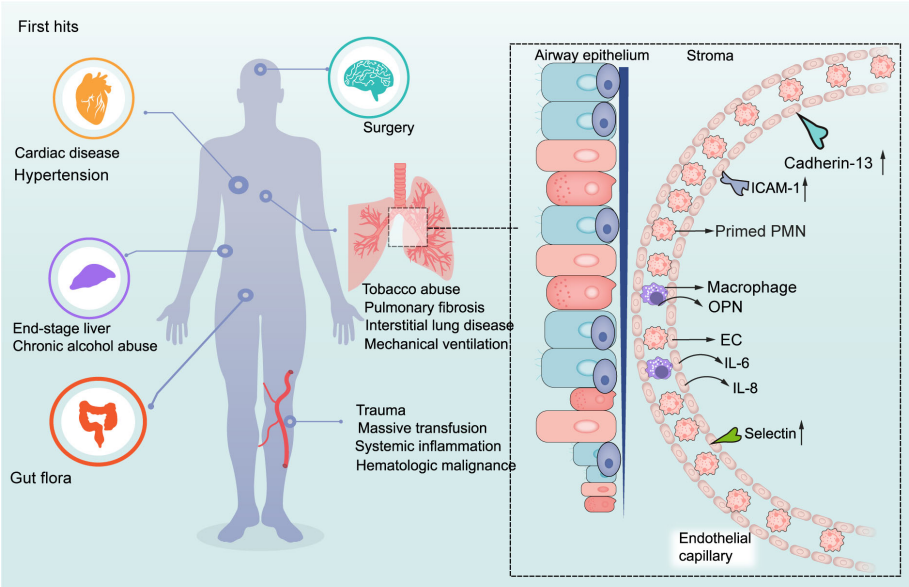

FIGURE 2
First hits in the pathogenesis of TRALI. The underlying diseases of patients stimulate the activation of ECs and macrophages, thus attracting PMNs from circulating pool to the injured lung.

uniquely influence TRALI progression (13, 14), representing the pulmonary reaction phase.

In wild-type BALB/c or C57BL/6 mice, the development of pulmonary edema requires monocytes/macrophages, while PMNs and platelets appear to be dispensable. Conversely, regulatory T cells (Tregs) and dendritic cells (DCs) are associated with lung injury amelioration (32). Meanwhile, given that ECs represent the key regulator of PMN transmigration, they may represent pivotal targets for TRALI induction (33). However, the interplay between pathogenic antibodies and their target cells remains unclear in the context of antibody-dependent TRALI pathogenesis. In this section, we discuss how antibodies or BRMs in transfused blood components respond to target cells and how the induced aberrant host response delineates the different pathogenic scenarios of TRALI (Figure 3).

2.2.1 PMNs

Based on patient autopsy reports and preclinical studies on the TRALI reaction, PMNs are regarded as the main pathogenic cells mediating lung injury (13, 26). Among the initially reported TRALI cases, anti-HLA class antibodies were the most frequently identified antibody types in blood products, of which anti-HLA class I antibodies were the most prevalent (21, 34). Indeed murine models that mimic human anti-HLA class I antibody-dependent TRALI—administration of anti-MHC class I mAbs (clone 34–1–2S) against murine $H2K^d$, or the $H\text{-}2^d$ antigen—has advanced our understanding of this disease. The essential role of PMNs in TRALI was first identified in preclinical models, in which *in vivo* ablation of PMNs reportedly protected mice from anti-MHC-I-mediated TRALI development (23, 32). In the first genetically manipulated *in vivo* murine TRALI model, endothelial-bound 34-1-2S reacted with the pulmonary PMN Fc gamma receptor (FcγR), leading to PMN activation and lung injury (22) (Figure 3A). Although resident PMNs do not regularly express HLA class II, high levels are expressed on the surface of activated PMNs (35). Moreover, evidence from two-hit rat models revealed that transfusion of donor antibodies against HLA class II stimulated PMN activation and TRALI induction (35, 36) (Figure 3B). In a rat anti-HNA-2a-mediated TRALI model, the antibody directly activated PMNs in the presence of cognate antigen on the surface of PMNs in an EC-independent manner (37). Unlike other anti-leukocyte antibodies that participated in TRALI development, anti-HNA-3a antibodies failed to induce direct PMN activation and appeared to primarily interact with ECs (38) (Figure 3D). Following the activation of ECs, von Willebrand factor (vWF) was produced and released into circulation; subsequently, anti-HNA-3a antibodies bound to the trimolecular complex comprising choline transporter-like protein-2, vWF, and CD11b/CD18 on the surface of PMNs, leading to PMN activation and agglutination *via* CD11b/CD18 signal transduction, which may promote TRALI-associated endothelial leakage (38) (Figure 3C).

In the case of antibody-independent TRALI, lyso-PCs generated during blood storage caused PMN-mediated EC leakage in an *in vitro* TRALI model, in which human pulmonary microvascular endothelial cells (HPMVECs) were primed with LPS and co-cultured with PMNs followed by the addition of lyso-PCs as the second hit (39) (Figure 3H). CD40—the CD40L receptor—is distributed on the surface of leukocytes, platelets, and ECs (40). The interaction between CD40 and CD40L has been proposed as a proinflammatory feature and a pivotal pathogenic response to inflammation and organ injury (41). Stored platelet microparticles that released sCD40L boosted PMN-dependent HPMVEC damage,

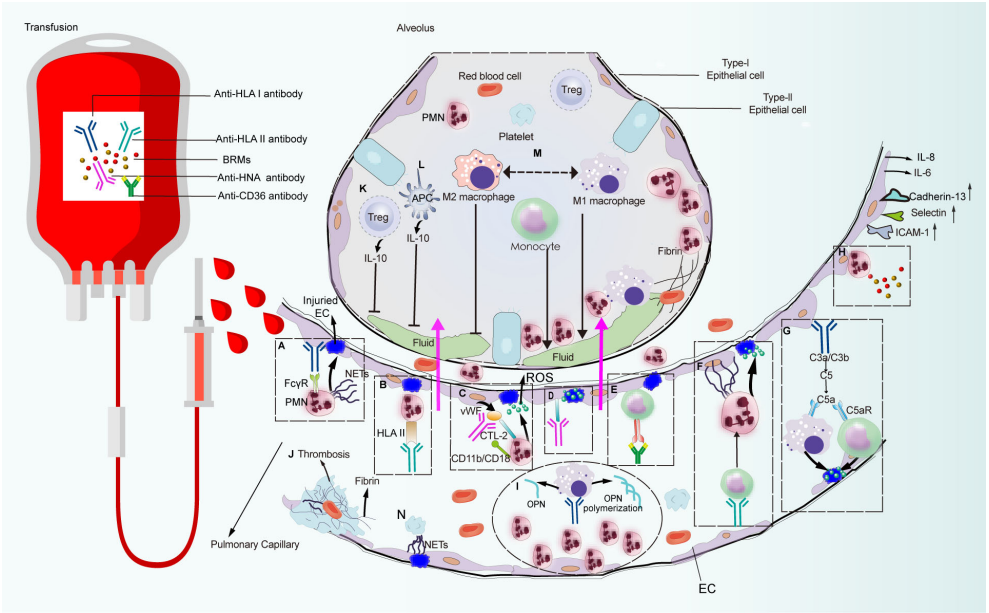

FIGURE 3
Pulmonary reaction and effector phase of TRALI pathogenesis. Pathways that are constituted with detrimental factors from blood products which connect with immune cells and non-hematopoietic cell lead to pulmonary edema or lung injury alleviation. Pathways **(A–N)** are systematically discussed in the main text. CTL-2, choline transporter-like protein-2.

which may contribute to TRALI onset (40). Indeed, blocking the CD40-CD40L interaction with an anti-CD40L antibody protected mice against 34-1-2S-mediated TRALI development by suppressing PMN migration into the alveolar space (42, 43).

Although the aberrant activation of PMNs is recognized as the main feature of TRALI, the underlying molecular mechanisms driving PMN activation remain elusive. MicroRNAs (miRNAs)—single-stranded non-coding RNAs constituting approximately 22 nucleotides—contributed to lung injury by interacting with the 3′-untranslated region of mRNA (44). More specifically, miR-144 caused 34-1-2S-mediated TRALI by activating the NF-κB/CXCR1 signaling pathway *via* KLF2 in a PMN-dependent manner (45) (Figure 4A). Additionally, protein tyrosine phosphatase-1B (PTP1B) activated the PI3Kγ/AKT/mTOR-dependent CXCR axis, which may be involved in PMN activation (46) (Figure 4B). Anti-human leukocyte antigen-A2 (HLA-A2) antibody can function as an initiator of TRALI (47). *In vitro* coculture of anti-HLA-A2 antibody with PMNs resulted in PMN activation and subsequent endothelial permeability (48). The anti-HLA-A2 antibody may activate PMNs by stimulating NF-κB/NLRP3 inflammasome activation *via* increased abundance of phosphorylated-Src, thus aggravating TRALI (49) (Figure 4C).

2.2.2 ECs

Anti-leukocyte antibodies are recognized as the main contributor to TRALI pathogenesis; however, the critical binding site of these antibodies remains unclear. HLA expression on nonleukocytic cells suggests ECs as probable targets for antibody binding. As early as 2011, infusion of 34-1-2S to a murine model of human TRALI suggested that the reaction between the antibody and MHC class I molecules on pulmonary ECs represented a probable initiating event for TRALI (50). This may be explained by the high expression of MHC-I on the surfaces of murine pulmonary ECs (51). Similarly, high pulmonary endothelial MHC-I expression has been observed in clinical TRALI (51). Given that the lung capillaries represent the first location encountered by the infused antibodies, the ECs may serve as a key site for antibody binding. Furthermore, targeted deletion of endothelial MHC-I alleviated 34-1-2S-mediated lung injury, while its restoration rendered mice susceptible to lung edema (51). Additionally, the interaction between 34-1-2S and pulmonary ECs may drive the production of complement component 5a (C5a) *via* activation of the complement cascade, thus contributing to TRALI development (50). Collectively, these findings highlight the importance of 34-1-2S engagement with endothelial MHC-I in the induction of TRALI.

ECs also express other leukocyte antigens, including HLA class II and HNA-3, the interaction of which, with their respective antibodies, reportedly contributed to TRALI development, i.e., alloantibodies against HNA-3a, not HNA-3b, have been linked to severe TRALI (52, 53). Anti-HNA-3a antibodies interacted with cognate antigens on the surface of pulmonary ECs in a PMN-independent manner, thereby precipitating TRALI (54, 55).

Moreover, ECs participate in antibody-independent TRALI *via* direct endothelial dysfunction. Transfusion of aged platelets elicited TRALI *via* acid sphingomyelinase (ASM)-forming ceramide-mediated endothelial apoptosis, further accelerating endothelial barrier failure (56). Furthermore, stored platelet-derived injurious

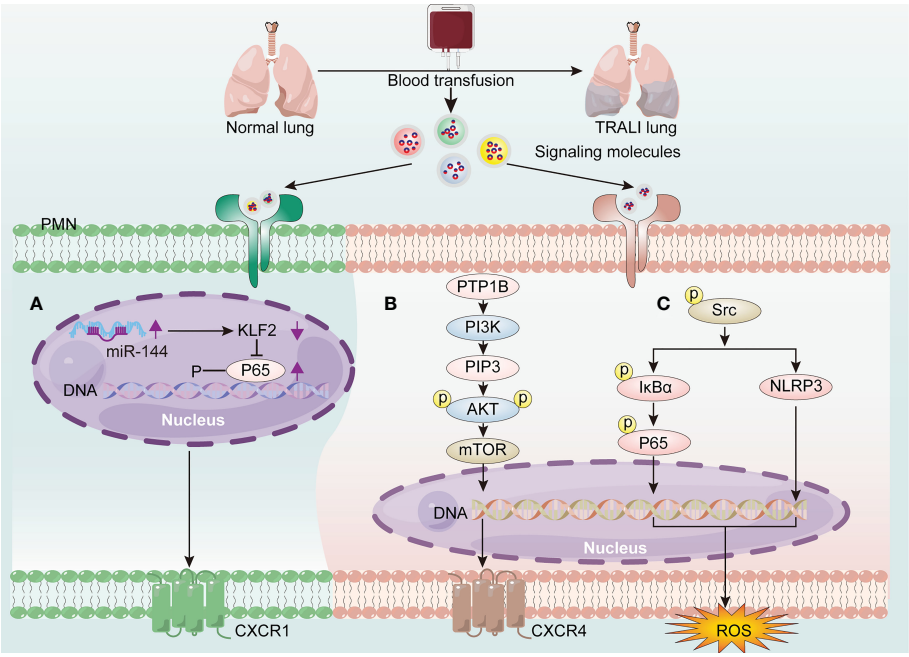

FIGURE 4
The molecular mechanisms of driving PMN activation in TRALI pathogenesis. Blood transfusion induces PMN activation *via* the generation of signaling molecules activating the receptors on PMNs, thereby exacerbating TRALI. **(A)** Up-regulated miR-144 promotes PMN activation through activating the NF-κB/CXCR1 signaling pathway *via* down-regulation of KLF2. **(B)** PTP1B activates PMNs *via* PI3Kγ/AKT/mTOR-dependent CXCR4 signaling. **(C)** HLA-A2 induces PMN-derived ROS production *via* activating NF-κB/NLRP3 inflammasome *via* phoosphorylate-Src elevation.

ceramide enhanced the formation of extracellular vesicles in an ASM-dependent manner, which transported ceramide to the lung, resulting in endothelial barrier failure and TRALI onset (57, 58). Moreover, red blood cell (RBC) transfusion was a hazard factor for the induction of pulmonary respiratory failure (59, 60). RBC transfusion-mediated lung injury may be related to pulmonary ECs undergoing necrotic cell death, i.e., necroptosis (61, 62).

Collectively, these data support the evidence that ECs may be crucial regulators of TRALI.

2.2.3 Monocytes/macrophages

The binding of anti-leukocyte antibodies to corresponding cognate antigens distributed on PMNs or pulmonary ECs may lead to PMN activation and induction of lung injury. However, given that PMN depletion did not prevent TRALI development in murine antibody-mediated TRALI (54), other cells have also been implicated. Although HLA class II antigen is not specifically expressed on PMNs or ECs, anti-HLA class II antibodies are consistently involved in TRALI onset. Indeed, plasma containing anti-HLA class II antibodies effectively sensitized peripheral blood mononuclear cells, leading to severe transfusion reactions *via* the production of inflammatory cytokines, such as IL-1β and IL-6, and chemokines (IL-8) by monocytes (63). Moreover, evidence from an *ex vivo* model showed that anti-HLA class II antibody-initiated monocyte activation was attributable to exaggerated HPMVEC permeability, which reflected endothelial damage in patients suffering from TRALI (64). Consistent with this result, anti-HLA class II antibody-containing plasma can cause matched monocyte activation, resulting in the initiation of a PMN amplification cascade and lung endothelial damage in an *in vitro* two-hit model (65) (Figure 3F). This finding has been further verified in an *ex vivo* lung model, which showed that anti-HLA class II antibody-mediated TRALI was dependent on monocytes, while PMNs were apparently dispensable (65). Following injection of 34-1-2S to severe combined immunodeficient (SCID) mice, the intact antibody reacted with its cognate antigen on peripheral blood monocytes, resulting in monocyte-dependent upregulation of MIP-2 expression, leading to recruitment of PMNs to the lung microvasculature, where the Fc domain of the antibody led to full TRALI initiation (66). Additionally, in place of FcγR-mediated PMNs activation, the C5a receptor on the surface of peripheral blood monocytes/macrophages responded to C5a derived from complement cascade activation, causing disease induction (50) (Figure 3G). Furthermore, individuals with CD36-deficient platelets and monocytes can develop isoantibodies against CD36 because of incompatible immune stimulation, which contributes to TRALI onset (67–69). The preliminary mechanism may be associated with anti-CD36 antibody-Fc receptor (FcR) binding to monocytes, thus inducing the TRALI reaction (70) (Figure 3E).

Macrophages have also been identified as major opsonins involved in TRALI induction. *In vivo* macrophage-derived OPN polymerization was involved in PMN chemotaxis (71), whereas macrophage elimination protected mice from antibody-mediated TRALI (26) (Figure 3I). Macrophages exert diverse functions, facilitated in part by their ability to undergo polarization (72), which enables them to readily adopt phenotypes based on stimulation within their microenvironment (73). Macrophages are roughly categorized as M1 or M2 according to phenotype. M1 macrophages are regarded as the proinflammatory phenotype with microbicidal potential, while M2 macrophages have a propensity to facilitate tissue repair and cell proliferation (72). Using a murine TRALI model, Wang et al. (74) confirmed that M1-polarized alveolar macrophages (AMs)—the proinflammatory phenotype—played a critical role in lung injury. Lung edema in TRALI mice can be abrogated by inhibiting the polarization of AMs toward the M1 phenotype (74) (Figure 3M).

These data suggest a clear role for monocytes/macrophages in TRALI pathogenesis.

2.2.4 Recipient platelets

Platelets derived from bone marrow megakaryocytes are commonly associated with thrombosis and hemostasis (75). However, beyond these traditional roles, platelets are key effectors of thromboinflammation and immune responses *via* crosstalk with various immune cells, such as PMNs (76). Moreover, considering the observed thrombocytopenia in TRALI patients, as well as the results of murine antibody-mediated TRALI models, platelets appear to be drivers of TRALI (13, 77). However, the evidence regarding the role of recipient platelets in aggravating lung injury is conflicting, i.e., the role of recipient platelets as either pathogenic or dispensable, in the context of TRALI development, within murine models injected with 34-1-2S is dependent on the experimental designs for assessing lung injury. On the one hand, treatment with rabbit polyclonal anti-mouse platelet serum to eliminate platelets, as well as 100 mg kg^{-1} aspirin or tirofiban to inhibit platelet reactivity, effectively prevented alveolar edema (23, 78, 79). Moreover, GPIb—a major platelet receptor—has been implicated in platelet activation and aggregation (76). However, platelet depletion, using an anti-GPIbα antibody, improved TRALI outcomes, without influencing its progression (80). On the other hand, several studies using different animal models have shown that platelet depletion or inhibition was dispensable in TRALI development. For example, neuraminidase-induced thrombocytopenia failed to effectively protect mice from TRALI (50, 81), diphtheria toxin-induced immunologic thrombocytopenia did not prevent PF4-cre/iDTR mice from 34-1-2S-associated lung edema (82), and pretreatment of mice with ML354—a protease receptor 4 pathway inhibitor—failed to prevent TRALI induction following activation of platelets *via ex vivo* stimulation (80).

Recently, novel insights regarding recipient platelets have been reported. Receptors bound to immunoglobulin G (IgG) antibody are uniquely expressed on human platelets and include IgG receptor I (FcγRI) and FcγRIIA, among others (83). Among these receptors, FcγRIIA/CD32A is the most extensively distributed FcγR on the surface of human platelets (83). Yet, its effects on TRALI have not been reported in mouse models, suggesting that the previous conclusions regarding the role of recipient platelets as main contributors to the pathogenicity of antibody-dependent TRALI are potentially incomplete. To address this gap in knowledge, EI Mdawar et al. (84) established an FcγRIIA/CD32A transgenic mouse model. When the humanized mouse model expressing the

FcγRIIA/CD32A receptor was challenged with 34-1-2S, aggravated lung edema was observed (84). The authors concluded that the associated pathogenesis was caused by TRALI induction triggering platelet activation and subsequent 5-hydroxytryptamine 2A serotonin release. Thus, recipient platelets appear to represent key effector cells in exaggerated lung injury; however, their contribution to TRALI onset and pathogenesis requires further investigation.

2.2.5 DCs/Tregs/IL-10

Conflicting evidence has been reported regarding the role of recipient T cells in other inflammatory lung injury models. For example, T-cell activation may aggravate endotoxin-induced acute lung injury (ALI) (85). Meanwhile, mice treated with LPS developed ARDS, whereas lethal lung injury was significantly ameliorated by decreasing CD3+ T cells *in vivo* (86). Conversely, murine ARDS induced by reovirus was critically dependent on T cells and their ability to secret interferon-γ (17). In contrast, reconstituted T cells protected SCID mice from lung injury, implicating T cells as protective factors against TRALI development (17). This was further confirmed *via* removal of Tregs, DCs, and IL-10, resulting in murine TRALI initiation (32), which was likely related to the protective effect elicited by Treg- and DC-secreted IL-10. Indeed, both patients with low levels of IL-10 and mice lacking IL-10 were susceptible to TRALI development (32, 87). Hence, the Treg-DC-IL-10 axis has been proposed as a protective mechanism against TRALI induction (Figures 3K, L). However, to date, the mechanism underlying the protective effect of IL-10 remains unclear and warrants further investigation.

2.3 Effector phase

In this phase, activated effector cells, including PMNs, ECs, monocytes/macrophages, and platelets, produced effector molecules, such as NETs (Figures 3A, N) and ROS (Figures 3C, D, F, G), which directly damage pulmonary vascular ECs, resulting in lung edema. Additionally, EC dysfunction may aggravate pulmonary vascular leakage. Moreover, dysregulated coagulation has been implicated in lung injury, including that associated with TRALI and severe acute respiratory syndrome coronavirus 2 (SARS-CoV-2) mediated ALI (77, 88).

2.3.1 NETs

NETs can effectively restrict pathogen spreading and kill microorganisms *via* the release of high doses of histones and granule contents by active immune cells (89). The role of NETs in TRALI was first reported in 2012 by Thomas, who observed NETs in the blood of patients and mice with TRALI (81). They further observed that PMN-derived NETs were released *in vitro* following challenge by an anti-leukocyte antibody. More recently, the formation of NETs *in vivo*, as well as their detrimental contributions, have been further validated in TRALI models (90, 91). The complement system has also been shown to function as a key trigger of NET production by assisting the 34-1-2S in PMN activation (51, 92). However, NETs are not exclusively produced by PMNs. Platelet-derived NETs can directly damage pulmonary ECs, further aggravating TRALI (93). Moreover, within a murine TRALI model, an increase in platelet–neutrophil interactions and NET formation was observed, with fewer NET produced following the administration of platelet-targeting therapeutics (78). Additionally, NET formation has been observed in antibody-independent TRALI. For example, under long-term storage, RBC hemolysis can occur and cause sufficient hemin accumulation in the solution (94). Hemin induced NET release, resulting in TRALI induction (94). Hence, NETs function as pivotal effector molecules of TRALI induction.

2.3.2 ROS

Upon exposure to inflammatory factors, the NADPH oxidase family members are activated, resulting in the production and release of a large amount of ROS, leading to lung disease (95). ROS are important effector molecules involved in TRALI pathogenesis. That is, trapped PMNs within the lung capillary bed being activated by anti-leukocyte antibodies and BRMs from transfused blood components, resulting in the production and release of ROS, which further destroy the ECs, causing capillary leakage and pulmonary edema (48, 96). PMNs are also recruited to the lungs, where they produce ROS that damage the ECs (26). Thus, PMN-derived ROS production blockade was an effective strategy for protecting mice from antibody-mediated TRALI (50, 97, 98). Activated monocytes/macrophages and pulmonary ECs also generated ROS, thus inducing deterioration of endothelial permeability and TRALI onset (50, 54). More importantly, gp91phox-KO mice, which lacked the ability to induce ROS, were protected from antibody-mediated TRALI, indicating that ROS were essential for TRALI induction (32). Storage of blood products can cause vesicle shedding and accumulation of hemin and lysoPC, which contributed to aberrant oxidative bursts, ROS production, and lung endothelial damage *in vitro* (39, 99–101). This may represent a potential pathogenesis for antibody-independent TRALI development.

2.3.3 Imbalanced coagulation and the fibrinolysis system

Microthrombosis occured in the pulmonary vascular walls of animals with TRALI (84). Hence, considering that ECs are the key initiator and regulator of coagulation (102), coagulopathy may contribute to deteriorated lung function following transfusion of pathogenic antibodies or BRMs that would destroy pulmonary ECs. Indeed, coagulopathy has been identified as a pivotal pathogenic characteristic in rat models of aged erythrocyte- or platelet-mediated TRALI (103, 104). A case-control study reported that blood transfusions in patients who underwent cardiovascular surgery and exhibited obvious pulmonary inflammatory reactions were accompanied by coagulation and fibrinolysis dysregulation, leading to worsened prognosis in the ICU (105), thus further demonstrating the potential role of coagulopathy in TRALI development. Moreover, intravital lung imaging revealed platelet adhesion to the pulmonary ECs as well as occasional thrombotic events in a murine 34-1-2S-mediated TRALI model (51). Coagulopathy was involved in the dysregulation of coagulation

and fibrinolytic pathways (106), leading to fibrin deposition in the lungs (77). Fibrin effusion in the lung alveoli was recognized as a main contributing factor to ALI and ARDS pathogenesis (107–109). Additionally, in a murine 34-1-2S-mediated TRALI model, increased coagulation, impaired fibrinolysis, and fibrin deposition were observed in the lungs (77) (Figure 3J). In fact, fibrin deposition in the lungs may activate ECs, thereby promoting the release of proinflammatory mediators and increasing vascular permeability and lung injury (77).

3 Management

The morbidity associated with TRALI has plummeted with the introduction of mitigation strategies that include donor management, blood component processing, and patient blood management (PBM). However, no specific therapies are available and therapeutic options primarily focus on supportive measures. Hence, additional research is needed to develop, standardize, and evaluate novel drugs for the treatment of TRALI. Recently, a full spectrum of potential targets, including anti-inflammatory and immunoregulatory factors, have been investigated as potential TRALI therapeutics. Recent progress in prevention strategies (Table 1) and treatments (Table 2) has been made and is described below.

3.1 Prevention

3.1.1 Antibody-mediated TRALI prevention strategies

3.1.1.1 Donor management

Considering that anti-HLA or anti-HNA antibodies are detected most frequently in multiparous donors, TRALI risk-reduction strategies, including the introduction of male-only donors, male-dominated plasma, exclusion of all-exposure donors, and antibody screening, have been introduced, resulting in a significant reduction in the morbidity associated with antibody-dependent TRALI in developed countries (4, 21, 110–112). However, anti-leukocyte antibody screening has not yet been routinely implemented because of financial complexities (136). Despite the use of these prevention strategies, additional research is needed, as anti-HLA antibodies were reportedly triggered in coronavirus disease 19 convalescent plasma donors and SARS-CoV-2 vaccination volunteers (137, 138). Therefore, TRALI prevention may also require screening antibodies against HLA antigens in donors following SARS-CoV-2 sensitization.

3.1.1.2 Solvent/detergent-treated pooled plasma

Solvent/detergent-treated pooled plasma (SDP) is manufactured by treating large pools of plasma with solvent detergent to ensure that the anti-leukocyte antibody levels are below the limit of detection (116). Since the adoption of SDP in Norway in 1993, no TRALI cases were reported over a 10-year period (113). As of 2020, no TRALI cases had been reported in association with SDP transfusion (115). However, in 2022, a definite TRALI case was observed following SDP transfusion (20, 116), resulting in a total of three reported TRALI cases following SDP transfusion to date (116). Although implementation of SDP transfusion has markedly reduced the incidence of TRALI, medical staff associated with SDP transfusions must realize the potential risk regarding severe complications, i.e., TRALI.

3.1.2 Antibody-independent TRALI prevention strategies

3.1.2.1 Leukoreduction

Leukoreduction is a procedure that intentionally filters leukocytes in donated samples to decrease the abundance of mediators derived from leukocytes and platelets, thereby diminishing transfusion adverse reactions (117, 119). A retrospective analysis revealed that leukoreduction of blood components reduced the occurrence of TRALI cases by 83% (117). Furthermore, previous *in vivo* animal studies demonstrated that TRALI could be attenuated by leukoreduction before storage because of the reduction of proinflammatory mediators (47, 118). Conversely, leukoreduction of packed RBC failed to efficiently prevent TRALI, as reported in a systematic review (119). Hence, the effect of blood component leukoreduction on TRALI incidence should continue to be monitored.

3.1.2.2 Pathogen reduction technology

The pathogen reduction technology (PRT) of Mirasol and Intercept$^{(TM)}$ has been proven effective in improving blood component safety by targeting pathogen nucleic acid or membrane lipid structures in donor samples (124, 139). However, the efficiency of PRT to reduce the risk of TRALI has been proven inconsistent in preclinical studies. An earlier *in vivo* study reported that blood products treated with Mirasol PRT failed to prevent rat TRALI (120). However, transfusion of Mirasol PRT-treated platelets has also prevented lung injury in immunodeficient mice (121). Meanwhile, transfusion of aged Mirasol PRT-treated RBC did not deteriorate this disease in a murine TRALI model parallel with standard-delivery RBC (122). These contradictory *in vivo* results may be because of discrepancies in experimental design.

The role of PRT in TRALI risk-reduction was also debated in clinical studies. An open label, prospective hemovigilance program confirmed that no TRALI cases occurred following transfusion with Intercept$^{(TM)}$-processed platelets (124). Similarly, data from a hemovigilance system involving 2181 transfusion records in Ghana demonstrated that Mirasol PRT-treated whole blood effectively prevented TRALI (123). However, a recent open label, sequential cohort study found that ARDS-associated morbidity did not differ significantly between patients receiving Intercept $^{(TM)}$ PRT platelets and those receiving conventional platelets (125). Therefore, comprehensive clinical trials are required to validate the effect of PRT blood components on TRALI risk-reduction.

3.1.2.3 Platelet additive solution

Following the introduction of risk-reduction strategies in 2014, the rate of TRALI did not differ between blood components (140). However, a significantly higher incidence of TRALI was sustained in female-donated platelets compared with that in male-donated

TABLE 1 Summary of the prevention strategies of TRALI.

Disease	Strategy		Type of study	Effects	Country	Year	Sources
Antibody dependent TRALI	Donor management	Male-only plasma	Retrospective study	Decline in TRALI	Australia	2022	Sivakaanthan et al. (21)
			Retrospective study	No TRALI cases reported	UK	2017	Bolton-Maggs et al. (110)
		Male-dominate plasma	Retrospective study	Decline in TRALI	Australia	2022	Sivakaanthan et al. (21)
		Exclusion of allo-exposure donors	Prospective study	Decline in TRALI	Netherlands	2012	Middelburg et al. (111)
		Screening for antibodies	Retrospective study	Decline in TRALI	Germany France UK Sweden USA	2012	Reesink et al. (112)
	SDP		Clinical study	No cases of TRALI	Norway	2003	Flesland et al. (113)
			Systematic review and meta-analysis	No cases of TRALI	Netherlands	2017	Saadah et al. (114)
			Clinical study	No cases of TRALI	Netherlands	2020	Saadah et al. (115)
			Retrospective study	TRALI occurrence	Netherlands	2022	Klanderman et al. (20)
			Case series	TRALI occurrence	Netherlands	2022	Klanderman et al. (116)
Antibody independent TRALI	Leukoreduction		Retrospective study	Decline in TRALI	USA	2010	Blumberg et al. (117)
			Preclinical study	TRALI mitigation	USA	2014	Silliman et al. (47)
			Preclinical study	TRALI mitigation	USA	2020	McQuinn et al. (118)
			Systematic review	Invalid in prevention TRALI	Ecuador	2015	Simancas-Racines et al. (119)
	PRT	Mirasol	Preclinical study	Invalid in prevention TRALI	USA	2010	Silliman et al. (120)
		Mirasol	Preclinical study	Incapable of inducing TRALI	USA	2015	Caudrillie et al. (121)
		Mirasol	Preclinical study	Incapable of inducing TRALI	USA	2017	Mallavia et al. (122)
		Mirasol	Retrospective study	Valid in prevention TRAL	Ghana	2019	Owusu-Ofori et al. (123)
		Intercept (TM)	Prospective study	No TRALI cases	Italy	2015	Knutson et al. (124)
		Intercept (TM)	Cohort study	No effect on prevention TRALI	USA	2022	Snyder et al. (125)
	PAS		Review	Reducing the incidence of TRALI	USA	2019	Kuldanek et al. (126)
			Review	Reducing the incidence of TRALI	Netherlands	2018	van der Meer et al. (127)
TRALI	PBM		Review	Decreasing the incidence of TRALI	USA	2017	Friedman et al. (128)
			Retrospective study	Decline the incidence of TRALI	Austria	2019	Tung et al. (129)
			Retrospective study	Avoiding TRALI occurrence	Sri Lanka	2022	Priyanjani et al. (130)

TRALI, transfusion-related acute lung injury; SDP, solvent/detergent treated pooled plasma; PRT, pathogen reduction technology; PAS, platelet additive solution; PBM, patient blood management.

TABLE 2 Summary of innovative treatments undergoing TRALI.

Disease	Targeting	Strategy	Delivery Route	Treatment Regiment	Results/ Outcomes	Proposed mechanism of action	Type of study	References
TRALI	Supportive care	Oxygen inhalation	Not mentioned	Not mentioned	Relieving respiratory distress	Maintaining hemodynamics	Review	Semple et al. (13), 2019
							Review	Kuldanek et al. (126), 2019
		Ventilation	Invasive	Not mentioned			Review	Kuldanek et al. (126), 2019
			Noninvasive	Not mentioned				
		Extra-corporeal membrane oxygenation	Intravenous catheterization	Not mentioned			Review	Kuldanek et al. (126), 2019
				Lasting 15 h after the operation			Case reports	Honda et al. (131), 2015
	Serum proinflammatory, anti-inflammatory markers levles, and oxidative stress	Ascorbic acid	I.V.	2.5 gm/6 h, 96 h	Better 7-days survival	Reduced most proinflammatory markers levels and oxidative stress; elevated anti-inflammatory marker	Clinical trial	Kassem et al. (132), 2022
	Gut glora	Broad spectrum; (vancomycin, ampicillin, neomycin, and metronidazole)	Oral	1 mg/mL, every 48 hours for 1 week	Preventing murine TRALI	Decreasing plasma MIP-2 levels and pulmonary PMN recruitment	Preclinical study	Kapur R et al. (24), 2018
Antibody-dependent TRALI	NETs	Aspirin	I.P.	100 μg/g, 30 min prior to LPS priming and again 2 h prior to MHC-I mAb challenge.	Alleviating lung injury	Decreasing NET formation and NET-associated platelets sequestration	Preclinical study	Caudrillier et al. (78), 2012
		DNase1	I.V.	10 mg/kg, at the same time of H2Kd mAb injection; 5 minutes after H2Kd mAb injection	Alleviating lung injury	Decreasing NET formation and NET-associated platelets sequestration	Preclinical study	Caudrillier et al. (78), 2012
		DNase1	Intranasal	50 μg/mouse, 10 min before or 90 min after H2Kd antibody injection.	Improving arterial oxygen saturation	Disrupting NET accumulation	Preclinical study	Thomas et al. (81), 2012
		Disulfiram	I.P.	50 mg/kg, 24 h and 3 h before H2Kd antibody injection.	Improving survival	Blockade of NET formation	Preclinical study	Adrover et al. (91), 2022
		MSI-1436	I.P.	10 mg/kg, 2 h before TRALI induction	Preventing murine TRALI and improving survival	Limiting NET production	Preclinical study	Song et al. (46), 2022
	ROS	IVIg	I.P.	2 g/kg, 18 h before 34-1-2S injection; 1 g/kg dose of IVIg 3 min post 34-1-2S injection	Preventing TRALI as well as reducing lung injury	Inhibiting PMN derived ROS production	Preclinical study	Semple et al. (97), 2012
	PMNs	MSI-1436	I.P.					

(Continued)

TABLE 2 Continued

Disease	Targeting	Strategy	Delivery Route	Treatment Regiment	Results/ Outcomes	Proposed mechanism of action	Type of study	References
				Optimal dose of 10 mg/kg, 2 h before 34-1-2S injection.	Preventing murine TRALI and improving survival	Promoting PMN aging	Preclinical study	Song et al. (46), 2022
		Dasatinib	Oral	Not mentioned	Alleviating lung injury	Inhibited PMN activation	Preclinical study	Le et al. (49), 2022
	ECs	IL-35	I.V.	100 μg/kg, once a day for 2 days before the TRALI model, and the model was generated on the third day, with a third injection before 34-1-2S injection.	Preventing TRALI	Inhibition of endothelial activation	Preclinical study	Qiao et al. (133), 2020
	Macrophage	anti-OPN antibody	I.V.	2.25 mg/kg, injected with TRALI induction antibodies	Preventing TRALI onset	Blocking OPN derived from macrophages	Preclinical study	Kapur et al. (26), 2019
		AAT	Exogenous gene delivery; hydrodynamic injection	A mixture of a pattB-CMV-AAT and a mouse codon-optimized PhiC31o vector was codelivered to hepatocytes by hydrodynamic injection	Alleviating lung injury	Suppressing AMs polarization toward the proinflammatory M1 phenotype	Preclinical study	Wang et al. (74), 2020
	Platelets	Sarpogrelate	I.V.	1 mg/kg,5min before 34-1-2S injection; injection after TRALI induction	Abolishing lung edema	Blockade of platelet FcγRIIA/CD32A activation mediated serotonin secretion	Preclinical study	El Mdawar et al. (84), 2021
		Tirofiban	I.V.	2 μg/g, 30min before 34-1-2S injection	Decreasing lung injury	Suppressing platelet activation and targeting pulmonary coagulation-fibrinolytic disorders	Preclinical study	Yuan et al. (134), 2023
	Anti-inflammatory cytokine	IL-10	I.V.	45 mg/kg, together with the TRALI induction antibodies or 15 min after injection of TRALI induction antibodies	Protecting and rescuing murine TRALI	Removal of a major anti-inflammatory brake.	Preclinical study	Kapur et al. (32), 2017
	Treg	IL-2/IL-2c	I.P.	IL-2 5μg/kg or IL-2c (1 mg of recombinant murine IL-2 and 10 mg of mouse IL-2 antibody) administered to mice for 5 consecutive days before TRALI model induction	Preventing murine TRALI	Activation of Treg-IL-10 axis	Preclinical study	He et al. (135), 2019

TRALI, transfusion-related acute lung injury; h, hour; I.V., intravenous injection; I.P., intraperitoneal injection; min, minute; MIP-2, macrophage inflammatory protein-2; NETs, neutrophil extracellular traps; ROS, reactive oxygen species; mAb, monoclonal antibody; IVIg, intravenous immunoglobulin; PMNs, polymorphonuclear neutrophils; ECs, endothelial cells; IL, interleukin; OPN, osteopontin; α1-antitrypsin, AAT; AM, alveolar macrophage; FcγR, IgG receptor; IL-2c, anti-IL-2 complexes; Treg, regulatory T cell.

platelets (140), which may be because of the platelets suspended in female plasma containing anti-HLA or anti-HNA antibodies. Meanwhile, buffy-coat-derived platelets suspended in platelet additive solution (PAS) can reduce TRALI-associated morbidity, which was similar to that reported in single-donor platelets (126, 127). Thus, additional strategies that may decrease the incidence of TRALI must be implemented, including replacement of traditional residual plasma with novel PAS in buffy coat pooled platelets.

3.1.3 TRALI PBM

PBM attempts to optimize the patient's hematologic capabilities, decrease bleeding, and limit unnecessary transfusions (141). Findings from the hemovigilance network in the United States in 2015 highlighted the ability of PBM to decrease the incidence of TRALI (128). Similarly, a decrease in TRALI incidence was observed in Austria following the introduction of PBM (129). A recent study further emphasized that proper PBM represented the standard tool for avoiding TRALI occurrence (130).

3.2 Treatment

3.2.1 Supportive care

To date, there are no established treatments for TRALI beyond supportive care, which comprises oxygen inhalation, ventilation, and extra-corporeal membrane oxygenation to effectively maintain hemodynamics (13, 126, 131). In rare cases of sickle cell disease, patients experiencing TRALI also receive 5% albumin, erythropoietin, and iron as supportive modalities (142). Although pulmonary edema is common, diuretics should be avoided because of the associated hypotension (143).

3.2.2 Clinical studies

Ascorbic acid, a water-soluble vitamin, can limit ROS damage to the epithelial barrier. A randomized controlled trial revealed that critically ill patients with TRALI exhibited a better 7-day survival following intravenous administration of high-dose ascorbic acid (132). To fully explore more effective TRALI treatments, future large-scale multi-center randomized controlled trials and in-depth clinical studies are needed.

3.2.3 Preclinical studies

Activation of ECs, PMNs, monocytes/macrophages and platelets leading to effector molecule production and pulmonary fibrin deposition is the key process of the onset of pulmonary edema, the hallmark of TRALI. Hence, blocking these pathways may effectively prevent TRALI initiation. Additionally, targeting gut flora and Tregs/IL-10 seems to be prospective prevention strategies or treatments.

3.2.3.1 Targeting gut flora

Since gut flora resulted in mice susceptibility to 34-1-2S-dependent TRALI, depletion of gut flora in mice may be a promising strategy for relieving TRALI. Utilizing broad-spectrum antibiotics composed of vancomycin, ampicillin, neomycin, and metronidazole in drinking water to kill gut flora can prevent TRALI in mice *via* decreasing plasma MIP-2 levels and PMN recruitment in the lungs (24).

3.2.3.2 Targeting effector molecules

Various compounds have been found to halt the effect of NETs. For instance, DNase I is an effective therapeutic drug for digesting NET present in the lungs (91). Combined aspirin and DNase1 treatment reduced NET formation and NET-associated platelet sequestration, thus alleviating TRALI (78). Moreover, intranasal DNase 1 treatment of mice before 34-1-2S infusion, or injection 90 min after TRALI occurrence, can disrupt NET accumulation in the alveoli and improve blood oxygenation (81). Meanwhile, inhibition of NET formation is also an effective means to prevent TRALI. Disulfiram—an existing FDA-approved drug for alcohol use disorder—effectively improved the survival of murine 34-1-2S-induced TRALI *via* blockade of NET formation (91).

Intravenous immunoglobulin (IVIg) is biologic components of polyclonal antibodies, extracted from human plasma of large healthy donor cohort blood banks. IVIg has proven beneficial for the clinical treatment of autoimmune diseases, chronic lymphocytic leukemia, and sepsis (144). To date, IVIg therapy remains off-label for patients with TRALI. Nevertheless, one study has assessed the efficacy of IVIg in a TRALI model and found that it prevented murine antibody-mediated TRALI and reduced lung injury at the level of PMN-derived ROS production, thus improving lung injury (97). Conversely, several clinical lines of evidence have reported that IVIg may contribute to TRALI induction (145, 146). Although IVIg may contribute to TRALI induction, this is extremely rare given the amount of IVIg infused annually. Due to these controversial findings, the therapeutic pathway associated with IVIg requires further elucidation.

3.2.3.3 Targeting PMNs

The pivotal role of PMNs in TRALI provides a basic principle for exploiting PMN-targeted therapies. PMN aging is described as a "programmed disarming" that decreases the capacity of PMNs to inflict damage after infiltrating target tissues (147). Based on this theory, it is proposed that therapeutic intervention to regulate PMN aging may protect against tissue damage. PTP1B regulates signaling events that are of fundamental importance to homeostatic control (46). PTP1B inhibitors, including MSI-1436 and DPM-1003, have been tested in clinical trials for obesity and metastatic breast cancer (46). Inhibition of PTP1B with MSI-1436 effectively promoted PMN aging, thus preventing murine TRALI and improving survival (46). Dasatinib —a tyrosine kinase inhibitor commonly used to improve leukemia survival rates (148)—provided a clinical benefit in PMN-mediated inflammatory diseases by influencing the proinflammatory functions of mature PMNs (148). Moreover, dasatinib inhibited PMN activation in a TRALI mouse model by negatively regulating the NF-κB/NLRP3 inflammasome activation (49).

3.2.3.4 Targeting endothelial activation

As endothelial activation is crucial to TRALI onset, it may represent an effective therapeutic target for preventing lung injury caused by blood transfusion. IL-35, which belongs to the IL-12 cytokine family, is regarded as a novel immune-suppressive cytokine (149). IL-35 may alleviate disease states by inhibiting pulmonary endothelial proliferation, apoptosis, and activation (133, 150). IL-35 treatment has been proven to prevent murine TRALI *via* inhibition of endothelial activation (133), which could provide new insights into therapeutic targets.

3.2.3.5 Targeting macrophages

The treatments for targeting macrophages, including blocking the production of key effectors by macrophages and regulating macrophage polarization, represent potential TRALI therapies. OPN derived from macrophages is a matricellular protein that served a

crucial role in PMN migration (26). Meanwhile, inhibition of OPN with an anti-OPN antibody in the presence of macrophages can prevent TRALI onset (26). Likewise, inducing polarization of macrophages toward the anti-inflammatory M2 phenotype has improved various disease states in preclinical models (151, 152). In particular, α1-antitrypsin (AAT) elicits tissue-protective effects as well as anti-inflammatory and immunomodulatory properties (74). Application of human AAT exogenous gene delivery technology to 34-1-2S-treated mouse livers successfully alleviated lung injury *via* suppressing M1 polarization (74). Hence, targeting macrophage-associated inflammatory proteins or promoting polarization toward the M2 phenotype may serve as prospective therapeutic strategies.

3.2.3.6 Targeting platelet activation

Sarpogrelate has been widely used in treating cardiovascular disorders *via* specifically antagonizing 5-HT2A receptor signaling (153). Thus, to investigate the role of 5-HT2A receptor in serotonin-mediated deterioration that caused pulmonary capillary leakage in humanized mice, sarpogrelate was employed (84). Administration of this drug to antibody-mediated TRALI in humanized mice abolished the exacerbation of lung edema (84). The significant effect of sarpogrelate on TRALI suggested that targeting activated platelet-mediated serotonin secretion may represent a potential TRALI therapy. Alternatively, tirofiban—a platelet receptor antagonist—possessed potential for preventing murine 34-1-2S-mediated TRALI *via* suppressing platelet activation and targeting pulmonary coagulation-fibrinolytic disorders (134).

3.2.3.7 Targeting Tregs/IL-10

Tregs are a subpopulation of $CD4^+$ T cells that maintain tissue tolerance *via* secretion of anti-inflammatory cytokines (e.g., IL-10) (154, 155). Treg-based therapies have been proven promising for autoimmune diseases and allograft rejection (155, 156). In particular, IL-2 is a trophic cytokine required for the expansion of effector cells as well as Tregs (135), and the IL-2/anti-IL-2 antibody complex (IL-2c) induces vigorous T-cell proliferation *in vivo* (135). In a murine antibody-mediated TRALI model, administration of IL-2/IL-2c rapidly expanded the Treg population, thereby increasing the level of IL-10, which enabled mice to recover from lung injury (157). Given that IL-10 possesses potent anti-inflammatory and tissue regenerative capabilities, IL-10 administration prophylactically protected and therapeutically rescued against TRALI *in vivo* (13, 32, 158). These findings indicate that induction of Treg IL-10 production, or direct IL-10 treatment represent promising therapeutic strategies for TRALI.

4 Conclusions

Although TRALI is a leading cause of transfusion-associated death, specific treatments are still lacking. Thus, understanding its pathogenesis is key to establishing effective disease management strategies. Recently, significant progress has been made in defining TRALI pathophysiology. In particular, based on the two-hit theory, we innovatively define a three-step pathogenesis model for TRALI that is composed of the priming step, pulmonary reaction, and effector phase. As depicted in this model, the patient risk factors, in combination with detrimental factors within the blood transfusion components, trigger a dynamic spectrum of clinical manifestations based on complex host responses. These responses involve immune cells, including PMNs, platelets, Tregs, monocytes, macrophages; non-immune cells, such as ECs; and effector molecules, such as NETs, ROS, and coagulation-fibrinolytic disorders. In fact, the three-step pathogenesis model especially in pulmonary reaction and effector phase may be potentially overlapping.As such, application of a TRALI pathogenesis stage-specific management strategies may serve to improve disease progression. Hence, a better understanding of modifiable risk factors may help identify those patients most susceptible to TRALI onset. Following the introduction of strategies to exclude anti-leukocyte antibodies, BRMs, and associated pathogenic molecules from blood products, the incidence of TRALI in clinical studies and preclinical models has decreased rapidly. Additionally, a large number of *in vivo* drug experiments targeting PMNs, macrophages, platelets, Tregs, ECs, NETs, ROS, and coagulation-fibrinolytic disorders have effectively prevented the occurrence of lung edema. As these interventions have demonstrated efficacy in preventing TRALI occurrence in preclinical studies, their early implementation might benefit disease prognosis. One potential therapeutic agent is ascorbic acid, which has been proven beneficial for TRALI recovery in critical patients within a clinical trial. Further in-depth research is required to investigate effective drugs for targeted therapies to achieve better clinical outcomes.

Author contributions

YY and ZL conceptualized the review. YY drafted the manuscript, created the figures, and constructed the tables. ZL edited the final version of manuscript. ZL obtained the funding and provided the financial resource. All authors contributed to the article and approved the submitted version.

Funding

This study was supported by the Technology Innovation Project of Chengdu Science and Technology Bureau (2022-YF05-02122-SN).

Acknowledgments

We gratefully appreciate the generous assistance from colleagues at the Department of Blood Transfusion, the Third People's Hospital of Chengdu, Affiliated Hospital of Southwest Jiaotong University.

Conflict of interest

The authors declare that the research was conducted in the absence of any commercial or financial relationships that could be construed as a potential conflict of interest.

Publisher's note

References

1. Morsing SKH, Zeeuw van der Laan E, van Stalborch AD, van Buul JD, Kapur R, Vlaar AP. A pulmonary endothelial amplification loop aggravates ex-vivo transfusion-related acute lung injury *Via* increased toll-like receptor 4 and intra-cellular adhesion molecule-1 expression. *Transfusion* (2022) 62(10):1961–6. doi: 10.1111/trf.17076

2. Guo K, Ma S. The immune system in transfusion-related acute lung injury prevention and therapy: update and perspective. *Front Mol Biosci* (2021) 8:639976. doi: 10.3389/fmolb.2021.639976

3. Vlaar APJ, Toy P, Fung M, Looney MR, Juffermans NP, Bux J, et al. A consensus redefinition of transfusion-related acute lung injury. *Transfusion* (2019) 59(7):2465–76. doi: 10.1111/trf.15311

4. US Food and Drug Administration. *Fatalities reported to fda following blood collection and transfusion annual summary for fy 2020* (2021). Available at: https://www.fda.gov/media/160859/download.

5. Zeeuw van der Laan EAN, van der Velden S, Porcelijn L, Semple JW, van der Schoot CE, Kapur R. Update on the pathophysiology of transfusion-related acute lung injury. *Curr Opin Hematol* (2020) 27(6):386–91. doi: 10.1097/moh.0000000000000607

6. Benson AB, Moss M, Silliman CC. Transfusion-related acute lung injury (Trali): a clinical review with emphasis on the critically ill. *Br J haematology* (2009) 147(4):431–43. doi: 10.1111/j.1365-2141.2009.07840.x

7. Vlaar AP, Juffermans NP. Transfusion-related acute lung injury: a clinical review. *Lancet (London England)* (2013) 382(9896):984–94. doi: 10.1016/s0140-6736(12)62197-7

8. Wallis JP. Transfusion-related acute lung injury (Trali)–under-Diagnosed and under-reported. *Br J anaesthesia* (2003) 90(5):573–6. doi: 10.1093/bja/aeg101

9. Vlaar AP, Binnekade JM, Prins D, van Stein D, Hofstra JJ, Schultz MJ, et al. Risk factors and outcome of transfusion-related acute lung injury in the critically ill: a nested case-control study. *Crit Care Med* (2010) 38(3):771–8. doi: 10.1097/CCM.0b013e3181cc4d4b

10. Brittingham TE. Immunologic studies on leukocytes. *Vox sanguinis* (1957) 2(4):242–8. doi: 10.1111/j.1423-0410.1957.tb03699.x

11. Popovsky MA, Abel MD, Moore SB. Transfusion-related acute lung injury associated with passive transfer of antileukocyte antibodies. *Am Rev Respir Dis* (1983) 128(1):185–9. doi: 10.1164/arrd.1983.128.1.185

12. Bayat B, Nielsen KR, Bein G, Traum A, Burg-Roderfeld M, Sachs UJ. Transfusion of target antigens to preimmunized recipients: a new mechanism in transfusion-related acute lung injury. *Blood Adv* (2021) 5(20):3975–85. doi: 10.1182/bloodadvances.2020003843

13. Semple JW, Rebetz J, Kapur R. Transfusion-associated circulatory overload and transfusion-related acute lung injury. *Blood* (2019) 133(17):1840–53. doi: 10.1182/blood-2018-10-860809

14. Peters AL, van Hezel ME, Juffermans NP, Vlaar AP. Pathogenesis of non-antibody mediated transfusion-related acute lung injury from bench to bedside. *Blood Rev* (2015) 29(1):51–61. doi: 10.1016/j.blre.2014.09.007

15. Silliman CC, Boshkov LK, Mehdizadehkashi Z, Elzi DJ, Dickey WO, Podlosky L, et al. Transfusion-related acute lung injury: epidemiology and a prospective analysis of etiologic factors. *Blood* (2003) 101(2):454–62. doi: 10.1182/blood-2002-03-0958

16. Silliman CC, Paterson AJ, Dickey WO, Stroneck DF, Popovsky MA, Caldwell SA, et al. The association of biologically active lipids with the development of transfusion-related acute lung injury: a retrospective study. *Transfusion* (1997) 37(7):719–26. doi: 10.1046/j.1537-2995.1997.37797369448.x

17. Fung YL, Kim M, Tabuchi A, Aslam R, Speck ER, Chow L, et al. Recipient T lymphocytes modulate the severity of antibody-mediated transfusion-related acute lung injury. *Blood* (2010) 116(16):3073–9. doi: 10.1182/blood-2010-05-284570

18. Menis M, Anderson SA, Forshee RA, McKean S, Johnson C, Warnock R, et al. Transfusion-related acute lung injury and potential risk factors among the inpatient us elderly as recorded in Medicare claims data, during 2007 through 2011. *Transfusion* (2014) 54(9):2182–93. doi: 10.1111/trf.12626

19. Yokoyama A, Sakamoto Y, Jo T, Urushiyama H, Tamiya H, Tanaka G, et al. Pulmonary disease as a risk factor for transfusion-related acute lung injury. *ERJ Open Res* (2021) 7(3):00039–2021. doi: 10.1183/23120541.00039-2021

20. Klanderman RB, van Mourik N, Eggermont D, Peters AL, Tuinman PR, Bosman R, et al. Incidence of transfusion-related acute lung injury temporally associated with Solvent/Detergent plasma use in the icu: a retrospective before and after implementation study. *Transfusion* (2022) 62(9):1752–62. doi: 10.1111/trf.17049

21. Sivakaanthan A, Swain F, Pahn G, Goodison K, Gutta N, Holdsworth R, et al. Transfusion-related acute lung injury (Trali): a retrospective review of reported cases in Queensland, Australia over 20 years. *Blood transfusion = Trasfusione del sangue* (2022) 20(6):454–64. doi: 10.2450/2022.0020-22

22. Looney MR, Su X, Van Ziffle JA, Lowell CA, Matthay MA. Neutrophils and their fc gamma receptors are essential in a mouse model of transfusion-related acute lung injury. *J Clin Invest* (2006) 116(6):1615–23. doi: 10.1172/jci27238

23. Looney MR, Nguyen JX, Hu Y, Van Ziffle JA, Lowell CA, Matthay MA. Platelet depletion and aspirin treatment protect mice in a two-event model of transfusion-related acute lung injury. *J Clin Invest* (2009) 119(11):3450–61. doi: 10.1172/jci38432

24. Kapur R, Kim M, Rebetz J, Hallström B, Björkman JT, Takabe-French A, et al. Gastrointestinal microbiota contributes to the development of murine transfusion-related acute lung injury. *Blood Adv* (2018) 2(13):1651–63. doi: 10.1182/bloodadvances.2018018903

25. Kapur R, Kim M, Shanmugabhavananthan S, Liu J, Li Y, Semple JW. C-reactive protein enhances murine antibody-mediated transfusion-related acute lung injury. *Blood* (2015) 126(25):2747–51. doi: 10.1182/blood-2015-09-672592

26. Kapur R, Kasetty G, Rebetz J, Egesten A, Semple JW. Osteopontin mediates murine transfusion-related acute lung injury *Via* stimulation of pulmonary neutrophil accumulation. *Blood* (2019) 134(1):74–84. doi: 10.1182/blood.2019000972

27. Tung JP, Chiaretti S, Dean MM, Sultana AJ, Reade MC, Fung YL. Transfusion-related acute lung injury (Trali): potential pathways of development, strategies for prevention and treatment, and future research directions. *Blood Rev* (2022) 53:100926. doi: 10.1016/j.blre.2021.100926

28. Peters AL, Van Stein D, Vlaar AP. Antibody-mediated transfusion-related acute lung injury; from discovery to prevention. *Br J haematology* (2015) 170(5):597–614. doi: 10.1111/bjh.13459

29. Morsing SKH, Zeeuw van der Laan E, van Stalborch AD, van Buul JD, Vlaar APJ, Kapur R. Endothelial cells of pulmonary origin display unique sensitivity to the bacterial endotoxin lipopolysaccharide. *Physiol Rep* (2022) 10(8):e15271. doi: 10.14814/phy2.15271

30. Giacalone VD, Margaroli C, Mall MA, Tirouvanziam R. Neutrophil adaptations upon recruitment to the lung: new concepts and implications for homeostasis and disease. *Int J Mol Sci* (2020) 21(3):851. doi: 10.3390/ijms21030851

31. Gao F, Lucke-Wold BP, Li X, Logsdon AF, Xu LC, Xu S, et al. Reduction of endothelial nitric oxide increases the adhesiveness of constitutive endothelial membrane icam-1 through src-mediated phosphorylation. *Front Physiol* (2017) 8:1124. doi: 10.3389/fphys.2017.01124

32. Kapur R, Kim M, Aslam R, McVey MJ, Tabuchi A, Luo A, et al. T Regulatory cells and dendritic cells protect against transfusion-related acute lung injury *Via* il-10. *Blood* (2017) 129(18):2557–69. doi: 10.1182/blood-2016-12-758185

33. Qian Y, Wang Z, Lin H, Lei T, Zhou Z, Huang W, et al. Trim47 is a novel endothelial activation factor that aggravates lipopolysaccharide-induced acute lung injury in mice *Via* K63-linked ubiquitination of Traf2. *Signal transduction targeted Ther* (2022) 7(1):148. doi: 10.1038/s41392-022-00953-9

34. Simtong P, Sudwilai Y, Cheunta S, Leelayuwat C, Romphruk AV. Prevalence of leucocyte antibodies in non-transfused Male and female platelet apheresis donors. *Transfusion Med (Oxford England)* (2021) 31(3):186–92. doi: 10.1111/tme.12781

35. Kelher MR, Banerjee A, Gamboni F, Anderson C, Silliman CC. Antibodies to major histocompatibility complex class ii antigens directly prime neutrophils and cause acute lung injury in a two-event in vivo rat model. *Transfusion* (2016) 56(12):3004–11. doi: 10.1111/trf.13817

36. Kelher MR, Silliman CC. Antibodies specific for mhc class ii antigens cause trali directly in a two-event in vivo model. *Blood* (2012) 120:21. doi: 10.1182/blood.V120.21.845.845

37. Sachs UJ, Hattar K, Weissmann N, Bohle RM, Weiss T, Sibelius U, et al. Antibody-induced neutrophil activation as a trigger for transfusion-related acute lung injury in an ex vivo rat lung model. *Blood* (2006) 107(3):1217–9. doi: 10.1182/blood-2005-04-1744

38. Bayat B, Tjahjono Y, Berghöfer H, Werth S, Deckmyn H, De Meyer SF, et al. Choline transporter-like protein-2: new Von willebrand factor-binding partner involved in antibody-mediated neutrophil activation and transfusion-related acute lung injury. *Arteriosclerosis thrombosis Vasc Biol* (2015) 35(7):1616–22. doi: 10.1161/atvbaha.115.305259

39. Wyman TH, Bjornsen AJ, Elzi DJ, Smith CW, England KM, Kelher M, et al. A two-insult in vitro model of pmn-mediated pulmonary endothelial damage: requirements for adherence and chemokine release. *Am J Physiol Cell Physiol* (2002) 283(6):C1592–603. doi: 10.1152/ajpcell.00540.2001

40. Xie RF, Hu P, Wang ZC, Yang J, Yang YM, Gao L, et al. Platelet-derived microparticles induce polymorphonuclear leukocyte-mediated damage of human pulmonary microvascular endothelial cells. *Transfusion* (2015) 55(5):1051–7. doi: 10.1111/trf.12952

41. Ots HD, Tracz JA, Vinokuroff KE, Musto AE. Cd40-Cd40l in neurological disease. *Int J Mol Sci* (2022) 23(8):4115. doi: 10.3390/ijms23084115

42. Tariket S, Hamzeh-Cognasse H, Laradi S, Arthaud CA, Eyraud MA, Bourlet T, et al. Evidence of Cd40l/Cd40 pathway involvement in experimental transfusion-related acute lung injury. *Sci Rep* (2019) 9(1):12536. doi: 10.1038/s41598-019-49040-0

43. Tariket S, Hamzeh-Cognasse H, Arthaud CA, Laradi S, Bourlet T, Berthelot P, et al. Inhibition of the Cd40/Cd40l complex protects mice against Ali-induced pancreas degradation. *Transfusion* (2019) 59(3):1090–101. doi: 10.1111/trf.15206

44. Lu Q, Yu S, Meng X, Shi M, Huang S, Li J, et al. Micrornas: important regulatory molecules in acute lung Injury/Acute respiratory distress syndrome. *Int J Mol Sci* (2022) 23(10):5545. doi: 10.3390/ijms23105545

45. Le A, Wu Y, Liu W, Wu C, Hu P, Zou J, et al. Mir-144-Induced Klf2 inhibition and nf-Kappab/Cxcr1 activation promote neutrophil extracellular trap-induced transfusion-related acute lung injury. *J Cell Mol Med* (2021) 25(14):6511–23. doi: 10.1111/jcmm.16650

46. Song D, Adrover JM, Felice C, Christensen LN, He XY, Merrill JR, et al. Ptp1b inhibitors protect against acute lung injury and regulate Cxcr4 signaling in neutrophils. *JCI Insight* (2022) 7(14):e158199. doi: 10.1172/jci.insight.158199

47. Silliman CC, Kelher MR, Khan SY, LaSarre M, West FB, Land KJ, et al. Experimental prestorage filtration removes antibodies and decreases lipids in rbc supernatants mitigating trali in vivo. *Blood* (2014) 123(22):3488–95. doi: 10.1182/blood-2013-10-532424

48. Khoy K, Nguyen MVC, Masson D, Bardy B, Drouet C, Paclet MH. Transfusion-related acute lung injury: critical neutrophil activation by anti-Hla-A2 antibodies for endothelial permeability. *Transfusion* (2017) 57(7):1699–708. doi: 10.1111/trf.14134

49. Le A, Liu W, Wu C, Hu P, Zou J, Wu Y, et al. Polymorphonuclear neutrophil activation by src phosphorylation contributes to hla-A2 antibody-induced transfusion-related acute lung injury. *Mol Immunol* (2022) 150:9–19. doi: 10.1016/j.molimm.2022.04.010

50. Strait RT, Hicks W, Barasa N, Mahler A, Khodoun M, Köhl J, et al. Mhc class I-specific antibody binding to nonhematopoietic cells drives complement activation to induce transfusion-related acute lung injury in mice. *J Exp Med* (2011) 208(12):2525–44. doi: 10.1084/jem.20110159

51. Cleary SJ, Kwaan N, Tian JJ, Calabrese DR, Mallavia B, Magnen M, et al. Complement activation on endothelium initiates antibody-mediated acute lung injury. *J Clin Invest* (2020) 130(11):5909–23. doi: 10.1172/jci138136

52. Gottschall JL, Triulzi DJ, Curtis B, Kakaiya RM, Busch MP, Norris PJ, et al. The frequency and specificity of human neutrophil antigen antibodies in a blood donor population. *Transfusion* (2011) 51(4):820–7. doi: 10.1111/j.1537-2995.2010.02913.x

53. Reil A, Wesche J, Greinacher A, Bux J. Geno- and phenotyping and immunogenicity of hna-3. *Transfusion* (2011) 51(1):18–24. doi: 10.1111/j.1537-2995.2010.02751.x

54. Bayat B, Tjahjono Y, Sydykov A, Werth S, Hippenstiel S, Weissmann N, et al. Anti-human neutrophil antigen-3a induced transfusion-related acute lung injury in mice by direct disturbance of lung endothelial cells. *Arteriosclerosis thrombosis Vasc Biol* (2013) 33(11):2538–48. doi: 10.1161/atvbaha.113.301206

55. Chiaretti S, Sultana A, Temple F, Burton M, Pahn G, Flower R, et al. Donor anti-Hna-3a antibodies induce monocytemediated hlmvec damage in a 2 insult in vitro model. *Internal Med J* (2019) 49:34. doi: 10.1111/imj.14678

56. McVey MJ, Kim M, Tabuchi A, Srbely V, Japtok L, Arenz C, et al. Acid sphingomyelinase mediates murine acute lung injury following transfusion of aged platelets. *Am J Physiol Lung Cell Mol Physiol* (2017) 312(5):L625–l37. doi: 10.1152/ajplung.00317.2016

57. McVey MJ, Weidenfeld S, Maishan M, Spring C, Kim M, Tabuchi A, et al. Platelet extracellular vesicles mediate transfusion-related acute lung injury by imbalancing the sphingolipid rheostat. *Blood* (2021) 137(5):690–701. doi: 10.1182/blood.2020005985

58. Cleary SJ, Looney MR. Chewing the fat on trali. *Blood* (2021) 137(5):586–7. doi: 10.1182/blood.2020010034

59. Sampson AC, Lassiter BP, Gregory Rivera M, Hair PS, Jackson KG, Enos AI, et al. Peptide inhibition of acute lung injury in a novel two-hit rat model. *PloS One* (2021) 16(10):e0259133. doi: 10.1371/journal.pone.0259133

60. Hu A, Chen W, Wu S, Pan B, Zhu A, Yu X, et al. An animal model of transfusion-related acute lung injury and the role of soluble Cd40 ligand. *Vox sanguinis* (2020) 115(4):303–13. doi: 10.1111/vox.12895

61. Qing DY, Conegliano D, Shashaty MG, Seo J, Reilly JP, Worthen GS, et al. Red blood cells induce necroptosis of lung endothelial cells and increase susceptibility to lung inflammation. *Am J Respir Crit Care Med* (2014) 190(11):1243–54. doi: 10.1164/rccm.201406-1095OC

62. Faust H, Lam LM, Hotz MJ, Qing D, Mangalmurti NS. Rage interacts with the necroptotic protein Ripk3 and mediates transfusion-induced danger signal release. *Vox sanguinis* (2020) 115(8):729–34. doi: 10.1111/vox.12946

63. Sakagawa H, Miyazaki T, Fujihara M, Sato S, Yamaguchi M, Fukai K, et al. Generation of inflammatory cytokines and chemokines from peripheral blood mononuclear cells by hla class ii antibody-containing plasma unit that was associated with severe nonhemolytic transfusion reactions. *Transfusion* (2007) 47 (1):154–61. doi: 10.1111/j.1537-2995.2007.01078.x

64. Wakamoto S, Fujihara M, Takahashi D, Niwa K, Sato S, Kato T, et al. Enhancement of endothelial permeability by coculture with peripheral blood mononuclear cells in the presence of hla class ii antibody that was associated with transfusion-related acute lung injury. *Transfusion* (2011) 51(5):993–1001. doi: 10.1111/j.1537-2995.2010.02910.x

65. Sachs UJ, Wasel W, Bayat B, Bohle RM, Hattar K, Berghöfer H, et al. Mechanism of transfusion-related acute lung injury induced by hla class ii antibodies. *Blood* (2011) 117(2):669–77. doi: 10.1182/blood-2010-05-286146

66. McKenzie CG, Kim M, Singh TK, Milev Y, Freedman J, Semple JW. Peripheral blood monocyte-derived chemokine blockade prevents murine transfusion-related acute lung injury (Trali). *Blood* (2014) 123(22):3496–503. doi: 10.1182/blood-2013-11-536755

67. Xu X, Chen D, Ye X, Xia W, Shao Y, Deng J, et al. Improvement of anti-Cd36 antibody detection *Via* monoclonal antibody immobilization of platelet antigens assay by using selected monoclonal antibodies. *Ann Lab Med* (2023) 43(1):86–91. doi: 10.3343/alm.2023.43.1.86

68. Ando M. Cd36, an important antigen on platelets and monocytes. *Vox sanguinis* (2020) 115(SUPPL 1):27. doi: 10.1111/vox.13031

69. Nakajima F, Nishimura M, Hashimoto S, Okazaki H, Tadokoro K. Role of anti-nak(a) antibody, monocytes and platelets in the development of transfusion-related acute lung injury. *Vox sanguinis* (2008) 95(4):318–23. doi: 10.1111/j.1423-0410.2008.01095.x

70. Wu Y, Santoso S, Fu Y. Anti-Cd36 antibodies induced transfusion-related acute lung injury in mice. *Vox sanguinis* (2020) 115(SUPPL 1):55–6. doi: 10.1111/vox.13031

71. Nishimichi N, Hayashita-Kinoh H, Chen C, Matsuda H, Sheppard D, Yokosaki Y. Osteopontin undergoes polymerization in vivo and gains chemotactic activity for neutrophils mediated by integrin Alpha9beta1. *J Biol Chem* (2011) 286(13):11170–8. doi: 10.1074/jbc.M110.189258

72. Orecchioni M, Ghosheh Y, Pramod AB, Ley K. Macrophage polarization: different gene signatures in M1(Lps+) vs. classically and M2(Lps-) vs. alternatively activated macrophages. *Front Immunol* (2019) 10:1084. doi: 10.3389/fimmu.2019.01084

73. Gharavi AT, Hanjani NA, Movahed E, Doroudian M. The role of macrophage subtypes and exosomes in immunomodulation. *Cell Mol Biol Lett* (2022) 27(1):83. doi: 10.1186/s11658-022-00384-y

74. Wang L, Wu T, Yan S, Wang Y, An J, Wu C, et al. M1-polarized alveolar macrophages are crucial in a mouse model of transfusion-related acute lung injury. *Transfusion* (2020) 60(2):303–16. doi: 10.1111/trf.15609

75. Burnouf T, Walker TL. The multifaceted role of platelets in mediating brain function. *Blood* (2022) 140(8):815–27. doi: 10.1182/blood.2022015970

76. Mandel J, Casari M, Stepanyan M, Martyanov A, Deppermann C. Beyond hemostasis: platelet innate immune interactions and thromboinflammation. *Int J Mol Sci* (2022) 23(7):3868. doi: 10.3390/ijms23073868

77. Yu Y, Jiang P, Sun P, Su N, Lin F. Pulmonary coagulation and fibrinolysis abnormalities that favor fibrin deposition in the lungs of mouse antibody-mediated transfusion-related acute lung injury. *Mol Med Rep* (2021) 24(2):601. doi: 10.3892/mmr.2021.12239

78. Caudrillier A, Kessenbrock K, Gilliss BM, Nguyen JX, Marques MB, Monestier M, et al. Platelets induce neutrophil extracellular traps in transfusion-related acute lung injury. *J Clin Invest* (2012) 122(7):2661–71. doi: 10.1172/jci61303

79. Ortiz-Muñoz G, Mallavia B, Bins A, Headley M, Krummel MF, Looney MR. Aspirin-triggered 15-Epi-Lipoxin A4 regulates neutrophil-platelet aggregation and attenuates acute lung injury in mice. *Blood* (2014) 124(17):2625–34. doi: 10.1182/blood-2014-03-562876

80. Cognasse F, Tariket S, Hamzeh-Cognasse H, Arthaud CA, Eyraud MA, Bourlet T, et al. Platelet depletion limits the severity but does not prevent the occurrence of experimental transfusion-related acute lung injury. *Transfusion* (2020) 60(4):713–23. doi: 10.1111/trf.15738

81. Thomas GM, Carbo C, Curtis BR, Martinod K, Mazo IB, Schatzberg D, et al. Extracellular DNA traps are associated with the pathogenesis of trali in humans and mice. *Blood* (2012) 119(26):6335–43. doi: 10.1182/blood-2012-01-405183

82. Hechler B, Maître B, Magnenat S, Heim V, El Mdawar MB, Gachet C, et al. Platelets are dispensable for antibody-mediated transfusion-related acute lung injury in the mouse. *J Thromb haemostasis JTH* (2016) 14(6):1255–67. doi: 10.1111/jth.13335

83. Beutier H, Hechler B, Godon O, Wang Y, Gillis CM, de Chaisemartin L, et al. Platelets expressing igg receptor Fcγriia/Cd32a determine the severity of experimental anaphylaxis. *Sci Immunol* (2018) 3(22):eaan5997. doi: 10.1126/sciimmunol.aan5997

84. El Mdawar MB, Maître B, Magnenat S, Tupin F, Jönsson F, Gachet C, et al. Platelet fcγriia-induced serotonin release exacerbates the severity of transfusion-related acute lung injury in mice. *Blood Adv* (2021) 5(23):4817–30. doi: 10.1182/bloodadvances.2021004336

85. Nakajima T, Lin KW, Li J, McGee HS, Kwan JM, Perkins DL, et al. T Cells and lung injury. *Impact Rapamycin Am J Respir Cell Mol Biol* (2014) 51(2):294–9. doi: 10.1165/rcmb.2013-0171OC

86. Yuan R, Li Y, Han S, Chen X, Chen J, He J, et al. Fe-curcumin nanozyme-mediated reactive oxygen species scavenging and anti-inflammation for acute lung injury. *ACS Cent Sci* (2022) 8(1):10–21. doi: 10.1021/acscentsci.1c00866

87. Kapur R, Kim M, Rebetz J, Rondina MT, Porcelijn L, Semple JW. Low levels of interleukin-10 in patients with transfusion-related acute lung injury. *Ann Trans Med* (2017) 5(16):339. doi: 10.21037/atm.2017.04.37

88. Lee C, Choi WJ. Overview of covid-19 inflammatory pathogenesis from the therapeutic perspective. *Arch pharmacal Res* (2021) 44(1):99–116. doi: 10.1007/s12272-020-01301-7

89. Herre M, Cedervall J, Mackman N, Olsson AK. Neutrophil extracellular traps in the pathology of cancer and other inflammatory diseases. *Physiol Rev* (2023) 103 (1):277–312. doi: 10.1152/physrev.00062.2021

90. Aroca-Crevillén A, Hidalgo A, Adrover JM. *In vivo* imaging of circadian net formation during lung injury by four-dimensional intravital microscopy. *Methods Mol Biol (Clifton NJ)* (2022) 2482:285–300. doi: 10.1007/978-1-0716-2249-0_19

91. Adrover JM, Carrau L, Daßler-Plenker J, Bram Y, Chandar V, Houghton S, et al. Disulfiram inhibits neutrophil extracellular trap formation and protects rodents from acute lung injury and sars-Cov-2 infection. *JCI Insight* (2022) 7(5):e157342. doi: 10.1172/jci.insight.157342

92. Jongerius I, Porcelijn L, van Beek AE, Semple JW, van der Schoot CE, Vlaar APJ, et al. The role of complement in transfusion-related acute lung injury. *Transfusion Med Rev* (2019) 33(4):236–42. doi: 10.1016/j.tmrv.2019.09.002

93. Chen D, Xu X, Xia W, Ye X, Bayat B, Bein G, et al. Anti-Cd36 antibodies induced endothelial disturbance via activation of pbmc: evidence of crucial Epitope(S). *Vox sanguinis* (2020) 115(SUPPL 1):58. doi: 10.1111/vox.13031

94. Kono M, Saigo K, Takagi Y, Takahashi T, Kawauchi S, Wada A, et al. Heme-related molecules induce rapid production of neutrophil extracellular traps. *Transfusion* (2014) 54(11):2811–9. doi: 10.1111/trf.12700

95. Li D, Cong Z, Lyu X, Wu C, Tao Y, Zhu X. [the role of nicotinamide-adenine dinucleotide phosphate oxidase nox family in acute lung injury]. *Zhonghua wei zhong bing ji jiu yi xue* (2019) 31(2):244–7. doi: 10.3760/cma.j.issn.2095-4352.2019.02.026

96. Segel GB, Halterman MW, Lichtman MA. The paradox of the neutrophil's role in tissue injury. *J leukocyte Biol* (2011) 89(3):359–72. doi: 10.1189/jlb.0910538

97. Semple JW, Kim M, Hou J, McVey M, Lee YJ, Tabuchi A, et al. Intravenous immunoglobulin prevents murine antibody-mediated acute lung injury at the level of neutrophil reactive oxygen species (Ros) production. *PloS One* (2012) 7(2):e31357. doi: 10.1371/journal.pone.0031357

98. Hidalgo A, Chang J, Jang JE, Peired AJ, Chiang EY, Frenette PS. Heterotypic interactions enabled by polarized neutrophil microdomains mediate thromboinflammatory injury. *Nat Med* (2009) 15(4):384–91. doi: 10.1038/nm.1939

99. Jank H, Salzer U. Vesicles generated during storage of red blood cells enhance the generation of radical oxygen species in activated neutrophils. *TheScientificWorldJournal* (2011) 11:173–85. doi: 10.1100/tsw.2011.25

100. Kono M, Saigo K, Takagi Y, Kawauchi S, Wada A, Hashimoto M, et al. Morphological and flow-cytometric analysis of haemin-induced human neutrophil activation: implications for transfusion-related acute lung injury. *Blood transfusion = Trasfusione del sangue* (2013) 11(1):53–60. doi: 10.2450/2012.0141-11

101. Yu C, Xu L, Chen LF, Guan YJ, Kim M, Biffl WL, et al. Prbc-derived plasma induces non-muscle myosin type iia-mediated neutrophil migration and morphologic change. *Immunopharmacol immunotoxicology* (2013) 35(1):71–9. doi: 10.3109/08923973.2012.677046

102. De Pablo-Moreno JA, Serrano LJ, Revuelta L, Sánchez MJ, Liras A. The vascular endothelium and coagulation: homeostasis, disease, and treatment, with a focus on the Von willebrand factor and factors viii and V. *Int J Mol Sci* (2022) 23 (15):8283. doi: 10.3390/ijms23158283

103. Vlaar AP, Hofstra JJ, Levi M, Kulik W, Nieuwland R, Tool AT, et al. Supernatant of aged erythrocytes causes lung inflammation and coagulopathy in a "Two-hit" in vivo syngeneic transfusion model. *Anesthesiology* (2010) 113(1):92–103. doi: 10.1097/ALN.0b013e3181de6f25

104. Vlaar AP, Hofstra JJ, Kulik W, van Lenthe H, Nieuwland R, Schultz MJ, et al. Supernatant of stored platelets causes lung inflammation and coagulopathy in a novel in vivo transfusion model. *Blood* (2010) 116(8):1360–8. doi: 10.1182/blood-2009-10-248732

105. Tuinman PR, Vlaar AP, Cornet AD, Hofstra JJ, Levi M, Meijers JC, et al. Blood transfusion during cardiac surgery is associated with inflammation and coagulation in the lung: a case control study. *Crit Care (London England)* (2011) 15(1):R59. doi: 10.1186/cc10032

106. Conway EM, Mackman N, Warren RQ, Wolberg AS, Mosnier LO, Campbell RA, et al. Understanding covid-19-Associated coagulopathy. *Nat Rev Immunol* (2022) 22(10):639–49. doi: 10.1038/s41577-022-00762-9

107. Sebag SC, Bastarache JA, Ware LB. Therapeutic modulation of coagulation and fibrinolysis in acute lung injury and the acute respiratory distress syndrome. *Curr Pharm Biotechnol* (2011) 12(9):1481–96. doi: 10.2174/138920111798281171

108. Ware LB, Matthay MA. The acute respiratory distress syndrome. *New Engl J Med* (2000) 342(18):1334–49. doi: 10.1056/nejm200005043421806

109. Bos LDJ, Ware LB. Acute respiratory distress syndrome: causes, pathophysiology, and phenotypes. *Lancet (London England)* (2022) 400 (10358):1145–56. doi: 10.1016/s0140-6736(22)01485-4

110. Bolton-Maggs PHB. Serious hazards of transfusion - conference report: celebration of 20 years of uk haemovigilance. *Transfusion Med (Oxford England)* (2017) 27(6):393–400. doi: 10.1111/tme.12502

111. Middelburg RA, Beckers EA, Porcelijn L, Lardy N, Wiersum-Osselton JC, Schipperus MR, et al. Allo-exposure status and leucocyte antibody positivity of blood donors show a similar relation with trali. *Transfusion Med (Oxford England)* (2012) 22 (2):128–32. doi: 10.1111/j.1365-3148.2012.01140.x

112. Reesink HW, Lee J, Keller A, Dennington P, Pink J, Holdsworth R, et al. Measures to prevent transfusion-related acute lung injury (Trali). *Vox sanguinis* (2012) 103(3):231–59. doi: 10.1111/j.1423-0410.2012.01596.x

113. Flesland O, Seghatchian J, Solheim BG. The Norwegian plasma fractionation project–a 12 year clinical and economic success story. *Transfusion apheresis Sci Off J World Apheresis Assoc Off J Eur Soc Haemapheresis* (2003) 28(1):93–100. doi: 10.1016/s1473-0502(02)00104-0

114. Saadah NH, van Hout FMA, Schipperus MR, le Cessie S, Middelburg RA, Wiersum-Osselton JC, et al. Comparing transfusion reaction rates for various plasma types: a systematic review and meta-Analysis/Regression. *Transfusion* (2017) 57 (9):2104–14. doi: 10.1111/trf.14245

115. Saadah NH, Schipperus MR, Wiersum-Osselton JC, van Kraaij MG, Caram-Deelder C, Beckers EAM, et al. Transition from fresh frozen plasma to Solvent/Detergent plasma in the Netherlands: comparing clinical use and transfusion reaction risks. *Haematologica* (2020) 105(4):1158–65. doi: 10.3324/haematol.2019.222083

116. Klanderman RB, Bulle EB, Heijnen JWM, Allen J, Purmer IM, Kerkhoffs JH, et al. Reported transfusion-related acute lung injury associated with Solvent/Detergent plasma - a case series. *Transfusion* (2022) 62(3):594–9. doi: 10.1111/trf.16822

117. Blumberg N, Heal JM, Gettings KF, Phipps RP, Masel D, Refaai MA, et al. An association between decreased cardiopulmonary complications (Transfusion-related acute lung injury and transfusion-associated circulatory overload) and implementation of universal leukoreduction of blood transfusions. *Transfusion* (2010) 50(12):2738–44. doi: 10.1111/j.1537-2995.2010.02748.x

118. McQuinn ER, Smith SA, Viall AK, Wang C, LeVine DN. Neutrophil extracellular traps in stored canine red blood cell units. *J veterinary Internal Med* (2020) 34(5):1894–902. doi: 10.1111/jvim.15876

119. Simancas-Racines D, Osorio D, Martí-Carvajal AJ, Arevalo-Rodriguez I. Leukoreduction for the prevention of adverse reactions from allogeneic blood transfusion. *Cochrane Database Systematic Rev* (2015) 2015(12):CD009745. doi: 10.1002/14651858.CD009745.pub2

120. Silliman CC, Khan SY, Ball JB, Kelher MR, Marschner S. Mirasol pathogen reduction technology treatment does not affect acute lung injury in a two-event in vivo model caused by stored blood components. *Vox sanguinis* (2010) 98(4):525–30. doi: 10.1111/j.1423-0410.2009.01289.x

121. Caudrillier A, Mallavia B, Rouse L, Marschner S, Looney MR. Transfusion of human platelets treated with mirasol pathogen reduction technology does not induce acute lung injury in mice. *PloS One* (2015) 10(7):e0133022. doi: 10.1371/journal.pone.0133022

122. Mallavia B, Kwaan N, Marschner S, Yonemura S, Looney MR. Mirasol pathogen reduction technology treatment of human whole blood does not induce acute lung injury in mice. *PloS One* (2017) 12(6):e0178725. doi: 10.1371/journal.pone.0178725

123. Owusu-Ofori A, Asamoah-Akuoko L, Acquah M, Wilkinson S, Ansa J, Brown B, et al. Hemovigilance on mirasol pathogen-reduced whole blood in Ghana. *Vox sanguinis* (2019) 114:67. doi: 10.1111/vox.12792

124. Knutson F, Osselaer J, Pierelli L, Lozano M, Cid J, Tardivel R, et al. A prospective, active haemovigilance study with combined cohort analysis of 19,175 transfusions of platelet components prepared with amotosalen-uva photochemical treatment. *Vox sanguinis* (2015) 109(4):343–52. doi: 10.1111/vox.12287

125. Snyder EL, Wheeler AP, Refaai M, Cohn CS, Poisson J, Fontaine M, et al. Comparative risk of pulmonary adverse events with transfusion of pathogen reduced and conventional platelet components. *Transfusion* (2022) 62(7):1365–76. doi: 10.1111/trf.16987

126. Kuldanek SA, Kelher M, Silliman CC. Risk factors, management and prevention of transfusion-related acute lung injury: a comprehensive update. *Expert Rev Hematol* (2019) 12(9):773–85. doi: 10.1080/17474086.2019.1640599

127. van der Meer PF, de Korte D. Platelet additive solutions: a review of the latest developments and their clinical implications. *Transfusion Med hemotherapy offizielles Organ der Deutschen Gesellschaft fur Transfusionsmedizin und Immunhamatologie* (2018) 45(2):98–102. doi: 10.1159/000487513

128. Friedman T, Javidroozi M, Lobel G, Shander A. Complications of allogeneic blood product administration, with emphasis on transfusion-related acute lung injury and transfusion-associated circulatory overload. *Adv Anesth* (2017) 35(1):159–73. doi: 10.1016/j.aan.2017.07.008

129. Tung JP. Transfusion-related acute lung injury (Trali): pathogenesis and diagnosis. *Pathology* (2019) 51:S44. doi: 10.1016/j.pathol.2018.12.103

130. Priyanjani R, Naotunna S, Senanayake D, Kuruppu D. How we investigated a case of transfusion related acute lung injury (Trali) at the histocompatibility reference laboratory, national blood centre, Sri Lanka. *Vox sanguinis* (2022) 117(SUPPL 1):231–2. doi: 10.1111/vox.13285

131. Honda A, Morita M, Taniguchi A, Tabuchi A, Kubo S. [Successful extracorporeal membrane oxygenation for a patient with nearly fatal hypoxemia induced by transfusion-related acute lung injury]. *Masui Japanese J anesthesiology* (2015) 64(11):1181–5.

132. Kassem AB, Ahmed I, Omran G, Megahed M, Habib T. Role of ascorbic acid infusion in critically ill patients with transfusion-related acute lung injury. *Br J Clin Pharmacol* (2022) 88(5):2327–39. doi: 10.1111/bcp.15167

133. Qiao J, He R, Yin Y, Tian L, Li L, Lian Z, et al. Ril-35 prevents murine transfusion-related acute lung injury by inhibiting the activation of endothelial cells. *Transfusion* (2020) 60(7):1434–42. doi: 10.1111/trf.15805

134. Yuan X, Jiang P, Qiao C, Su N, Sun P, Lin F, et al. Platelet suppression by tirofiban ameliorates pulmonary coagulation and fibrinolysis abnormalities in the lungs of mouse antibody-mediated transfusion-related acute lung injury. *Shock (Augusta Ga)* (2023) 59(4):603–11. doi: 10.1097/shk.0000000000002080

135. Hong SW, O E, Lee JY, Yi J, Cho K, Kim J, et al. Interleukin-2/Antibody complex expanding Foxp3(+) regulatory T cells exacerbates Th2-mediated allergic airway inflammation. *BMB Rep* (2019) 52(4):283–8. doi: 10.5483/BMBRep.2019.52.4.271

136. Schönbacher M, Aichinger N, Weidner L, Jungbauer C, Grabmer C, Schuha B, et al. Leukocyte-reactive antibodies in female blood donors: the Austrian experience. *Transfusion Med hemotherapy offizielles Organ der Deutschen Gesellschaft fur Transfusionsmedizin und Immunhamatologie* (2021) 48(2):99–108. doi: 10.1159/000509946

137. Dada A, Elhassan K, Bawayan RM, Albishi G, Hefni L, Bassi S, et al. Sars-Cov-2 triggers the development of class I and class ii hla antibodies in recovered convalescent plasma donors. *Intervirology* (2022) 65(4):230–5. doi: 10.1159/000524016

138. Nissen-Meyer LSH, Czapp E, Naper C, Jensen T, Boulland LML. Screening for antibodies to hla class I in apheresis donors following covid-19 or sars-Cov-2 vaccination. *Transfusion apheresis Sci Off J World Apheresis Assoc Off J Eur Soc Haemapheresis* (2022) 61(5):103567. doi: 10.1016/j.transci.2022.103567

139. Devine DV, Schubert P. Pathogen inactivation technologies: the advent of pathogen-reduced blood components to reduce blood safety risk. *Hematology/oncology Clinics North America* (2016) 30(3):609–17. doi: 10.1016/j.hoc.2016.01.005

140. Vossoughi S, Gorlin J, Kessler DA, Hillyer CD, Van Buren NL, Jimenez A, et al. Ten years of trali mitigation: measuring our progress. *Transfusion* (2019) 59(8):2567–74. doi: 10.1111/trf.15387

141. Roman M, Fashina O, Tomassini S, Abbasciano RG, Lai F, Richards T, et al. Reporting conflicts of interest in randomised trials of patient blood management interventions in patients requiring major surgery: a systematic review and meta-analysis. *BMJ Open* (2022) 12(8):e054582. doi: 10.1136/bmjopen-2021-054582

142. Arzoun H, Srinivasan M, Adam M, Thomas SS, Lee B, Yarema A. A systematic review on the management of transfusion-related acute lung injury in transfusion-dependent sickle cell disease. *Cureus* (2022) 14(2):e22101. doi: 10.7759/cureus.22101

143. Ackfeld T, Schmutz T, Guechi Y, Le Terrier C. Blood transfusion reactions-a comprehensive review of the literature including a Swiss perspective. *J Clin Med* (2022) 11(10):2859. doi: 10.3390/jcm11102859

144. Tocut M, Kolitz T, Shovman O, Haviv Y, Boaz M, Laviel S, et al. Outcomes of icu patients treated with intravenous immunoglobulin for sepsis or autoimmune diseases. *Autoimmun Rev* (2022) 21(12):103205. doi: 10.1016/j.autrev.2022.103205

145. Baudel JL, Vigneron C, Pras-Landre V, Joffre J, Marjot F, Ait-Oufella H, et al. Transfusion-related acute lung injury (Trali) after intravenous immunoglobulins: French multicentre study and literature review. *Clin Rheumatol* (2020) 39(2):541–6. doi: 10.1007/s10067-019-04832-7

146. Guo Y, Tian X, Wang X, Xiao Z. Adverse effects of immunoglobulin therapy. *Front Immunol* (2018) 9:1299. doi: 10.3389/fimmu.2018.01299

147. Adrover JM, Aroca-Crevillén A, Crainiciuc G, Ostos F, Rojas-Vega Y, Rubio-Ponce A, et al. Programmed 'Disarming' of the neutrophil proteome reduces the magnitude of inflammation. *Nat Immunol* (2020) 21(2):135–44. doi: 10.1038/s41590-019-0571-2

148. Futosi K, Németh T, Pick R, Vántus T, Walzog B, Mócsai A. Dasatinib inhibits proinflammatory functions of mature human neutrophils. *Blood* (2012) 119(21):4981–91. doi: 10.1182/blood-2011-07-369041

149. Wan N, Rong W, Zhu W, Jia D, Bai P, Liu G, et al. Tregs-derived interleukin 35 attenuates endothelial proliferation through Stat1 in pulmonary hypertension. *Ann Trans Med* (2021) 9(11):926. doi: 10.21037/atm-21-1952

150. Li M, Liu Y, Fu Y, Gong R, Xia H, Huang X, et al. Interleukin-35 inhibits lipopolysaccharide-induced endothelial cell activation by downregulating inflammation and apoptosis. *Exp Cell Res* (2021) 407(2):112784. doi: 10.1016/j.yexcr.2021.112784

151. Liu M, Meng X, Xuan Z, Chen S, Wang J, Chen Z, et al. Effect of er miao San on peritoneal macrophage polarisation through the mirna-33/Nlrp3 signalling pathway in a rat model of adjuvant arthritis. *Pharm Biol* (2022) 60(1):846–53. doi: 10.1080/13880209.2022.2066700

152. Kaneda MM, Messer KS, Ralainirina N, Li H, Leem CJ, Gorjestani S, et al. Pi3kγ is a molecular switch that controls immune suppression. *Nature* (2016) 539(7629):437–42. doi: 10.1038/nature19834

153. Han A, Lee T, Lee J, Song SW, Lee SS, Jung IM, et al. A multicenter, randomized, open-labelled, non-inferiority trial of sustained-release sarpogrelate versus clopidogrel after femoropopliteal artery intervention. *Sci Rep* (2023) 13(1):2502. doi: 10.1038/s41598-023-29006-z

154. Sugiyama D, Hinohara K, Nishikawa H. Significance of regulatory T cells in cancer immunology and immunotherapy. *Exp Dermatol* (2023) 32(3):256–63. doi: 10.1111/exd.14721

155. Yu Y, Jiang P, Sun P, Su N, Lin F. Analysis of therapeutic potential of preclinical models based on Dr3/Tl1a pathway modulation (Review). *Exp Ther Med* (2021) 22(1):693. doi: 10.3892/etm.2021.10125

156. Goswami TK, Singh M, Dhawan M, Mitra S, Emran TB, Rabaan AA, et al. Regulatory T cells (Tregs) and their therapeutic potential against autoimmune disorders - advances and challenges. *Hum Vaccines immunotherapeutics* (2022) 18(1):2035117. doi: 10.1080/21645515.2022.2035117

157. He R, Li L, Kong Y, Tian L, Tian X, Fang P, et al. Preventing murine transfusion-related acute lung injury by expansion of Cd4(+) Cd25(+) Foxp3(+) tregs using il-2/Anti-Il-2 complexes. *Transfusion* (2019) 59(2):534–44. doi: 10.1111/trf.15064

158. Zhang W, Xiao D, Li X, Zhang Y, Rasouli J, Casella G, et al. Sirt1 inactivation switches reactive astrocytes to an anti-inflammatory phenotype in cns autoimmunity. *J Clin Invest* (2022) 132(22):e151803. doi: 10.1172/jci151803

frontiers | Frontiers in Immunology

TYPE Original Research
PUBLISHED 29 May 2023
DOI 10.3389/fimmu.2023.1151528

OPEN ACCESS

EDITED BY
Adan Chari Jirmo,
Hannover Medical School, Germany

REVIEWED BY
Katherina Psarra,
Evaggelismos General Hospital, Greece
Jacqueline Margaret Cliff,
Brunel University London, United Kingdom

*CORRESPONDENCE
Yuri F. van der Heijden
yuri.vanderheijden@vumc.org

†These authors have contributed equally to this work and share first authorship

RECEIVED 26 January 2023
ACCEPTED 17 May 2023
PUBLISHED 29 May 2023

CITATION
Krause R, Warren CM, Simmons JD, Rebeiro PF, Maruri F, Karim F, Sterling TR, Koethe JR, Leslie A and van der Heijden YF (2023) Failure to decrease HbA1c levels following TB treatment is associated with elevated Th1/Th17 CD4+ responses. *Front. Immunol.* 14:1151528. doi: 10.3389/fimmu.2023.1151528

Failure to decrease HbA1c levels following TB treatment is associated with elevated Th1/Th17 CD4+ responses

Robert Krause[1,2†], Christian M. Warren[3†], Joshua D. Simmons[3†], Peter F. Rebeiro[3,4,5], Fernanda Maruri[3,5], Farina Karim[1,2,5], Timothy R. Sterling[3,5], John R. Koethe[3], Al Leslie[1,2,6] and Yuri F. van der Heijden[3,5,7*]

[1]Africa Health Research Institute (AHRI), Durban, South Africa, [2]College of Health Sciences, School of Laboratory Medicine & Medical Sciences, University of KwaZulu Natal, Durban, South Africa, [3]Division of Infectious Diseases, Department of Medicine, Vanderbilt University School of Medicine, Nashville, TN, United States, [4]Department of Biostatistics, Vanderbilt University School of Medicine, Nashville, TN, United States, [5]Vanderbilt Tuberculosis Center, Vanderbilt University School of Medicine, Nashville, TN, United States, [6]Division of Infection and Immunity, University College London, London, United Kingdom, [7]The Aurum Institute, Johannesburg, South Africa

Introduction: The rising global burden of metabolic disease impacts the control of endemic tuberculosis (TB) in many regions, as persons with diabetes mellitus (DM) are up to three times more likely to develop active TB than those without DM. Active TB can also promote glucose intolerance during both acute infection and over a longer term, potentially driven by aspects of the immune response. Identifying patients likely to have persistent hyperglycemia following TB treatment would enable closer monitoring and care, and an improved understanding of underlying immunometabolic dysregulation.

Methods: We measured the relationship of plasma cytokine levels, T cell phenotypes and functional responses with the change in hemoglobin A1c (HbA1c) before and after treatment of pulmonary TB in a prospective observational cohort in Durban, South Africa. Participants were stratified based on stable/increased HbA1c (n = 16) versus decreased HbA1c (n = 46) levels from treatment initiation to 12 month follow-up.

Results: CD62 P-selectin was up- (1.5-fold) and IL-10 downregulated (0.85-fold) in plasma among individuals whose HbA1c remained stable/increased during TB treatment. This was accompanied by increased pro-inflammatory TB-specific IL-17 production (Th17). In addition, Th1 responses were upregulated in this group, including TNF-α production and CX3CR1 expression, with decreased IL-4 and IL-13 production. Finally, the TNF-α+ IFNγ+ CD8+ T cells were associated with stable/increased HbA1c. These changes were all significantly different in the stable/increased HbA1c relative to the decreased HbA1c group.

Discussion: Overall, these data suggest that patients with stable/increased HbA1c had an increased pro-inflammatory state. Persistent inflammation and elevated T cell activity in individuals with unresolved dysglycemia following TB treatment may indicate failure to fully resolve infection or may promote persistent dysglycemia in these individuals, and further studies are needed to explore potential mechanisms.

KEYWORDS

hyperglycemia, tuberculosis, diabetes, HIV, HbA1c, IL-17, TNF-α, CX3CR1

Introduction

The convergence of tuberculosis (TB) and type 2 diabetes mellitus (DM) threatens the life and livelihood of individuals in many resource-constrained settings. Concerns about the impact of DM on TB are particularly relevant in sub-Saharan Africa, which already bears over 80% of the world's HIV-associated TB burden. The prevalence of DM is projected to rise steeply in the coming decades (1–3). An estimated 12.6% of the adult (age 20-79 years) sub-Sahara-African population have impaired glucose tolerance, 5.2% have type 2 diabetes, and over 50% of diabetes cases remain undiagnosed (4).

The interaction of TB and metabolic dysregulation is complex; while impaired glucose tolerance, including overt DM as well as prediabetes, increases the risk of active TB disease, the immune response to TB may also drive adverse changes in metabolic health (5–7). The increased risk of active TB in patients with DM has been attributed to multiple immunologic alterations, including monocyte and macrophage defects that contribute to delayed adaptive immune responses and altered *M. tuberculosis* (*Mtb*) specific pro- and anti-inflammatory T-helper type 1 (Th1) and Th17 responses (8, 9). Previous studies have also shown that patients with prediabetes and active TB have increased circulating levels of Th1, Th2, Th17, and regulatory cytokines (10, 11).

Although not all individuals with prediabetes go on to develop overt diabetes (12–15), the alterations in immune function in persons with prediabetes and DM that contribute to active TB disease overlap, in part, with studies linking immunologic biomarkers to the development of metabolic disease in the absence of infectious conditions. In the general population, a reduced proportion of naïve and regulatory (T_{reg}) CD4+ T cells (16–18), higher circulating memory CD4+ T cells (16, 19), and a shift towards pro-inflammatory Th1 and Th17 helper cells (18) was associated with prevalent diabetes. Taken together, these findings suggest a potential bidirectional relationship in which altered immunity in glucose intolerance predisposes to active TB disease, which subsequently may worsen metabolic function.

The potential for an immune response against infectious conditions to promote metabolic dysregulation has been investigated in persons with HIV (PWH) (20, 21), but there are fewer data among individuals with TB. We and others, have previously demonstrated that elevation of soluble receptor of tumor necrosis factor (TNF)-α-1 (sTNFR1) and interleukin-6 (IL-6), and increased expression of CD45RO and CD57 on CD4+ T cells, are associated with increased incidence of DM among PWH (16, 22, 23). Additionally, higher baseline frequencies of CD4+ T effector memory RA+ (T_{EMRA}) cells (CD45RA+ CD27-) and senescent T cells (CD4+ CD28-) have been associated with incident diabetes in PWH (21). It is unclear, however, if these factors are also associated with DM in patients with TB disease.

In this study we sought to build upon the immunometabolism model linking alterations in adaptive immunity to the development of DM to explore impaired glucose tolerance (hemoglobin A1c [HbA1c] ≥5.7%) in TB disease using longitudinal data from drug-susceptible TB patients in South Africa. We assessed a broad range of innate and adaptive immune markers among individuals undergoing treatment for active TB to identify factors associated with the persistence or worsening of glucose intolerance.

Methods

Study population

Participants enrolled in the Africa Health Research Institute (AHRI) site in Durban, South Africa of the Regional Prospective Observational Research in Tuberculosis consortium of South Africa (RePORT SA) were eligible for inclusion. All participants included in the study were individuals with pulmonary, drug-susceptible, culture-confirmed *Mycobacterium tuberculosis* (*Mtb*). Study enrollment opened in December 2017 and closed in November 2019. Individual baseline measures of weight (kg), height (m), body mass index (BMI), HbA1c (%), age (years), sex (self-reported, male or female), HIV status (by Western Blot and PCR, positive or negative) as well as antiretroviral therapy (ART) use, and blood samples (CD4+ T-lymphocyte counts) were collected at the time of treatment initiation (baseline); HbA1c and CD4+ counts were measured again at 12-15 months (follow-up). HbA1c levels were defined as normal (<5.7%), prediabetes (5.7-6.4%), and diabetes (≥6.5%), with the HbA1c characteristics of the study population at baseline and follow up summarized in Supplementary Table 1. These HbA1c based definitions are based on the American Diabetes Association guidelines (24).

This study was approved by the Vanderbilt Institutional Review Board (IRB#191176). Informed consent was obtained under the Biomedical Research Ethics Committee (BREC) at the University of Kwazulu-Natal (UKZN) Ref No: BE423/19, and the RePORT South Africa study (IRB#160918) at Vanderbilt.

T-lymphocyte stimulation conditions and flow cytometry

Peripheral blood mononuclear cells (PBMC) were isolated by density gradient centrifugation through Histopaque 1077 (SIGMA) according to standard procedure. To induce cytokine production, 10^6 PBMC each were stimulated for 6 hours with the mitogens PMA and ionomycin or *Mtb* peptides (MTB300) or left unstimulated. Cells were then washed in PBS and surface stained in a 25 µl antibody mix containing a Live/Dead™ fixable Aqua-dead cell staining reagent (1:200 dilution, Invitrogen, Carlsbad, CA, USA). Combinations of the surface antibodies as listed in Supplementary Table 2 or 3 from BD Biosciences (Franklin Lakes, NJ, USA) or from BioLegend (San Diego, CA, USA). *Ex vivo* surface marker staining was completed for 20 min in the dark at room temperature (RT), followed by two washes with PBS. Cells were then fixed in 2% PFA ready for acquisition. Alternatively for intracellular cytokine staining (ICS) the cells were permeabilized, following surface marker staining, with 100 µl BD FixPerm at 4°C for 20 min, washed twice with BD PermWash buffer and blocked with 100 µl of a 20% goat serum PBS solution. Finally, cells were stained with a 25 µl cytokine antibody mix for 20 min at RT, washed with PermWash buffer and suspended in 2% PFA. Cells were acquired on a FACSAria Fusion III flow cytometer (BD), and data analyzed with FlowJo version 9.9.6 software (Tree Star).

T-lymphocyte cluster determinations

An unsupervised analysis workflow that includes dimension reduction and clustering was applied to each identified cell type (CD4+ and CD8+) from each cytometric experiment (ICS and *ex vivo*) independently. The workflow was executed using the R programming language version 4.1. To start, FCS files were down sampled to 5000 events with seed set to 123 for reproducibility. The down sampled data was then concatenated and transformed (25). The flowjo_biexp function from the flowWorkspace (26) package was used to transform the data. Transformation parameters, such as maxValue, pos, neg, and widthBasis were parsed from a FlowJo workspace XML file. The XML file was exported from the same workspace where the FCS files were previously gated for CD4+ T and CD8+ T cells and other known populations. The HarmonyMatrix function from the harmony package (27) was then used to help mitigate any batch effects. The do_pca argument was set to FALSE and the biexponential-transformed data was used as the input embedding on which the harmony algorithm would act directly. Uniform Manifold Approximation and Projection (UMAP) was used to facilitate visualization of the corrected, multidimensional space. This was done with the umap function from the uwot package (28) with nearest neighbors (n_neighbors) set to 30. Data points were initialized (init) using the "spca" setting and effective minimum distance between embedded points (min_dist) was set to 0.1. The FlowSOM function from the FlowSOM package (29) was used to iteratively cluster the multidimensional, batch-corrected data. A range of 3 to 25 clusters was tested with seed set to 123. Heatmaps representative of each cluster's phenotype were produced per iteration (30). These heatmaps were used to guide the selection of an appropriate number of meta-clusters (nClus). For the CD4+ T cell ICS experiment analysis, a cluster number of 10 was chosen. A cluster number of 9 was chosen for each of the other three data sets analyzed (CD8+ T cell ICS, CD4+ T cell ex vivo, and CD8+ T cell ex vivo analyses). Cluster frequencies were calculated and used for downstream statistical testing.

Plasma cytokine and CMV serostatus assays

Patient plasma cytokine levels were measured using the Thermo Fisher human inflammation panel 20 Plex kit (cat. no. EPX200-12185-901) and the Luminex Bio-Rad Bio-Plex™ 200 system. To control for the effect of CMV infection, which often elicits Th1 biased T cell responses (20, 31), the patient CMV serostatus was assessed by the GenWay CMV IgG ELISA test kit (cat. no. GWB-892399).

Outcome

The primary outcome in these analyses was individual follow-up HbA1c measure in relation to baseline HbA1c; the HbA1c outcome was dichotomized as decreased (follow-up measure < baseline measure) or stable/increased (follow-up measure ≥ baseline measure).

Statistical analysis

Participant demographic and clinical characteristics were compared by HbA1c change over time (decreased versus stable/increased) using Chi-square tests for categorical variables and Kruskall-Wallis tests for continuous variables. Differences in the percentages of CD4+ cells of particular phenotypes (percent of individuals' total CD4+ population, defined by surface receptor and cytokine characteristics) were also examined across outcome categories, comparing follow-up to baseline measures, under multiple stimulation conditions. These differences were assessed for each phenotype under each stimulation condition both by Kruskal-Wallis test, and if considered of potential interest for hypothesis generation ($p<0.10$), by linear regression, adjusting for baseline HbA1c measure. All analyses were conducted in Stata 15.1 (StataCorp, College Station, TX). Family-wise error rate corrections were not applied for multiple testing, as hypothesis tests for specific markers were determined *a priori* as per Kumar et al. (11), but

Bonferroni-corrected p-values are provided in the footnotes of each table for the reader's consideration.

Results

Of 62 total participants, approximately 1/3 (n = 23) had normal HbA1c levels at baseline, half (n = 33) had prediabetes, and the remainder (n = 6) were categorized as having diabetes (24). Three of the six patients with HbA1c ≥6.5% at baseline self-reported DM. The HbA1c levels of the study population are summarized in Supplementary Table 1. The HbA1c levels for the prediabetes and diabetes groups tended to decrease following treatment, with the prediabetes group showing a significant decrease ($p < 0.0001$) in baseline to follow-up HbA1c values. Since the HbA1c levels varied considerably at baseline versus follow-up, we separated participants into those with any increased (n = 10) or decreased (n = 46) follow-up HbA1c relative to baseline. We did not implement a threshold to qualify an alteration as increased or decreased, rather any change was considered. Participants without change in HbA1c (n = 6) were included in the increased HbA1c group; four of the six had normal HbA1c.

Table 1 compares the population demographics/characteristics of the two groups. Neither group differed significantly by age, sex, or HIV status. All 62 participants were CMV IgG positive. Most patients (n = 51 [82%]) were cured or had treatment completion; seven had treatment failure, three did not complete treatment, and one had relapse after cure. Due to our small study sample size and since several studies have investigated the associated factors for progression from prediabetes to diabetes or reversion to normoglycemia (12–15), we focused on measuring immune-associated changes relating to HbA1c fluctuations following TB treatment and did not consider participants with overt diabetes as a separate group.

First, we assessed plasma cytokine levels of all participants to determine if changes in HbA1c following TB treatment were associated with changes in systemic markers of inflammation (Table 2). Only two markers showed significant changes between study groups. CD62 P-selectin, a marker of chronic inflammation (32), was significantly higher in the patients with stable/increased HbA1c following treatment relative to those in whom HbA1c was reduced. Conversely, the anti-inflammatory cytokine IL-10 was significantly reduced in participants with stable/increased HbA1c but remained unchanged in patients with decreased HbA1c. Although no significant differences were observed for the other soluble factors measured, including proinflammatory markers such as IL-6 and IL-1b, these data suggested an association between increasing HbA1c and a more proinflammatory state following TB treatment.

To determine if stable/increased HbA1c levels were associated with differences in T cell immunity, PBMC samples were stimulated as described and an unbiased clustering approach used to identify CD4+ or CD8+ T cell phenotypes of interest (Figure 1A). The main cytokine producing CD4+ populations, clusters 2-7 (Figure 1B), all grouped together and displayed either an effector memory (CD45RO+ CCR7-) or a TEMRA (CD45RO-CCR7-) phenotype. This approach identified a PMA-stimulated IL-17+ TNF-α+ CD4+ cluster (cluster 6) which was positively associated with HbA1c levels (Figures 1C, D). At follow-up after TB treatment, the capacity of CD4+ T cells to produce IL-17 was increased in patients with stable/increased HbA1c. This population has an effector memory phenotype (CD45RO+ CCR7-) and comprises about 0.6% of total CD4+ T cells. In addition, *Mtb*-specific T cells, which produced IL-17 but not TNF-α+ following

TABLE 1 Study population characteristics (N=62).

	Decreased-HbA1c (n=46)		Stable/increased-HbA1c (n=16)		
Characteristic	N	%	N	%	p-value*
Age, years**	33.5	(27, 43)	37	(31.5, 41.5)	0.53
Sex					0.31
Male	28	60.9	12	75	
Female	18	39.1	4	25	
HIV-Status					0.57
Negative	18	39.1	5	31.2	
Positive	28	60.9	11	68.8	
HIV-Positive, ART-Receipt					0.51
No	16/28	57.1	5/11	45.5	
Yes	12/28	42.9	6/11	54.5	
HbA1c at Baseline**	6	(5.7, 6.2)	5.3	(5.1, 5.6)	
HbA1c at Follow-up**	5.5	(5.3, 5.8)	5.5	(5.2, 5.6)	

*X^2 test for categorical variables; Kruskall-Wallis test for continuous variables **Continuous variables presented as "median (interquartile range)"

TABLE 2 Comparison of Fold-change (follow-up vs Baseline) in plasma cytokine levels relative to HbA1c change during follow-up (increase vs. decrease), (N=62).

	Decreased HbA1c		Stable/increased HbA1c		
Marker	Median fold change	IQR	Median fold change	IQR	p-value*
IFN alpha	0.92	(0.76, 1.1)	0.97	(0.81, 1.1)	0.47
IL-10	**1**	**(0.89, 1.3)**	**0.85**	**(0.76, 1)**	**0.04**
IL-13	0.99	(0.77, 1.2)	0.88	(0.83, 1.1)	0.35
IL-4	0.96	(0.81, 1.2)	0.92	(0.81, 1.2)	0.94
CD62E (E-selectin)	0.51	(0.32, 0.94)	0.63	(0.34, 0.98)	0.68
CD62P (P-selectin)	**0.67**	**(0.45, 1.2)**	**1.5**	**(0.79, 2.2)**	**0.01**
GM-CSF	1	(0.89, 1.2)	0.88	(0.77, 0.98)	0.06
IFN gamma	0.93	(0.71, 1.1)	0.84	(0.7, 0.96)	0.3
IL1 alpha	0.89	(0.78, 1)	0.77	(0.67, 1.1)	0.3
IL1 beta	0.98	(0.77, 1.2)	0.95	(0.79, 1.2)	0.75
IL-12p70	0.88	(0.73, 1.1)	0.85	(0.7, 1)	0.88
IL-17A (CTLA-8)	0.98	(0.75, 1.2)	0.86	(0.72, 0.97)	0.14
IL-6	0.93	(0.79, 1)	0.83	(0.72, 0.99)	0.52
IL-8 (CXCL8)	0.74	(0.47, 0.88)	0.77	(0.54, 0.97)	0.54
IP-10 (CXCL10)	0.27	(0.07, 0.64)	0.4	(0.18, 0.71)	0.52
MCP1 (CCL2)	1.1	(0.83, 1.3)	1.3	(0.79, 1.7)	0.44
MIP1 alpha (CCL3)	0.79	(0.67, 1)	0.85	(0.76, 1.1)	0.33
MIP1 beta (CCL4)	0.93	(0.69, 1.1)	0.96	(0.78, 1.1)	0.72
ICAM-1	0.82	(0.62, 0.99)	0.89	(0.61, 1.1)	0.37
TNF alpha	1	(0.78, 1.1)	0.95	(0.89, 0.61)	0.61

*X^2 test for categorical variables; Kruskall-Wallis test for continuous variables. Continuous variables presented as "median fold change (interquartile range)" percentages. Bold proportions/distributions are significantly different ($p<0.05$). Bonferroni-corrected threshold for multiple testing is $p=0.0025$.

stimulation with MTB300, were also significantly elevated in participants who had stable/increased HbA1c. These cells had a TEMRA (CD45RO- CCR7-) phenotype. To confirm these differences identified using an unbiased approach, we gated on total cytokine production for CD4+ T cells using conventional Boolean gating (Table 3; Supplementary Figure 1). Despite seeing no difference in plasma TNF-α, this revealed a significant increase in TNF-α production from CD4+ T cells stimulated with MTB300 antigen in patients with stable/increased HbA1c. Together these data suggest that stable/increased HbA1c following TB treatment was associated with elevated Th1 and Th17 CD4+ responses. In contrast, the capacity for Th2 responses (based on the production of IL-4/-13) was reduced in participants with stable/increased HbA1c, reaching significance at follow-up with PMA stimulation (Supplementary Table 4).

An additional phenotyping flow panel was used, and unbiased clustering revealed distinct clusters suggestive of activated and exhausted T cells (based on the expression of HLA-DR, PD-1, CD57 and CX3CR1) (Figures 2A, B). Of these, cluster 6, distinguished by expression of CX3CR1 in the absence of HLA-DR or CD57, showed a positive association with stable/increased HbA1c (Figure 2C). Furthermore, looking at total CX3CR1+ CD4+ T cells, their frequency was higher at baseline and follow-up in the patients with stable/increased HbA1c (~1.4 fold higher). In addition, cluster 8 (CD57+) almost doubled in frequency from baseline to follow-up for patients with stable/increased HbA1c, but this did not reach statistical significance.

Examining CD8+ T cell responses in the same way we found that a PMA stimulated IFNγ+ TNF-α+ effector memory CD8+ T cell population (cluster 9) was upregulated in patients with stable/increased HbA1c at follow-up (Figure 3). As expected, the IL-17, IL-4 and IL-13 expression were confined to CD4+ T cells, with little or no detection in CD8+ populations. From the phenotyping panel (Figure 4), cluster 2, consistent with CD8+

10.3389/fimmu.2023.1151528

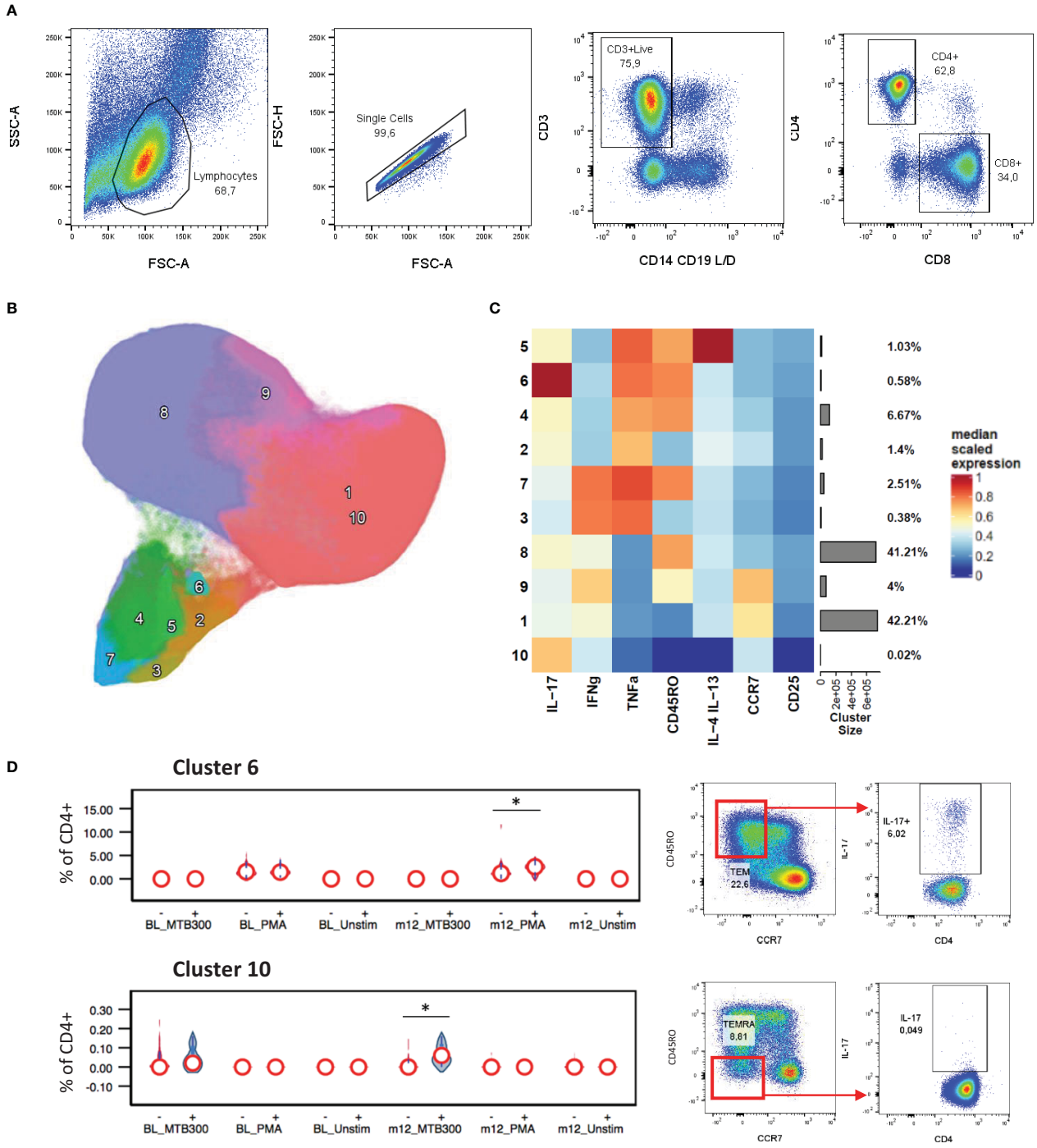

FIGURE 1
CD4+ cytokine profiles associated with HbA1c levels. General gating strategy to identify CD4+ and CD8+ T cells **(A)**. UMAP projection of the 10 FlowSOM generated CD4+ T cell clusters **(B)**. The resulting cluster frequency and median fluorescence intensity of detected markers expressed by each cluster were presented as a heatmap **(C)**. Clusters 6 and 10 significantly associated with stable/increased HbA1c category **(D)**. Participant groups with increased or decreased HbA1c levels were represented with "+" or "-" respectively. Respective flow cytometry dot plots were included alongside, displaying IL-17 production. Statistical analyses were done using Kruskal-Wallis test and P values are denoted as * < 0.05.

TEMRA CD57+ population, was lower in patients with stable/increased HbA1c at both baseline and follow-up but reached significance at follow-up (Figure 4C). A similar trend, although not significant, was observed for cluster 6, which expressed markers of activation and proliferation (HLA-DR+ Ki67+).

Discussion

In our drug-susceptible TB study cohort with high proportion of PWH, we investigated the immune factors associated with persistent glucose intolerance following treatment of active disease. Longitudinal sampling allowed us to group patients based on stable/increased HbA1c

TABLE 3 Manual gating of total cytokine production by CD4+ T cells.

	Decreased-HbA1c		Stable/increased-HbA1c		
Characteristic	Median %	IQR	Median %	IQR	p-value*
TNF-α+ Only, BL+ PMA	20	(12, 27)	19	(11, 28)	0.93
TNF-α+ Only, BL+ TB300	**0.011**	**(0, 0.027)**	**0.05**	**(0.012, 0.073)**	**0.03**
TNF-α+ Only, BL+ Unstim	0	(0, 0.02)	0.005	(0, 0.031)	0.23
TNF-α+ Only, m12+ PMA	25	(18, 30)	23	(18, 32)	0.85
TNF-α+ Only, m12+ TB300	**0.008**	**(0, 0.015)**	**0.029**	**(0.005, 0.041)**	**0.01**
TNF-α+ Only, m12+ Unstim	0.001	(0, 0.013)	0.011	(0, 0.03)	0.12

*$\chi 2$ test for categorical variables; Kruskall-Wallis test for continuous variables. Continuous variables presented as "median (interquartile range)" percentages. Bold proportions/distributions are significantly different ($p<0.05$). Bonferroni-corrected threshold for multiple testing is $p=0.008$.

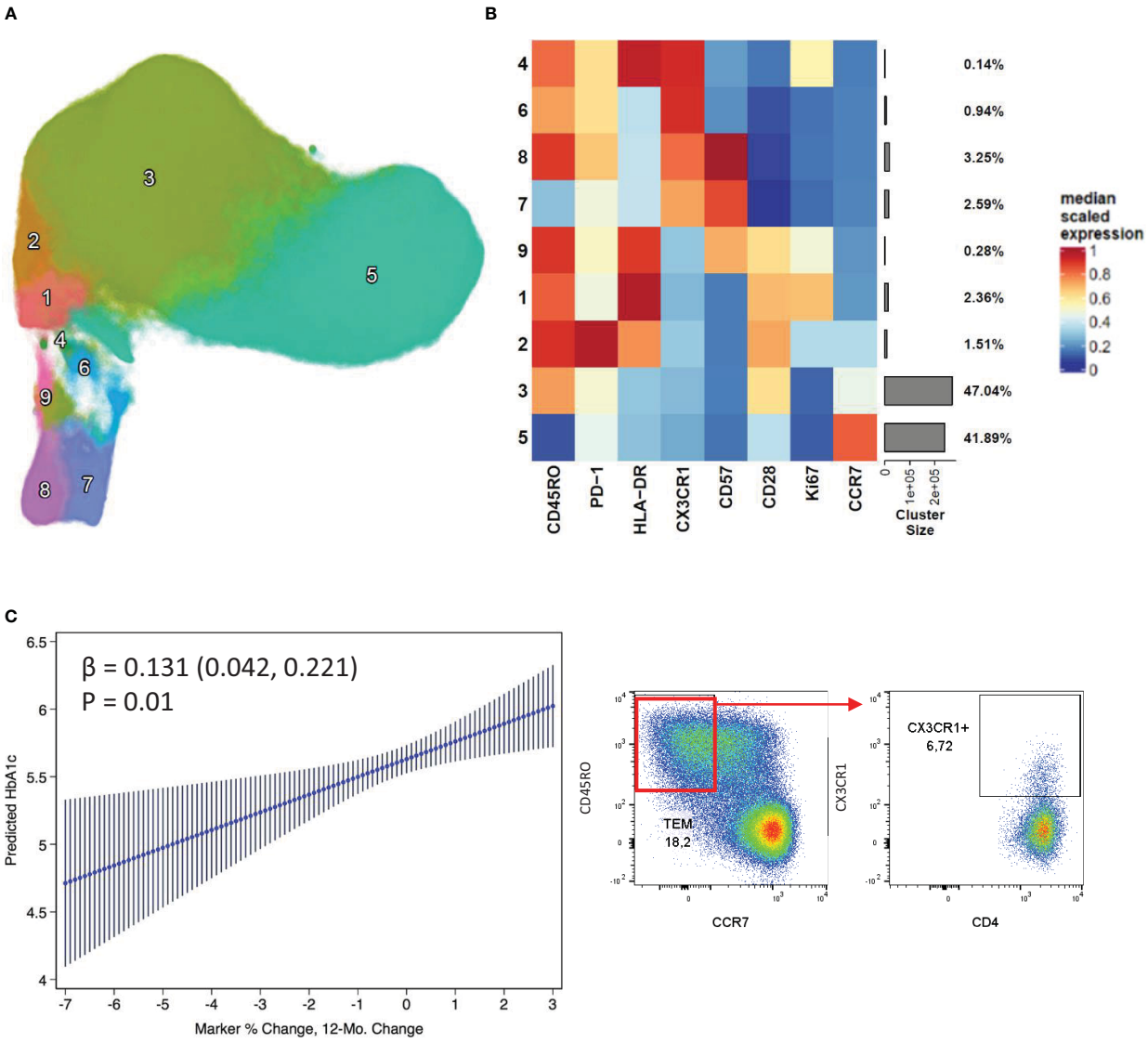

FIGURE 2
CD4+ CX3CR1 surface expression associated with increased HbA1c change. Nine distinct clusters were identified by FlowSOM and projected as a UMAP **(A)**. The cluster frequency and marker expression intensity were presented as a heatmap **(B)**. Linear regression of a CX3CR1 expressing cluster 6 which associated positively with stable/increased HbA1c **(C)**. Respective flow cytometry dot plots were included alongside, displaying CX3CR1 expression.

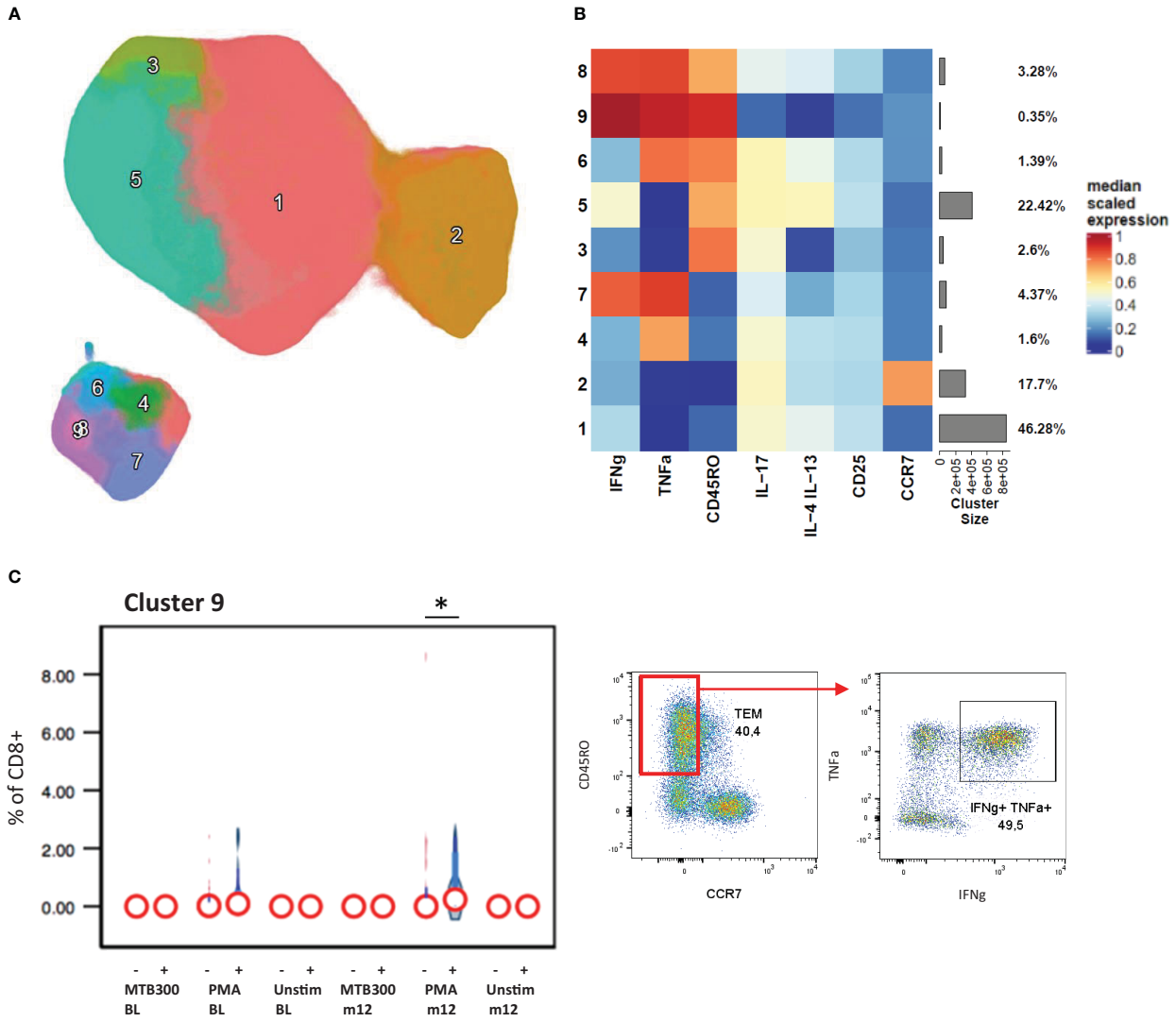

FIGURE 3
CD8+ cytokine profiles associated with HbA1c levels. The CD8+ T cells clustered into 9 distinct populations by FlowSOM analysis and displayed by UMAP projection **(A)**. The cluster frequency and marker expression intensity were compared in the resulting heatmap **(B)**. Cluster 9 associated significantly with stable/increased HbA1c category **(C)**. Participant groups with increased or decreased HbA1c levels were represented with "+" or "-" respectively. Respective flow cytometry dot plots were included alongside, displaying IFNg and TNFα co-expression. Statistical analyses were done using Kruskal-Wallis test and P values are denoted as * < 0.05.

or decreased HbA1c. Stable/increased HbA1c one year after TB treatment initiation was associated with a pro-inflammatory state reflected by elevated plasma cytokines, Th1 (CX3CR1+) and Th17 CD4+ T cell responses.

Six patients had an HbA1c ≥6.5% at baseline, three of whom received anti-diabetic medications, though they did not start these medications during follow up. Despite a relatively low proportion of patients with DM in our cohort, over half (56%) had HbA1c levels consistent with prediabetes at baseline. We found that most patients had resolution of hyperglycemia after TB treatment, consistent with well-documented transient hyperglycemia (33). It is unclear whether the hyperglycemia observed in our study and others increases long-term risks for development of DM (34).

Although most participants did not have baseline HbA1c levels indicative of overt DM, and most had resolution of hyperglycemia, those with increased HbA1c levels tended to display a more pro-inflammatory state characterized by elevated CD62 P-selectin and depressed IL-10 plasma levels. Although less pronounced, likely due to the small sample size, this is in keeping with similar trends observed by Randeria et al. who compared type 2 diabetics (HIV and TB negative) to healthy controls (35). HIV and TB co-infection as well as the effect of ART may have influenced our findings. Nonetheless we observed elevated soluble CD62 P-selectin, which serves as an indicator of vascular inflammation and is characteristic of type 2 diabetes (36–38). Several studies have described either an increased expression of IL-10 in plasma of persons with type 2 diabetes (35) or unchanged/reduced levels (39, 40)

10.3389/fimmu.2023.1151528

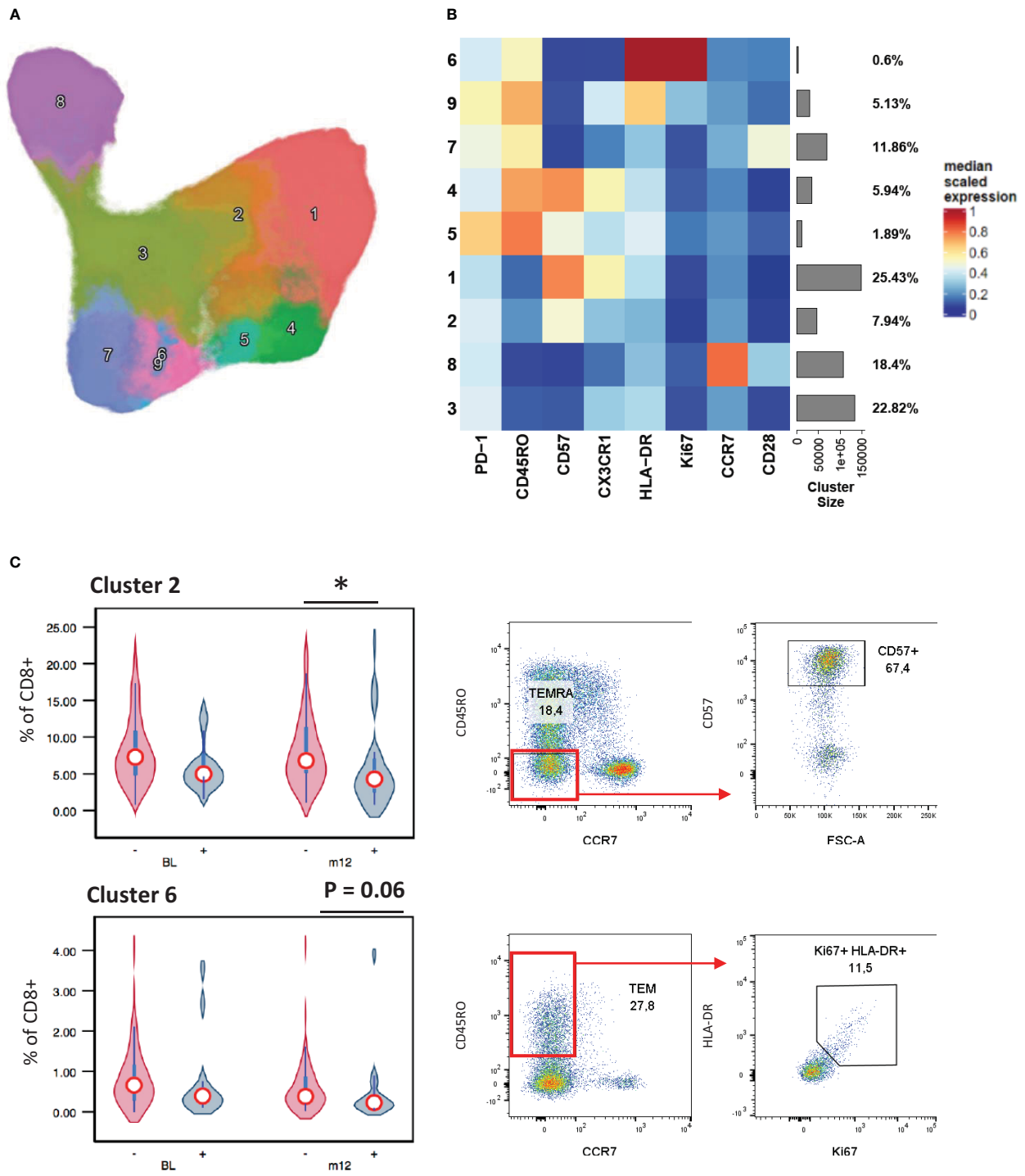

FIGURE 4
CD8+ surface marker expression associated with HbA1c levels. A UMAP projection of the 9 unique CD8+ T cell clusters identified by FlowSOM analysis **(A)**. The population frequencies and their relative marker expression levels were summarized in a heatmap **(B)**. Cluster 2 associated stable/increased with HbA1c category **(C)**. Participant groups with increased or decreased HbA1c levels were represented with "+" or "-" respectively. Respective flow cytometry dot plots were included alongside, displaying CD57+ TEMRA and Ki67 and HLA-DR co-expressing TEM. Statistical analyses were done using Kruskal-Wallis test and P values are denoted as * < 0.05.

relative to healthy controls. Interestingly, glucose intolerance reduces IL-10 signaling efficiency, resulting in increased TNF-α production (39).

Although we did not observe a difference in TNF-α, we did detect reduced IL-10 plasma levels. Reduced IL-10 signaling has been associated with type 2 diabetes (40). Together the lower IL-10 levels and reduced signaling tie in well with a pro-inflammatory T cell response. In this regard, participants with HbA1c levels that increased or remained stable over time had an increased capacity of CD4+ T cells to produce IL-17 and TNFα (following PMA stimulation), and for *Mtb*-specific CD4+ T cells to produce IL-17 alone following stimulation with the TB-antigen pool MTB300 (41).

Recent data from a human TST challenge model suggest that TB-specific Th17 T cell responses are associated with TB pathogenesis (42). Although most participants had successful treatment and were culture negative at the end of TB therapy, it is possible that incomplete Mtb killing may occur within the lungs of some TB patients, as demonstrated in human studies using direct sampling of the lung environment (43). If so, then residual infection might be expected to prevent the resolution of HbA1c and be associated with persistent inflammation and pathogenic IL-17 T cell responses. Regardless, dysglycemia is associated with decreased Th1 and Th17 responses to *Mtb* antigens in individuals with latent TB infection (44, 45), suggesting a different relationship following TB treatment. Interestingly, the depression of these responses was linked to elevated IL-10, which was significantly lower in individuals following treatment who had stable or increased HbA1c levels, supporting this hypothesis.

In addition, we observed an association between CD4+ T cell expression of CX3CR1, a marker associated with Th1 effector populations (46, 47), and stable/increased HbA1c levels. Lau et al. also found DM was associated with an increase in CX3CR1 expressing T cells and a reduced Th2 response (48). The CX3CR1-fractalkine axis mediates the migration of CX3CR1 expressing lymphocytes to inflamed tissue endothelium (46, 49). These T cells often have anti-viral and cytotoxic properties and are associated with CMV and HIV infection (31, 50). All participants in this study had CMV reactive plasma and 69% of participants in the stable/increased HbA1c group were HIV positive, therefore this increased CX3CR1+ CD4+ T cell frequency is also consistent with their anti-viral properties. Nonetheless, CX3CR1 expression on CD4+ T cells associated positively with stable/increased HbA1c. This, in turn, is consistent with this phenotype's association with the progression of metabolic disease (20).

Our study had limitations. First, our sample size was small. Despite the small number of patients with DM at baseline, we were able to demonstrate the association of stable/increased HbA1c with elevated Th1 and Th17 CD4+ responses, providing direction for further study. Second, we had a single follow-up measurement of HbA1c and CD4+ cells 12-15 months after TB treatment initiation. Although this timeframe allowed time for a complete course of treatment, it remains unclear what risk, if any, is conferred by the dysregulation we observed in those whose HbA1c remained stable or increased. Finally, our investigations were exploratory and need to be confirmed in additional contexts and populations.

Conclusion

Identifying markers that associate with glucose intolerance could help identify metabolically fragile individuals who need closer monitoring/treatment. Monitoring the pro-inflammatory T cell response in hyperglycemic patients after TB treatment could prove useful in this regard. Further work investigating the mechanisms linking these immune pathways to metabolic dysregulation and poor clinical outcomes are needed.

Data availability statement

The original contributions presented in the study are included in the article/Supplementary Material. Further inquiries can be directed to the corresponding author.

Ethics statement

This study was approved by the Vanderbilt Institutional Review Board (IRB#191176). Informed consent was obtained under the Biomedical Research Ethics Committee (BREC) at the University of Kwazulu-Natal (UKZN) Ref No: BE423/19, and the RePORT South Africa study (IRB#160918) at Vanderbilt. The patients/participants provided their written informed consent to participate in this study.

Author contributions

RK, CW and JS share co-first authorship. RK conducted experimental work, analysis and wrote the manuscript. CW contributed to analysis and writing. JS contributed to analysis and writing. PR contributed to statistical analysis and writing. FM, FK and TS contributed to study design, administration and writing. JK contributed to study design, analysis and writing. AL contributed to study design and writing. YV contributed to study design, funding, analysis and writing. All authors contributed to the article and approved the submitted version.

Funding

This work was supported by the following grant from the U.S. Civilian Research and Development Foundation: DAA9-19-65379-1, DAA9-19-65380-1, OISE-16-62060-1, OISE-16-62061-1.

Conflict of interest

Author PR consulted for Gilead & Janssen pharmaceuticals; money paid to institution grant funding from NIH/NIAID.

The remaining authors declare that the research was conducted in the absence of any commercial or financial relationships that could be construed as a potential conflict of interest.

Publisher's note

Supplementary material

The Supplementary Material for this article can be found online at: https://www.frontiersin.org/articles/10.3389/fimmu.2023.1151528/full#supplementary-material

References

1. Critchley JA, Restrepo BI, Ronacher K, Kapur A, Bremer AA, Schlesinger LS, et al. Defining a research agenda to address the converging epidemics of tuberculosis and diabetes: part 1: epidemiology and clinical management. *Chest* (2017) 152(1):165–73. doi: 10.1016/j.chest.2017.04.155

2. Shaw JE, Sicree RA, Zimmet PZ. Global estimates of the prevalence of diabetes for 2010 and 2030. *Diabetes Res Clin Pract* (2010) 87(1):4–14. doi: 10.1016/j.diabres.2009.10.007

3. World Health Organization. *Global report on diabetes*. Geneva: WHO Press (2016).

4. IDF. *International diabetes federation diabetes atlas*. Brussels, Belgium: International Diabetes Federation (2021).

5. Tenorio AR, Zheng Y, Bosch RJ, Krishnan S, Rodriguez B, Hunt PW, et al. Soluble markers of inflammation and coagulation but not T-cell activation predict non-AIDS-defining morbid events during suppressive antiretroviral treatment. *J Infect Dis* (2014) 210(8):1248–59. doi: 10.1093/infdis/jiu254

6. du Bruyn E, Peton N, Esmail H, Howlett PJ, Coussens AK, Wilkinson RJ. Recent progress in understanding immune activation in the pathogenesis in HIV-tuberculosis co-infection. *Curr Opin HIV AIDS* (2018) 13(6):455–61. doi: 10.1097/COH.0000000000000501

7. Pickup JC. Inflammation and activated innate immunity in the pathogenesis of type 2 diabetes. *Diabetes Care* (2004) 27(3):813–23. doi: 10.2337/diacare.27.3.813

8. Kumar NP, Sridhar R, Banurekha VV, Jawahar MS, Nutman TB, Babu S. Expansion of pathogen-specific T-helper 1 and T-helper 17 cells in pulmonary tuberculosis with coincident type 2 diabetes mellitus. *J Infect Dis* (2013) 208(5):739–48. doi: 10.1093/infdis/jit241

9. Vallerskog T, Martens GW, Kornfeld H. Diabetic mice display a delayed adaptive immune response to mycobacterium tuberculosis. *J Immunol* (2010) 184(11):6275–82. doi: 10.4049/jimmunol.1000304

10. Ronacher K, van Crevel R, Critchley JA, Bremer AA, Schlesinger LS, Kapur A, et al. Defining a research agenda to address the converging epidemics of tuberculosis and diabetes: part 2: underlying biologic mechanisms. *Chest* (2017) 152(1):174–80. doi: 10.1016/j.chest.2017.02.032

11. Kumar NP, Banurekha VV, Nair D, Sridhar R, Kornfeld H, Nutman TB, et al. Coincident pre-diabetes is associated with dysregulated cytokine responses in pulmonary tuberculosis. *PloS One* (2014) 9(11):e112108. doi: 10.1371/journal.pone.0112108

12. Alizadeh Z, Baradaran HR, Kohansal K, Hadaegh F, Azizi F, Khalili D. Are the determinants of the progression to type 2 diabetes and regression to normoglycemia in the populations with pre-diabetes the same? *Front Endocrinol (Lausanne)* (2022) 13:1041808. doi: 10.3389/fendo.2022.1041808

13. Kowall B, Rathmann W, Heier M, Holle R, Peters A, Thorand B, et al. Impact of weight and weight change on normalization of prediabetes and on persistence of normal glucose tolerance in an older population: the KORA S4/F4 study. *Int J Obes (Lond)* (2012) 36(6):826–33. doi: 10.1038/ijo.2011.161

14. Alvarsson M, Hilding A, Ostenson CG. Factors determining normalization of glucose intolerance in middle-aged Swedish men and women: a 8-10-year follow-up. *Diabetes Med* (2009) 26(4):345–53. doi: 10.1111/j.1464-5491.2009.02685.x

15. Lee EY, Lee YH, Yi SW, Shin SA, Yi JJ. BMI and all-cause mortality in normoglycemia, impaired fasting glucose, newly diagnosed diabetes, and prevalent diabetes: a cohort study. *Diabetes Care* (2017) 40(8):1026–33. doi: 10.2337/dc16-1458

16. Olson NC, Doyle MF, de Boer IH, Huber SA, Jenny NS, Kronmal RA, et al. Associations of circulating lymphocyte subpopulations with type 2 diabetes: cross-sectional results from the multi-ethnic study of atherosclerosis (MESA). *PloS One* (2015) 10(10):e0139962. doi: 10.1371/journal.pone.0139962

17. Wagner NM, Brandhorst G, Czepluch F, Lankeit M, Eberle C, Herzberg S, et al. Circulating regulatory T cells are reduced in obesity and may identify subjects at increased metabolic and cardiovascular risk. *Obes (Silver Spring)* (2013) 21(3):461–8. doi: 10.1002/oby.20087

18. Zeng C, Shi X, Zhang B, Liu H, Zhang L, Ding W, et al. The imbalance of Th17/Th1/Tregs in patients with type 2 diabetes: relationship with metabolic factors and complications. *J Mol Med (Berl)* (2012) 90(2):175–86. doi: 10.1007/s00109-011-0816-5

19. Rattik S, Engelbertsen D, Wigren M, Ljungcrantz I, Ostling G, Persson M, et al. Elevated circulating effector memory T cells but similar levels of regulatory T cells in patients with type 2 diabetes mellitus and cardiovascular disease. *Diabetes Vasc Dis Res* (2019) 16(3):270–80. doi: 10.1177/1479164118817942

20. Wanjalla CN, McDonnell WJ, Ram R, Chopra A, Gangula R, Leary S, et al. Single-cell analysis shows that adipose tissue of persons with both HIV and diabetes is enriched for clonal, cytotoxic, and CMV-specific CD4+ T cells. *Cell Rep Med* (2021) 2(2):100205. doi: 10.1016/j.xcrm.2021.100205

21. Bailin SS, Kundu S, Wellons M, Freiberg MS, Doyle MF, Tracy RP, et al. Circulating CD4+ TEMRA and CD4+ CD28- T cells and incident diabetes among persons with and without HIV. *Aids* (2022) 36(4):501–11. doi: 10.1097/QAD.0000000000003137

22. Brown TT, Tassiopoulos K, Bosch RJ, Shikuma C, McComsey GA. Association between systemic inflammation and incident diabetes in HIV-infected patients after initiation of antiretroviral therapy. *Diabetes Care* (2010) 33(10):2244–9. doi: 10.2337/dc10-0633

23. Betene ADC, De Wit S, Neuhaus J, Palfreeman A, Pepe R, Pankow JS, et al. Interleukin-6, high sensitivity c-reactive protein, and the development of type 2 diabetes among HIV-positive patients taking antiretroviral therapy. *J Acquir Immune Defic Syndr* (2014) 67(5):538–46. doi: 10.1097/QAI.0000000000000354

24. Sherwani SI, Khan HA, Ekhzaimy A, Masood A, Sakharkar MK. Significance of HbA1c test in diagnosis and prognosis of diabetic patients. *biomark Insights* (2016) 11:95–104. doi: 10.4137/BMI.S38440

25. Ellis BHP, Hahne F, Le Meur N, Gopalakrishnan N, Spidlen J, Jiang M, et al. flowCore: basic structures for flow cytometry data. r package version 2.8.0. *BMC Bioinformatics* (2022). doi: 10.1186/1471-2105-10-106

26. Finak GJM. flowWorkspace: infrastructure for representing and interacting with gated and ungated cytometry data sets. r package version 4.8.0. *Bioconductor* (2022). doi: 10.18129/B9.bioc.flowWorkspace

27. Korsunsky IMN, Fan J, Slowikowski K, Raychaudhuri S. Harmony: fast, sensitive, and accurate integration of single cell data. r package version 0.1.1. *Nat Methods* (2022). doi: 10.1038/s41592-019-0619-0

28. Mellville J. Uwot: the uniform manifold approximation and projection (UMAP) method for dimensionality reduction. r package version 0.1.14. *CRAN* (2022). Available at: https://github.com/jlmelville/uwot.

29. Van Gassen S. FlowSOM: uisng self-organizing maps for visualization and interpretation of cytometry data. *Cytom Part J Int Soc Anal Cytol* (2015) 87:636–45. doi: 10.1002/cyto.a.22625

30. Gu Z. Complex heatmaps reveal patterns and correlations in multidimensional genomic data. *Bioinformatics* (2016) 32:2847–9. doi: 10.1093/bioinformatics/btw313

31. Abana CO, Pilkinton MA, Gaudieri S, Chopra A, McDonnell WJ, Wanjalla C, et al. Cytomegalovirus (CMV) epitope-specific CD4(+) T cells are inflated in HIV(+) CMV(+) subjects. *J Immunol* (2017) 199(9):3187–201. doi: 10.4049/jimmunol.1700851

32. Kirwan DE, Chong DLW, Friedland JS. Platelet activation and the immune response to tuberculosis. *Front Immunol* (2021) 12:631696. doi: 10.3389/fimmu.2021.631696

33. Boillat-Blanco N, Ramaiya KL, Mganga M, Minja LT, Bovet P, Schindler C, et al. Transient hyperglycemia in patients with tuberculosis in Tanzania: implications for diabetes screening algorithms. *J Infect Dis* (2016) 213(7):1163–72. doi: 10.1093/infdis/jiv568

34. Magee MJ, Salindri AD, Kyaw NTT, Auld SC, Haw JS, Umpierrez GE. Stress hyperglycemia in patients with tuberculosis disease: epidemiology and clinical implications. *Curr Diabetes Rep* (2018) 18(9):71. doi: 10.1007/s11892-018-1036-y

35. Randeria SN, Thomson GJA, Nell TA, Roberts T, Pretorius E. Inflammatory cytokines in type 2 diabetes mellitus as facilitators of hypercoagulation and abnormal clot formation. *Cardiovasc Diabetol* (2019) 18(1):72. doi: 10.1186/s12933-019-0870-9

36. Preston RA, Coffey JO, Materson BJ, Ledford M, Alonso AB. Elevated platelet p-selectin expression and platelet activation in high risk patients with uncontrolled severe hypertension. *Atherosclerosis* (2007) 192(1):148–54. doi: 10.1016/j.atherosclerosis.2006.04.028

37. Kaur R, Kaur M, Singh J. Endothelial dysfunction and platelet hyperactivity in type 2 diabetes mellitus: molecular insights and therapeutic strategies. *Cardiovasc Diabetol* (2018) 17(1):121. doi: 10.1186/s12933-018-0763-3

38. Gross PL. Soluble p-selectin is the smoke, not the fire. *Blood* (2017) 130(2):101–2. doi: 10.1182/blood-2017-05-786319

39. Barry JC, Shakibakho S, Durrer C, Simtchouk S, Jawanda KK, Cheung ST, et al. Hyporesponsiveness to the anti-inflammatory action of interleukin-10 in type 2 diabetes. *Sci Rep* (2016) 6:21244. doi: 10.1038/srep21244

40. van Exel E, Gussekloo J, de Craen AJ, Frolich M, Bootsma-Van Der Wiel A, Westendorp RG, et al. Low production capacity of interleukin-10 associates with the metabolic syndrome and type 2 diabetes: the Leiden 85-plus study. *Diabetes* (2002) 51(4):1088–92. doi: 10.2337/diabetes.51.4.1088

41. Scriba TJ, Carpenter C, Pro SC, Sidney J, Musvosvi M, Rozot V, et al. Differential recognition of mycobacterium tuberculosis-specific epitopes as a function of tuberculosis disease history. *Am J Respir Crit Care Med* (2017) 196(6):772–81. doi: 10.1164/rccm.201706-1208OC

42. Pollara G, Turner CT, Rosenheim J, Chandran A, Bell LCK, Khan A, et al. Exaggerated IL-17A activity in human in vivo recall responses discriminates active tuberculosis from latent infection and cured disease. *Sci Transl Med* (2021) 13(592):eabg7673. doi: 10.1126/scitranslmed.abg7673

43. Malherbe ST, Shenai S, Ronacher K, Loxton AG, Dolganov G, Kriel M, et al. Persisting positron emission tomography lesion activity and mycobacterium tuberculosis mRNA after tuberculosis cure. *Nat Med* (2016) 22(10):1094–100. doi: 10.1038/nm.4177

44. Kumar NP, Moideen K, George PJ, Dolla C, Kumaran P, Babu S. Coincident diabetes mellitus modulates Th1-, Th2-, and Th17-cell responses in latent tuberculosis in an IL-10- and TGF-beta-dependent manner. *Eur J Immunol* (2016) 46(2):390–9. doi: 10.1002/eji.201545973

45. Kumar NP, Moideen K, Dolla C, Kumaran P, Babu S. Prediabetes is associated with the modulation of antigen-specific Th1/Tc1 and Th17/Tc17 responses in latent mycobacterium tuberculosis infection. *PloS One* (2017) 12(5):e0178000. doi: 10.1371/journal.pone.0178000

46. Nishimura M, Umehara H, Nakayama T, Yoneda O, Hieshima K, Kakizaki M, et al. Dual functions of fractalkine/CX3C ligand 1 in trafficking of perforin+/granzyme b+ cytotoxic effector lymphocytes that are defined by CX3CR1 expression. *J Immunol* (2002) 168(12):6173–80. doi: 10.4049/jimmunol.168.12.6173

47. Batista NV, Chang YH, Chu KL, Wang KC, Girard M, Watts TH. T Cell-intrinsic CX3CR1 marks the most differentiated effector CD4(+) T cells, but is largely dispensable for CD4(+) T cell responses during chronic viral infection. *Immunohorizons* (2020) 4(11):701–12. doi: 10.4049/immunohorizons.2000059

48. Lau EYM, Carroll EC, Callender LA, Hood GA, Berryman V, Pattrick M, et al. Type 2 diabetes is associated with the accumulation of senescent T cells. *Clin Exp Immunol* (2019) 197(2):205–13. doi: 10.1111/cei.13344

49. Fong AM, Robinson LA, Steeber DA, Tedder TF, Yoshie O, Imai T, et al. Fractalkine and CX3CR1 mediate a novel mechanism of leukocyte capture, firm adhesion, and activation under physiologic flow. *J Exp Med* (1998) 188(8):1413–9. doi: 10.1084/jem.188.8.1413

50. Pachnio A, Ciaurriz M, Begum J, Lal N, Zuo J, Beggs A, et al. Cytomegalovirus infection leads to development of high frequencies of cytotoxic virus-specific CD4+ T cells targeted to vascular endothelium. *PloS Pathog* (2016) 12(9):e1005832. doi: 10.1371/journal.ppat.1005832

frontiers | Frontiers in Immunology

TYPE Original Research
PUBLISHED 12 June 2023
DOI 10.3389/fimmu.2023.1121864

OPEN ACCESS

EDITED BY
Miguel Angel Alejandre Alcazar,
University Hospital of Cologne, Germany

REVIEWED BY
Michael B. Fessler,
National Institute of Environmental Health Sciences (NIH), United States
Marten A. Hoeksema,
Amsterdam UMC, Netherlands

*CORRESPONDENCE
Tobias Schmid
t.schmid@biochem.uni-frankfurt.de

RECEIVED 12 December 2022
ACCEPTED 30 May 2023
PUBLISHED 12 June 2023

CITATION
Bauer R, Meyer SP, Raue R, Palmer MA, Guerrero Ruiz VM, Cardamone G, Rösser S, Heffels M, Roesmann F, Wilhelm A, Lütjohann D, Zarnack K, Fuhrmann DC, Widera M, Schmid T and Brüne B (2023) Hypoxia-altered cholesterol homeostasis enhances the expression of interferon-stimulated genes upon SARS-CoV-2 infections in monocytes.
Front. Immunol. 14:1121864.
doi: 10.3389/fimmu.2023.1121864

Hypoxia-altered cholesterol homeostasis enhances the expression of interferon-stimulated genes upon SARS-CoV-2 infections in monocytes

Rebekka Bauer[1], Sofie Patrizia Meyer[1], Rebecca Raue[1], Megan A. Palmer[1], Vanesa Maria Guerrero Ruiz[1], Giulia Cardamone[1], Silvia Rösser[1], Milou Heffels[1], Fabian Roesmann[2], Alexander Wilhelm[2], Dieter Lütjohann[3], Kathi Zarnack[4], Dominik Christian Fuhrmann[1,5], Marek Widera[2], Tobias Schmid[1,5]* and Bernhard Brüne[1,5,6,7]

[1]Institute of Biochemistry I, Faculty of Medicine, Goethe University Frankfurt, Frankfurt, Germany, [2]Institute of Medical Virology, University Hospital Frankfurt, Goethe University Frankfurt, Frankfurt, Germany, [3]Institute of Clinical Chemistry and Clinical Pharmacology, University of Bonn, Bonn, Germany, [4]Buchmann Institute for Molecular Life Sciences (BMLS), Faculty of Biological Sciences, Goethe University Frankfurt, Frankfurt, Germany, [5]German Cancer Consortium (DKTK), Partner Site Frankfurt, Frankfurt, Germany, [6]Frankfurt Cancer Institute, Goethe University Frankfurt, Frankfurt, Germany, [7]Fraunhofer Institute for Translational Medicine and Pharmacology ITMP, Frankfurt, Germany

Hypoxia contributes to numerous pathophysiological conditions including inflammation-associated diseases. We characterized the impact of hypoxia on the immunometabolic cross-talk between cholesterol and interferon (IFN) responses. Specifically, hypoxia reduced cholesterol biosynthesis flux and provoked a compensatory activation of sterol regulatory element-binding protein 2 (SREBP2) in monocytes. Concomitantly, a broad range of interferon-stimulated genes (ISGs) increased under hypoxia in the absence of an inflammatory stimulus. While changes in cholesterol biosynthesis intermediates and SREBP2 activity did not contribute to hypoxic ISG induction, intracellular cholesterol distribution appeared critical to enhance hypoxic expression of chemokine ISGs. Importantly, hypoxia further boosted chemokine ISG expression in monocytes upon infection with severe acute respiratory syndrome coronavirus type 2 (SARS-CoV-2). Mechanistically, hypoxia sensitized toll-like receptor 4 (TLR4) signaling to activation by SARS-CoV-2 spike protein, which emerged as a major signaling hub to enhance chemokine ISG induction following SARS-CoV-2 infection of hypoxic monocytes. These data depict a hypoxia-regulated immunometabolic mechanism with implications for the development of systemic inflammatory responses in severe cases of coronavirus disease-2019 (COVID-19).

KEYWORDS

hypoxia, immunometabolism, cholesterol, SREBP2, COVID-19, systemic inflammation

1 Introduction

The availability of molecular oxygen (O_2) is critical for many cellular functions, most notably cellular energy production via oxidative phosphorylation. Thus, various mechanisms evolved to cope with hypoxia, especially with respect to metabolic rewiring in order to protect cells from detrimental effects due to the lack of oxygen (1, 2). Not surprisingly, hypoxia and the resulting adaptive processes are tightly linked to numerous diseases including cancer, as well as metabolic and inflammatory disorders (3). The multilayered crosstalk between metabolic changes and immune responses also forms the basis for the emerging field of immunometabolism (4). While the concept of immunometabolism was termed merely 10 years ago, initial evidence dates back to the early 1990s, when increased expression of the pro-inflammatory cytokine tumor necrosis factor α (TNFα) was observed in rodent models of obesity and was shown to contribute to the development of insulin resistance (5). Along similar lines, altered cholesterol dynamics affect immune functions, as exemplified by observations that upon excessive uptake of low density lipoprotein (LDL)-cholesterol macrophages acquire a pro-inflammatory, foam cell phenotype within atherosclerotic lesions (6). Moreover, using statins to lower plasma LDL-cholesterol concentrations elicited potent anti-inflammatory effects in patients with inflammatory diseases like rheumatoid arthritis or metabolic syndrome (7, 8). Furthermore, intracellular cholesterol trafficking and biosynthetic signaling were shown to activate the inflammasome (9, 10), whereas accumulation of the cholesterol precursor mevalonate induced a trained immunity phenotype in monocyte-derived cells (11). Of note, changes in cholesterol biosynthesis flux also altered anti-viral responses by enhancing interferon (IFN) signaling (12, 13). The connection between IFN signaling and cholesterol metabolism appears to be bidirectional though, as cholesterol biosynthesis enzymes were downregulated in response to viral infection or IFN treatment (14, 15).

In this study, we observed a coinciding transcriptional upregulation of cholesterol biosynthesis enzymes and IFN-stimulated genes (ISGs) in hypoxic monocytes. Mechanistically, hypoxia-evoked changes in cholesterol dynamics enhanced toll-like receptor (TLR) signaling and consequently IFN responses. Hypoxia further increased chemokine ISG production in monocytes upon infection with severe acute respiratory syndrome coronavirus type 2 (SARS-CoV-2), thereby providing a novel concept how hypoxemia, i.e., low blood oxygen levels, might favor systemic inflammation in severe cases of coronavirus disease-2019 (COVID-19).

2 Materials and methods

2.1 Chemicals

All chemicals were purchased from Thermo Fisher Scientific GmbH (Dreieich, Germany), if not indicated otherwise. Fatostatin hydrobromide, TAK-242, IKK-16 hydrochloride, lathosterol, 7-dehydrocholesterol, and desmosterol were purchased from Cayman Chemical (Ann Harbor, MI, USA), PF-429242 dihydrochloride, ketoconazole, methyl-β-cyclodextrin-complexed (water-soluble) cholesterol, mevalonolactone, and geranylgeraniol from Sigma-Aldrich (Taufkirchen, Germany), U18666A from Enzo Life Sciences (Lausen, Switzerland), simvastatin from Selleck Chemicals (Planegg, Germany), NB-598 maleate from Adooq Bioscience (Irvine, CA, USA), enpatoran from TargetMol (Wellesley Hills, MA, USA), T0901317 from Tocris (Wiesbaden-Nordenstadt, Germany), TJ-M2010-5 from Hycultec GmbH (Beutelsbach, Germany), and BX-795 from MedChemExpress (Monmouth Junction, NJ, USA).

2.2 Cell culture

THP-1 cells were obtained from ATCC, and THP-1 STING- and MAVS-KO cells as well as the corresponding original WT THP-1 cells were kindly provided by Prof. Veit Hornung (LMU Munich, Germany) (16). THP-1 cells were cultured in Roswell Park Memorial Institute (RPMI) 1640 medium, supplemented with 100 U/mL penicillin, 100 µg/mL streptomycin, and 10% or 5% FBS (Capricorn Scientific GmbH, Ebsdorfergrund, Germany or Sigma-Aldrich), dependent on the cholesterol concentration of the respective FBS batch. For experiments performed under low FBS levels, the percentage of FBS was reduced to $1/10^{th}$ of the FBS amount used for maintaining the cells. Cells were kept at 37°C in a humidified atmosphere with 5% CO_2. For hypoxic incubations, cells were transferred to a hypoxia workstation (SCI-tive, Baker Ruskinn, Bridgend, South Wales, UK) at 37°C with 5% CO_2 and 1% O_2.

2.3 IFNAR neutralization

THP-1 cells were treated with 5 µg/mL α-IFNAR2 antibody (Clone MMHAR-2 Mab, PBL assay science, Piscataway, NJ, USA; cat. no. 21385) or IgG2a isotype control antibody (Clone C1.18.4, Bio X Cell, Lebanon, NH, USA; cat. no. BE0085) prior to normoxic or hypoxic incubation for 24 h.

2.4 SARS-CoV-2 infection

Lung-derived A549-AT cells, constitutively expressing ACE2 and TMPRSS2 (17), were infected with SARS-CoV-2 strain FFM1 (accession number MT358638.1) (18) using a multiplicity of infection (MOI) of 0.1 in Minimum Essential Medium (MEM) containing 1% FBS, 100 U/mL penicillin, 100 µg/mL streptomycin, and 4 mM L-glutamine (all Sigma-Aldrich). After 1 h inoculation at 37°C and 5% CO_2, cells were washed once with PBS and fresh medium was added. 48 h post infection (hpi), virus-containing supernatants were centrifuged and stored at -80°C until further usage.

Monocytic THP-1 cells were cultured for 24 h in RPMI 1640 with 1% FBS, 100 U/mL penicillin, and 100 µg/mL streptomycin

(all Sigma-Aldrich) at 37°C with 5% CO_2 and either 21% or 1% O_2. Optionally, 10 µM fatostatin, 10 µM TAK-242, or 0.1% DMSO (Carl Roth, Karlsruhe, Germany) were added 1 h before starting hypoxic cultures. Experiments involving SARS-CoV-2 were carried out in an oxygen-adjustable incubator in a biosafety level 3 (BSL3) facility. After 24 h normoxic or hypoxic incubations, THP-1 cells were infected with the SARS-CoV-2 containing virus supernatants. Supernatants of non-infected A549-AT were used as controls. Cells were washed 1 hpi with PBS, and either directly lysed for RNA isolation, or incubated for additional 5 h, before freezing debris-free supernatants at -80°C for subsequent ELISAs and lysing cells for RNA isolation. Sample inactivation for further processing was performed with previously evaluated methods (19).

2.5 Stimulation with SARS-CoV-2 spike protein

THP-1 cells were pre-incubated for 24 h under normoxia or hypoxia before 5 µg/mL recombinant SARS-CoV-2 spike trimer (S1 +S2) (BPS Bioscience, San Diego, CA, USA; cat. no. 100728) or 0.04% glycerol (Sigma-Aldrich) as vehicle control were added for additional 8 h normoxic or hypoxic incubations.

2.6 RNA isolation, reverse transcription, and quantitative polymerase chain reaction

Total RNA from THP-1 cells was extracted using either TRIzol or the RNeasy mini kit (for SARS-CoV-2 experiments; Qiagen, Hilden, Germany) according to the manufacturer's instructions. The Maxima First Strand cDNA synthesis kit was used for reverse transcription and qPCR analyses were performed using PowerUp SYBR Green Master Mix on QuantStudio 3 and 5 PCR Real-Time Systems (Thermo Fisher Scientific). Primers were ordered from Biomers (Ulm, Germany) and are listed in Supplementary Table S1, except the primer for *IRF7* (Hs_IRF7_1_SG QuantiTect Primer Assay), which was purchased from Qiagen.

2.7 Differential gene expression analysis

Previously, we characterized transcriptome-wide changes in *de novo* synthesis and RNA stability under hypoxia in monocytes by a metabolic labeling approach. Here, we focused on total mRNA changes within the previously published comprehensive metabolic RNA sequencing data of THP-1 cells incubated for 8 h and for 72 h under hypoxia (acute hypoxia (= AH) and chronic hypoxia (= CH), respectively), or under normoxia (N) (GSM5994456 to GSM5994464) (20). For differential gene expression analyses, raw reads were quality-, adapter-, and polyA-trimmed using Cutadapt (21) and unique molecular identifier and linker sequences were removed before the processed reads were aligned to the human genome (GRCh38) with Ensembl gene annotation (release 80) using STAR (version 2.7.6a) (22). Transcript counts were determined using htseq-count with default parameters (23) and Ensembl gene annotation (release 80). Differentially expressed genes were determined using DESeq2 in R (24). Log_2-transformed fold changes in genes were shrunken using the estimator "ashr". Adjusted *p*-values (*padj*) were determined using Benjamini-Hochberg correction, and differentially regulated transcripts between N, AH, and CH were visualized with ComplexHeatmaps (25). Hereto, read counts were corrected for library size using DESeq2 size factors and subjected to a row-wise *z*-score normalization. Transcripts were grouped into three groups by *k*-means clustering. For the identification of enriched functional annotation clusters, transcripts downregulated (first cluster) or upregulated (second and third clusters) by hypoxia were analyzed separately using the Database for Annotation, Visualization and Integrated Discovery (DAVID) against the gene sets "GOTERM_BP_DIRECT" and "UP_KW_BIOLOGICAL_PROCESS" (26, 27). A list of all detected transcripts (basemean > 0, for all conditions) served as background data set.

2.8 Interferome analysis

Transcripts constituting the functional annotation cluster "immune cell activation" within the hypoxic upregulated transcripts were used as input for Interferome v2.01 (28). Interferome v2.01 compared the input transcripts with a comprehensive database of collected gene expression data from different cell types after treatment with type I, II, or III IFNs. For further analyses, we used only the interferon-stimulated genes (ISGs) from all identified interferon-regulated genes (IRGs) within the "immune cell activation" cluster. The distribution of the putative type I, II, and/or III IFN targets was visualized using VennDiagram (29), and the library-size and row-wise *z*-score normalized read counts of the so-identified ISGs under N, AH, and CH were visualized with ComplexHeatmaps (25).

2.9 Immunoblots

All reagents used for immunoblotting were purchased from Sigma-Aldrich, if not indicated otherwise. THP-1 cells were resuspended in lysis buffer (10 mM Tris-HCl, 6.65 M Urea, 10% glycerol, 1% SDS (Carl Roth), pH 7.4; freshly supplemented with 1 mM DTT (Carl Roth), protease inhibitor and phosphatase inhibitor mixes (cOmplete and phosSTOP, respectively (Roche, Grenzach-Wyhlen, Germany)), and sonicated. 70 µg total protein were separated by sodium dodecylsulfate polyacrylamide gel electrophoresis and transferred onto nitrocellulose membranes (GE Healthcare, Chalfont St Giles, UK). Proteins were detected using specific antibodies for LSS (Proteintech, Planegg-Martinsried, Germany; cat. no. 13715-1-AP), β-tubulin (Abcam, Cambridge, UK; cat. no. ab7780), pSTAT1 (Tyr701; Cell Signaling, Leiden, Netherlands; cat. no. 7649S), or STAT1 (Cell Signaling; cat. no. 9172S) and appropriate IRDye secondary antibodies (LI-COR Biosciences, Bad Homburg, Germany), and visualized using the Odyssey infrared imaging system (LI-COR Biosciences).

2.10 Immunofluorescent staining

THP-1 cells were incubated for 8 h under normoxia or hypoxia and subsequently fixed with ROTI®Histofix (Carl Roth) for 10 min at 4°C. After transferring to object slides using a cytospin centrifuge, cells were permeabilized with 0.1% triton X in PBS for 10 min, followed by blocking with 10% normal goat serum (Sigma-Aldrich) with 100 mM glycine. Primary rabbit anti-SREBP2 antibody (Cayman Chemical; cat. no. 10007663) was incubated at 1:500 in 2% normal goat serum overnight at 4°C. F(ab')2 goat anti-rabbit IgG Alexa fluor™ plus 488 secondary antibody (Thermo Fisher Scientific; cat. no. A48282) was incubated at 1:500 in 2% normal goat serum for 45 min at room temperature. Cells were counterstained with 1 µg/mL 4',6-diamidino-2-phenylindole (DAPI) for 1 min. Whole slide scans were performed using Vectra Polaris (Akoya Biosciences, Marlborough, MA, USA) at 20x magnification. Image analysis was performed in QuPath v0.4.2 (30), cell detection with a 5 µm expansion was performed on annotations of the whole cytospin area. Mean nuclear intensity values per cell were generated for analysis.

2.11 ELISAs

CCL2 and CXCL10 protein levels in the supernatants of SARS-CoV-2 infected THP-1 cells were quantified using SimpleStep ELISA kits from Abcam according to the manufacturer's instructions.

2.12 Sterol measurements

THP-1 cells were incubated for up to 24 h under normoxia or hypoxia. Optionally, cells were pre-incubated with 1 µM simvastatin, 10 µM NB-598, 10 µM ketoconazole, or 0.1% DMSO for 1 h. Sterol content was determined by gas chromatography-mass spectrometry-selected ion monitoring (GC-MS-SIM) as previously described (31–33). Briefly, cell pellets were dried in a speedvac concentrator (12 mbar; Savant AES 1000) and weighed. Cholesterol and cholesterol precursors were extracted using chloroform. After alkaline hydrolysis, the concentrations of the cholesterol precursors lanosterol, 24,25-dihydrolanosterol, lathosterol, and desmosterol were measured with GC-MS-SIM in selected ion monitoring mode. The trimethylsilyl-ethers of the sterols were separated on a DB-XLB (30 m length x 0.25 mm internal diameter, 0.25 µm film) column (Agilent Technologies, Waldbronn, Germany) using the 6890N Network GC system (Agilent Technologies). Epicoprostanol (Steraloids, Newport, RI, USA) was used as an internal standard, to quantify the non-cholesterol sterols (Medical Isotopes, Pelham, NH, USA) on a 5973 Network MSD (Agilent Technologies). Total cholesterol was measured by GC-flame ionization detection on an HP 6890 GC system (Hewlett Packard, Waldbronn, Germany), equipped with a DB-XLB (30 m length x 0.25 mm internal diameter, 0.25 µm film) column (Agilent Technologies) using 5α-cholestane (Steraloids) as internal standard.

2.13 Statistical analysis

Data are reported as means ± SEM of at least three independent experiments. Statistical analyses were carried out using GraphPad Prism v9.3.1 (GraphPad Software, San Diego, CA, USA) or R v4.0.5 (34). Statistical significance was estimated either using two-tailed paired t-test, one-way or two-way repeated measures ANOVA with Holm-Šídák's multiple comparisons test as applicable. If residuals were assumed to be not normally distributed (based on quantile-quantile (Q-Q) plots), data were log-transformed before statistical testing.

3 Results

3.1 Hypoxia enhances expression of cholesterol biosynthesis enzymes and increases IFN signaling

Since hypoxia is a major contributing factor to various immune system-associated diseases, we determined RNA dynamics in human monocytic THP-1 cells in response to acute (8 h 1% O_2 = AH) and chronic (72 h 1% O_2 = CH) hypoxia (20). In line with the major regulatory impact of hypoxia, 2632 transcripts appeared differentially expressed (*padj* < 0.05, |log2FC| > 0.3) between normoxia (21% O_2 = N) and hypoxia (AH and/or CH), however, following different regulatory dynamics (Figure 1A). While 1268 targets decreased under acute and/or chronic hypoxia (first cluster), 1364 targets increased either cumulatively during hypoxic incubations (second cluster) or only in response to CH (third cluster) (Supplementary Table S2). Functionally, cell cycle and respiration emerged as top enriched annotations amongst the downregulated transcripts, whereas cholesterol metabolism and immune cell activation were enriched within the upregulated candidates (Figure 1B; Supplementary Table S2). In fact, the majority of enzymes involved in the cholesterol biosynthesis cascade were upregulated, mostly already under AH (Figures 1A, C). To obtain further insights into the dynamics of cholesterol biosynthesis gene expression under hypoxia, we determined expression of representative genes in THP-1 cells over a time course of up to 72 h of hypoxia. mRNA expression of the selected candidates *lanosterol synthase* (*LSS*) and *methylsterol monooxygenase 1* (*MSMO1*) increased after 8 h of hypoxia, reaching maximal levels at 24 - 48 h, thereafter decreasing (Figure 1D). In line, LSS protein expression increased after 24 h and remained elevated up to 72 h of hypoxia (Figure 1E).

Of note, changes in cholesterol metabolism were previously linked to altered immune responses (35), especially to interferon (IFN) signaling (12, 13). Since "immune cell activation" emerged as the second most enriched function within the differentially induced genes in hypoxic THP-1 monocytes (Figure 1B), we determined the contribution of interferon-stimulated genes (ISGs) to the hypoxia-induced immune response using the Interferome v2.01 database (28). Of note, 75% (60 of 80) of the immune activation-associated transcripts regulated under hypoxia in THP-1 cells were potential ISGs. Of these the vast majority, i.e., 60% (= 36), were proposed

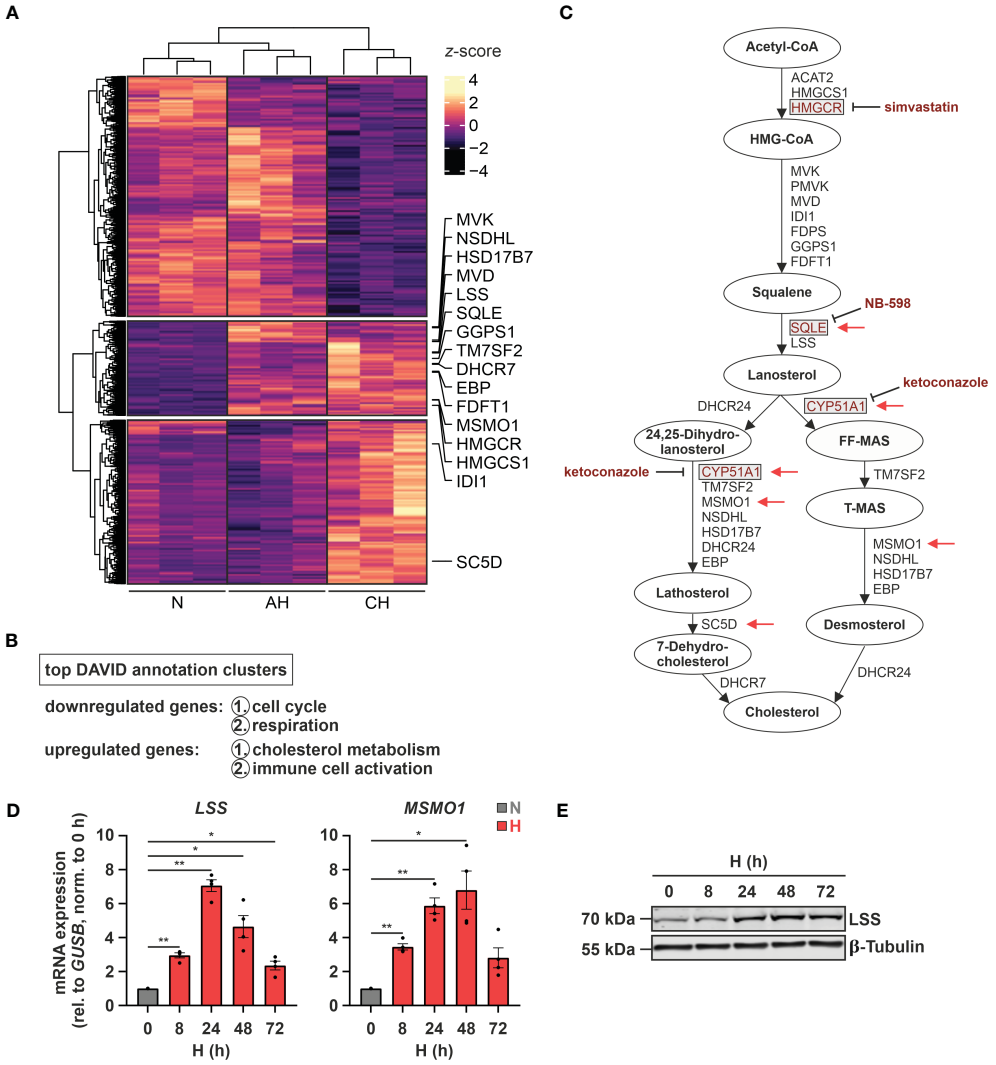

FIGURE 1
Hypoxia induces cholesterol biosynthesis enzymes. **(A)** RNA expression in THP-1 cells exposed to hypoxia (H; 1% O_2) for 8 h (acute hypoxia = AH) or 72 h (chronic hypoxia = CH) was determined relative to normoxic THP-1 cells (N; 21% O_2) by RNA-Seq (n = 3). Differentially expressed genes (*padj* < 0.05, |log2FC| > 0.3) were visualized in a heatmap (*z*-score normalized counts) and categorized by *k*-means clustering. Cholesterol biosynthesis genes are highlighted. **(B)** Top two functional annotation clusters of down- or upregulated transcripts identified by DAVID (26, 27). **(C)** Schematic representation of the cholesterol biosynthesis cascade. Oxygen-demanding steps are highlighted by red arrows and selected inhibitors as well as their target enzymes are marked in red. **(D, E)** THP-1 cells were incubated under N (grey) or H (red) for the indicated times (n = 4). **(D)** *LSS* and *MSMO1* mRNA expression was analyzed by RT-qPCR and normalized to *GUSB* expression. **(E)** LSS protein expression was determined by Western blot analysis. β-tubulin served as loading control. The blot is representative of four independent experiments. All data are means ± SEM and were statistically analyzed using one-way repeated measures ANOVA with Holm-Šídák's multiple comparisons test (*p < 0.05, **p < 0.01).

targets of both type I and II IFNs, 28% (= 17) were exclusive type II IFN targets, two exclusive type I IFN targets, and five associated with type I, II, as well as III IFNs (Figure 2A; Supplementary Table S3). Interestingly, in contrast to cholesterol biosynthesis-associated targets most ISGs (49 of 60) were predominantly induced under CH (Figure 2B; Supplementary Table S3). Refined hypoxia time course experiments validated maximal induction of *2'-5'-oligoadenylate synthetase 1* (*OAS1*), *interferon regulatory factor 7* (*IRF7*), and *interferon α-inducible protein 6* (*IFI6*) at 48 h of hypoxia, whereas *interferon β1* (*IFNB1*) was maximal after 24 h (Figure 2C). To determine whether early IFN-β induction in hypoxia might contribute to the expression of some of the ISGs increasing later on, we blocked IFN-β-receptor-dependent signaling in hypoxic THP-1 cells (24 h) using an α-interferon-α/β-receptor subunit 2 (IFNAR2) antibody (5 μg/mL). While *IFNB1* and *IRF7* expression was not influenced by IFNAR2 neutralization compared to the respective IgG2a-isotype control, *OAS1* and *IFI6* induction were markedly reduced upon IFNAR2 blockage (Figure 2D). In line with activation of type I IFN receptor signaling, the downstream effector signal transducer and activator of transcription 1 (STAT1) was phosphorylated (Tyr701) after 8 - 24h of hypoxia (Supplementary Figure 1).

Taken together, hypoxia enhances the expression of nearly all enzymes of the cholesterol biosynthesis cascade and at the same time induces a broad range of ISGs in monocytic THP-1 cells, in part by a secondary IFNAR-dependent amplification loop.

10.3389/fimmu.2023.1121864

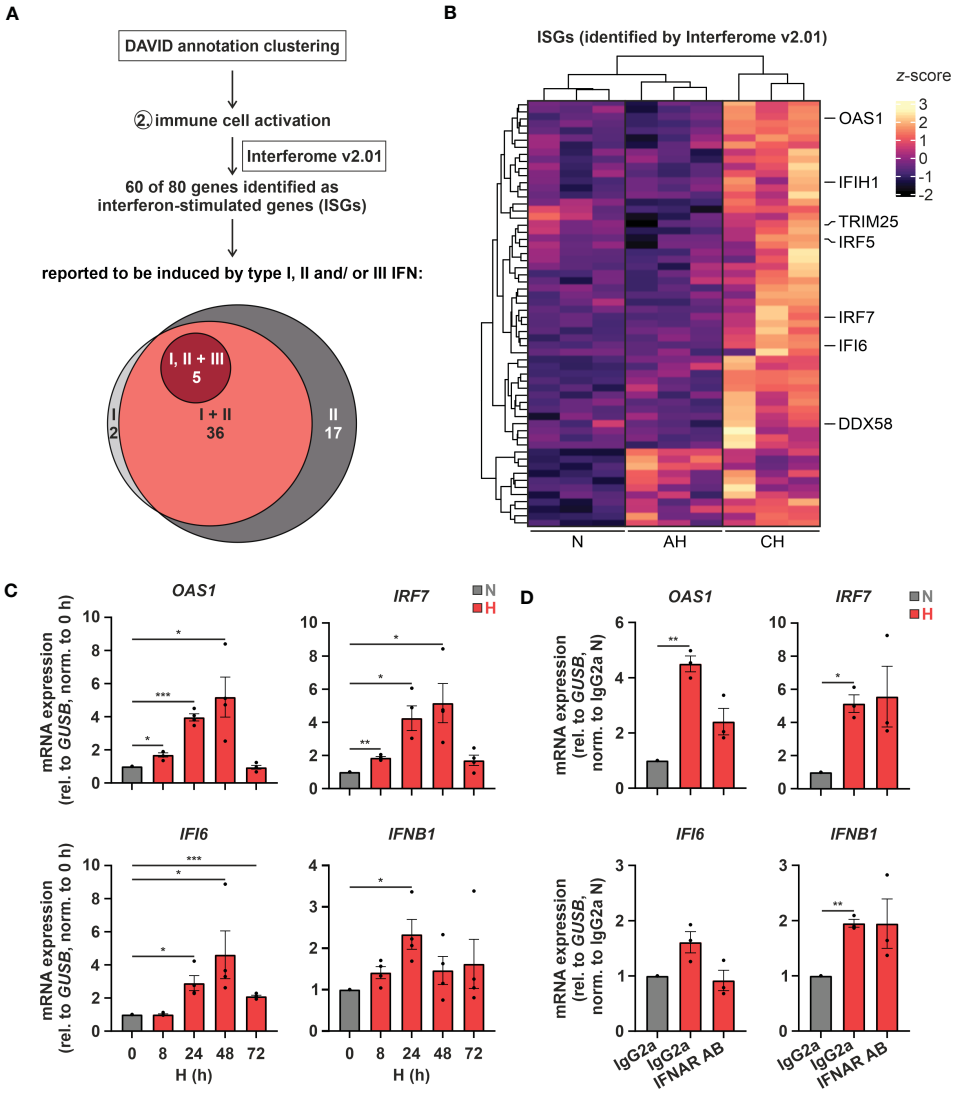

FIGURE 2
Hypoxia increases interferon (IFN) signaling. **(A)** IFN-stimulated genes (ISGs) within the transcripts constituting the functional annotation cluster "immune cell activation" were identified using Interferome v2.01 (28). Venn diagram depicts proposed ISGs regulated by type I, II, and/or III IFNs according to Interferome v2.01. **(B)** Heatmap representing differentially expressed, hypoxia-induced ISGs (*z*-score normalized count data) under normoxia (N), acute hypoxia (AH; 8 h), and chronic hypoxia (CH; 72h) (n = 3; *padj* < 0.05, |log2FC| > 0.3). Selected ISGs are highlighted. **(C)** THP-1 cells were incubated under N (grey) or H (red) for the indicated times (n = 4) or **(D)** treated with 5 µg/mL α-IFNAR2 antibody or an IgG2a-isotype control and incubated under N (grey) or H (red) for 24 h (n = 3). *OAS1, IRF7, IFI6*, and *IFNB1* mRNA expression was analyzed by RT-qPCR and normalized to *GUSB* expression. All data are means ± SEM and were statistically analyzed by one-way repeated measures ANOVA with Holm-Šídák's multiple comparisons test (*$p < 0.05$, **$p < 0.01$, ***$p < 0.001$).

3.2 Hypoxic ISG induction is not directly affected by cholesterol biosynthesis intermediates

Considering previous reports showing that a disturbance in cholesterol metabolism may increase IFN signaling (12, 13), we asked whether changes in cholesterol metabolism might also contribute to ISG induction under hypoxia. To this end, we initially measured sterol levels in THP-1 cells in the course of hypoxia. In accordance with several oxygen-demanding steps within the cholesterol biosynthesis cascade (Figure 1C, red arrows), lathosterol and desmosterol, i.e., sterol intermediates downstream of the major oxygen-demanding reactions, were reduced, while the early cholesterol precursors lanosterol and 24,25-dihydrolanosterol markedly accumulated under hypoxia (Figure 3A; Supplementary Figure 2). Levels of total cholesterol appeared to be only minimally attenuated by reduced oxygen, though at much higher total amounts than the other sterols. Noteworthy, while changes in lanosterol and lathosterol were almost maximal already at 4 h of hypoxia (Figure 3A), expression of cholesterol biosynthesis enzymes as well as of ISGs remained unaltered at this early time point (Supplementary Figure 3), suggesting that changes in cholesterol metabolites might contribute to the observed gene expression changes. To prevent or mimic hypoxic accumulation of lanosterol and 24,25-dihydrolanosterol, we next pre-treated THP-1 cells with either the

10.3389/fimmu.2023.1121864

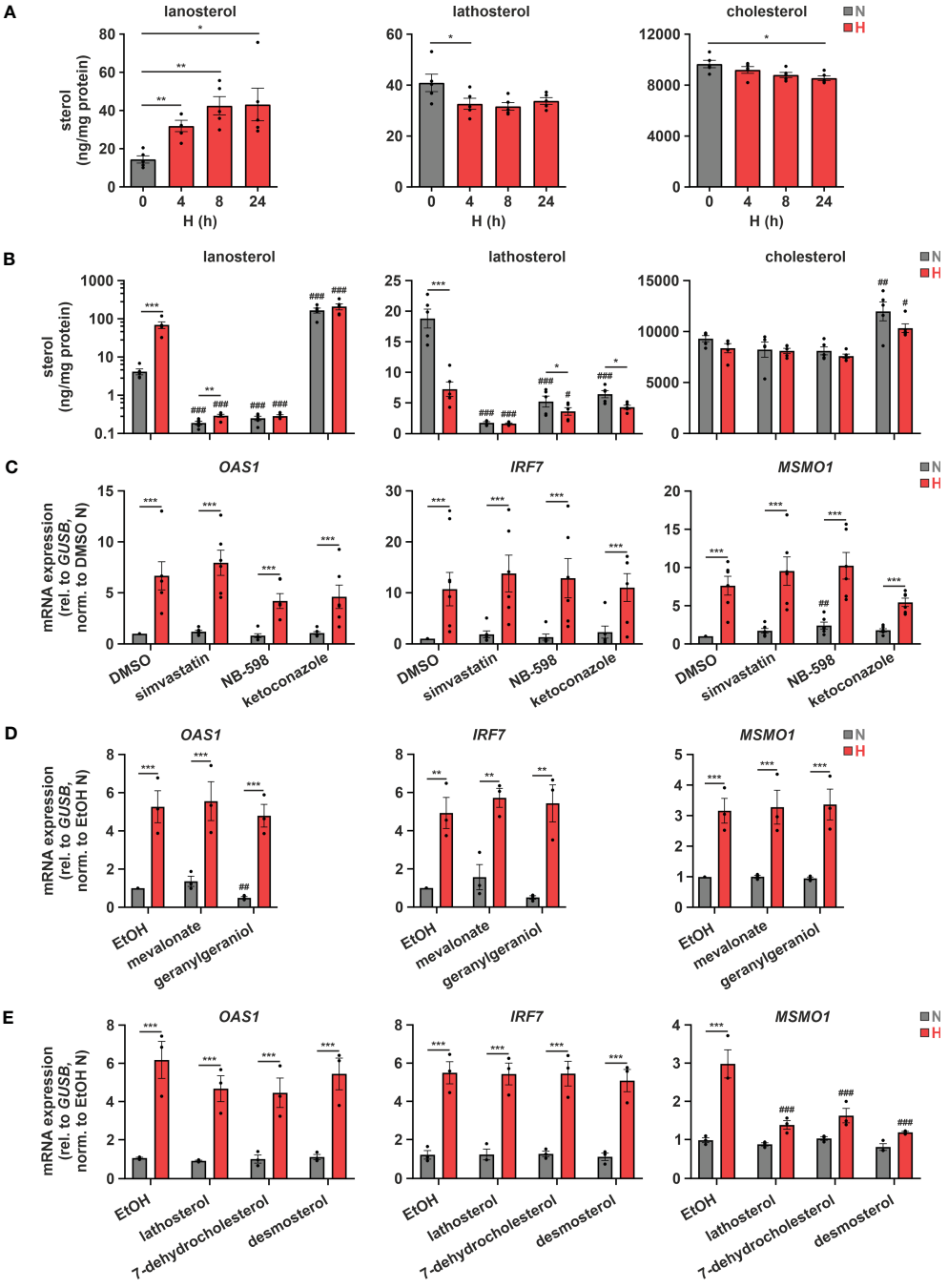

FIGURE 3
Hypoxic ISG induction is not directly affected by cholesterol biosynthesis intermediates. **(A)** THP-1 cells were incubated under N (grey) or H (red) for the indicated times (n = 5). Sterol levels were measured by GC-MS. **(B, C)** THP-1 cells were pre-incubated for 1 h with 1 μM simvastatin, 10 μM NB-598, 10 μM ketoconazole, or DMSO, prior to incubation under N (grey) or H (red) for 24 h (n = 5). **(B)** Cellular sterol levels were measured by GC-MS. **(C)** *OAS1*, *IRF7*, and *MSMO1* mRNA expression was analyzed by RT-qPCR and normalized to *GUSB* expression. **(D, E)** THP-1 cells were pre-incubated for 1 h with **(D)** the early cholesterol precursors mevalonate (300 μM) or geranylgeraniol (15 μM) (n = 3), **(E)** the late cholesterol precursors lathosterol, 7-dehydrocholesterol, or desmosterol (each 5 μM) (n = 3), or appropriate solvent controls, prior to incubation under N (grey) or H (red) for 24 h. *OAS1*, *IRF7*, and *MSMO1* mRNA expression was analyzed by RT-qPCR and normalized to *GUSB* expression. All data are means ± SEM and were statistically analyzed using one-way repeated measures ANOVA with Holm-Šídák's multiple comparisons test **(A)**, or two-way repeated measures ANOVA with Holm-Šídák's multiple comparisons test **(B–E)** (*$p < 0.05$, **$p < 0.01$, ***$p < 0.001$; #$p < 0.05$, ##$p < 0.01$, ###$p < 0.001$ (compared to respective solvent controls)).

3-hydroxy-3-methylglutaryl-CoA reductase (HMGCR) inhibitor simvastatin (1 μM), the squalene epoxidase (SQLE) inhibitor NB-598 (10 μM), or the cytochrome P450 51A1 (CYP51A1, lanosterol 14α-demethylase) inhibitor ketoconazole (10 μM) for 1 h before incubating them for 24 h under normoxia or hypoxia (see Figure 1C for interventions). Inhibition of HMGCR and SQLE significantly reduced lanosterol and lathosterol levels already under normoxia and prevented hypoxia-mediated accumulation of lanosterol (Figure 3B). As expected, inhibition of the lanosterol/24,25-dihydrolanosterol-metabolizing enzyme CYP51A1 reduced the

late intermediate lathosterol, while it massively increased lanosterol under normoxia, even overruling the hypoxia-induced increase. As observed under hypoxia, cholesterol levels displayed only slight changes in response HMGCR and SQLE inhibition, but surprisingly increase markedly upon ketoconazole treatment. Despite pronounced changes in sterol *de novo* synthesis, all three inhibitors only minimally affected *MSMO1* levels under normoxia and did not alter its hypoxic induction (Figure 3C). These findings suggest that total cholesterol levels are an imprecise measure to predict changes in intracellular cholesterol dynamics. Similarly, *OAS1* and *IRF7*, i.e., IFNAR-dependent and -independent ISGs, respectively, remained unaffected by the three inhibitors under normoxia and hypoxia, indicating that accumulation of early cholesterol precursors did not contribute to hypoxic ISG induction. To determine if cholesterol biosynthesis intermediates might still be involved in hypoxic ISG induction, we supplemented THP-1 cells with early (mevalonate (300 μM), geranylgeraniol (15 μM)) or late cholesterol precursors (lathosterol, 7-dehydrocholesterol, desmosterol (5 μM each)) prior to 24 h of hypoxia. Corroborating the observation that cholesterol biosynthesis inhibitors did not alter hypoxic ISG induction, supplementation of neither early nor late cholesterol precursors substantially attenuated the hypoxia-mediated increase in *OAS1* and *IRF7* expression (Figures 3D, E). In line with the oxygen requirements for cholesterol biosynthesis, early cholesterol intermediates did not affect hypoxic *MSMO1* induction (Figure 3D), while late intermediates almost completely prevented the hypoxic increase in *MSMO1* expression (Figure 3E).

Subcellular changes in cholesterol concentrations provide a rheostat to control the activities of the transcription factors sterol regulatory element-binding protein 2 (SREBP2), which is activated after sterol depletion at the endoplasmic reticulum (ER) to enhance cholesterol biosynthesis and uptake (36), and liver X receptor (LXR), which is activated by desmosterol or oxysterols to reduce cholesterol uptake and enhance cholesterol export (Figure 4A) (37). First, we addressed the involvement of SREBP2, the master regulator of the enzymes involved in cholesterol biosynthesis, in the hypoxic induction of the cholesterol biosynthesis enzymes. Indeed, after 8 h of hypoxia nuclear SREBP2 levels, reflecting active SREBP2, were increased (Figure 4B). Furthermore, pre-incubation of THP-1 cells with the established SREBP2 inhibitors PF-429242 (1 μM) or fatostatin (10 μM) effectively blocked hypoxic *MSMO1* induction (Figures 4C, D). While SREBP2 was previously described to directly bind and activate IFN response genes (38), and inhibition of SREBP2 cleavage and release from the Golgi with the S1P (site 1 protease) inhibitor PF-429242 completely blocked SREBP2 target expression even under normoxia, it did not affect hypoxic *OAS1* and *IRF7* induction (Figure 4C). In contrast, inhibition of SREBP2 activation with fatostatin (10 μM), which selectively blocked the hypoxic increase in *MSMO1* expression, also attenuated the hypoxic ISG expression (Figure 4D). To further test if cholesterol homeostasis changes might affect ISG expression, we incubated THP-1 cells with the LXR agonist T0901317 (1 μM). In line with reduced cholesterol biosynthesis and desmosterol levels, expression of the cholesterol exporter *ATP binding cassette subfamily A member 1* (*ABCA1*), a proto-typical LXR target, was reduced under hypoxia (Supplementary Figure 4). Interestingly, small molecule-based activation of LXR significantly increased the hypoxic ISG induction (Figure 4E).

Conclusively, our data indicate that while the hypoxic ISG induction in monocytes is not directly affected by changes in cholesterol biosynthetic flux, modulation of subcellular cholesterol dynamics might contribute to the enhanced ISG expression under hypoxia.

3.3 Intracellular cholesterol distribution determines hypoxic chemokine ISG induction

As altering ER-to-Golgi dynamics with fatostatin or cholesterol import/export processes via LXR activation both impacted hypoxic ISG induction, we aimed to gain further insights into the potential relevance of subcellular cholesterol dynamics. Since cellular cholesterol homeostasis relies on a tightly regulated interplay between cholesterol uptake, *de novo* synthesis, transport between different compartments, and eventually export (Figure 5A), we next addressed ISG induction under conditions when extracellular cholesterol resources are limited. Therefore, we reduced the availability of exogenous cholesterol by lowering the amount of fetal bovine serum (FBS) in the medium. Reduced exogenous cholesterol availability enhanced *OAS1* and *IRF7* expression under normoxia and hypoxia to a similar extend (Figure 5B). In contrast, low FBS exclusively enhanced the hypoxic expression of the well-characterized chemokine ISGs *CC motif chemokine ligand 2* (*CCL2*) and *CXC motif chemokine ligand 10* (*CXCL10*), which were previously shown to be induced upon cholesterol disturbances (12). To assess if the ISG-inducing effects of low FBS might indeed be due to decreased uptake of cholesterol, we used the Niemann-Pick C1 protein (NPC1) inhibitor U18666A, which prevents redistribution of LDL-derived cholesterol from lysosomes to cellular organelles such as ER and mitochondria, but also to the plasma membrane (Figure 5A). Strikingly, while hypoxic *OAS1* and *IRF7* induction remained unaltered by NPC1 inhibition at high FBS, their serum depletion-dependent increase under hypoxia was prevented (Figure 5B). In contrast, *CXCL10* induction by both FBS reduction and/or hypoxia remained largely unaffected, and *CCL2* even increased upon NPC1 inhibition under both normoxia and hypoxia, which was further enhanced when combined with FBS depletion. The differential responses of the ISGs to low serum and/or NPC1 inhibition point towards a complex, cholesterol-associated regulatory network, specific for each ISG. Therefore, we next tested if supplementation of THP-1 cells with methyl-β-cyclodextrin (MβCD)-complexed cholesterol under low serum conditions might affect hypoxic ISG expression patterns. While cholesterol supplementation did not affect *OAS1* and *IRF7* expression at all, it enhanced *CCL2* and *CXCL10* expression predominantly under normoxia (Figure 5C). Consequently, the hypoxic induction of chemokine ISGs in serum reduced conditions appeared to be attenuated by cholesterol addition. Not surprisingly, cholesterol supplementation massively reduced both normoxic and hypoxic *MSMO1* expression. Moreover, forced cholesterol loading of THP-1 cells with MβCD-cholesterol under low serum conditions overruled

10.3389/fimmu.2023.1121864

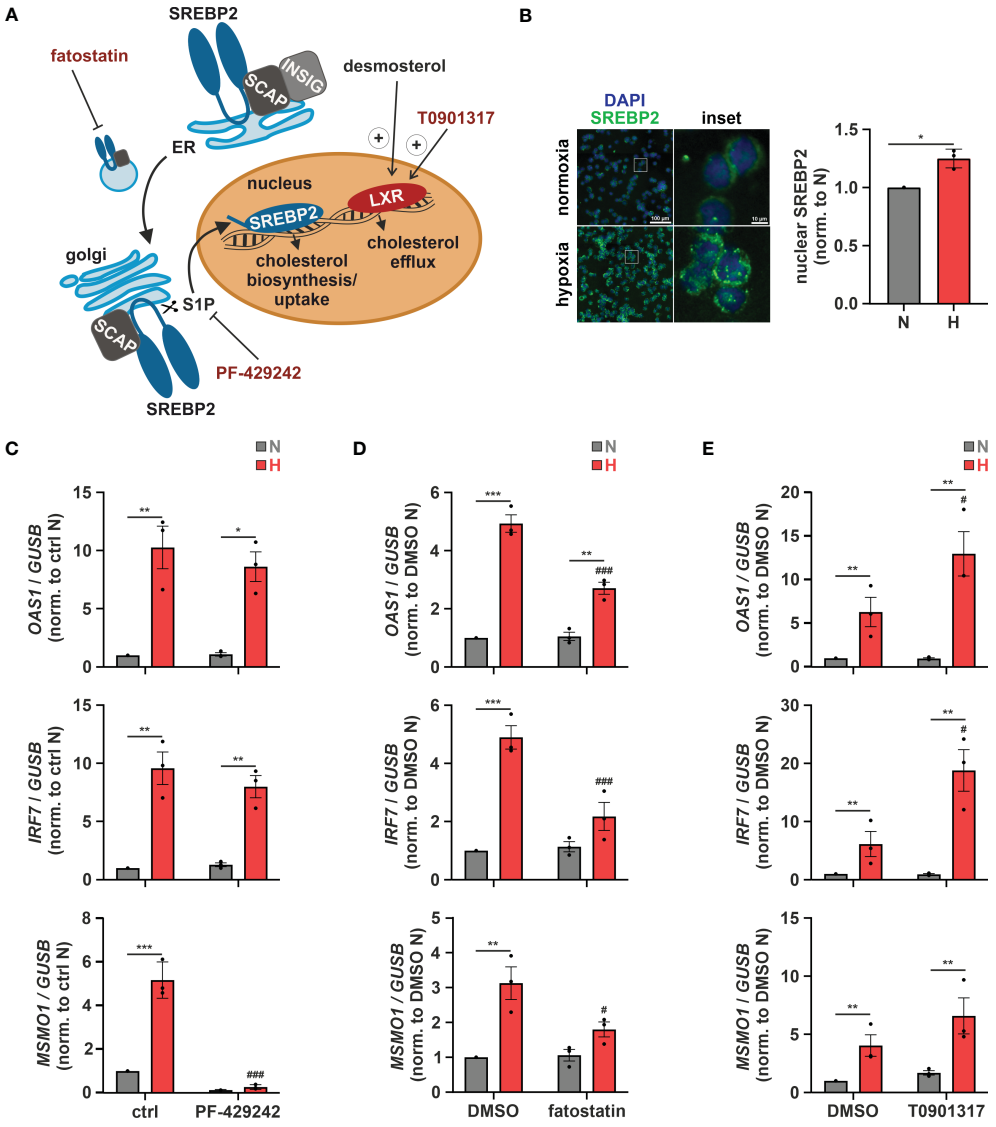

FIGURE 4
Altered cholesterol homeostasis affects hypoxic ISG induction. **(A)** Overview of the mechanisms of activation of the cholesterol-associated transcription factors LXR and SREBP2. The LXR agonist T0901317 as well as the SREBP2 inhibitors PF-429242 and fatostatin are highlighted in red. **(B)** THP-1 cells were incubated under N (grey) or H (red) for 8 h (n = 3). Immunofluorescence staining for SREBP2 (green) was performed. Nuclei were counterstained with DAPI (blue). Mean fluorescence intensity was quantified for nuclear SREBP2. Images are representative of three independent experiments. **(C–E)** THP-1 cells were pre-incubated for 1 h with **(C)** 1 μM PF-429242, **(D)** 10 μM fatostatin, **(E)** 1 μM T0901317, or appropriate solvent controls, prior to incubation under N (grey) or H (red) for 24 h (n = 3). *OAS1*, *IRF7*, and *MSMO1* mRNA expression was analyzed by RT-qPCR and normalized to *GUSB* expression. Data are means ± SEM and were statistically analyzed using two-tailed paired t-test **(B)**, or two-way repeated measures ANOVA with Holm-Šídák's multiple comparisons test **(C–E)** (*$p < 0.05$, **$p < 0.01$, ***$p < 0.001$; #$p < 0.05$, ###$p < 0.001$ (compared to ctrl or DMSO, respectively)).

the changes elicited by the NPC1 inhibitor for all ISGs as well as for *MSMO1* (Figure 5C). These findings underscore the notion that the impact of intracellular cholesterol dynamics on the expression of ISGs in the context of hypoxia is extremely versatile.

Functionally, interferon-associated immune responses are of special interest when considering virus infections. The β-coronavirus SARS-CoV-2 was first detected in 2019 and described to be the causative agent of a novel lung disease named COVID-19, in which severe clinical manifestations are caused by dysregulated host immune responses (39–41). As COVID-19 is a respiratory disease, which, in severe cases leads to hypoxemia, i.e., low blood oxygen levels, we wondered if hypoxia might influence SARS-CoV-2 infections. Therefore, we incubated THP-1 cells for 24 h under normoxia or hypoxia before adding infectious SARS-CoV-2 (strain FFM1) (18) for 1 h under low serum conditions. Due to technical considerations, all infections had to be carried out under normoxia. Of note, primary monocytes were previously shown to express only low levels of the main SARS-CoV-2 receptor angiotensin-converting enzyme 2 (ACE2) and its associated transmembrane serine protease 2 (TMPRSS2) (42). Despite the fact that THP-1 monocytes only minimally express ACE2, they were substantially infected with SARS-CoV-2 as indicated by the expression of viral *M*

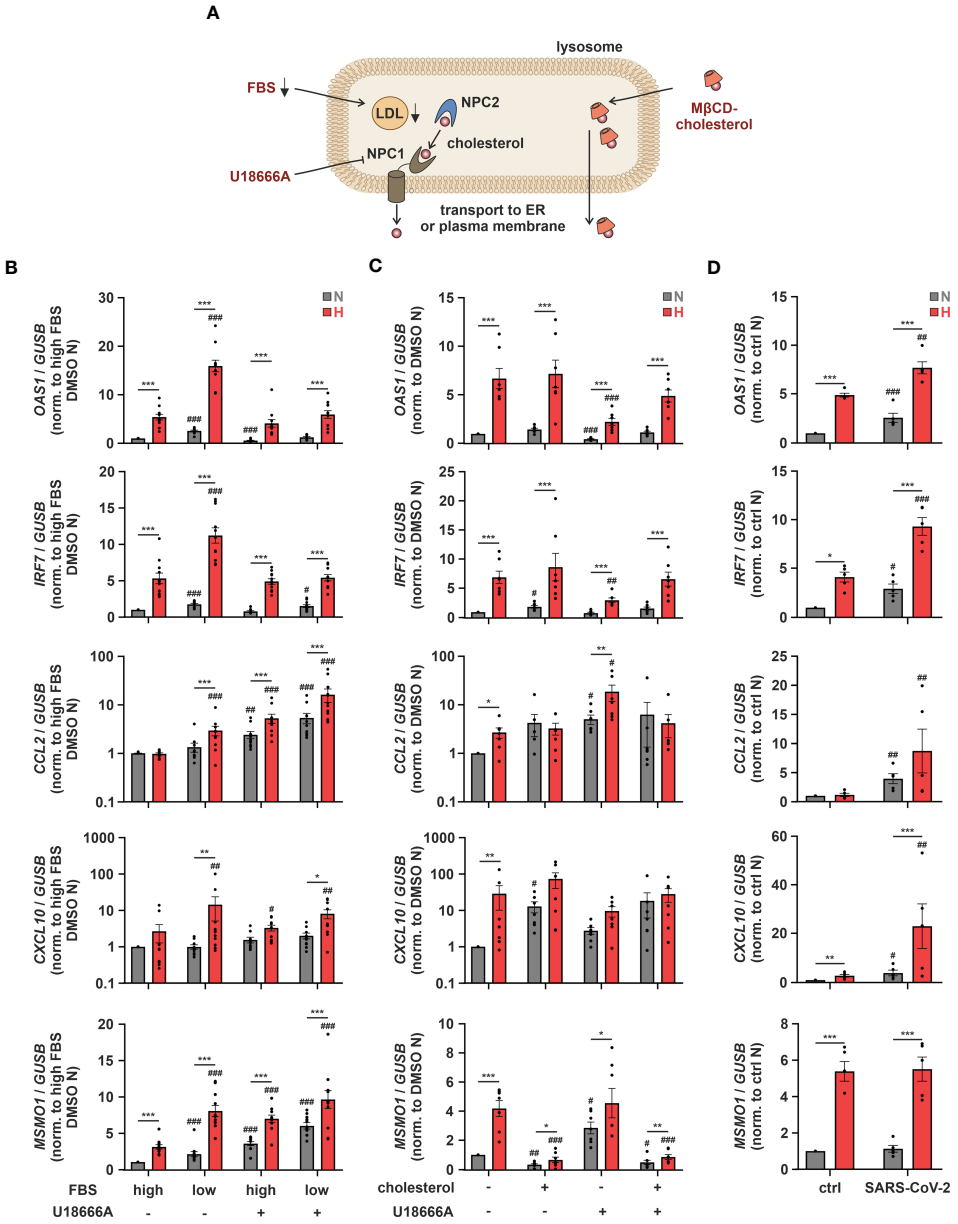

FIGURE 5
Intracellular cholesterol distribution determines hypoxic chemokine ISG induction. **(A)** Overview of the lysosomal cholesterol distribution machinery. Relevant interventions are indicated in red. **(B)** THP-1 cells were pre-incubated for 1 h with 5 µM U18666A or DMSO in medium containing high or low levels of FBS prior to incubation under N (grey) or H (red) for 24 h (n = 11). **(C)** THP-1 cells were pre-incubated for 1 h with 5 µM U18666A or DMSO in medium containing low levels of FBS ± 0.25 mg/mL methyl-β-cyclodextrin-complexed cholesterol prior to incubation under N (grey) or H (red) for 24 h (n = 7). **(D)** THP-1 cells were incubated under N (grey) or H (red) for 24 h in medium containing low levels of FBS prior to infection with SARS-CoV-2 (strain FFM1) under N. RNA was isolated 1 hour post infection (n = 5). *OAS1*, *IRF7*, *CCL2*, *CXCL10*, and *MSMO1* mRNA expression was analyzed by RT-qPCR and normalized to *GUSB* expression. All data are means ± SEM and were statistically analyzed using two-way repeated measures ANOVA with Holm-Šídák's multiple comparisons test (*p < 0.05, **p < 0.01, ***p < 0.001; #p < 0.05, ##p < 0.01, ###p < 0.001 (compared to to FBS high/DMSO **(B)**, FBS low/DMSO **(C)**, or FBS low/ctrl **(D)**, respectively)).

gene (C_t = 24.10 ± 0.96), yet hypoxic priming only slightly increased virus abundance (Supplementary Figure 5). The infection of THP-1 cells was not productive, though, as no active replication of the virus (subgenomic RNA4 encoding E gene) was observed. In line with previous reports suggesting mild interferon responses to SARS-CoV-2 infections (43), *OAS1* and *IRF7* were only slightly elevated in THP-1 cells after infection with SARS-CoV-2 under normoxia and hypoxia. Remarkably, *CCL2* and *CXCL10*, both of which are increased in patients developing a systemic inflammatory response syndrome following SARS-CoV-2 infections (44), showed a strong hypoxic induction upon subsequent infection with SARS-CoV-2 (Figure 5D).

Taken together, our data show that cholesterol homeostasis impinges on diverse mechanisms regulating various sub-groups of ISGs under conditions of low oxygen tensions. Of note, hypoxic elevation of chemokine ISGs, which were massively enhanced upon

concomitant SARS-CoV-2 infection, appeared to be extremely sensitive to extracellular cholesterol availability and the distribution thereof.

3.4 TLR4 signaling contributes to hypoxic ISG induction

As hypoxia-enhanced chemokine production in response to SARS-CoV-2 infection might be of major relevance with respect to COVID-19-related systemic inflammation, we further characterized the underlying regulatory principles. We next aimed to determine potentially involved pattern recognition receptors (PRRs). To this end, we first used THP-1 cells deficient for mitochondrial antiviral signaling protein (MAVS) (16), which integrates activity of retinoic acid-inducible gene I (RIG-1) and melanoma differentiation-associated protein 5 (MDA5) (45), or for stimulator of interferon response cGAMP interactor (STING) (16), which is activated by cyclic GMP-AMP synthase (cGAS) (46). In line with the complex, ISG-specific regulation, hypoxic *OAS1*, *IRF7*, and *CXCL10* induction under low serum conditions was lower in MAVS-deficient cells than in STING-knockout (KO) or the corresponding wildtype (WT) THP-1 cells, while hypoxic *CCL2* induction remained unaltered (Supplementary Figure 6). Since neither the cGAS/STING nor the RIG-1/MDA5/MAVS axis appeared sufficient for the hypoxic chemokine ISG induction, we asked if toll-like receptors (TLRs) might be involved as well, since they have been shown to not only regulate classical pro-inflammatory cytokines, but also ISGs (Figure 6A) (47). Of the 10 known TLRs, *TLR1*, *TLR2*, *TLR4*, and *TLR9* were most abundant, *TLR5*, *TLR6*, and *TLR7* were expressed at intermediate levels, whereas *TLR3*, *TLR8*, and *TLR10* appeared not to be expressed at all in THP-1 cells (Supplementary Figure 7A). While *TLR2* and *TLR5* expression did not change in response to hypoxia and/or serum deprivation, expression of *TLR1*, *TLR6*, *TLR7*, and *TLR9* was enhanced by hypoxia and further increased upon serum depletion (Figure 6B; Supplementary Figure 7B), as observed for *OAS1*, *IRF7*, and *CXCL10* (Figure 5B). Interestingly, similar to *CCL2* (Figure 5B), *TLR4* was only elevated under hypoxia at low FBS concentrations (Figure 6B). To test a general involvement of TLRs in the hypoxic ISG induction, we inhibited myeloid differentiation primary response 88 (MyD88), the intracellular signal transduction adapter for most TLRs, using TJ-M2010-5 (10 μM) (Figure 6A). MyD88 inhibition reduced hypoxic induction of *OAS1* and *IRF7* more efficiently under low serum conditions and completely abrogated hypoxia-induced chemokine ISG expression (Figure 6C). While TLR-mediated activation of MyD88/inhibitors of nuclear factor kappa B (NF-κB) kinase α/β (IKKα/β)/NF-κB signaling is well established to drive pro-inflammatory cytokine expression, TLR-dependent ISG induction commonly relies on the TIR-domain containing adaptor-inducing interferon-β (TRIF)/TANK-binding kinase 1 (TBK1)/IKKε/IRF axis (48). To shed further light on the involved signaling cascade, we inhibited TBK1 using BX-795 (0.5 μM) or canonical IKKs using IKK-16 (0.1 μM), both of which known to be critical for TLR-dependent activation of ISGs (49). While both TBK1 and IKK inhibition significantly reduced hypoxic induction of *OAS1* and *IRF7*, *MSMO1* expression was not altered (Figure 6D). Moreover, the prominent hypoxic induction of the chemokine ISGs *CCL2* and *CXCL10* under low serum conditions remained largely unaffected by TBK1 inhibition, whereas IKK inhibition appeared to efficiently reduce *CXCL10* induction, yet leaving *CCL2* unaltered. These findings not only suggest that MyD88- rather than TRIF-dependent signaling underlies the hypoxic chemokine ISG induction, but again underscore the complexity of mechanisms contributing to the hypoxic elevation of the different ISGs.

Since TLR7 and 8 are activated by single stranded RNA viruses such as SARS-CoV-2, and TLR4 has recently been proposed to be activated by SARS-CoV-2 as well (50), we next asked, if they might be also involved in the hypoxic ISG induction. To this end, we used the selective TLR4 inhibitor TAK-242 (10 μM) or the TLR7/8 inhibitor enpatoran (0.1 μM). While enpatoran efficiently blocked ISG expression induced by the specific TLR7/8 agonist resiquimod (R848) (Supplementary Figure 8), it did not affect hypoxic induction of any of the tested ISGs irrespective of the serum conditions (Figure 6E). In contrast, TLR4 inhibition not only prevented the low serum-dependent increase of the hypoxic *OAS1* and *IRF7* induction, it further blocked chemokine ISG expression altogether. As a side note, reduced hypoxic *MSMO1* induction after TLR4 or MyD88 inhibition corroborated the bidirectionality between IFN signaling and cholesterol metabolism (14).

In summary, TLR4-dependent signaling appears of major importance for the cholesterol dynamic-associated, hypoxic induction of ISGs in monocytes. Herein, chemokine ISGs, such as *CCL2* and *CXCL10*, displayed the strongest addiction to intact TLR4/MyD88 signaling. Moreover, owing to the hypoxic upregulation of various TLRs, a general sensitization of TLR signaling under hypoxia might be predicted.

3.5 Hypoxic priming increases the production of chemokine ISGs after SARS-CoV-2 infection via TLR4 activation

Since TLR4 contributed to hypoxic ISG induction and relevant ISGs increased after SARS-CoV-2 infection in monocytic THP-1 cells, and further taking into account that a direct binding and activation of TLR4 by SARS-CoV-2 spike protein was recently proposed (50), we wondered if SARS-CoV-2 spike protein alone might induce the hypoxic phenotype. Therefore, we pre-incubated THP-1 cells in serum-reduced conditions under either normoxia or hypoxia for 24 h, and continued incubations for additional 8 h in the presence or absence of SARS-CoV-2 spike protein (5 μg/mL). While expression of *OAS1* and *IRF7* only minimally increased in the presence of SARS-CoV-2 spike protein, *CCL2* and *CXCL10*, i.e., chemokine ISGs associated with severe cases of SARS-CoV-2 infections, robustly increased (Figure 7A). This became evident already under normoxia and was further enhanced under hypoxia. Inhibition of TLR4 with TAK-242 (10 μM) drastically diminished hypoxia- and SARS-CoV-2 spike protein-induced *CCL2* and *CXCL10* expression and also attenuated hypoxic induction of *OAS1* and *IRF7*. Of note, fatostatin (10 μM) diminished hypoxia-

10.3389/fimmu.2023.1121864

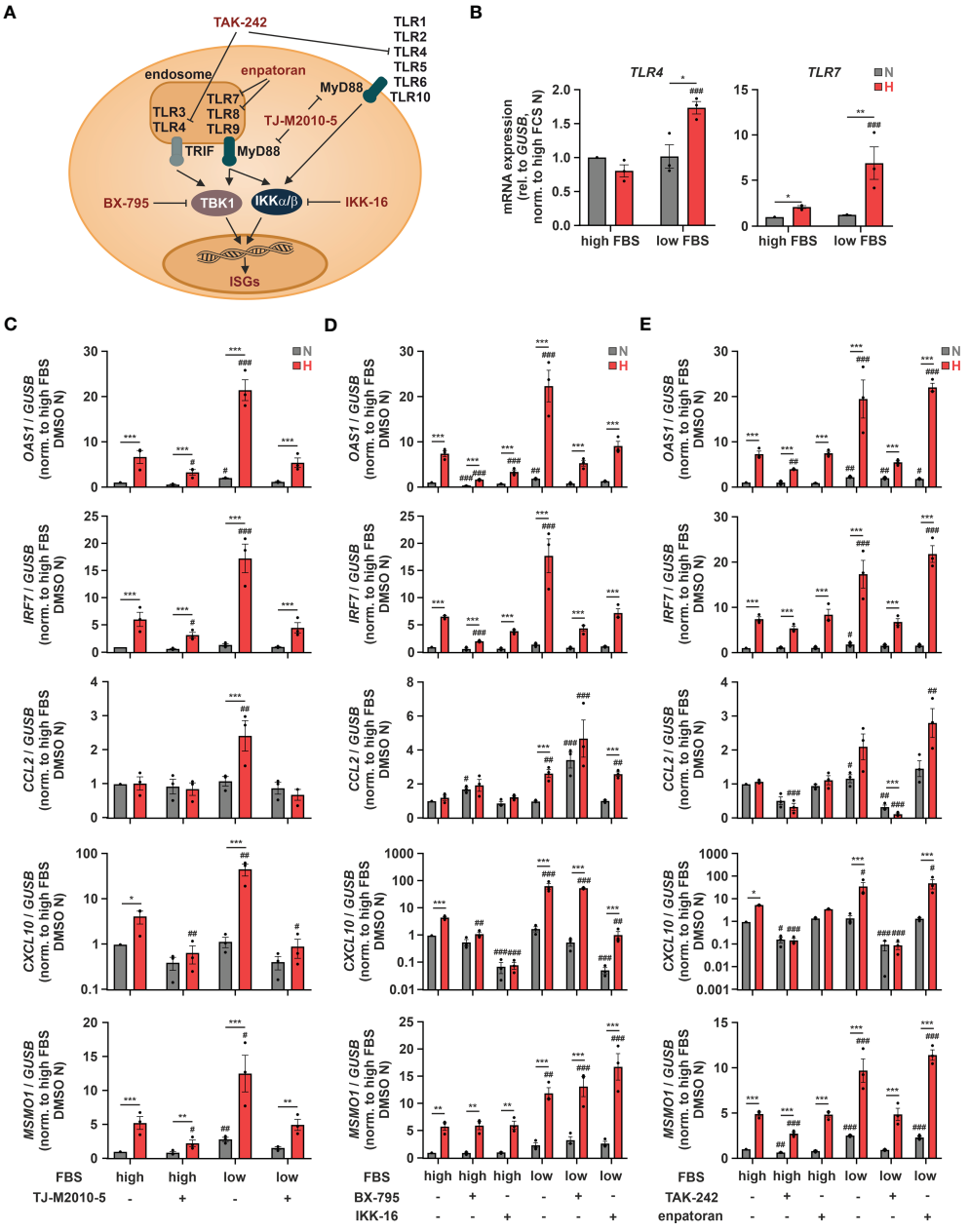

FIGURE 6
TLR4 signaling contributes to hypoxic ISG induction. **(A)** Overview of toll-like receptors (TLRs), adaptor proteins, and kinases regulating ISG induction. Relevant inhibitors are highlighted in red. **(B)** THP-1 cells were incubated under N (grey) or H (red) for 24 h in medium containing high or low levels of FBS (n = 3). *TLR4* and *TLR7* mRNA expression was analyzed by RT-qPCR and normalized to *GUSB* expression. **(C–E)** THP-1 cells were pre-incubated for 1 h with **(C)** 10 μM TJ-M2010-5 (MyD88 inhibitor), **(D)** 0.5 μM BX-795 (TBK1/IKKε inhibitor), 0.1 μM IKK-16 (IKKα/β inhibitor), **(E)** 10 μM TAK-242 (TLR4 inhibitor), 0.1 μM enpatoran (TLR7/8 inhibitor), or DMSO in medium containing high or low levels of FBS prior to incubation under N (grey) or H (red) for 24 h (n = 3). *OAS1*, *IRF7*, *CCL2*, *CXCL10*, and *MSMO1* mRNA expression was analyzed by RT-qPCR and normalized to *GUSB* expression. All data are means ± SEM and were statistically analyzed using two-way repeated measures ANOVA with Holm-Šídák's multiple comparisons test (*$p < 0.05$, **$p < 0.01$, ***$p < 0.001$; #$p < 0.05$, ##$p < 0.01$, ###$p < 0.001$ (compared to to FBS high **(B)** or FBS high/DMSO **(C–E)**, respectively)).

enhanced expression of ISGs and *MSMO1* also in the context of stimulation with SARS-CoV-2 spike protein. Having established that SARS-CoV-2 spike protein induces comparable ISG responses in THP-1 monocytes as the infectious virus and enhances chemokine ISG expression in response to hypoxia, we reached out to determine if TLR4 and cholesterol dynamics are also involved in interferon-associated immune responses in monocytic THP-1 cells upon infection with SARS-CoV-2 in a hypoxic environment. To this end, we primed THP-1 cells for 24 h under hypoxia prior to infecting them with SARS-CoV-2 (FFM1 strain) for 6 h under normoxia. Owing to the reoxygenation, expression of the SREBP2 target *MSMO1* was not elevated in hypoxia-primed THP-1 cells after infection (Figure 7B). In contrast to the spike protein, SARS-CoV-2 infection induced *OAS1* and *IRF7* expression already under normoxic conditions, still showing a slight enhancement by hypoxic priming. *CCL2* and *CXCL10* mRNA levels on the other hand were

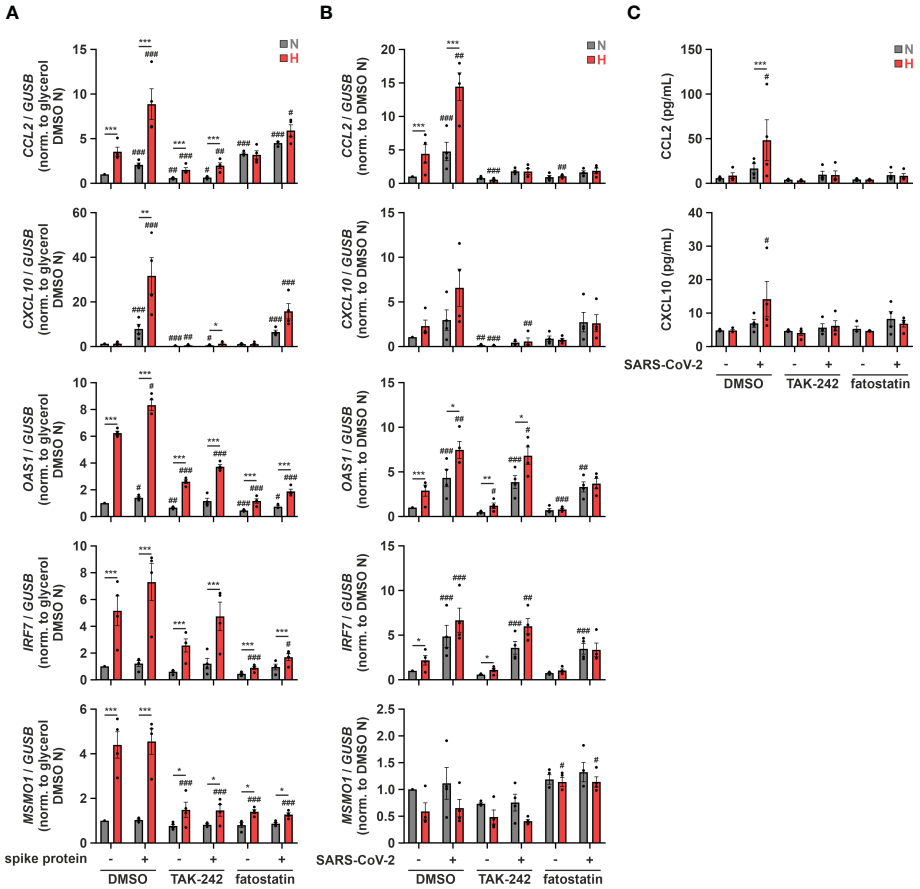

FIGURE 7
Hypoxic priming increases production of chemokine ISGs after SARS-CoV-2 infection via TLR4 activation. **(A)** THP-1 cells were pre-incubated for 1 h with 10 µM TAK-242, 10 µM fatostatin, or DMSO in medium containing low levels of FBS prior to incubation under N (grey) or H (red) for 32 h 5 µg/mL SARS-CoV-2 spike protein or glycerol were added for the last 8 h (n = 4). *CCL2*, *CXCL10*, *OAS1*, *IRF7*, and *MSMO1* mRNA expression was analyzed by RT-qPCR and normalized to *GUSB* expression. **(B, C)** THP-1 cells were pre-incubated for 1 h with 10 µM TAK-242, 10 µM fatostatin, or DMSO in medium containing low levels of FBS prior to incubation under N (grey) or H (red) for 24 h Subsequently, cells were infected with SARS-CoV-2 (strain FFM1) under N (n = 4). **(B)** RNA was isolated 6 hours post infection. *CCL2*, *CXCL10*, *OAS1*, *IRF7*, and *MSMO1* mRNA expression was analyzed by RT-qPCR and normalized to *GUSB* expression. **(C)** Secreted CCL2 and CXCL10 protein levels were determined by ELISA in supernatants 6 hours post infection. All data are means ± SEM and were statistically analyzed using two-way repeated measures ANOVA with Holm-Šídák's multiple comparisons test (*$p < 0.05$, **$p < 0.01$, ***$p < 0.001$; #$p < 0.05$, ##$p < 0.01$, ###$p < 0.001$ (compared to to FBS low/DMSO)).

comparable in cells infected with SARS-CoV-2 or treated with spike protein only, displaying a marked increase after hypoxic priming. Interestingly, whereas TLR4 inhibition (TAK-242, 10 µM) did not alter enhanced *OAS1* and *IRF7* expression in response to hypoxic priming and SARS-CoV-2 infection, it completely abolished the expression of chemokine ISGs *CCL2* and *CXCL10* (Figure 7B), despite the fact that the infection rate was not affected (Supplementary Figure 9). Interfering with intracellular cholesterol dynamics using fatostatin (10 µM) selectively prevented the hypoxia-evoked increase of the ISGs, irrespective of the presence or absence of SARS-CoV-2, without affecting the virus infection rate (Figure 7B; Supplementary Figure 9). To validate the functional relevance of chemokine ISG expression changes in the context of SARS-CoV-2 infection of monocytic cells under conditions of reduced oxygen availability, we finally determined protein amounts of CCL2 and CXCL10 in the supernatants of THP-1 cells. In line with mRNA expression changes, hypoxia markedly enhanced secretion of CCL2 and CXCL10 upon infection with SARS-CoV-2 (Figure 7C). Hypoxic induction again was completely abolished when either TLR4 or SCAP-associated trafficking were inhibited.

Our data suggest that hypoxia increases expression of chemokine ISGs in monocytic THP-1 cells upon infection with SARS-CoV-2 by enhancing spike protein-mediated TLR4 signaling. Severe cases of COVID-19 are characterized by hypoxemia, implying that monocytes regularly encounter hypoxic conditions. Our findings therefore provide a concept of how hypoxia might prime monocytes for TLR4-dependent chemokine ISG production in response to SARS-CoV-2 infection, thus potentially contributing to systemic inflammation.

4 Discussion

In this study, we characterized a so far unknown connection between hypoxia-evoked disturbances in cholesterol metabolism

and altered IFN responses in monocytes. Cholesterol biosynthesis flux was reduced under hypoxia, resulting in a compensatory SREBP2 activation and consequently enhanced expression of cholesterol biosynthesis enzymes. Also, a broad range of ISGs was induced under hypoxia, but their hypoxic regulation was independent of SREBP2 activity. While a complex regulatory network affected various subgroups of ISGs, intracellular distribution of cholesterol appeared crucial for the hypoxic, TLR4/MyD88-mediated induction of chemokine ISGs. Hypoxia further enhanced chemokine ISG expression in monocytes upon infection with SARS-CoV-2, potentially contributing to systemic inflammatory responses in severe cases of COVID-19 (Figure 8).

Our observation that early cholesterol biosynthesis intermediates accumulated, while late intermediates were reduced under hypoxic conditions in THP-1 monocytes, corroborates previous findings of an altered sterol composition under hypoxia (51–53). Moreover, massive and rapid accumulation of lanosterol and 24,25-dihydrolanosterol agrees with previous findings that squalene epoxidase remains active under low oxygen tensions for an extended period of time, thus allowing cholesterol biosynthetic flux to reach lanosterol and 24,25-dihydrolanosterol (51, 54). In contrast to earlier reports claiming that SREBP2 is not activated under hypoxia (55–57), we found a strong feedback activation of SREBP2 despite marginal changes in total cholesterol levels. Supplementation of late cholesterol precursors sufficed to block SREBP2 activity, which suggests that local cholesterol availability (e.g., at the ER) rather than total cholesterol levels are critical in hypoxic monocytes. Differences in sub-cellular cholesterol dynamics or cellular cholesterol requirements might account for the pronounced cell type-specificity of SREBP2 activation in the context of hypoxia. Interestingly, the key enzyme of the cholesterol biosynthesis cascade HMGCR was previously shown to be a direct target of the hypoxia-inducible factor 1 (HIF-1) (58), which might contribute to the enhanced formation of early cholesterol intermediates as well.

Strikingly, expression of IFN response targets closely followed cholesterol biosynthesis changes in hypoxic monocytes, pointing to a potential interplay. Indeed, there is increasing evidence that cholesterol metabolism and IFN responses are tightly interwoven. On the one hand, IFNs and viral infections appear to reduce SREBP2 target expression (14, 15), while on the other hand, cholesterol intermediates were shown to affect ISG expression. Specifically, the early cholesterol intermediate lanosterol repressed IFN signaling in macrophages (59), whereas accumulation of the direct cholesterol precursor 7-dehydrocholesterol or reduced desmosterol levels enhanced ISG expression (13, 60). Furthermore, York et al. (12) provide evidence for an immunometabolic circuit where type I IFN shifts the balance

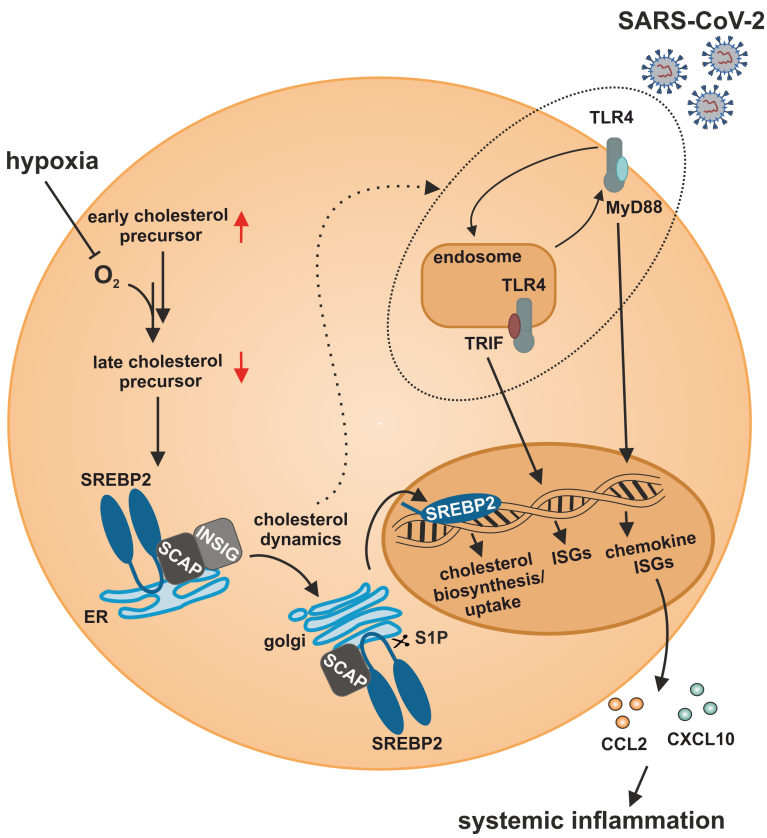

FIGURE 8
Model of the impact of hypoxia on IFN responses to SARS-CoV-2 infection in monocytes. Hypoxia alters cholesterol biosynthesis flux and subcellular cholesterol dynamics, consequently enhancing TLR4/MyD88-dependent chemokine ISG production in response to SARS-CoV-2 infection.

from cholesterol synthesis to uptake, without altering total cholesterol availability. A reduced flux through the cholesterol biosynthesis cascade in turn enhances IFN responses, putatively via lowered cholesterol levels at the ER (12). On a mechanistic side note, SREBP2 was further shown to directly bind to and activate the promotor of various ISGs (38). In contrast, hypoxia-induced ISG expression in monocytes occurred independently of SREBP2, as inhibition of the activating cleavage of SREBP2 by S1P did not attenuate hypoxic ISG induction. Surprisingly though, fatostatin, a commonly used SREBP2 inhibitor, efficiently reduced hypoxia-dependent ISG expression. Fatostatin prevents SREBP2 activation by inhibiting SCAP-coupled ER-to-Golgi transfer. SCAP-associated trafficking was further shown to enhance inflammatory and IFN signaling independent of SREBP2 activation (9, 61). Since cholesterol supplementation did not affect hypoxic *OAS1* and *IRF7* expression, a direct SCAP effect appeared unlikely. Considering SCAP-independent effects of fatostatin, such as a general interference with ER-to-Golgi transport or the inhibition of tubulin polymerization (62, 63), hypoxic ISG induction in monocytes might result from altered intracellular trafficking processes due to changes in subcellular cholesterol distribution instead. Indeed, cholesterol has been shown to influence intracellular trafficking by altering membrane properties or regulating motor proteins (64, 65). As a side note, differentiated, primary macrophages did not show the same phenotype as the monocytic THP-1 cells (data not shown), which might be due to differences in cell culture conditions, likely affecting cellular cholesterol availability and uptake. Yet, further studies are needed to elucidate the exact differences in hypoxic ISG induction between monocytes and macrophages, also with respect to the functional relevance in the context of inflammatory diseases.

Our data suggest that elevated ISG expression under hypoxia demands sensitization of TLR signaling linked to altered intracellular cholesterol dynamics. In fact, associations between cholesterol distribution and TLR trafficking are well-characterized (66, 67) and intracellular trafficking (e.g., between plasma membrane, endosome, or lysosome) has been shown to be critical for activation and termination of TLR signaling as well as recycling (68). Localization is of particular importance in the case of TLR4. TLR4 exclusively activates MyD88-dependent NF-κB signaling when it resides at the plasma membrane, whereas endosomal TLR4 additionally activates TRIF to elicit type I IFN signals (69). In line, accumulation of both TLR4 and cholesterol in endosomal compartments was previously shown to enhance NF-κB as well as IFN signaling upon LPS-treatment in NPC1-deficient cells (70).The observation that TLR4-dependent ISG induction prevailed in hypoxic THP-1 monocytes agrees with the previously described TLR4-dependent upregulation of IFN responses in microglia during ischemia/reperfusion (71). The strict dependency of the hypoxic chemokine ISG induction on MyD88 further corroborates a recent report showing that the direct interaction of cholesterol with MyD88 contributes to signaling amplification of the latter (72). Strikingly, hypoxic induction of chemokine ISGs in monocytes appeared particularly sensitive to changes in intracellular cholesterol trafficking as they showed a more pronounced increase in the hypoxic induction compared to the other ISGs when either extracellular cholesterol availability was reduced or the proper distribution of extracellularly supplied cholesterol was attenuated by inhibition of NPC1. Considering that NPC1 inhibition interferes with cholesterol distribution not only to the ER but also to mitochondria, it can be speculated that changes in mitochondrial integrity, due to altered sterol shuttling to the mitochondria, might contribute to hypoxic ISG induction as well. In line, it is well established that mitochondrial DNA in the cytosol elicits interferon responses (73). Nevertheless, this mechanism was proposed to rely on intact cGAS/STING signaling, which appeared to be not required for the hypoxic ISG induction in THP-1 cells.

While IFN responses are of specific relevance in the context of viral infections (74), SARS-CoV-2 infections were initially deemed to elicit only low levels of type I and III IFNs (41). Interestingly, while we observed a moderate induction of *OAS1* and *IRF7*, chemokine ISGs were markedly induced in response to SARS-CoV-2 infection in hypoxic monocytes. As inhibition of TLR4 activation or interference with cholesterol dynamics completely abolished the enhanced IFN response, TLR sensitization under hypoxia emerged as a potential mechanism. While cholesterol dynamics appeared to be crucial for the hypoxic elevation of all ISGs in the context of SARS-CoV-2 infection, TLR4 was specifically relevant for enhanced chemokine ISGs. Considering the complex regulation of IFN responses via various PRRs, the observation that MAVS also contribute to the hypoxic induction of some ISGs further supports the notion that the hypoxic ISG response integrates numerous receptor-dependent but also -independent signals. Monocytes and monocyte-derived macrophages were previously proposed to resist infection with SARS-CoV-2 due to only minimal expression of the main SARS-CoV-2 receptor ACE2 and its associated serine protease TMPRSS2 (42). Here, we observed infection of THP-1 monocytes with SARS-CoV-2, which corroborates recent findings that monocytes, despite the lack of intrinsic ACE2 expression, can be infected by SARS-CoV-2 (75). In line with previous observations that monocytes/macrophages show no productive infection with SARS-CoV-2 (76), we also did not detect active replication (subgenomic RNA4 encoding E gene). Still, increased production of ISGs and IFN-mediated inflammatory responses after SARS-CoV-2 infection of monocyte-derived cells were previously described (76, 77) and the relevance of monocytes/macrophages with respect to the clinical outcome of COVID-19 is widely accepted (78, 79). Our data suggest that hypoxia-enhanced chemokine ISG responses to SARS-CoV-2 are mediated via TLR4, which likely is activated via the spike protein, as recently suggested (50). Nevertheless, while the exact role of IFN signaling for the pathogenesis of COVID-19 is still controversially discussed and likely depends on the stage of the disease (80–82), our finding that hypoxia specifically enhances chemokine ISG expression in the context of SARS-CoV-2 infection suggests that monocytes within a hypoxemic environment might contribute to the progression from a local inflammatory disease to a systemic inflammatory response syndrome (83–85). Cholesterol homeostasis was not only identified to be important for the infection with SARS-CoV-2 (86), but activation of SREBP2 in blood mononuclear cells was put forward as an indicator of disease severity as it correlated with the development of a cytokine storm in severe cases of COVID-19 (85).

Taken together, we identified hypoxia-mediated changes in cholesterol homeostasis to induce interferon responses in monocytes. Our finding that hypoxic monocytes produce elevated chemokine ISG levels upon SARS-CoV-2 infection in a TLR4- and cholesterol-dependent manner might open new therapeutic opportunities to prevent systemic progression of severe COVID-19 cases.

Data availability statement

The datasets presented in this study can be found in online repositories. The names of the repository/repositories and accession number(s) can be found in the article/Supplementary Material.

Author contributions

RB, DF, TS and BB conceived the study and designed the experiments. RB and SM performed the experiments. VR, GC, SR, RR, MH and MP contributed to the acquisition of data. DL conducted the sterol measurements. RB, KZ and TS analyzed the data. FR, AW and MW supported the BSL3 experiments. RB and TS wrote the original draft. MW, TS and BB acquired funding. All authors contributed to the article and approved the submitted version.

Funding

This work was supported by the DFG (BR999/25-1 to BB; SFB 1039, B04 to BB; GRK 2336, TP06 to BB and TS; WI5086/1-1 to MW) and the Goethe Corona Fonds (to MW and TS). Parts of this work were supported by the Clusterproject ENABLE and the High-Performance Center TheraNova funded by the Hessian Ministry for Science and the Arts (MW), and the Federal Ministry of Education and Research (BMBF; grant 02WRS1621C (MW)).

Acknowledgments

The authors would like to thank Anja Kerksiek, Christiane Pallas, Bettina Wenzel, and Tanja Keppler for excellent technical assistance.

Conflict of interest

The authors declare that the research was conducted in the absence of any commercial or financial relationships that could be construed as a potential conflict of interest.

Publisher's note

Supplementary material

The Supplementary Material for this article can be found online at: https://www.frontiersin.org/articles/10.3389/fimmu.2023.1121864/full#supplementary-material

SUPPLEMENTARY TABLE 2
Hypoxia-induced gene expression changes and associated functions.

SUPPLEMENTARY TABLE 3
Putative hypoxia-induced ISGs identified by Interferome.

References

1. Nakazawa MS, Keith B, Simon MC. Oxygen availability and metabolic adaptations. *Nat Rev Cancer* (2016) 16:663–73. doi: 10.1038/nrc.2016.84

2. Fuhrmann DC, Brüne B. Mitochondrial composition and function under the control of hypoxia. *Redox Biol* (2017) 12:208–15. doi: 10.1016/j.redox.2017.02.012

3. Luo Z, Tian M, Yang G, Tan Q, Chen Y, Li G, et al. Hypoxia signaling in human health and diseases: implications and prospects for therapeutics. *Signal Transduct Target Ther* (2022) 7:218. doi: 10.1038/s41392-022-01080-1

4. Mathis D, Shoelson SE. Immunometabolism: an emerging frontier. *Nat Rev Immunol* (2011) 11:81. doi: 10.1038/nri2922

5. Hotamisligil GS, Shargill NS, Spiegelman BM. Adipose expression of tumor necrosis factor-α: direct role in obesity-linked insulin resistance. *Science* (1993) 259:87–91. doi: 10.1126/science.7678183

6. Moore KJ, Tabas I. Macrophages in the pathogenesis of atherosclerosis. *Cell* (2011) 145:341–55. doi: 10.1016/j.cell.2011.04.005

7. Li G, Zhao J, Li B, Zhang X, Ma J, Ma X, et al. The anti-inflammatory effects of statins on patients with rheumatoid arthritis: a systemic review and meta-analysis of 15 randomized controlled trials. *Autoimmun Rev* (2018) 17:215–25. doi: 10.1016/j.autrev.2017.10.013

8. Tabrizi R, Tamtaji OR, Mirhosseini N, Lankarani KB, Akbari M, Dadgostar E, et al. The effects of statin use on inflammatory markers among patients with metabolic syndrome and related disorders: a systematic review and meta-analysis of randomized controlled trials. *Pharmacol Res* (2019) 141:85–103. doi: 10.1016/j.phrs.2018.12.010

9. Guo C, Chi Z, Jiang D, Xu T, Yu W, Wang Z, et al. Cholesterol homeostatic regulator SCAP-SREBP2 integrates NLRP3 inflammasome activation and cholesterol biosynthetic signaling in macrophages. *Immunity* (2018) 49:842–856.e7. doi: 10.1016/j.immuni.2018.08.021

10. de la Roche M, Hamilton C, Mortensen R, Jeyaprakash AA, Ghosh S, Anand PK. Trafficking of cholesterol to the ER is required for NLRP3 inflammasome activation. *J Cell Biol* (2018) 217:3560–76. doi: 10.1083/jcb.201709057

11. Bekkering S, Arts RJW, Novakovic B, Kourtzelis I, van der Heijden CDCC, Li Y, et al. Metabolic induction of trained immunity through the mevalonate pathway. *Cell* (2018) 172:135–146.e9. doi: 10.1016/j.cell.2017.11.025

12. York AG, Williams KJ, Argus JP, Zhou QD, Brar G, Vergnes L, et al. Limiting cholesterol biosynthetic flux spontaneously engages type I IFN signaling. *Cell* (2015) 163:1716–29. doi: 10.1016/j.cell.2015.11.045

13. Xiao J, Li W, Zheng X, Qi L, Wang H, Zhang C, et al. Targeting 7-dehydrocholesterol reductase integrates cholesterol metabolism and IRF3 activation to eliminate infection. *Immunity* (2020) 52:109–122.e6. doi: 10.1016/j.immuni.2019.11.015

14. Blanc M, Hsieh WY, Robertson KA, Watterson S, Shui G, Lacaze P, et al. Host defense against viral infection involves interferon mediated down-regulation of sterol biosynthesis. *PloS Biol* (2011) 9:e1000598. doi: 10.1371/journal.pbio.1000598

15. Reboldi A, Dang EV, McDonald JG, Liang G, Russell DW, Cyster JG. 25-hydroxycholesterol suppresses interleukin-1–driven inflammation downstream of type I interferon. *Science* (2014) 345:679–84. doi: 10.1126/science.1254790

16. Mankan AK, Schmidt T, Chauhan D, Goldeck M, Höning K, Gaidt M, et al. Cytosolic RNA:DNA hybrids activate the cGAS –STING axis. *EMBO J* (2014) 33:2937–46. doi: 10.15252/embj.201488726

17. Widera M, Wilhelm A, Toptan T, Raffel JM, Kowarz E, Roesmann F, et al. Generation of a sleeping beauty transposon-based cellular system for rapid and sensitive screening for compounds and cellular factors limiting SARS-CoV-2 replication. *Front Microbiol* (2021) 12:701198. doi: 10.3389/fmicb.2021.701198

18. Toptan T, Hoehl S, Westhaus S, Bojkova D, Berger A, Rotter B, et al. Optimized qRT-PCR approach for the detection of intra- and extra-cellular SARS-CoV-2 RNAs. *IJMS* (2020) 21:4396. doi: 10.3390/ijms21124396

19. Widera M, Westhaus S, Rabenau HF, Hoehl S, Bojkova D, Cinatl J, et al. Evaluation of stability and inactivation methods of SARS-CoV-2 in context of laboratory settings. *Med Microbiol Immunol* (2021) 210:235–44. doi: 10.1007/s00430-021-00716-3

20. Bauer R, Meyer SP, Kloss KA, Guerrero Ruiz VM, Reuscher S, Zhou Y, et al. Functional RNA dynamics are progressively governed by RNA destabilization during the adaptation to chronic hypoxia. *Int J Mol Sci* (2022) 23:5824. doi: 10.3390/ijms23105824

21. Martin M. Cutadapt removes adapter sequences from high-throughput sequencing reads. *EMBnet J* (2011) 17:10. doi: 10.14806/ej.17.1.200

22. Dobin A, Davis CA, Schlesinger F, Drenkow J, Zaleski C, Jha S, et al. STAR: ultrafast universal RNA-seq aligner. *Bioinformatics* (2013) 29:15–21. doi: 10.1093/bioinformatics/bts635

23. Anders S, Pyl PT, Huber W. HTSeq–a Python framework to work with high-throughput sequencing data. *Bioinformatics* (2015) 31:166–9. doi: 10.1093/bioinformatics/btu638

24. Love MI, Huber W, Anders S. Moderated estimation of fold change and dispersion for RNA-seq data with DESeq2. *Genome Biol* (2014) 15:550. doi: 10.1186/s13059-014-0550-8

25. Gu Z, Eils R, Schlesner M. Complex heatmaps reveal patterns and correlations in multidimensional genomic data. *Bioinformatics* (2016) 32:2847–9. doi: 10.1093/bioinformatics/btw313

26. Huang DW, Sherman BT, Lempicki RA. Systematic and integrative analysis of large gene lists using DAVID bioinformatics resources. *Nat Protoc* (2009) 4:44–57. doi: 10.1038/nprot.2008.211

27. Sherman BT, Hao M, Qiu J, Jiao X, Baseler MW, Lane HC, et al. DAVID: a web server for functional enrichment analysis and functional annotation of gene lists (2021 update). *Nucleic Acids Res* (2022) 50:W216–21. doi: 10.1093/nar/gkac194

28. Rusinova I, Forster S, Yu S, Kannan A, Masse M, Cumming H, et al. INTERFEROME v2.0: an updated database of annotated interferon-regulated genes. *Nucleic Acids Res* (2012) 41:D1040–6. doi: 10.1093/nar/gks1215

29. Chen H, Boutros PC. VennDiagram: a package for the generation of highly-customizable Venn and Euler diagrams in r. *BMC Bioinf* (2011) 12:35. doi: 10.1186/1471-2105-12-35

30. Bankhead P, Loughrey MB, Fernández JA, Dombrowski Y, McArt DG, Dunne PD, et al. QuPath: open source software for digital pathology image analysis. *Sci Rep* (2017) 7:16878. doi: 10.1038/s41598-017-17204-5

31. Snodgrass RG, Benatzy Y, Schmid T, Namgaladze D, Mainka M, Schebb NH, et al. Efferocytosis potentiates the expression of arachidonate 15-lipoxygenase (ALOX15) in alternatively activated human macrophages through LXR activation. *Cell Death Differ* (2021) 28:1301–16. doi: 10.1038/s41418-020-00652-4

32. Mackay DS, Jones PJH, Myrie SB, Plat J, Lütjohann D. Methodological considerations for the harmonization of non-cholesterol sterol bio-analysis. *J Chromatogr B* (2014) 957:116–22. doi: 10.1016/j.jchromb.2014.02.052

33. Lütjohann D, Stellaard F, Kerksiek A, Lötsch J, Oertel BG. Serum 4β-hydroxycholesterol increases during fluconazole treatment. *Eur J Clin Pharmacol* (2021) 77:659–69. doi: 10.1007/s00228-020-03041-5

34. R Core Team. *R: a language and environment for statistical computing* (2021). Available at: https://www.R-project.org/.

35. Tall AR, Yvan-Charvet L. Cholesterol, inflammation and innate immunity. *Nat Rev Immunol* (2015) 15:104–16. doi: 10.1038/nri3793

36. Wang X, Briggs MR, Hua X, Yokoyama C, Goldstein JL, Brown MS. Nuclear protein that binds sterol regulatory element of low density lipoprotein receptor promoter. II. purification and characterization. *J Biol Chem* (1993) 268:14497–504. doi: 10.1016/S0021-9258(19)85266-3

37. Bilotta MT, Petillo S, Santoni A, Cippitelli M. Liver X receptors: regulators of cholesterol metabolism, inflammation, autoimmunity, and cancer. *Front Immunol* (2020) 11:584303. doi: 10.3389/fimmu.2020.584303

38. Kusnadi A, Park SH, Yuan R, Pannellini T, Giannopoulou E, Oliver D, et al. The cytokine TNF promotes transcription factor SREBP activity and binding to inflammatory genes to activate macrophages and limit tissue repair. *Immunity* (2019) 51:241–257.e9. doi: 10.1016/j.immuni.2019.06.005

39. Zhou P, Yang X-L, Wang X-G, Hu B, Zhang L, Zhang W, et al. A pneumonia outbreak associated with a new coronavirus of probable bat origin. *Nature* (2020) 579:270–3. doi: 10.1038/s41586-020-2012-7

40. Zhu N, Zhang D, Wang W, Li X, Yang B, Song J, et al. A novel coronavirus from patients with pneumonia in China, 2019. *N Engl J Med* (2020) 382:727–33. doi: 10.1056/NEJMoa2001017

41. Blanco-Melo D, Nilsson-Payant BE, Liu W-C, Uhl S, Hoagland D, Møller R, et al. Imbalanced host response to SARS-CoV-2 drives development of COVID-19. *Cell* (2020) 181:1036–1045.e9. doi: 10.1016/j.cell.2020.04.026

42. Zankharia U, Yadav A, Yi Y, Hahn BH, Collman RG. Highly restricted SARS-CoV-2 receptor expression and resistance to infection by primary human monocytes and monocyte-derived macrophages. *J Leukoc Bio* (2022) 112:569–76. doi: 10.1002/JLB.4COVA1121-579RR

43. Kim Y-M, Shin E-C. Type I and III interferon responses in SARS-CoV-2 infection. *Exp Mol Med* (2021) 53:750–60. doi: 10.1038/s12276-021-00592-0

44. Merad M, Martin JC. Pathological inflammation in patients with COVID-19: a key role for monocytes and macrophages. *Nat Rev Immunol* (2020) 20:355–62. doi: 10.1038/s41577-020-0331-4

45. Kawai T, Takahashi K, Sato S, Coban C, Kumar H, Kato H, et al. IPS-1, an adaptor triggering RIG-i- and Mda5-mediated type I interferon induction. *Nat Immunol* (2005) 6:981–8. doi: 10.1038/ni1243

46. Ablasser A, Goldeck M, Cavlar T, Deimling T, Witte G, Röhl I, et al. cGAS produces a 2'-5'-linked cyclic dinucleotide second messenger that activates STING. *Nature* (2013) 498:380–4. doi: 10.1038/nature12306

47. Fitzgerald KA, Kagan JC. Toll-like receptors and the control of immunity. *Cell* (2020) 180:1044–66. doi: 10.1016/j.cell.2020.02.041

48. Ullah MO, Sweet MJ, Mansell A, Kellie S, Kobe B. TRIF-dependent TLR signaling, its functions in host defense and inflammation, and its potential as a therapeutic target. *J Leukoc Biol* (2016) 100:27–45. doi: 10.1189/jlb.2RI1115-531R

49. Liu Z-M, Yang M-H, Yu K, Lian Z-X, Deng S-L. Toll-like receptor (TLRs) agonists and antagonists for COVID-19 treatments. *Front Pharmacol* (2022) 13:989664. doi: 10.3389/fphar.2022.989664

50. Zhao Y, Kuang M, Li J, Zhu L, Jia Z, Guo X, et al. SARS-CoV-2 spike protein interacts with and activates TLR4. *Cell Res* (2021) 31:818–20. doi: 10.1038/s41422-021-00495-9

51. Nguyen AD, McDonald JG, Bruick RK, DeBose-Boyd RA. Hypoxia stimulates degradation of 3-Hydroxy-3-methylglutaryl-coenzyme a reductase through accumulation of lanosterol and hypoxia-inducible factor-mediated induction of insigs. *J Biol Chem* (2007) 282:27436–46. doi: 10.1074/jbc.M704976200

52. Zhu J, Jiang X, Chehab FF. FoxO4 interacts with the sterol regulatory factor SREBP2 and the hypoxia inducible factor HIF2α at the CYP51 promoter. *J Lipid Res* (2014) 55:431–42. doi: 10.1194/jlr.M043521

53. Song B-L, Javitt NB, DeBose-Boyd RA. Insig-mediated degradation of HMG CoA reductase stimulated by lanosterol, an intermediate in the synthesis of cholesterol. *Cell Metab* (2005) 1:179–89. doi: 10.1016/j.cmet.2005.01.001

54. Kucharzewska P, Christianson HC, Belting M. Global profiling of metabolic adaptation to hypoxic stress in human glioblastoma cells. *PloS One* (2015) 10:e0116740. doi: 10.1371/journal.pone.0116740

55. Cao R, Zhao X, Li S, Zhou H, Chen W, Ren L, et al. Hypoxia induces dysregulation of lipid metabolism in HepG2 cells via activation of HIF-2a. *Cell Physiol Biochem* (2014) 34:1427–41. doi: 10.1159/000366348

56. Dolt KS, Karar J, Mishra MK, Salim J, Kumar R, Grover SK, et al. Transcriptional downregulation of sterol metabolism genes in murine liver exposed to acute hypobaric hypoxia. *Biochem Biophys Res Commun* (2007) 354:148–53. doi: 10.1016/j.bbrc.2006.12.159

57. Kondo A, Yamamoto S, Nakaki R, Shimamura T, Hamakubo T, Sakai J, et al. Extracellular acidic pH activates the sterol regulatory element-binding protein 2 to promote tumor progression. *Cell Rep* (2017) 18:2228–42. doi: 10.1016/j.celrep.2017.02.006

58. Pallottini V, Guantario B, Martini C, Totta P, Filippi I, Carraro F, et al. Regulation of HMG-CoA reductase expression by hypoxia. *J Cell Biochem* (2008) 104:701–9. doi: 10.1002/jcb.21757

59. Araldi E, Fernández-Fuertes M, Canfrán-Duque A, Tang W, Cline GW, Madrigal-Matute J, et al. Lanosterol modulates TLR4-mediated innate immune responses in macrophages. *Cell Rep* (2017) 19:2743–55. doi: 10.1016/j.celrep.2017.05.093

60. Zhang X, McDonald JG, Aryal B, Canfrán-Duque A, Goldberg EL, Araldi E, et al. Desmosterol suppresses macrophage inflammasome activation and protects against vascular inflammation and atherosclerosis. *Proc Natl Acad Sci USA* (2021) 118:e2107682118. doi: 10.1073/pnas.2107682118

61. Chen W, Li S, Yu H, Liu X, Huang L, Wang Q, et al. ER adaptor SCAP translocates and recruits IRF3 to perinuclear microsome induced by cytosolic microbial DNAs. *PloS Pathog* (2016) 12:e1005462. doi: 10.1371/journal.ppat.1005462

62. Gholkar AA, Cheung K, Williams KJ, Lo Y-C, Hamideh SA, Nnebe C, et al. Fatostatin inhibits cancer cell proliferation by affecting mitotic microtubule spindle assembly and cell division. *J Biol Chem* (2016) 291:17001–8. doi: 10.1074/jbc.C116.737346

63. Shao W, Machamer CE, Espenshade PJ. Fatostatin blocks ER exit of SCAP but inhibits cell growth in a SCAP-independent manner. *J Lipid Res* (2016) 57:1564–73. doi: 10.1194/jlr.M069583

64. Sarkar P, Kumar GA, Shrivastava S, Chattopadhyay A. Chronic cholesterol depletion increases f-actin levels and induces cytoskeletal reorganization via a dual mechanism. *J Lipid Res* (2022) 63:100206. doi: 10.1016/j.jlr.2022.100206

65. Lebrand C, Corti M, Goodson H, Cosson P, Cavalli V, Mayran N, et al. Late endosome motility depends on lipids via the small GTPase Rab7. *EMBO J* (2002) 21:1289–300. doi: 10.1093/emboj/21.6.1289

66. Azzam KM, Fessler MB. Crosstalk between reverse cholesterol transport and innate immunity. *Trends Endocrinol Metab* (2012) 23:169–78. doi: 10.1016/j.tem.2012.02.001

67. Sun Y, Ishibashi M, Seimon T, Lee M, Sharma SM, Fitzgerald KA, et al. Free cholesterol accumulation in macrophage membranes activates toll-like receptors and p38 mitogen-activated protein kinase and induces cathepsin K. *Circ Res* (2009) 104:455–65. doi: 10.1161/CIRCRESAHA.108.182568

68. McGettrick AF, O'Neill LA. Localisation and trafficking of toll-like receptors: an important mode of regulation. *Curr Opin Immunol* (2010) 22:20–7. doi: 10.1016/j.coi.2009.12.002

69. Ciesielska A, Matyjek M, Kwiatkowska K. TLR4 and CD14 trafficking and its influence on LPS-induced pro-inflammatory signaling. *Cell Mol Life Sci* (2021) 78:1233–61. doi: 10.1007/s00018-020-03656-y

70. Suzuki M, Sugimoto Y, Ohsaki Y, Ueno M, Kato S, Kitamura Y, et al. Endosomal accumulation of toll-like receptor 4 causes constitutive secretion of cytokines and activation of signal transducers and activators of transcription in niemann-pick disease type c (NPC) fibroblasts: a potential basis for glial cell activation in the NPC brain. *J Neurosci* (2007) 27:1879–91. doi: 10.1523/JNEUROSCI.5282-06.2007

71. McDonough A, Lee RV, Noor S, Lee C, Le T, Iorga M, et al. Ischemia/Reperfusion induces interferon-stimulated gene expression in microglia. *J Neurosci* (2017) 37:8292–308. doi: 10.1523/JNEUROSCI.0725-17.2017

72. Hayakawa S, Tamura A, Nikiforov N, Koike H, Kudo F, Cheng Y, et al. Activated cholesterol metabolism is integral for innate macrophage responses by amplifying Myd88 signaling. *JCI Insight* (2022) 7:e138539. doi: 10.1172/jci.insight.138539

73. Sprenger H-G, MacVicar T, Bahat A, Fiedler KU, Hermans S, Ehrentraut D, et al. Cellular pyrimidine imbalance triggers mitochondrial DNA–dependent innate immunity. *Nat Metab* (2021) 3:636–50. doi: 10.1038/s42255-021-00385-9

74. Katze MG, He Y, Gale M. Viruses and interferon: a fight for supremacy. *Nat Rev Immunol* (2002) 2:675–87. doi: 10.1038/nri888

75. Yao Y, Subedi K, Liu T, Khalasawi N, Pretto-Kernahan CD, Wotring JW, et al. Surface translocation of ACE2 and TMPRSS2 upon TLR4/7/8 activation is required for SARS-CoV-2 infection in circulating monocytes. *Cell Discov* (2022) 8:89. doi: 10.1038/s41421-022-00453-8

76. Zheng J, Wang Y, Li K, Meyerholz DK, Allamargot C, Perlman S. Severe acute respiratory syndrome coronavirus 2–induced immune activation and death of monocyte-derived human macrophages and dendritic cells. *J Infect Dis* (2021) 223:785–95. doi: 10.1093/infdis/jiaa753

77. Wilk AJ, Rustagi A, Zhao NQ, Roque J, Martínez-Colón GJ, McKechnie JL, et al. A single-cell atlas of the peripheral immune response in patients with severe COVID-19. *Nat Med* (2020) 26:1070–6. doi: 10.1038/s41591-020-0944-y

78. Junqueira C, Crespo Â, Ranjbar S, de Lacerda LB, Lewandrowski M, Ingber J, et al. FcγR-mediated SARS-CoV-2 infection of monocytes activates inflammation. *Nature* (2022) 606:576–84. doi: 10.1038/s41586-022-04702-4

79. Sefik E, Qu R, Junqueira C, Kaffe E, Mirza H, Zhao J, et al. Inflammasome activation in infected macrophages drives COVID-19 pathology. *Nature* (2022) 606:585–93. doi: 10.1038/s41586-022-04802-1

80. Soltani-Zangbar MS, Parhizkar F, Abdollahi M, Shomali N, Aghebati-Maleki L, Shahmohammadi Farid S, et al. Immune system-related soluble mediators and COVID-19: basic mechanisms and clinical perspectives. *Cell Commun Signal* (2022) 20:131. doi: 10.1186/s12964-022-00948-7

81. Eskandarian Boroujeni M, Sekrecka A, Antonczyk A, Hassani S, Sekrecki M, Nowicka H, et al. Dysregulated interferon response and immune hyperactivation in severe COVID-19: targeting STATs as a novel therapeutic strategy. *Front Immunol* (2022) 13:888897. doi: 10.3389/fimmu.2022.888897

82. Channappanavar R, Perlman S. Pathogenic human coronavirus infections: causes and consequences of cytokine storm and immunopathology. *Semin Immunopathol* (2017) 39:529–39. doi: 10.1007/s00281-017-0629-x

83. Grant RA, Morales-Nebreda L, Markov NS, Swaminathan S, Querrey M, Guzman ER, et al. Circuits between infected macrophages and T cells in SARS-CoV-2 pneumonia. *Nature* (2021) 590:635–41. doi: 10.1038/s41586-020-03148-w

84. Grieb P, Swiatkiewicz M, Prus K, Rejdak K. Hypoxia may be a determinative factor in COVID-19 progression. *Curr Res Pharmacol Drug Discov* (2021) 2:100030. doi: 10.1016/j.crphar.2021.100030

85. Lee W, Ahn JH, Park HH, Kim HN, Kim H, Yoo Y, et al. COVID-19-activated SREBP2 disturbs cholesterol biosynthesis and leads to cytokine storm. *Signal Transduct Target Ther* (2020) 5:186. doi: 10.1038/s41392-020-00292-7

86. Wang R, Simoneau CR, Kulsuptrakul J, Bouhaddou M, Travisano KA, Hayashi JM, et al. Genetic screens identify host factors for SARS-CoV-2 and common cold coronaviruses. *Cell* (2021) 184:106–119.e14. doi: 10.1016/j.cell.2020.12.004

frontiers | Frontiers in Immunology

TYPE Original Research
PUBLISHED 12 June 2023
DOI 10.3389/fimmu.2023.1114129

OPEN ACCESS

EDITED BY
Melanie Albrecht,
Paul-Ehrlich-Institut (PEI), Germany

REVIEWED BY
Pankaj Baral,
Kansas State University, United States
Krzysztof Guzik,
Jagiellonian University, Poland

*CORRESPONDENCE
Jialin Liu
ljl11243@rjh.com.cn
Jing Xu
xj40952@rjh.com.cn
Mi Zhou
zhouim11@aliyun.com

†These authors have contributed equally to this work and share first authorship

RECEIVED 02 December 2022
ACCEPTED 17 May 2023
PUBLISHED 12 June 2023

CITATION
Tang Y, Yu Y, Li R, Tao Z, Zhang L, Wang X, Qi X, Li Y, Meng T, Qu H, Zhou M, Xu J and Liu J (2023) Phenylalanine promotes alveolar macrophage pyroptosis *via* the activation of CaSR in ARDS. *Front. Immunol.* 14:1114129. doi: 10.3389/fimmu.2023.1114129

Phenylalanine promotes alveolar macrophage pyroptosis *via* the activation of CaSR in ARDS

Yiding Tang[1†], Yue Yu[1†], Ranran Li[1], Zheying Tao[1], Li Zhang[1], Xiaoli Wang[1], Xiaoling Qi[1], Yinjiaozhi Li[1], Tianjiao Meng[1], Hongping Qu[1], Mi Zhou[2*], Jing Xu[1*] and Jialin Liu[1*]

[1]Department of Critical Care Medicine, Ruijin Hospital, Shanghai Jiao Tong University School of Medicine, Shanghai, China, [2]Department of Cardiac Surgery, Ruijin Hospital affiliated to School of Medicine, Shanghai Jiao Tong University, Shanghai, China

Acute respiratory distress syndrome (ARDS) is associated with high mortality rates in patients admitted to the intensive care unit (ICU) patients with overwhelming inflammation considered to be an internal cause. The authors' previous study indicated a potential correlation between phenylalanine levels and lung injury. Phenylalanine induces inflammation by enhancing the innate immune response and the release of pro-inflammatory cytokines. Alveolar macrophages (AMs) can respond to stimuli *via* synthesis and release of inflammatory mediators through pyroptosis, one form of programmed cell death acting through the nucleotide-binging oligomerization domain-like receptors protein 3 (NLRP3) signaling pathway, resulting in the cleavage of caspase-1 and gasdermin D (GSDMD) and the release of interleukin (IL) -1β and IL-18, aggravating lung inflammation and injury in ARDS. In this study, phenylalanine promoted pyroptosis of AMs, which exacerbated lung inflammation and ARDS lethality in mice. Furthermore, phenylalanine initiated the NLRP3 pathway by activating the calcium-sensing receptor (CaSR). These findings uncovered a critical mechanism of action of phenylalanine in the context of ARDS and may be a new treatment target for ARDS.

KEYWORDS

acute respiratory disease syndrome (ARDS), alveolar macrophage (AM), phenylalanine, pyroptosis, CaSR

Introduction

ARDS, characterized by hypoxemia and bilateral pulmonary edema, and is associated with high mortality rates (34.9%-46.1%) in ICU patients. Overwhelming inflammation is considered to be an internal cause of ARDS (1). Accumulating evidence has revealed the essential roles of metabolites in immune activation and regulation (2). Our previous, which that targeted at the functional metabolites in patients with ARDS indicated a potential correlation between phenylalanine levels and lung injury (3).

Phenylalanine is an essential amino acid that increases in inflammation and the immune response, and has been proposed to predict disease severity in critically ill patients. A recent study reported the accumulation of phenylalanine was associated with inflammatory markers of coronavirus disease 2019(COVID-19) (4). Phenylalanine induces inflammation by enhancing the innate immune response and inducing the release of pro-inflammatory cytokines (5). However, the specific mechanism of action of phenylalanine in the lung inflammation in ARDS remains unclear.

Most airspace leukocytes are AMs. As resident inflammatory cells, they respond to stimuli in the alveolar spaces by synthesizing and releasing inflammatory mediators, which are also vital to inflammation during ARDS. The activation of AMs after exposure to pathogen triggers an inflammatory cascade (6). Pyroptosis is considered to be a mechanism of uncontrolled inflammation, and is a form of programmed cell death, with the cleavage of caspase-1 and GSDMD as well as the release of IL-1β and IL-18 (7). AMs can be activated by pathogen-associated molecular patterns including those of the NLR family. Induced macrophage pyroptosis acts through the NLRP3 inflammasome signaling pathway and aggravates lung inflammation and causes severe lung injury in ARDS (8). Blockade of NLRP3 inflammasome signaling in AMs may suppress pyroptosis and, consequently mitigate lung inflammation and injury in patients with ARDS (9).

In the present study, we demonstrated that phenylalanine promoted pyroptosis in AMs, thus exacerbating lung inflammation and ARDS lethality in mice. We further revealed that phenylalanine initiated NLRP3 pathway by activating CaSR. Thus, our findings may have uncovered a critical mechanism of action of phenylalanine in the context of ARDS lethality.

Materials and methods

Patients

This study was approved by Ruijin Hospital Ethics Committee of Shanghai Jiao Tong University School of Medicine. All patients who fulfilled the criteria for ARDS according to the Berlin definition were enrolled in the study (10). Patients < 18 years of age, individuals with any autoimmune diseases, those participating in another clinical trial, and those with other chronic respiratory diseases were excluded.

Sample acquisition and phenylalanine assessment

Blood samples and bronchoalveolar lavage fluid (BALF) were collected within 9 h of ARDS diagnosis for metabolomic analysis. Collectively, 59 patients were enrolled in this study. Blood samples (2 mL) were collected in heparin tubes and centrifuged at 500×g at 4°C for 5 min, the supernatants were extracted and stored at −80°C untill further use. Phenylalanine levels were assessed using mass spectrometry/high-performance liquid chromatography (Hypersil GOLD HPLC column [ThermoFisher, Waltham, MA, USA] coupled to a QTRAP 6500 [SCIEX, Framingham, MA, USA]). by Mass Spectrometry Platform, National Research Center for Translational Medicine, Ruijin Hospital Affiliated to Shanghai Jiao Tong University (SJTU) School of Medicine, Shanghai, China.

Animal experiments

Animal experiments were performed using 8–10-week-old C57BL/6 mice purchased from Shanghai Jihui Laboratory Animal Care Co., Ltd. and maintained at in-house facilities under pathogen-free conditions. The animal study was approved by the University Committee for Laboratory Animals and performed in accordance with guidelines of the Shanghai Institutes for Biological Sciences Council on Animal Care. ARDS model animals were established in accordance with a previous report, in which the mice were intratracheally injected with 50 μL bacterial lipopolysaccharide (LPS, Thermo Fisher, #L2630) with the concentration of 6 mg/ml or an equal volume of phosphate-buffered saline (PBS) as sham control (3). ARDS mice were administered with phenylalanine or PBS (25 mg/ml in total volume of 200μl intravenously) 24h before, immediately after and 12h after intratracheal injection of LPS three times. To illustrate the effect of phenylalanine on ARDS lethality, mice were pretreated with phenylalanine or PBS 24 h before the intratracheal injection of LPS, and another dose of phenylalanine or PBS every 24 h until death over the consequent 7 days. To deplete AMs, mice were intratracheally injected with 75 μL of Clodronate Liposomes (CL, Yeason, #40337ES10) 24 h before and soon after the ARDS model was established. Mice in the control group were administered with the same volume of liposomes. BALF and lung tissues were isolated for subsequent experiments 24 h after the final CL injection. To test the role of activated CaSR, another group of mice was administered Calhex231 *via* saline/dimethyl sulfoxide injection intraperitoneally 4 h after phenylalanine administration based on ARDS mice administered phenylalanine.

Assessment of lung injury

BALF was obtained from the mice *via* tracheal cannulation in a total volume of 1.5 ml PBS. The samples were then placed on ice and directly transferred for further processing. BALF was centrifuged at 500 ×g for 5 minutes at 4°C. The supernatant was tested to determine the concentration of IL-1β, IL-18, and protein concentration using a commercially available kit in accordance with manufacturer's instructions. Red blood cell lysate was added to the cell precipitate, and the mixture was centrifuged at 500 ×g for 5 min at 4°C after storage for 3 minutes at 4°C. Cells were cultured in RPMI 1640 medium containing fetal bovine serum (FBS) (0.5%) for 2 h and washed with RPMI 1640/0.5% FBS. Lung tissues were prepared for hematoxylin and eosin (H&E) staining.

Flowcytometry of lung cells

Lung tissue from the mice was crushed into small pieces and digested using 50 μL collagenase I (0.1 mg/mL) (Collagenase, Type 1, Sangon Biotech, Shanghai, China) at 37 °C for 1 h to prepare a single-cell suspension. The following fluorescent antibodies were purchased from Biolegend: APC/Cyanine7 anti-mouse CD45, 103116; PE anti-mouse CD11c, 117307; Brilliant Violet 421 anti-mouse F4/80, 123131; PerCP-Cy™5.5 rat anti-mouse I-A/I-E, 107626; Phycoerythrin/Cy7 anti-mouse/human CD11b, 101216; Brilliant Violet 605 anti-mouse Gr-1, 108439; APC Anti-mouse TCR 118116. Dead/live staining (LIVE/DEAD™ Fixable Aqua Dead Cell Stain Kit) from Invitrogen (Carlsbad, CA, USA) was used to distinguish dead cells and debris.

Acquisition of bone marrow-derived macrophages and cell culture

Bone marrow cells from 8-week-old C57BL/6 mice were collected by flushing the femurs and tibias and then the cells culturing in α-MEM (Gibco) containing 10% FBS, 100 IU/ml penicillin and 100 mg/ml streptomycin. Culture medium was transferred to another dish on the second day to cultivate non-adherent cells with addition of 10 ng/ml Granulocyte-Macrophage Colony-Stimulating Factor (GM-CSF, # 315-03, Peprotech, USA) at 37°C in a 5% CO2 incubator. The medium was replaced after 3-5 days, and adherent bone marrow-derived macrophages (BMDMs) were used within two passages.

BMDMs were exposed to 100 ng/ml LPS to enhance their proinflammatory phenotype with application of 600 μM Phenylalanine and/or 10 μM Calhex 231 for 4 h. Thirty minutes before the end of the experiment, 2mM ATP was added to the cells. After treatment, the cells were either lysed for Western blotting or collected for flow cytometry to assess pyroptosis.

Confirmation of pyroptosis

Western blotting and flow cytometry were performed to confirm pyroptosis. The protein concentrations of all samples were estimated using a commercially available BCA kit (Thermo Fischer). Equal amounts of proteins were separated using 10% sodium dodecyl sulfate-polyacrylamide gel electrophoresis and transferred onto a PVDF membrane (Millipore) using a protein transfer system. The membranes were blocked using 5% skim milk powder in TBST buffer for 1 h at room temperature (RT). The blots were then incubated overnight at 4°C with the primary antibodies including mouse anti-rabbit HSP90 (1:2000, Proteintech), mouse anti-rabbit GSDMD (1:1000, Santa Cruz), mouse anti- rabbit N-GSDMD (1:1000, Proteintech), mouse anti-rabbit caspase-1 (1:1000, Santa Cruz), mouse anti-rabbit N-caspase-1 (1:1000, Santa Cruz) and mouse anti-mouse GAPDH (1:1000, Santa Cruz). Subsequently, blots were incubated with anti-mouse or anti-rabbit IgG antibodies (1:5000, Cell signaling) for 1 h at RT. The blots were developed using a commercially available enhanced chemiluminescence detection kit. Each experiment was performed at least twice using cell populations obtained from separate mouse groups. Cells administered different treatments were processed according to manufacturer's instructions for the annexin V/propidium iodide (PI) assay (CAT#40302ES20, Yeasen, China).

Measurement of calcium concentration in BMDM

Cells were plated in black 96-well plates at 30,000 cells/well and left to stabilize overnight in a 37°C/5% CO2 incubator. The calcium-regulated intracellular calcium indicator, Fluo-4 AM (Yeasen, 40704ES72) was used to monitor real-time elevations in intracellular calcium following activation or inhibition of the CaSR according to manufacturer's instructions. Data were acquired using a plate reader at 37°C, with excitation at 494 nm and emission at 516 nm (Synergy Neo, USA).

Immunofluorescence

Lung tissue slices and BMDMs were isolated as previously described. The slices or cells were fixed using pre-cooled 4% paraformaldehyde for 15 min, washed with PBS, blocked in 3% bovine serum albumin for 1 h, and reacted with rabbit anti-GSDMD (1:100, Bio-Techne China Co. Ltd., China) primary antibody overnight. After washing the samples three times, samples were stained with Alexa Fluor 488 goat anti-rabbit IgG (1:1000, Abcam, USA) for 1 h in the dark. After washing with PBS, the sample slides were incubated with an anti-fluorescence quencher (DAPI) before capping the microscope slides. Slides were observed under a laser-scanning confocal microscope (LSM880, Zeiss, Oberkochen, Germany). Images were analyzed using ZEN software (Zeiss, Germany).

Statistical analysis

Statistical analyses were performed using GraphPad Prism version 9 (GraphPad Inc, San Diego, CA, USA) and SPSS version 24 (IBM Corporation, Armonk, NY, USA). Two-tailed unpaired t-tests, chi-squared tests and Fisher's exact tests were used for analysis. Receiver operating characteristic (ROC) curve analyses were reported as the area under the ROC curve (AUC). Differences with $P < 0.05$ were considered to be statistically significant. We repeated cell experiments for more than three times and extract protein for WB. Grayscale value in Figures 1H, 2J collected relative data reading from Image J. Unless specific notes in the figure legend, all the rest plots in Figures 1–4 showed data of one experiment meanwhile every kind of experiment had been repeated for more than three times.

10.3389/fimmu.2023.1114129

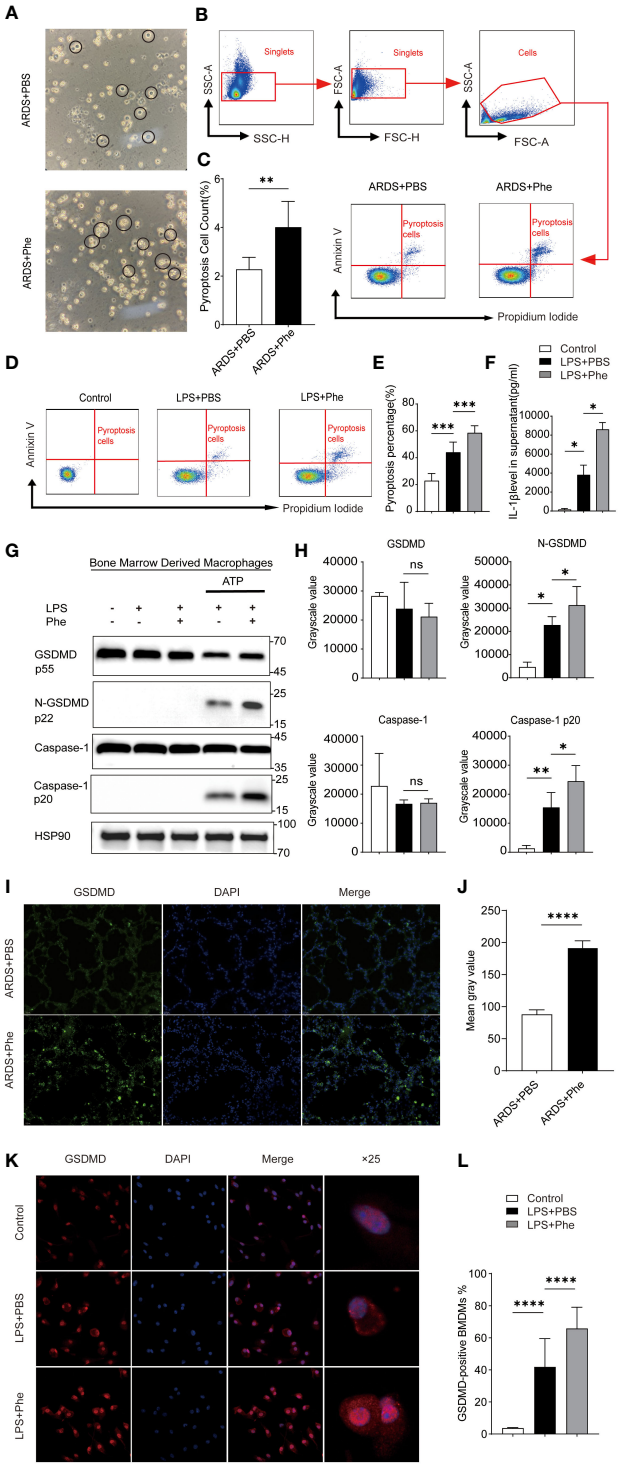

FIGURE 1
Pyroptosis occurred in AMs of ARDS mice administered phenylalanine and LPS-induced BMDMs treated with phenylananine. **(A)** Two morphological types of AMs in BALF of ARDS mice. **(B)** Cytometry gating workflow of dish-adherent cells in BALF from ARDS mice. **(C)** Pyroptosis (PI+, annexin V+) of dish-adherent cells in BALF from ARDS mice. **(D)** Pyroptosis (PI+, annexin V+) of BMDM cultured in different media. **(E)** Pyroptosis percentage of BMDMs cultured in different media. **(F)** IL-1β level in supernatent of different treatment. **(G)** Western blot of BMDMs cultured in different media. **(H)** Grayscale values for each blot of BMDMs cultured in different media. **(I)** Immunofluorescence detection of GSDMD expression in the lungs of ARDS mice. **(J)** Mean gray value for GSDMD expression in the lungs of ARDS mice. 4**(K)** Immunofluorescence detection of GSDMD expression in BMDM. **(L)** The proportion of GSDMD-positive BMDMs under different treatment. ns means no significance, * means p<0.05, **means p<0.01, ***means p<0.001, ****means p<0.0001.

10.3389/fimmu.2023.1114129

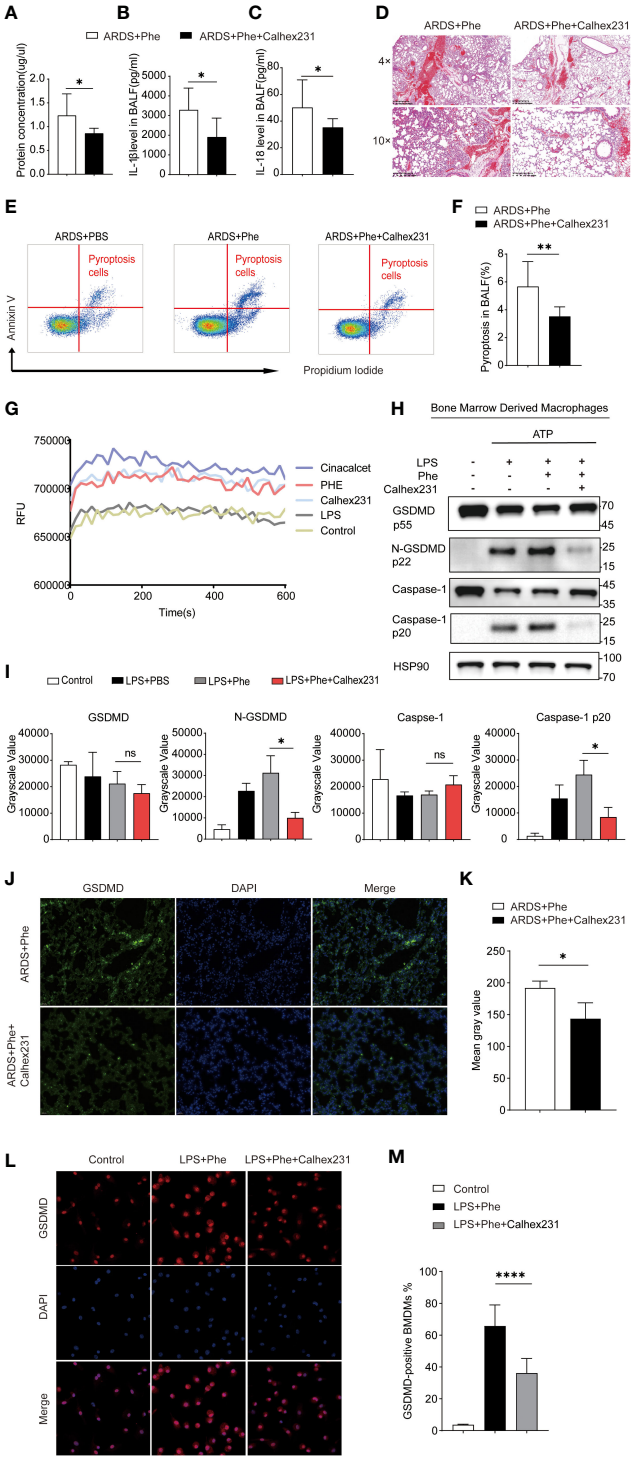

FIGURE 2
Phenylalanine administration induced pyroptosis *via* CaSR. **(A)** Protein concentration of BALF drawn from two groups of mice. **(B)** IL-1β level in BALF drawn from two groups of mice. **(C)** IL-18 level in BALF drawn from two groups of mice **(D)** Hematoxylin-Eosin staining of two groups of mice. **(E)** Cytometry gating workflow of dish-adherent cells in BALF from two groups of ARDS mice marked with PI and Annexin V. **(F)** Pyroptosis (PI+, annexin V+) proportion of dish-adherent cells in BALF from two groups of ARDS mice. **(G)** Instant relative fluorescence units (RFU) of BMDM treated with different stimulation. **(H)** Western blot of BMDM treated with different stimulation. **(I)** Grayscale values for each blot of BMDMs from different culture. **(J)** Immunofluorescence detection of GSDMD expression in the lungs of ARDS mice with or with out Calhex231. **(K)** Mean gray values for GSDMD expression in the lungs of ARDS mice with or with out Calhex231. **(L)** Immunofluorescence detection of GSDMD-positive BMDMs with or with out Calhex231. **(M)** GSDMD-positive BMDMs percentage with or with out Calhex231. ns means no significance, * means p<0.05, ****means p<0.0001.

10.3389/fimmu.2023.1114129

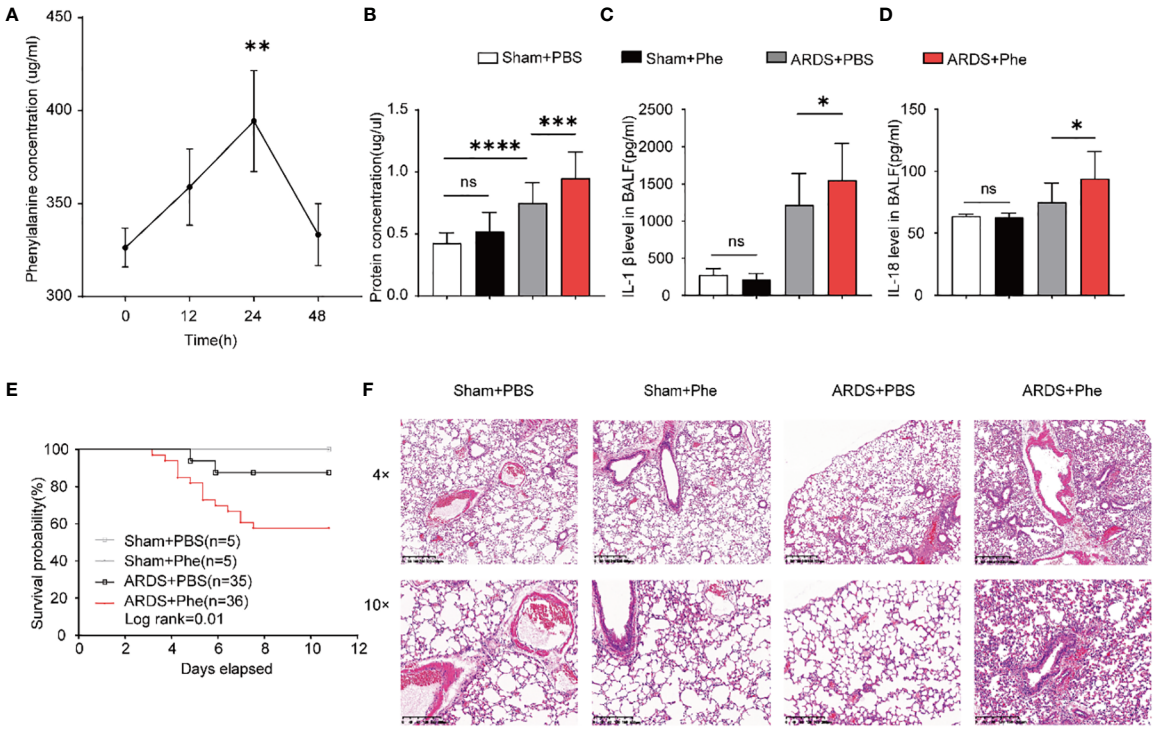

FIGURE 3
More severe lung injury in phenylalanine-administered ARDS mice. **(A)** The accumulation of phenylalanine in BALF after intravenous injection. **(B)** Protein concentration of BALF drawn from four groups of mice. **(C)** IL-1β level in BALF drawn from four groups of mice. **(D)** IL-18 level in BALF drawn from four groups of mice **(E)** Probability of survival of four groups of mice (collected data of experiments repeated for three times). **(F)** HE staining of four groups of mice. Ns, no significance. **p<0.01. ***p<0.001. ****p<0.0001.

Results

Increased serum phenylalanine level was associated with a non-survival outcome in patients with ARDS

From September 2020 to August 2022, 59 patients who fulfilled the Berlin definition criteria for ARDS were enrolled in this study and divided into survival and non-survival groups based on outcomes. The characteristics of each trial participant at the time of plasma collection, including age, sex, ARDS etiology, coexisting conditions, disease severity scores, laboratory results, and outcomes, are summarized in Table 1. Appropriate measures were taken to ensure that there was no difference in age or sex between the groups of ARDS patients. As shown, the ratio of partial pressure of oxygen (PaO_2)/fraction of inspired oxygen (FiO_2) was significantly higher in survivors than non-survivors, which indicates that the latter experienced impaired lung ventilation and further pulmonary dysfunction. After assessing serum phenylalanine levels in each patient, a significant increase was found in non-survivors compared to survivors (Figure 5A). Using ROC analysis, a cut-off value was found that, when serum phenylalanine level reached 3796 μg/ml, the survival of ARDS patients significantly decreased from 69.70% to 26.67 (Figure 5B). The ROC curve, according to this cut-off value, was used to assess the ability of phenylalanine level to predict survival rate. (Figure 5C).

Phenylalanine administration aggravated lung inflammation and injury in ARDS mice

Phenylalanine levels were first evaluated in mice challenged with a lethal dose of LPS (25 mg/kg body weight body weight) to confirm the results in samples from patients with ARDS (Supplementary Figure 1). To determine whether phenylalanine affected the pathogenesis and prognosis of ARDS, its effect was confirmed in ARDS mice administered three intravenous doses of phenylalanine. Individual BALF samples were obtained from the mice and immediately processed 24h after intratracheal administration of LPS. First, the accumulation of phenylalanine in BALF after intravenous injection was confirmed (Figure 3A). The groups of mice exhibited different protein concentrations. Among non-ARDS mice, there was no statistically significant difference regardless of whether phenylalanine was administered. In ARDS mice, the group administered phenylalanine exhibited higher protein levels, indicating more severe lung injury. (Figure 3B). Similarly, IL-1β and IL-18 levels also revealed a more serious outcome of

10.3389/fimmu.2023.1114129

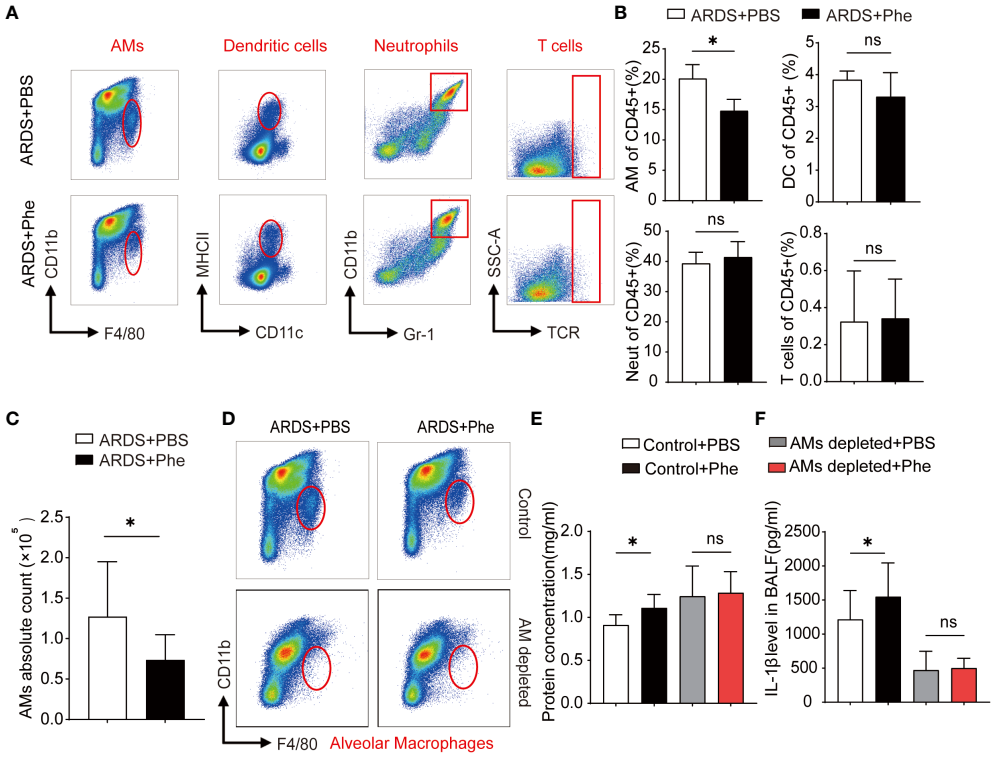

FIGURE 4
Decreased AMs found in ARDS mice administered Phe. **(A)** Cytometry of four types of immunocytes located in the lungs of ARDS mice administered with PBS or Phe. **(B)** Proportion of related immunocytes in CD45 positive cells. **(C)** Absolute numbers of AMs in ARDS mice administered with PBS or Phe. **(D)** Flow cytometry of AMs in the lung tissue of macrophage-depleted ARDS mice administered with PBS or Phe. **(E)** Protein concentration of BALF drawn from AM-eliminated or control ARDS mice administered PBS or Phe. **(F)** IL-1β level in BALF drawn from four groups of ARDS mice. ns means no significance, * means p<0.05.

phenylalanine-administered ARDS mice compared to control ARDS mice, and the difference disappeared in the sham groups (Figures 3C, D). None of the sham mice died during the chronic administration procedure. However, ARDS mice injected with phenylalanine every 12h tended exhibit significantly higher mortality rates than PBS-administered ARDS mice (Figure 3E). H&E staining of lung tissues revealed more diffusion in phenylalanine-injected ARDS mice than in PBS-injected ARDS mice at both 4× and 10× magnification. No significant differences were observed between the two sham groups (Figure 3F).

Phenylalanine administration reduced AMs in ARDS mice

After demonstrating severe lung injury in phenylalanine-administered ARDS mice, more studies involving the two groups were performed. First, the composition of intrapulmonary immunocytes in ARDS mice was analyzed. Using these methods, intrapulmonary cells were isolated and immunocytes were divided into dendritic cells (DCs), neutrophils (Neuts), AMs, and T cells (Supplementary Figure 2). Comparison of the immunocyte composition of the two groups of ARDS mice revealed more intrapulmonary AMs in PBS-administered ARDS mice than in phenylalanine-administered ARDS mice, whereas no significant difference was observed in DCs, Neuts, and T cells (Figure 4A). Statistical analysis confirmed a significantly lower percentage of intrapulmonary AMs in the phenylalanine-treated ARDS mice than in the PBS-treated ARDS mic (Figure 4B). To further support this finding, the absolute number of AMs was calculated (Figure 4C), which suggested that the difference in AMs resulted in more severe lung injury in phenylalanine-treated ARDS mice. Therefore, intrapulmonary AMs in ARDS mice were further depleted to explore whether there was a difference in the severity of lung injury without AMs (Figure 4D). Results revealed that protein concentration and IL-1β level in BALF after the depletion of AMs demonstrated no significant difference between the two groups (Figures 4E, F).

Phenylalanine administration induced pyroptosis in activated AMs

After confirming that AMs may be the key cells that lead to phenotypic differences between ARDS mice with different levels of phenylalanine, BALF was extracted from the two groups of ARDS mice and cells were cultured to divide them into AMs (adherent cells) and Neuts (suspended cells). It was clear that the morphology of AMs can be roughly divided into two types: steady state, with round and complete cell membrane and opaque interior; and those in a state of pyroptosis with cell swelling and expansion and many

10.3389/fimmu.2023.1114129

TABLE 1 Characteristics of enrolled ARDS patients.

Total	59	Survival	Non-survival	P-value
Numbers		27	32	/
Age		64.6 ± 15.4	69.0 ± 12.0	0.23
APACHEII		14.2 ± 5.8	15.9 ± 8.2	0.53
Gender, Female, n(%)		7(26)	16(50)	0.07
Etiology of ARDS, n(%)				
	Sepsis	5(23)	5(21)	0.99
	Pneumonia	7(32)	14(58)	0.20
	Aspiration	1(4)	0	0.49
	Trauma	1(5)	1(3)	1.00
	Others	11(41)	9(28)	0.58
Coexisting conditions, n(%)				
	Diabetes	6(7)	4(13)	0.50
	Renal failure	8(30)	6(19)	0.55
	Hepatic disease	3(11)	8(25)	0.18
	Coronary artery disease	3(11)	3(9)	1.00
	Cancer	1(4)	4(13)	0.35
	COPD	1(4)	1(3)	1.00
The severity of ARDS, n(%)				
	Mild	7(30)	7(25)	0.78
	Moderate	12(52)	14(50)	
	Severe	4(17)	7(25)	
	PaO2/FiO2	208.5 ± 108.0	154.1 ± 74.5	0.04*
	PEEP, cmH_2O	8.0 ± 2.8	8.4 ± 3.5	0.68
	CRP	127.0 ± 94.3	132.9 ± 92.0	0.64
	PCT	10.9 ± 16.5	6.9 ± 16.4	0.26
Cell counts, $\times10^9$/L				
	Leukocytes	14.4 ± 8.0	13.9 ± 9.0	0.83
	Neutrophils	11.8 ± 7.8	15.6 ± 16.8	0.30
	Lymphocytes	3.7 ± 5.8	1.1 ± 1.6	0.03*
Outcomes of patients				
	Ventilator days	18.7 ± 16.3	15.5 ± 14.7	0.48
	ICU stay, days	48.1 ± 69.6	39.2 ± 46.6	0.59

Quantitative data are presented as mean ± SD, Qualitative data are presented as number(percentage), P values obtained with Fisher's two-tailed t test probability using survival (n = 27) and non-survival (n = 32) patients; APACHEII acute physiology and chronic health evaluation; ARDS acute respiratory distress syndrome; COPD chronic obstructive pulmonary disease; PEEP positive end-expiratory pressure; CRP C-reactive protein; PCT procalcitonin; ICU intensive care unit. * P value <0.05.

bubble-like protrusions (Figure 1A). The PBS-treated ARDS mice exhibited more intact and opaque AMs, whereas the phenylalanine-treated ARDS mice exhibited more pyroptotic cells. Flow cytometry analysis of these adherent cells stained with PI and annexin V revealed that the proportion of pyroptotic cells (double-positive) was significantly higher in phenylalanine-treated ARDS mice (Figures 1B, C). Similar *in vitro* tests were performed on BMDMs from the same source as AMs. The proportion of pyroptotic cells was significantly higher in the medium supplemented with phenylalanine (Figures 1D, E). IL-1β level of supernatant also exhibited a significant increase when cells were treated with phenylalanine (Figure 1F). In addition, Western blotting demonstrated significantly upregulated expression of cleaved-GSDMD and cleaved-caspase-1 in BMDMs treated with

phenylalanine (Figures 1G, H). Immunofluorescence detection detection increased expression of GSDMD in the lungs of phenylalanine-treated ARDS mice (Figure 1I), which was confirmed by quantification of the mean gray value (Figure 1J). When detecting GSDMD in cells, GSDMD expression was obviously promoted in BMDMs with LPS and phenylalanine (Figure 1K). The proportion of GSDMD-positive BMDM expressing phenylalanine was significantly higher (Figure 1L). Collectively, these results demonstrated that pyroptosis occurred and was promoted in both AMs of ARDS mice administered phenylalanine and in BMDMs treated with phenylalanine.

Phenylalanine administration induced pyroptosis *via* the calcium-sensitive receptor

Phenylalanine is a positive allosteric regulator of the CaSR, which is involved in various cellular interactions (11). Moreover, GSDMD and caspase-1 are downstream effector molecules present in their cleaved forms when activated. Therefore, the authors hypothesized that phenylalanine may promote the cleavage of GSDMD and caspase-1 by activating the CaSR to induce pyroptosis. To verify the role of the CaSR, its specific inhibitor Calhex231 was applied to ARDS mice to observe relief of lung injury and inflammation. The protein concentrations of IL-1β and IL-18 in BALF decreased (Figures 2A–C). H&E staining of the lung tissue exhibited less diffusion in Calhex231-administered ARDS mice (Figure 2D). In addition, a significantly lower proportion of pyroptosis in BALF cells from mice administered Calhex231 was found (Figures 2E, F). By determining calcium influx into cells, measured in relative fluorescence units (RFU), cells treated with phenylalanine exhibited significantly higher calcium influx, and CaSR-specific stimulants further promoted calcium influx into cells (Figure 2G). In addition, Western blot analysis of BMDMs in different media revealed that the expression of cleaved-GSDMD and cleaved-caspase-1 was significantly downregulated when the medium was supplemented with Calhex231 (Figures 2H, I). When phenylalanine-administered ARDS mice were applied with Calhex231, the expression of GSDMD in the lungs was significantly downregulated (Figures 2J, K). GSDMD-positive BMDMs drastically decreased in the presence of Calhex231. Accordingly, fewer GSDMD-positive BMDMs were detected in Calhex231-administered cells in comparison to only Phe-treated BMDMs (Figures 2L, M). We further assessed the role of caspases and NLRP3 with their inhibitors Z-Val-Ala-Asp-FMK (Supplementary Figure 3) and MCC950 (Supplementary Figure 4). This indicates that pyroptosis was associated with the CASR *via* activation of NLRP3 and Caspase-1.

Discussion

To our knowledge, this is the first study to reveal a novel role for phenylalanine in mediating ARDS *via* induction of pyroptosis in AMs. We first observed that increased phenylalanine levels in ARDS patients was associated with mortality. In mice with ARDS, phenylalanine administration has been shown to be closely associated with increased AM pyroptosis, along with elevated levels of IL-1β and IL-18. We performed *in vivo* and *in vitro* investigations to further confirm that phenylalanine was responsible for the increase in AM pyroptosis *via* the activation of the CaSR-initiated NLRP3 inflammasome pathway. CaSR inhibition significantly alleviates LPS-induced inflammation and decreases the frequency of AM pyroptosis. For the first time, we have elucidated a complete pathway of how elevated phenylalanine levels trigger AM pyroptosis, resulting in inflammation when exposed to higher levels of phenylalanine and leading to ARDS lethality, which expands the current understanding of the role of small-molecule metabolites in pulmonary inflammation. These findings may provide new treatment targets for patients with ARDS.

Metabolites have been proposed as novel biomarkers reflecting the severity of ARDS owing to their quick response to the influence of external factors (12). In fact, metabolites are not only downstream products but also active drivers of biological processes serving as molecular signals (13). Our study highlights the association between

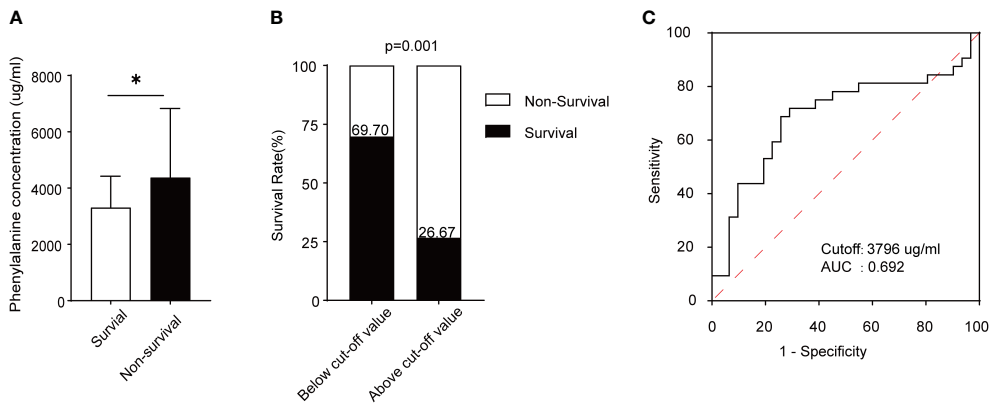

FIGURE 5
Phenylalanine concentration and its prediction capacity in survival and non-survival ARDS patients. **(A)** Serum phenylalanine concentration in the two groups of patients. **(B)** Survival rate of ARDS patients according to the cut-off value. **(C)** ROC curve and AUC according to the cut-off value. *means p<0.05

elevated phenylalanine levels and poor outcomes in patients with ARDS. In our study, the administration of phenylalanine aggravated lung inflammation, reflected by elevated levels of IL-1β and IL-18 in BALF. These results implicate phenylalanine as a "bioactive metabolite" in physiological reactions in ARDS. Phenylalanine is an essential amino acid (14) that is absorbed into plasma and is mainly converted to tyrosine in the liver (15). The lungs do not directly use phenylalanine; however, consistent with previous research by Tan et al. (16), our study found that the lungs take up phenylalanine, which was demonstrated by the accumulation of phenylalanine in BALF after intravenous injection (Supplementary Figure 1). These results provided basic evidence that phenylalanine directly interacts with lung cells.

AMs, the major immunocytes regulating lung inflammation and acute lung injury (ALI), respond to invasive stimuli *via* pyroptosis (17), which is a caspase-1-dependent death pathway. Activated caspase-1 cleaves GSDMD to generate mature GSDMD that induces plasma membrane pore formation, resulting in cell swelling, plasma membrane rupture, and the release of pro-inflammatory cytokines such as IL-1β and IL-18 (18). It has been reported that excessive pyroptosis can cause partial or systemic inflammation and even lead to lethality (19). Zhu et al. found that AM pyroptosis was elevated when the lung structure was disrupted by cigarette smoke (20). In addition, Wu et al. reported that caspase-1 was activated in LPS-induced ALI, thereby facilitating AMs pyroptosis (21). In our study, phenylalanine administration promoted pyroptosis in AMs, which in turn is believed to induce severe lung injury. Depletion of AMs eliminated the adverse outcomes caused by phenylalanine. Therefore, AM pyroptosis resulting from elevated phenylalanine levels is the main trigger of severe lung injury in ARDS.

The NLRP3 inflammasome is a critical component of the innate immune system (22). The activation of the NLRP3 pyrolytic pathway requires two signals simultaneously. The first includes pathogenic agents, such as LPS, or cytokines, and the former includes lysosomes and ATP. The first signal increases the activation of caspase-1 and GSDMD in the pyroptotic pathway, whereas the second signal is a key step in the cleavage and assembly of inflammasomes (23). Recent studies have shown that elevated calcium (Ca^{2+}) concentrations can promote the combination of NLRP3 and ASC proteins to form activated inflammasomes, thereby ensuring the conduction of downstream pathways (24). Our results suggest that phenylalanine upregulates intracellular Ca^{2+} concentrations by activating CaSR, a regulator of calcium homeostasis, and its inhibition can downregulate pyroptosis. Phenylalanine does not affect NLRP3 expression. Among all aromatic L-amino acids, phenylalanine is most likely to bind and activate the CaSR (25). Therefore, our results indicate that phenylalanine serves as a secondary signal that may bind to the CaSR and recruit Ca^{2+}, accelerating the assembly of NLRP3 and ASC, and finally leading to the activation of NLRP3 mediated pyroptosis. CaSR, a member of the aromatic L-amino acid receptor family, is a G-protein-coupled receptor distributed in the lung tissue and expressed in macrophages (26). It is widely associated with inflammation in diverse diseases involving the cardiovascular system (27), such as vascular calcification, atherosclerosis, myocardial infarction, hypertension, obesity (28) and the respiratory system, such as asthma (29) and acute lung injury (30). Results of our study demonstrated that CaSR inhibition alleviated phenylalanine-induced lung injury, inflammation, and AM pyroptosis, further confirming that phenylalanine plays a role *via* the CaSR.

We have limited clinical samples and there may still exist other minor pathways to pyroptosis in above situation. Nevertheless, we demonstrated a novel mechanism by which elevated phenylalanine levels promote inflammation *via* the CaSR and aggravates ARDS through the induction of AM pyroptosis, which may be a new target for treating ARDS.

Data availability statement

The raw data supporting the conclusions of this article will be made available by the authors, without undue reservation.

Ethics statement

The studies involving human participants were reviewed and approved by Ruijin Hospital Ethics Committee of Shanghai Jiao Tong University School of Medicine. The patients/participants provided their written informed consent to participate in this study. The animal study was reviewed and approved by Shanghai Institutes for Biological Sciences Council on Animal Care.

Author contributions

YT designed research studies, conducted experiments, acquired clinical data, analyzed data, wrote the manuscript. YY collected clinical samples. RL designed research studies. ZT analyzed data. LZ conducted experiments. XW, XQ, YL, TM and HQ collected clinical samples. MZ provided reagents. JX designed research studies and wrote the manuscript. JL designed research studies and revised the manuscript. YT is in the first place of first author and YY is in the second place of the co-first author. JL is in the first place of respondence, JX is in the second place of respondence and MZ is in the third place of respondence. All authors contributed to the article and approved the submitted version.

Funding

This study was supported by the National Natural Science Foundation of China (82202405) awarded to JX, Scientific Research Project Plan of Shanghai Municipal Health Commission (20204Y0145 and 20224Y0029) awarded to JX. National Natural Science Foundation of China (81970005), Leading Talents in Health and Wellness of Shanghai Municipal Health Commission (2022XD021) awarded to JL, and the scientific research project plan of Shanghai Municipal Health Commission (20204Y0145) awarded to XW.

Acknowledgments

Special thanks to Mass Spectrometry Platform, National Research Center for Translational Medicine, Ruijin Hospital Affiliated to Shanghai Jiao Tong University (SJTU) School of Medicine, Shanghai, China.

Conflict of interest

The authors declare that the research was conducted in the absence of any commercial or financial relationships that could be construed as a potential conflict of interest.

Publisher's note

Supplementary material

The Supplementary Material for this article can be found online at: https://www.frontiersin.org/articles/10.3389/fimmu.2023.1114129/full#supplementary-material

References

1. Bellani G, Laffey JG, Pham T, Fan E, Brochard L, Esteban A, et al. Epidemiology, patterns of care, and mortality for patients with acute respiratory distress syndrome in intensive care units in 50 countries. *JAMA* (2016) 315:788–800. doi: 10.1001/jama.2016.0291

2. Pearce EL, Pearce EJ. Metabolic pathways in immune cell activation and quiescence. *Immunity* (2013) 38:633–43. doi: 10.1016/j.immuni.2013.04.005

3. Xu J, Pan T, Qi X, Tan R, Wang X, Liu Z, et al. Increased mortality of acute respiratory distress syndrome was associated with high levels of plasma phenylalanine. *Respir Res* (2020) 21:99. doi: 10.1186/s12931-020-01364-6

4. Luporini RL, Pott-Junior H, Di Medeiros Leal MCB, Castro A, Ferreira AG, Cominetti MR, et al. Phenylalanine and COVID-19: tracking disease severity markers. *Int Immunopharmacol* (2021) 101:108313. doi: 10.1016/j.intimp.2021.108313

5. Wyse ATS, Dos Santos TM, Seminotti B, Leipnitz G. Insights from animal models on the pathophysiology of hyperphenylalaninemia: role of mitochondrial dysfunction, oxidative stress and inflammation. *Mol Neurobiol* (2021) 58:2897–909. doi: 10.1007/s12035-021-02304-1

6. Joshi N, Walter JM, Misharin AV. Alveolar macrophages. *Cell Immunol* (2018) 330:86–90. doi: 10.1016/j.cellimm.2018.01.005

7. Kesavardhana S, Malireddi RKS, Kanneganti TD. Caspases in cell death, inflammation, and pyroptosis. *Annu Rev Immunol* (2020) 38:567–95. doi: 10.1146/annurev-immunol-073119-095439

8. Wu XB, Sun HY, Luo ZL, Cheng L, Duan XM, Ren JD. Plasma-derived exosomes contribute to pancreatitis-associated lung injury by triggering NLRP3-dependent pyroptosis in alveolar macrophages. *Biochim Biophys Acta Mol Basis Dis* (2020) 1866:165685. doi: 10.1016/j.bbadis.2020.165685

9. Machado MG, Patente TA, Rouille Y, Heumel S, Melo EM, Deruyter L, et al. Acetate improves the killing of streptococcus pneumoniae by alveolar macrophages *via* NLRP3 inflammasome and glycolysis-HIF-1alpha axis. *Front Immunol* (2022) 13:773261. doi: 10.3389/fimmu.2022.773261

10. Matthay MA, Zemans RL, Zimmerman GA, Arabi YM, Beitler JR, Mercat A, et al. Acute respiratory distress syndrome. *Nat Rev Dis Primers* (2019) 5:18. doi: 10.1038/s41572-019-0069-0

11. Conigrave AD, Quinn SJ, Brown EM. L-amino acid sensing by the extracellular Ca2+-sensing receptor. *Proc Natl Acad Sci USA* (2000) 97:4814–9. doi: 10.1073/pnas.97.9.4814

12. Wei Y, Huang H, Zhang R, Zhu Z, Zhu Y, Lin L, et al. Association of serum mannose with acute respiratory distress syndrome risk and survival. *JAMA Netw Open* (2021) 4:e2034569. doi: 10.1001/jamanetworkopen.2020.34569

13. Husted AS, Trauelsen M, Rudenko O, Hjorth SA, Schwartz TW. GPCR-mediated signaling of metabolites. *Cell Metab* (2017) 25:777–96. doi: 10.1016/j.cmet.2017.03.008

14. Eriksson JG, Guzzardi MA, Iozzo P, Kajantie E, Kautiainen H, Salonen MK. Higher serum phenylalanine concentration is associated with more rapid telomere shortening in men. *Am J Clin Nutr* (2017) 105:144–50. doi: 10.3945/ajcn.116.130468

15. Morgan MY, Milsom JP, Sherlock S. Plasma ratio of valine, leucine and isoleucine to phenylalanine and tyrosine in liver disease. *Gut* (1978) 19:1068–73. doi: 10.1136/gut.19.11.1068

16. Tan R, Li J, Liu F, Liao P, Ruiz M, Dupuis J, et al. Phenylalanine induces pulmonary hypertension through calcium-sensing receptor activation. *Am J Physiol Lung Cell Mol Physiol* (2020) 319:L1010–20. doi: 10.1152/ajplung.00215.2020

17. Li H, Li Y, Song C, Hu Y, Dai M, Liu B, et al. Neutrophil extracellular traps augmented alveolar macrophage pyroptosis *via* AIM2 inflammasome activation in LPS-induced ALI/ARDS. *J Inflammation Res* (2021) 14:4839–58. doi: 10.2147/JIR.S321513

18. Liu X, Zhang Z, Ruan J, Pan Y, Magupalli VG, Wu H, et al. Inflammasome-activated gasdermin d causes pyroptosis by forming membrane pores. *Nature* (2016) 535:153–8. doi: 10.1038/nature18629

19. Wang Z, Gu Z, Hou Q, Chen W, Mu D, Zhang Y, et al. Zebrafish GSDMEb cleavage-gated pyroptosis drives septic acute kidney injury in vivo. *J Immunol* (2020) 204:1929–42. doi: 10.4049/jimmunol.1901456

20. Zhu Z, Lian X, Su X, Wu W, Zeng Y, Chen X. Exosomes derived from adipose-derived stem cells alleviate cigarette smoke-induced lung inflammation and injury by inhibiting alveolar macrophages pyroptosis. *Respir Res* (2022) 23:5. doi: 10.1186/s12931-022-01926-w

21. Wu D, Pan P, Su X, Zhang L, Qin Q, Tan H, et al. Interferon regulatory factor-1 mediates alveolar macrophage pyroptosis during LPS-induced acute lung injury in mice. *Shock* (2016) 46:329–38. doi: 10.1097/SHK.0000000000000595

22. Li Z, Guo J, Bi L. Role of the NLRP3 inflammasome in autoimmune diseases. *BioMed Pharmacother* (2020) 130:110542. doi: 10.1016/j.biopha.2020.110542

23. Huang Y, Xu W, Zhou R. NLRP3 inflammasome activation and cell death. *Cell Mol Immunol* (2021) 18:2114–27. doi: 10.1038/s41423-021-00740-6

24. Jager E, Murthy S, Schmidt C, Hahn M, Strobel S, Peters A, et al. Calcium-sensing receptor-mediated NLRP3 inflammasome response to calciprotein particles drives inflammation in rheumatoid arthritis. *Nat Commun* (2020) 11:4243. doi: 10.1038/s41467-020-17749-6

25. Chen X, Wang L, Cui Q, Ding Z, Han L, Kou Y, et al. Structural insights into the activation of human calcium-sensing receptor. *Elife* (2021) 10. doi: 10.7554/eLife.68578a

26. D'Espessailles A, Santillana N, Sanhueza S, Fuentes C, Cifuentes M. Calcium sensing receptor activation in THP-1 macrophages triggers NLRP3 inflammasome and human preadipose cell inflammation. *Mol Cell Endocrinol* (2020) 501:110654. doi: 10.1016/j.mce.2019.110654

27. Sundararaman SS, van der Vorst EPC. Calcium-sensing receptor (CaSR), its impact on inflammation and the consequences on cardiovascular health. *Int J Mol Sci* (2021) 22(5):2478. doi: 10.3390/ijms22052478

28. Villarroel P, Villalobos E, Reyes M, Cifuentes M. Calcium, obesity, and the role of the calcium-sensing receptor. *Nutr Rev* (2014) 72:627–37. doi: 10.1111/nure.12135

29. Riccardi D, Ward JPT, Yarova PL, Janssen LJ, Lee TH, Ying S, et al. Topical therapy with negative allosteric modulators of the calcium-sensing receptor (calcilytics) for the management of asthma: the beginning of a new era? *Eur Respir J* (2022) 60(2):2102103. doi: 10.1183/13993003.02103-2021

30. Lee JW, Park HA, Kwon OK, Park JW, Lee G, Lee HJ, et al. NPS 2143, a selective calcium-sensing receptor antagonist inhibits lipopolysaccharide-induced pulmonary inflammation. *Mol Immunol* (2017) 90:150–7. doi: 10.1016/j.molimm.2017.07.012

frontiers | Frontiers in Immunology

TYPE Mini Review
PUBLISHED 01 September 2023
DOI 10.3389/fimmu.2023.1244586

OPEN ACCESS

EDITED BY
Slaven Crnkovic,
Medical University of Graz, Austria

REVIEWED BY
Cassiano Felippe Gonçalves-de-Albuquerque,
Rio de Janeiro State Federal University, Brazil

*CORRESPONDENCE
Steven P. Templeton
sptemple@iupui.edu

RECEIVED 22 June 2023
ACCEPTED 21 August 2023
PUBLISHED 01 September 2023

CITATION
Lim J-Y and Templeton SP (2023) Regulation of lung inflammation by adiponectin.
Front. Immunol. 14:1244586.
doi: 10.3389/fimmu.2023.1244586

Regulation of lung inflammation by adiponectin

Joo-Yeon Lim and Steven P. Templeton*

Department of Microbiology and Immunology, Indiana University School of Medicine-Terre Haute, Terre Haute, IN, United States

Adiponectin is an insulin sensitizing hormone that also plays a role in the regulation of inflammation. Although adiponectin can exert pro-inflammatory effects, more studies have reported anti-inflammatory effects, even in non-adipose tissues such as the lung. Obesity is considered an inflammatory disease, is a risk factor for lung diseases, and is associated with decreased levels of plasma adiponectin. The results of recent studies have suggested that adiponectin exerts anti-inflammatory activity in chronic obstructive pulmonary disease, asthma and invasive fungal infection. The signaling receptors of adiponectin, AdipoR1 and AdipoR2, are expressed by epithelial cells, endothelial cells, and immune cells in the lung. In this mini-review, we discuss the anti-inflammatory mechanisms of adiponectin in lung cells and tissues.

KEYWORDS

adiponectin, lung immune response, adiponectin receptors, COPD, asthma, inflammatory pulmonary disease, infectious lung disease, obesity

Introduction

Adiponectin (APN) is a protein abundantly produced by adipocytes. It is present at high concentrations in plasma and regulates glucose levels, lipid metabolism, and insulin sensitivity. Plasma APN levels are relatively high in lean and healthy individuals. Decreased circulating levels of APN in obese individuals could enhance the risk of insulin resistance, type 2 diabetes, and cardiovascular disease (1). APN has also been reported to be produced by lymphocytes, skeletal muscle cells, cardiomyocytes, osteoblasts, and liver cells (2–5).

APN binds to signaling adiponectin receptors AdipoR1 and AdipoR2 (6) and the non-signaling receptor T-cadherin (7). While AdipoR1 binds to the globular form of APN, AdipoR2 preferentially binds to the high-molecular weight (HMW) form (8). The HMW isoform is consist of several linked hexamers and trimers (9). Interestingly, females have higher circulating levels of total APN with higher proportions of HMW isoform compares to males (10–12). Unlike the expression of APN, there are no sex differences in the expression of AdipoRs in adipose tissue (13).

Obesity is associated with a higher incidence of various diseases, including pulmonary disorders, such as asthma, chronic obstructive pulmonary disease, and pulmonary hypertension, and is also associated with decreased plasma adiponectin (14–18). Obesity-associated dysregulation of immune responses, inflammatory vigor, and adipose

tissue immune cell infiltration are also believed to contribute to infectious disease pathogenesis (19).

According to the World Health Organization (WHO), the two most common chronic lung diseases are COPD and asthma, causing restricted airflow and breathing problem. APN has been implicated to play a role in the pathophysiology of COPD. Many studies revealed decreased serum APN in COPD patients (20). With a steadily increasing population of immunocompromised patients, disease caused by fungal infections remain a great threat to public health. Among lung fungal pathogens, such as *Aspergillus*, *Cryptococcus*, and *Pneumocystis*, Aspergillosis (approximately 57%) by Aspergillus spp. was most common (21). While the APN roles have been more thoroughly investigated in COPD and asthma, fewer studies have implicated in APN lung diseases. APN is required for metabolism and has a regulatory role in inflammation, primarily exerting anti-inflammatory effects. Here, we specifically review published studies that examine the anti-inflammatory activity of APN in inflammatory pulmonary diseases and cells of the lung.

APN and lung disorder

APN and COPD

Chronic Obstructive Pulmonary Disease (COPD) is a globally increasing cause of mortality with increasing prevalence over the past 20 years (22). Population aging, smoking and exposure to air pollution are leading risk factors for COPD (22–24). COPD patients showed increased numbers of lung inflammatory cells such as neutrophils, macrophages, and $CD8^+$ T cells, with increased production of chemokines and cytokines (25). A mouse model of COPD with tobacco smoke exposure showed increased APN production in bronchoalveolar lavage fluid (BALF) and APN gene expression by airway epithelial cells (26), suggesting that APN has the potential to modulate the inflammatory response in COPD. Another study used an elastase-induced emphysema model to identify the possible role of APN in the pathogenesis of COPD (27). Elastase-induced emphysema is associated with reduced APN concentration. APN-deficient (APN KO) mice show a progressive COPD-like phenotype characterized by progressive emphysema, increased endothelial apoptosis and increased TNF-α activity. APN is associated with inflammation in COPD and is positively correlated with as the neutrophil-recruiting chemokine IL-8 (26). APN can therefore be a biomarker for disease severity and progression in patients of COPD (28).

APN and asthma

Asthma is a chronic inflammatory disorder that affects airways in the lungs narrowed and swollen by inflammation and blocked by excess mucus. The most common asthma triggers include air pollen, dust products, animal dander, tobacco smoke and a wide range of fungi (29). In an obesity-related asthma mouse model used by Zhu et al., APN level in serum and BALF as well as adiponectin receptor (AdipoR) mRNA expression in lung were decreased and exogenous APN treatment increased both the APN level and AdipoR expression (30). In a mouse model of asthma by Medoff et al., ovalbumin (OVA)-sensitized and challenged APN KO mice exhibited increased pulmonary vascular remodeling, eosinophilic inflammation, and inflammatory chemokine gene expression compared to control mice (31). Furthermore, Obesity is associated with low-grade inflammation and enhances chronic inflammation in the airways of asthmatic obese patients. Expression of AdipoR2 and T-cadherin genes in bronchial epithelial cells was higher among obese patients with asthma than obese controls (32). Obesity in mice was associated with increased BALF macrophages, neutrophils and eosinophils, and increased Th2 cytokine production, including IL-13 and IL-5. Administration of exogenous APN reduced inflammation in obese mice, suggesting a therapeutic potential for the adiponectin pathway (33), and an APN receptor agonist reduced IL-4, IL-17, IL-23, and TNF-α in an OVA/lipopolysaccharide (LPS)-induced obese asthmatic model (34). In summary, APN treatment alleviated pathological changes in lung with reduction of eosinophils, total cell numbers in BALF, the eosinophil-attracting chemokine eotaxin and myeloperoxidase levels, which suggests that APN regulates cell migration into the airway and clearance of pulmonary inflammation in obesity-related asthma (30, 31).

In obese asthmatics, low APN was found more frequently than high (35) and non-obese individuals had higher levels of serum APN compared to obese (36). However, two other studies found no correlation between APN and obesity (37, 38). The differences in results of these studies might be related to demographic differences in age, gender, race, and disease severity. Although clinical data depend mainly on the serum APN, results from animal models and cell cultures demonstrate a potential benefit of APN pathway-stimulating therapy in asthmatics (35).

APN and pulmonary aspergillosis

In invasive aspergillosis patients, excessive inflammation is associated with increased mortality (39). However, the effects of APN on anti-fungal immune responses in the lung remains unclear.

Fungal spores are easily aerosolized and inhaled (40). Different manifestations of *Aspergillus* infection include allergic bronchopulmonary aspergillosis, chronic pulmonary aspergillosis, and invasive aspergillosis. Allergic bronchopulmonary aspergillosis is considered poorly controlled asthma, while invasive aspergillosis occurs in immunocompromised patients such as those with COPD, solid organ or bone marrow transplant recipients, intensive care unit patients, and patients with severe viral infection (HIV, influenza A virus, COVID-19) (41–45). Invasive aspergillosis has an extremely high mortality rate (50-90%) in immunocompromised patients (46). *Aspergillus fumigatus* is most prevalent and the major cause of aspergillosis (47). APN KO mice with invasive aspergillosis exhibit increased disease pathology

including decreased survival rate, increased fungal burden in the lung, increased cytokine production (IL-6 and TNF-α), and increased eosinophil recruitment (48). Aspiration of *Aspergillus fumigatus* conidia or chitin, one of the fungal cell wall components induced increased eosinophil recruitment in APN KO mice compared to wild-type controls (48, 49), and recombinant murine APN inhibited chitin-mediated eosinophil recruitment (49). Thus, it is likely that APN inhibits excessive inflammation in invasive aspergillosis, either directly or indirectly by enhancing antifungal immunity.

The roles of adiponectin in COPD, asthma, and pulmonary aspergillosis is summarized in Figure 1. Recent studies suggest a role for APN in regulating the inflammatory response in aspergillosis, COPD and asthma in either animal models or human patients (28, 35, 38). However, there are limited studies examining the role of APN during fungal infection in murine lungs (48, 49). Moreover, the number of the immunocompromised individuals is rapidly increasing, due to increased use of immunosuppressive therapies. Despite immune suppression, aspergillosis patients can succumb to an uncontrolled inflammatory response. Moreover, COPD and asthma patients showed increased hypersensitivity to *Aspergillus fumigatus* (29, 50, 51). More research is need to further unravel the anti-inflammatory mechanisms of the APN pathway in lung disease, especially in the context of fungal infection.

APN and bacterial and viral infections

Tuberculosis is a bacterial infectious disease that most often affects the lungs, which is caused by *Mycobacterium tuberculosis*. One-third of the world population is infected with this pathogen. Infection of *M. tuberculosis* alters adipose tissue morphology and contributes to an acute loss of body fat, which worsens pulmonary pathology. Comparing the lungs of *M. tuberculosis*-infected fat-ablated mice to infected fat-unablated mice, the levels of cytokines, such as TNF-α, IFN-γ, CD68, IL-12, and IL-10 were increased (52). APN may promote a reduction of TNF-α in the lungs in *M. tuberculosis*-infected mice (52). In acute lung injury model, APN attenuates LPS-induced lung injury in acute lung injury model (53). These reports suggest that APN regulates pulmonary pathology during bacterial infection.

Epidemiological evidence suggests an association between obesity and increased susceptibility to viral pneumonias associated with influenza, SARS-CoV-2, and COVID-19 cases (19, 54, 55). APN level is reduced in the patients infected with influenza A virus and COVID-19 with respiratory failure (56–58). Overexpression of IL-6, a key adipocyte-secreted inflammatory mediator, is an important risk factor worsening outcomes in influenza virus infection (59). In COVID-19, APN is generated by lymphocytes and downregulates the bone marrow production of

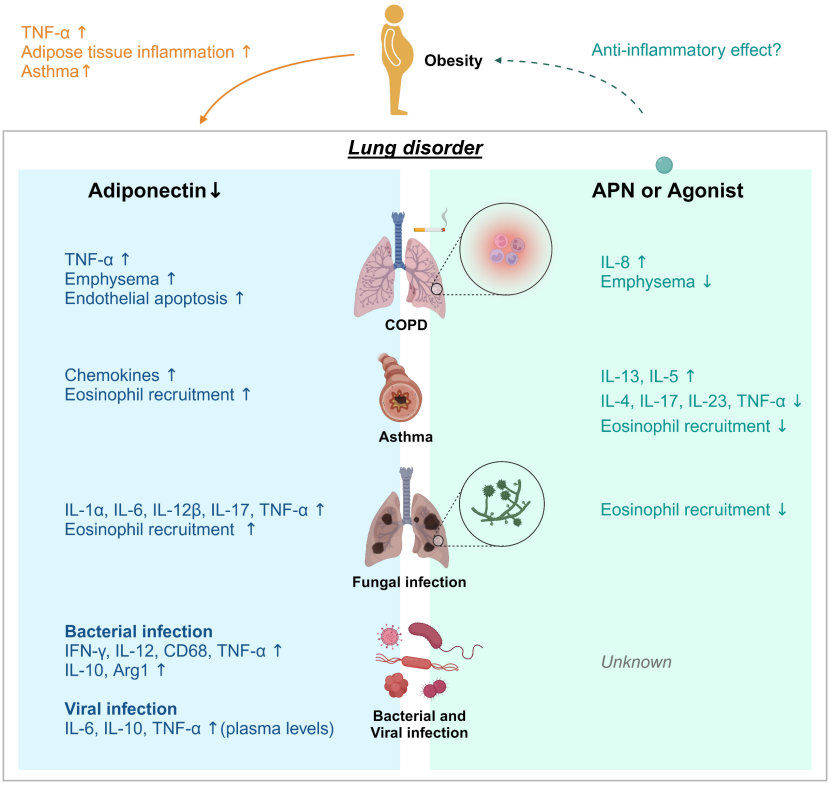

FIGURE 1
Adiponectin effect on lung disease. Obesity and aging are associated with loss of muscle mass, insulin resistance, and features of metabolic syndromes. Adiponectin (APN) activity is linked to metabolism and inhibition of inflammation. Decreases/deficiencies in plasma APN, even due to obesity, may contribute to adipose tissue inflammation, induction of asthma and TNF-α production in adipose and non-adipose tissues such as the lung. APN regulates inflammation in chronic pulmonary disease (COPD), asthma, fungal, bacterial, and viral infection. Adiponectin deficiency in COPD, aspergillosis, viral infection or tuberculosis resulted in increased expression of the proinflammatory cytokines TNF-α and IL-6, further suggesting that APN functions exerts anti-inflammatory activity. However, the effects of APN or AdipoRon on viral infection remain unknown. Treatment with APN or its agonist affects cytokine production; a decrease of IL-13 and IL-5 in asthma model and an increase of IL-8 in COPD, and increased IL-4, 1L-17, IL-23, and TNF-α in asthma. APN treatment also inhibited lung eosinophil recruitment in response to chitin.

granulocytes, with the activation of regulatory T cells (60). While the levels of cytokines in lung in COVID-19 patients have not been analyzed, the plasma levels of IL-6, TNF-α, and IL-10 were highly increased in severe COVID-19 patients with comparable levels to non-COVID-19 patients (61). So far, no study evaluated the effect of APN or AdipoRon on SARS-CoV-2 infection (62). These studies suggest that the APN pathway could be manipulated to provide protection against detrimental inflammation in response to viral infection.

Anti-inflammatory activity of adiponectin on lung cells

APN/AdipoRs in lung immune cells

APN and AdipoRs are expressed in the lung, suggesting an important role for the APN pathway in lung biological processes (63). Alveolar macrophages from APN KO mice released higher matrix metalloproteinases and TNF-α, which was suppressed by APN pretreatment (63). In humans, APN release from lung explants is negatively correlated with body mass index (64). Lung macrophages express both of the signaling APN receptors AdipoR1 and AdipoR2 (64). Lung macrophages treated with APN or its AdipoR1/R2 agonist AdipoRon resulted in decreased LPS- and poly (I:C)-induced production of TNF-α, IL-6, CXCL1 and CXCL8 (64). In the murine macrophage-like cell line RAW264, the globular domain of APN binds to the AdipoR1 and inhibits the TLR-induced NF-κB activity (65).

In lean mice, lung regulatory T cells ($CD3^+$ $CD4^+$ $Foxp3^+$ cells) increased AdipoR1 expression, while obese mice with allergic inflammation had reduced AdipoR1 expression in lung regulatory T cells and increased expression in BALF eosinophils (66). Thus, adiponectin exerts anti-inflammatory effects on lung cells, likely due to signaling through adiponectin receptors.

APN/AdipoRs in lung fibroblast, epithelial cells, and endothelial cells

Idiopathic pulmonary fibrosis is a common pulmonary disease, with high mortality, especially in older people. The idiopathic pulmonary fibrosis mouse model of bleomycin challenge induced a remarkable collagen fiber accumulation with extensive alveolar damage. Furthermore, APN treatment attenuated bleomycin-induced histopathology and inhibits TGF-β1-induced fibrosis in human lung fibroblasts with decreased TNF-α, IL-6, IL-1β, and IL-18 expression (67). Paraquat is an herbicide used worldwide and exposure to paraquat may cause acute injury and fibrosis in humans (68). In a pulmonary fibrosis model induced by paraquat, APN attenuated the fibrosis with decreased TGF-β1 and α-smooth muscle actin by regulating the NF-κB pathway (69). Human lung fibroblasts also express both AdipoR1 and AdipoR2, and APN treatment increased fibroblast expression of AdipoR1 but not AdipoR2. Knockdown of AdipoR1 using siRNA reversed the APN-mediated protective effect against paraquat-mediated fibrosis, demonstrating the importance of the APN-AdipoR1 pathway in fibroblasts for protection against pulmonary fibrosis (69).

In contrast, airway epithelial cells express significant levels of APN and AdipoR1, but not AdipoR2 in COPD patients and cultures of human lung epithelial cells (26). APN attenuated A549 cellular apoptosis and ameliorated cytotoxic effects induced by TNF-α and IL-1β by inhibiting NF-κB transactivation through AdipoR1. APN increased mRNA expression of the anti-inflammatory cytokine IL-10 in lung epithelial A549 cells (70). In summary, these studies provide evidence for a direct effect of APN on proliferation and inflammation of A549 epithelial cells with a protective role of APN in lung cells.

Hallmark features of acute lung injury include immune and endothelial cell activation and loss of vascular integrity (71). When acute lung injury was induced in control and APN KO mice by administration of LPS, APN KO mice appeared more ill with increased BALF protein concentration, increased production of TNF-α and IL-6, and decreased level of IL-10 in lung homogenates (53). Compared to the control mice with LPS injection, increased expression of IL-6, E-selectin, and Nox2 were detected in endothelial cells of APN KO mice (33). APN localizes to pulmonary vascular endothelium and APN deficiency leads to an age-dependent inflammatory vascular phenotype (72). APN deficiency also impairs mitochondrial function, promotes endothelial cell activation, and increases the susceptibility to LPS-induced acute lung injury (73). These finding suggests that parenchymal cells of the lung may play a role in the protective actions of APN.

Molecular mechanism of APN action on lung disease

In obesity-related asthma mice, APN treatment relieved inflammation and improved AMPK activity with a decrease in iNOS, Bcl-2, and NF-κB levels in lung (30). Treatment of Compound C, the AMPK inhibitor, reverses the effects of APN (30). It has been reported that APN directly binds to AdipoR1 and mediates signaling by activating AMPK.

M. tuberculosis infection increases the levels of both PPAR-γ and PPAR-α, key regulators of adipogenesis and lipid oxidation in the lungs (52). In LPS-induced acute lung injury model, NF-κB activation is APN is increased in APN KO mice (53).

In healthy mice, APN treatment induces the activation of p38 MAPK in $Helios^-$ regulatory T cells and upregulates the expression of AdipoR1 (74). In human epithelial cell line A549, activation of the APN-AdipoR1 pathway reduces cytotoxic effects inhibiting NF-κB activation and cytokine gene expression through ERK1/2 and AKT (70).

TABLE 1 Effects of APN in different lung cell types.

Cell types	Cell source	Function	Reference
Alveolar macrophages	APN KO mice	APN suppresses high matrix metalloproteinases and TNF-α	(63)
Human lung macrophages	LPS- and poly (I:C) infection *in vitro*	APN inhibits infection-induced production of TNF-α, IL-6, CXCL1 and CXCL8	(64)
Murine macrophage-like cells RAW264	Cell line	APN binds to AdipoR1 and inhibits the TLR-induced NF-κB activity	(65)
Lung regulatory T cells	Obese mice challenged with ovalbumin	Allergic inflammation reduces AdipoR1 expression	(66)
Human lung fibroblasts HELF	TGF-β1-induced fibrosis *in vitro*	APN inhibits the production of TNF-α, IL-6, IL-1β and IL-18	(67)
Human lung fibroblasts WI-38	Paraquat-induced fibrosis *in vitro*	APN increase AdipoR1 but not AdipoR2	(69)
Airway epithelial cells A549	Cell line	APN induces release of IL-8, and IL-10	(26)
		APN attenuates apoptosis and inhibits TNF-α and IL-1β by inhibiting NF-κB activity through AdipoR1	(70)
Endothelial cells	APN KO mice with LPS injection	Increased production of IL-6, E-selectin, and Nox2 is detected	(53)

APN, Adiponectin; AdipoR, adiponectin receptors; APN KO mice, Adiponectin-deficient mice; LPS, Lipopolysaccharide.

Conclusions and perspectives

There is increasing data suggesting that APN exerts an anti-inflammatory effect in the lung. Lung cells, including immune cells, epithelial cells, and endothelial cells, express AdipoRs, indicating they also have signaling ability upon binding to APN or an AdipoR agonist such as AdipoRon. Although both pro- and anti-inflammatory properties have been reported, anti-inflammatory function of APN was mainly observed in lung cells (Table 1). APN can trigger the activation of AMPK, PPAR, ERK, and AKT through its receptors. It is well known that APN improves different lung diseases; enhancing the signaling might prove a therapeutic target. However, further research will clarify the roles and mechanism of APN pathway-induced protection in lung diseases, including fungal, bacterial, and viral infection, which could result in novel therapies that protect against infection, excessive inflammation, and other lung pathologies.

Author contributions

J-YL and ST wrote the manuscript. J-YL prepared illustrations. J-YL and ST revised the manuscript. All authors contributed to the article and approved the submitted version.

Funding

The research was funded by National Institutes of Health/National Institute of Allergy and Infectious Diseases [R21 AI163574] (ST).

Acknowledgments

Figures were created with BioRender.com.

Conflict of interest

The authors declare that the research was conducted in the absence of any commercial or financial relationships that could be construed as a potential conflict of interest.

Publisher's note

References

1. Li S, Shin HJ, Ding EL, Van Dam RM. Adiponectin levels and risk of type 2 diabetes: a systemic review and meta-analysis. *JAMA* (2009) 302:179–88. doi: 10.1001/jama.2009.976

2. Ma H, Gomez V, Lu L, Yang X, Wu X, Xiao SY. Expression of adiponectin and its receptors in livers of morbidly obese patients with non-alcoholic fatty liver disease. *J Gastroenterol Hepatol* (2009) 24:233–7. doi: 10.1111/J.1440-1746.2008.05548.X

3. Crawford LJA, Peake R, Price S, Morris TCM, Irvine AE. Adiponectin is produced by lymphocytes and is a negative regulator of granulopoiesis. *J Leukoc Biol* (2010) 88:807–11. doi: 10.1189/JLB.1109723

4. Berner HS, Lyngstadaas SP, Spahr A, Monjo M, Thommesen L, Drevon CA, et al. Adiponectin and its receptors are expressed in bone-forming cells. *Bone* (2004) 35:842–9. doi: 10.1016/J.BONE.2004.06.008

5. Delaigle AM, Jonas JC, Bauche IB, Cornu O, Brichard SM. Induction of adiponectin in skeletal muscle by inflammatory cytokines: *In vivo* and in *vitro* studies. *Endocrinology* (2004) 145:5589–97. doi: 10.1210/en.2004-0503

6. Yamauchi T, Kamon J, Ito Y, Yokomizo T, Kita S, Sugiyama T, et al. Cloning of adiponectin receptors that mediate antidiabetic metabolic effects. *Nature* (2003) 423:762–9. doi: 10.1038/nature01705

7. Hug C, Wang J, Ahmad NS, Bogan JS, Tsao TS, Lodish HF. T-cadherin is a receptor for hexameric and high-molecular-weight forms of Acrp30/adiponectin. *Proc Natl Acad Sci U S A* (2004) 101:10308–13. doi: 10.1073/PNAS.0403382101

8. Diep Nguyen T. Adiponectin: Role in physiology and pathophysiology. *Int J Prev Med* (2020) 11:136. doi: 10.4103/ijpvm.ijpvm_193_20

9. Garcia P, Sood A. Adiponectin in pulmonary disease and critically ill patients. *Curr Med Chem* (2012) 19:5493–500. doi: 10.2174/092986712803833263

10. Peake PW, Kriketos AD, Campbell LV, Shen Y, Charlesworth JA. The metabolism of isoforms of human adiponectin: studies in human subjects and in experimental animals. *Eur J Endocrinol* (2005) 153:409–17. doi: 10.1530/EJE.1.01978

11. Eglit T, Lember M, Ringmets I, Rajasalu T. Gender differences in serum high-molecular-weight adiponectin levels in metabolic syndrome. *Eur J Endocrinol* (2013) 168:385–91. doi: 10.1530/EJE-12-0688

12. Rudnicki M, Abdifarkosh G, Rezvan O, Nwadozi E, Roudier E, Haas TL. Female mice have higher angiogenesis in perigonadal adipose tissue than males in response to high-fat diet. *Front Physiol* (2018) 23:1452. doi: 10.3389/fphys.2018.01452

13. Rasmussen MS, Lihn AS, Pedersen SB, Bruun JM, Rasmussen M, Richelsen B. Adiponectin receptors in human adipose tissue: effects of obesity, weight loss, and fat depots. *Obesity* (2006) 14:28–35. doi: 10.1038/OBY.2006.5

14. Peters U, Dixon AE, Forno E. Obesity and asthma. *J Allergy Clin Immunol* (2018) 141:1169–79. doi: 10.1016/j.jaci.2018.02.004

15. Dixon AE, Peters U. The effect of obesity on lung function. *Expert Rev Respir Med* (2018) 12:755–67. doi: 10.1080/17476348.2018.1506331

16. Verberne LDM, Leemrijse CJ, Swinkels ICS, Van Dijk CE, De Bakker DH, Nielen MMJ. Overweight in patients with chronic obstructive pulmonary disease needs more attention: a cross-sectional study in general practice. *NPJ Prim Care Respir Med* (2017) 27:63. doi: 10.1038/S41533-017-0065-3

17. Medoff BD. Fat, fire and muscle - The role of adiponectin in pulmonary vascular inflammation and remodeling. *Pulm Pharmacol Ther* (2013) 26:420–6. doi: 10.1016/j.pupt.2012.06.006

18. Adamczak M, Więcek A, Funahashi T, Chudek J, Kokot F, Matsuzawa Y. Decreased plasma adiponectin concentration in patients with essential hypertension. *Am J Hypertens* (2003) 16:72–5. doi: 10.1016/s0895-7061(02)03197-7

19. Alarcon PC, Damen MSMA, Madan R, Deepe GS, Spearman P, Way SS, et al. Adipocyte inflammation and pathogenesis of viral pneumonias: an overlooked contribution. *Mucosal Immunol* (2021) 14:1224–34. doi: 10.1038/s41385-021-00404-8

20. Lin YH, Jiang TX, Hu SX, Shi YH. Association between serum adiponectin concentrations and chronic obstructive pulmonary disease: a meta-analysis. *Biosci Rep* (2020) 40:BSR20192234. doi: 10.1042/BSR20192234

21. Li Z, Li Y, Chen Y, Li J, Li S, Li C, et al. Trends of pulmonary fungal infections from 2013 to 2019: an AI-based real-world observational study in Guangzhou, China. *Emerg Microbes Infect* (2021) 10:450. doi: 10.1080/22221751.2021.1894902

22. Rodrigues S de O, da Cunha CMC, Soares GMV, Silva PL, Silva AR, Gonçalves-De-albuquerque CF. Mechanisms, pathophysiology and currently proposed treatments of chronic obstructive pulmonary disease. *Pharmaceuticals* (2021) 14:979. doi: 10.3390/PH14100979

23. Adeloye D, Song P, Zhu Y, Campbell H, Sheikh A, Rudan I. Global, regional, and national prevalence of, and risk factors for, chronic obstructive pulmonary disease (COPD) in 2019: a systematic review and modelling analysis. *Lancet Respir Med* (2022) 10:447–58. doi: 10.1016/S2213-2600(21)00511-7

24. Christenson SA, Smith BM, Bafadhel M, Putcha N. Chronic obstructive pulmonary disease. *Lancet* (2022) 399:2227–42. doi: 10.1016/S0140-6736(22)00470-6

25. Barnes PJ, Shapiro SD, Pauwels RA. Chronic obstructive pulmonary disease: molecular and cellular mechanisms. *Eur Respir J* (2003) 22:672–88. doi: 10.1183/09031936.03.00040703

26. Miller M, Cho JY, Pham A, Ramsdell J, Broide DH. Adiponectin and functional adiponectin receptor 1 are expressed by airway epithelial cells in chronic obstructive pulmonary disease. *J Immunol* (2009) 182:684–91. doi: 10.4049/JIMMUNOL.182.1.684

27. Nakanishi K, Takeda Y, Tetsumoto S, Iwasaki T, Tsujino K, Kuhara H, et al. Involvement of endothelial apoptosis underlying chronic obstructive pulmonary disease-like phenotype in adiponectin-null mice: Implications for therapy. *Am J Respir Crit Care Med* (2011) 183:1164–75. doi: 10.1164/rccm.201007-1091OC

28. Jaswal S, Saini V, Kaur J, Gupta S, Kaur H, Garg K. Association of adiponectin with lung function impairment and disease severity in chronic obstructive pulmonary disease. *Int J Appl Basic Med Res* (2018) 8:14–8. doi: 10.4103/IJABMR.IJABMR_65_17

29. Namvar S, Labram B, Rowley J, Herrick S. *Aspergillus fumigatus*—Host interactions mediating airway wall remodelling in asthma. *J Fungi (Basel)* (2022) 8:159. doi: 10.3390/jof8020159

30. Zhu L, Chen X, Chong L, Kong L, Wen S, Zhang H, et al. Adiponectin alleviates exacerbation of airway inflammation and oxidative stress in obesity-related asthma mice partly through AMPK signaling pathway. *Int Immunopharmacol* (2019) 67:396–407. doi: 10.1016/j.intimp.2018.12.030

31. Medoff BD, Okamoto Y, Leyton P, Weng M, Sandall BP, Raher MJ, et al. Adiponectin deficiency increases allergic airway inflammation and pulmonary vascular remodeling. *Am J Respir Cell Mol Biol* (2009) 41:397–406. doi: 10.1165/RCMB.2008-0415OC

32. Sideleva O, Suratt BT, Black KE, Tharp WG, Pratley RE, Forgione P, et al. Obesity and asthma: an inflammatory disease of adipose tissue not the airway. *Am J Respir Crit Care Med* (2012) 186:598–605. doi: 10.1164/RCCM.201203-0573OC

33. Shore SA, Terry RD, Flynt L, Xu A, Hug C. Adiponectin attenuates allergen-induced airway inflammation and hyperresponsiveness in mice. *J Allergy Clin Immunol* (2006) 118:389–95. doi: 10.1016/j.jaci.2006.04.021

34. Elaidy SM, Essawy SS, Hussain MA, El-Kherbetawy MK, Hamed ER. Modulation of the IL-23/IL-17 axis by fenofibrate ameliorates the ovalbumin/lipopolysaccharide-induced airway inflammation and bronchial asthma in rats. *Naunyn Schmiedebergs Arch Pharmacol* (2018) 391:309–21. doi: 10.1007/S00210-017-1459-Z

35. Otelea MR, Arghir OC, Zugravu C, Rascu A. Adiponectin and asthma: Knowns, unknowns and controversies. *Int J Mol Sci* (2021) 22:8971. doi: 10.3390/ijms22168971

36. Ozde C, Dogru M, Erdogan F, Ipek IO, Ozde S, Karakaya O. The relationship between adiponectin levels and epicardial adipose tissue thickness in non-obese children with asthma. *Asian Pac J Allergy Immunol* (2015) 33:289–95. doi: 10.12932/AP0599.33.4.2015

37. Zhang X, Zheng J, Zhang L, Liu Y, Chen GP, Zhang HP, et al. Systemic inflammation mediates the detrimental effects of obesity on asthma control. *Allergy Asthma Proc* (2018) 39:43–50. doi: 10.2500/AAP.2018.39.4096

38. Nasiri Kalmarzi R, Ataee P, Mansori M, Moradi G, Ahmadi S, Kaviani Z, et al. Serum levels of adiponectin and leptin in asthmatic patients and its relation with asthma severity, lung function and BMI. *Allergol Immunopathol (Madr)* (2017) 45:258–64. doi: 10.1016/J.ALLER.2016.09.004

39. Camargo JF, Husain S. Immune correlates of protection in human invasive aspergillosis. *Clin Infect Dis* (2014) 59:569–77. doi: 10.1093/CID/CIU337

40. Richardson M, Bowyer P, Sabino R. The human lung and *Aspergillus*: You are what you breathe in? *Med Mycol* (2019) 57:S145–54. doi: 10.1093/mmy/myy149

41. Koehler P, Cornely OA, Böttiger BW, Dusse F, Eichenauer DA, Fuchs F, et al. COVID-19 associated pulmonary aspergillosis. *Mycoses* (2020) 63:528–34. doi: 10.1111/myc.13096

42. Arastehfar A, Carvalho A, van de Veerdonk FL, Jenks JD, Koehler P, Krause R, et al. COVID-19 associated pulmonary aspergillosis (CAPA)—from immunology to treatment. *J Fungi (Basel)* (2020) 6:91. doi: 10.3390/jof6020091

43. Mardani M, Hakamifard A. COVID-19 and immunocompromised conditions: Ongoing challenging issue. *Eur J Inflammation* (2021) 19:1–3. doi: 10.1177/20587392211016114

44. Denning DW, Morgan EF. Quantifying deaths from aspergillosis in HIV positive people. *J Fungi (Basel)* (2022) 8:1131. doi: 10.3390/jof8111131

45. Koehler P, Bassetti M, Kochanek M, Shimabukuro-Vornhagen A, Cornely OA. Intensive care management of influenza-associated pulmonary aspergillosis. *Clin Microbiol Infect* (2019) 25:1501–9. doi: 10.1016/j.cmi.2019.04.031

46. Inoue K, Muramatsu K, Nishimura T, Fujino Y, Matsuda S, Fushimi K, et al. Association between early diagnosis of and inpatient mortality from invasive pulmonary aspergillosis among patients without immunocompromised host factors: a nationwide observational study. *Int J Infect Dis* (2022) 122:279–84. doi: 10.1016/j.ijid.2022.05.048

47. Dagenais TRTT, Keller NP. Pathogenesis of *Aspergillus fumigatus* in invasive aspergillosis. *Clin Microbiol Rev* (2009) 22:447–65. doi: 10.1128/CMR.00055-08

48. Amarsaikhan N, Tsoggerel A, Hug C, Templeton SP. The metabolic cytokine adiponectin inhibits inflammatory lung pathology in invasive aspergillosis. *J Immunol* (2019) 203:956–63. doi: 10.4049/JIMMUNOL.1900174

49. Amarsaikhan N, Stolz DJ, Wilcox A, Sands EM, Tsoggerel A, Gravely H, et al. Reciprocal inhibition of adiponectin and innate lung immune responses to chitin and. *Aspergillus fumigatus Front Immunol* (2019) 10:1057. doi: 10.3389/FIMMU.2019.01057

50. Redes JL, Basu T, Ram-Mohan S, Ghosh CC, Chan EC, Sek AC, et al. *Aspergillus fumigatus*-secreted alkaline protease 1 mediates airways hyperresponsiveness in severe asthma. *Immunohorizons* (2019) 3:368–77. doi: 10.4049/immunohorizons.1900046

51. Bafadhel M, McKenna S, Agbetile J, Fairs A, Desai D, Mistry V, et al. *Aspergillus fumigatus* during stable state and exacerbations of COPD. *Eur Respir J* (2014) 43:64–71. doi: 10.1183/09031936.00162912

52. Ayyappan JP, Ganapathi U, Lizardo K, Vinnard C, Subbian S, Perlin DS, et al. Adipose tissue regulates pulmonary pathology during TB Infection. *mBio* (2019) 16: e027771–18. doi: 10.1128/mBio.02771-18

53. Konter JM, Parker JL, Baez E, Li SZ, Ranscht B, Denzel M, et al. Adiponectin attenuates lipopolysaccharide-induced acute lung injury through suppression of endothelial cell activation. *J Immunol* (2012) 188:854–63. doi: 10.4049/JIMMUNOL.1100426

54. Lighter J, Phillips M, Hochman S, Sterling S, Johnson D, Francois F, et al. Obesity in patients younger than 60 years is a risk factor for COVID-19 hospital admission. *Clin Infect Dis* (2020) 71:896–7. doi: 10.1093/CID/CIAA415

55. Popkin BM, Du S, Green WD, Beck MA, Algaith T, Herbst CH, et al. Individuals with obesity and COVID-19: A global perspective on the epidemiology and biological relationships. *Obes Rev* (2020) 21:e13128. doi: 10.1111/OBR.13128

56. Tsatsanis C, Margioris AN, Kontoyiannis DP. Association between H1N1 infection severity and obesity-adiponectin as a potential etiologic factor. *J Infect Dis* (2010) 202:459–60. doi: 10.1086/653842

57. Kearns SM, Ahern KW, Patrie JT, Horton WB, Harris TE, Kadl A. Reduced adiponectin levels in patients with COVID-19 acute respiratory failure: A case-control study. *Physiol Rep* (2021) 9:e14843. doi: 10.14814/PHY2.14843

58. Perrotta F, Scialò F, Mallardo M, Signoriello G, D'Agnano V, Bianco A, et al. Adiponectin, leptin, and resistin are dysregulated in patients infected by SARS-CoV-2. *Int J Mol Sci* (2023) 24:1131. doi: 10.3390/ijms24021131

59. Yu X, Zhang X, Zhao B, Wang J, Zhu Z, Teng Z, et al. Intensive cytokine induction in pandemic H1N1 influenza virus infection accompanied by robust production of IL-10 and IL-6. *PLoS One* (2011) 6:e28680. doi: 10.1371/JOURNAL.PONE.0028680

60. Crawford LJA, Peake R, Price S, Morris TCM, Irvine AE. Adiponectin is produced by lymphocytes and is a negative regulator of granulopoiesis. *J Leukoc Biol* (2010) 88:807–11. doi: 10.1189/JLB.1109723

61. Flikweert AW, Kobold ACM, van der Sar-van der Brugge S, Heeringa P, Rodenhuis-Zybert IA, Bijzet J, et al. Circulating adipokine levels and COVID-19 severity in hospitalized patients. *Int J Obes* (2023) 47:126–37. doi: 10.1038/s41366-022-01246-5

62. Al-Kuraishy HM, Al-Gareeb AI, Bungau SG, Radu AF, Batiha GES. The potential molecular implications of adiponectin in the evolution of SARS-CoV-2: Inbuilt tendency. *J King Saud Univ Sci* (2022) 34:102347. doi: 10.1016/j.jksus.2022.102347

63. Summer R, Little FF, Ouchi N, Takemura Y, Aprahamian T, Dwyer D, et al. Alveolar macrophage activation and an emphysema-like phenotype in adiponectin-deficient mice. *Am J Physiol Lung Cell Mol Physiol* (2008) 294:L1035–42. doi: 10.1152/AJPLUNG.00397.2007

64. Salvator H, Grassin-Delyle S, Brollo M, Couderc LJ, Abrial C, Victoni T, et al. Adiponectin inhibits the production of TNF-α, IL-6 and chemokines by human lung macrophages. *Front Pharmacol* (2021) 12:718929. doi: 10.3389/FPHAR.2021.718929

65. Yamaguchi N, Argueta JGM, Masuhiro Y, Kagishita M, Nonaka K, Saito T, et al. Adiponectin inhibits Toll-like receptor family-induced signaling. *FEBS Lett* (2005) 579:6821–6. doi: 10.1016/J.FEBSLET.2005.11.019

66. Ramos-Ramírez P, Malmhäll C, Johansson K, Adner M, Lötvall J, Bossios A. Lung regulatory t cells express adiponectin receptor 1: Modulation by obesity and airway allergic inflammation. *Int J Mol Sci* (2020) 21:8990. doi: 10.3390/ijms21238990

67. Wang X, Yang J, Wu L, Tong C, Zhu Y, Cai W, et al. Adiponectin inhibits the activation of lung fibroblasts and pulmonary fibrosis by regulating the nuclear factor kappa B (NF-κB) pathway. *Bioengineered* (2022) 13:10098–110. doi: 10.1080/21655979.2022.2063652

68. Dinis-Oliveira RJ, Duarte JA, Sánchez-Navarro A, Remião F, Bastos ML, Carvalho F. Paraquat poisonings: Mechanisms of lung toxicity, clinical features, and treatment. *Crit Rev Toxicol* (2008) 38:13–71. doi: 10.1080/10408440701669959

69. Yao R, Cao Y, He YR, Lau WB, Zeng Z, Liang ZA. Adiponectin attenuates lung fibroblasts activation and pulmonary fibrosis induced by paraquat. *PLoS One* (2015) 10: e0125169. doi: 10.1371/JOURNAL.PONE.0125169

70. Nigro E, Scudiero O, Sarnataro D, Mazzarella G, Sofia M, Bianco A, et al. Adiponectin affects lung epithelial A549 cell viability counteracting TNFa and IL-1ß toxicity through AdipoR1. *Int J Biochem Cell Biol* (2013) 45:1145–53. doi: 10.1016/j.biocel.2013.03.003

71. Orfanos SE, Mavrommati I, Korovesi I, Roussos C. Pulmonary endothelium in acute lung injury: From basic science to the critically ill. *Intensive Care Med* (2004) 30:1702–14. doi: 10.1007/S00134-004-2370-X

72. Summer R, Fiack CA, Ikeda Y, Sato K, Dwyer D, Ouchi N, et al. Adiponectin deficiency: A model of pulmonary hypertension associated with pulmonary vascular disease. *Am J Physiol Lung Cell Mol Physiol* (2009) 297:432–8. doi: 10.1152/AJPLUNG.90599.2008

73. Shah D, Torres C, Bhandari V. Adiponectin deficiency induces mitochondrial dysfunction and promotes endothelial activation and pulmonary vascular injury. *FASEB J* (2019) 33:13617–31. doi: 10.1096/fj.201901123R

74. Ramos-Ramírez P, Malmhäll C, Tliba O, Rådinger M, Bossios A. Adiponectin/AdipoR1 axis promotes IL-10 release by human regulatory T cells. *Front Immunol* (2021) 12:677550/BIBTEX. doi: 10.3389/FIMMU.2021.677550/BIBTEX

frontiers | Frontiers in Immunology

TYPE Original Research
PUBLISHED 01 November 2023
DOI 10.3389/fimmu.2023.1167605

OPEN ACCESS

EDITED BY
Adan Chari Jirmo,
Hannover Medical School, Germany

REVIEWED BY
Mats W. Johansson,
Morgridge Institute for Research,
United States
Stephanie DeStefano,
Hannover Medical School, Germany

*CORRESPONDENCE
Degan Lu
deganlu@126.com

RECEIVED 16 February 2023
ACCEPTED 12 October 2023
PUBLISHED 01 November 2023

CITATION
Peng H, Sun F, Jiang Y, Guo Z, Liu X, Zuo A and Lu D (2023) Semaphorin 7a aggravates TGF-β1-induced airway EMT through the FAK/ERK1/2 signaling pathway in asthma. *Front. Immunol.* 14:1167605. doi: 10.3389/fimmu.2023.1167605

Semaphorin 7a aggravates TGF-β1-induced airway EMT through the FAK/ERK1/2 signaling pathway in asthma

Haiying Peng, Fei Sun, Yunxiu Jiang, Zihan Guo, Xinyi Liu, Anli Zuo and Degan Lu*

Department of Respiratory, The First Affiliated Hospital of Shandong First Medical University & Shandong Provincial Qianfoshan Hospital, Shandong Institute of Respiratory Diseases, Shandong Institute of Anesthesia and Respiratory Critical Medicine, Jinan, China

Background: TGF-β1 can induce epithelial-mesenchymal transition (EMT) in primary airway epithelial cells (AECs). Semaphorin7A (Sema7a) plays a crucial role in regulating immune responses and initiating and maintaining transforming growth factor β1 TGF-β1-induced fibrosis.

Objective: To determine the expression of Sema7a, in serum isolated from asthmatics and non-asthmatics, the role of Sema7a in TGF-β1 induced proliferation, migration and airway EMT in human bronchial epithelial cells (HBECs) *in vitro*.

Methods: The concentrations of Sema7a in serum of asthmatic patients was detected by enzyme-linked immunosorbent assay (ELISA). The expressions of Sema7a and integrin-β1 were examined using conventional western blotting and real-time quantitative PCR (RT-PCR). Interaction between the Sema7a and Integrin-β1 was detected using the Integrin-β1 blocking antibody (GLPG0187). The changes in EMT indicators were performed by western blotting and immunofluorescence, as well as the expression levels of phosphorylated Focal-adhesion kinase (FAK) and Extracellular-signal-regulated kinase1/2 (ERK1/2) were analyzed by western blot and their mRNA expression was determined by RT-PCR.

Results: We described the first differentially expressed protein of sema7a, in patients with diagnosed bronchial asthma were significantly higher than those of healthy persons ($P<0.05$). Western blotting and RT-PCR showed that Sema7a and Integrin-β1 expression were significantly increased in lung tissue from the ovalbumin (OVA)-induced asthma model. GLPG0187 inhibited TGF-β1-mediated HBECs EMT, proliferation and migration, which was associated with Focal-adhesion kinase (FAK) and Extracellular-signal-regulated kinase1/2 (ERK1/2) phosphorylation.

Conclusion: Sema7a may play an important role in asthma airway remodeling by inducing EMT. Therefore, new therapeutic approaches for the treatment of chronic asthma, could be aided by the development of agents that target the Sema7a.

KEYWORDS

asthma, semaphorin 7A, airway remodeling, epithelial-mesenchymal transition, TGF-β1

1 Introduction

Asthma, characterized by airway inflammation, airway hyperresponsiveness (AHR), and airway remodeling (AR), is a chronic and heterogenic disease of the respiratory system mainly due to occupational or environmental exposure to industrial products, microorganisms, and other allergens (1, 2). The prevalence of asthma is still on the rise, with an estimated 358 million people worldwide affected by asthma, according to a global burden of disease study in 2015 (3). Most asthmatic patients can be controlled with bronchodilators and inhaled corticosteroids (4). However, an estimated 5-10% of patients are refractory to the treatment and thus require further therapy and even hospitalization, which results in impaired quality of life and a disproportionate cost to healthcare systems (5). AR may play an important role in the clinical severity of refractory asthma (6, 7). Therefore, it is necessary to further understand the factors that regulate the pathological features of asthma, including chronic inflammation and AR.

The chronic inflammatory response in the airways of asthmatic patients may result in alterations in the composition and distribution of cellular constituents of the airway wall, which is termed AR (8, 9). As a key feature of asthma, AR leads to irreversible airflow obstruction and persistent airway hyperresponsiveness and contributes to the symptomatology of the disease as well as irreversible loss of lung function (10, 11). Currently, inhaled corticosteroids and long-acting β2 agonists remain the mainstay for guideline-based control and management for asthma (12). However, such therapeutics are neither proven to prevent nor reverse AR although they can ameliorate inflammation (13). Moreover, AR may occur early in childhood to an equivalent degree in the airways, not necessarily subsequent to inflammation (14). Therefore, it is necessary to further explore the pathogenesis of AR in allergic asthma.

The semaphorin (Sema) protein family consists of more than 20 members and are extracellular signaling proteins that are instrumental in the development and maintenance of several organs and tissues (15). As a member of the Sema family, Sema7a (also known as CD108) is a glycosylphosphatidylinositol-linked membrane protein and is expressed constitutively and broadly in a variety of lymphoid, bone, endothelial, and nerve cells (16, 17). By binding to its receptor, integrin-β1 or plexin C1, with high affinity, Sema7a stimulates cytokine production in some inflammatory cells and is essential to the effector phase of the inflammatory immune response (18–20). The interaction of Sema7a with its receptor activates multiple signaling pathways, including phosphorylated focal-adhesion kinase phosphorylated (p-FAK), phosphorylated extracellular-signal-regulated kinase 1/2 (p-ERK1/2), nuclear factor kappa B (NF-κB), transforming growth factor β2 (TGF-β2)/Smad, and others (21, 22). A battery of studies has found that the Sema7a-integrin-β1 axis is a pivotal pathway in cell migration, angiogenesis and endothelial damage and is implicated in some disorders (22–24). Nevertheless, whether Sema7a has a role in the development of allergic asthma remains obscure.

Epithelial-mesenchymal transformation (EMT) is characterized by epithelial cell damage–repair-redamage-repair and is considered to be an initiating factor in AR in asthma (25, 26). As the first barrier to contact allergens, the bronchial epithelium plays an important role in airway EMT by secreting a variety of proinflammatory factors (27). Many signaling pathways, including transforming growth factor (TGF-β), epidermal growth factor (EGF), and tumor necrosis factor (TNF-α), are involved in the EMT process (28). Among them, TGF-β1 is a major inducer of EMT (29, 30). When expressed in the pulmonary epithelium, TGF-β1 can lead to the development of several AR features, including subepithelial fibrosis, epithelial shedding, and extracellular matrix deposition in the subepithelial layer by inducing EMT in bronchial epithelial cells (29, 31). In primary airway epithelial cells (AECs) obtained from asthmatic patients, TGF-β1 can induce EMT in a Smad3-dependent manner, suggesting dysregulated epithelial repair in asthmatic airways (32). Although some studies have documented that Sema7a contributes to atherosclerosis by mediating endothelial dysfunction and promotes the growth and migration of oral tongue squamous carcinoma cells by regulating the course of EMT (21, 33), little is known about whether Sema7a is involved in AR in allergic asthma by promoting the process of EMT.

To sum up, the expressions of Sema7a in serum of asthmatic patients and in lung tissue of ovalbumin (OVA) -induced mice were first examined. Then, whether the expression of Sema7a was associated with pathological features of allergic asthma was evaluated. Next, the roles of Sema7a in TGF-β1-induced EMT in human bronchial epithelial cells (HBECs) were investigate. Finally, the main signaling pathways involved in the effect of Sema7a were further probed. Our findings suggest that Sema7a may play a fundamental role in AR by inducing EMT through the FAK and ERK1/2 signaling pathway in HBECs and mice model of chronic asthma.

2 Methods

2.1 Humans

Ten patients with asthma were consecutively recruited from the Department of Respiratory Medicine and Intensive Care Medicine at the First Affiliated Hospital of Shandong First Medical University between October 1, 2021, and April 30, 2022. All of them met the criteria for asthma described in the report of the Global Initiative for Asthma (34). The disease activity of asthma was assessed according to the Asthma Control Test (ACT). Serum samples were collected, and those whose percentage of eosinophils in peripheral blood exceeded 3% were enrolled. A total of 20 healthy individuals who underwent health check-up in our hospital and whose age and sex were matched with those of asthmatic patients were selected as controls. None of them have chronic airway diseases/cancer or autoimmune diseases. This study was approved by the Medical Ethics Committee of The First Affiliated Hospital of Shandong First Medical University. Informed consent was obtained from all subjects who were enrolled in the present study.

2.2 Mice

A total of 18 female BALB/c mice aged 6-8 weeks were purchased from Pengyue Experimental Animal Breeding Co. Ltd. (Jinan, China) and housed in the Laboratory Animal Center of our hospital under SPF conditions. The feeding environment of the mice included a temperature–controlled house with 12 h light–dark cycles and free access to a standard laboratory diet and water (35). The mice were randomly divided into 3 groups: the control group (control, n=6), asthma group (asthma, n=6) and anti-Sema7a group (anti-Sema7a, n=6). All animal procedures were performed according to the National Institutes of Health (NIH) Guide for the Care and Use of Laboratory Animals (36). Moreover, all protocols were approved by the Ethics Committee for Laboratory Animals Care and Use in First Affiliated Hospital of Shandong First Medical University, Shandong, China.

2.3 Experimental model of chronic asthma

As described previously (37), the asthma group was sensitized with 0.2 ml sensitinogen (20 μg OVA+2 mg aluminum hydroxide) (Sigma–Aldrich, Beijing, China) on days 1, 7 and 14. From day 21 on, the OVA-sensitized mice were exposed to aerosolized 3% OVA (Sigma–Aldrich, Beijing, China) after anesthesia with 1% sodium pentobarbital (38) in a 30 cm×24 cm×50 cm chamber for 8 consecutive weeks: three times a week, 30 min each time. Anti-Sema7a antibody (6 μg/mouse) (AF1835, goat IgG; R&D Systems, Minneapolis, MN, USA) was administered intratracheally 30 min before each of the antigen challenges. In addition, mice in the control group were sensitized and challenged with phosphate-buffered saline (PBS) alone (Figure 1A).

2.4 Measurement of allergen-induced AHR

Airway responsiveness (R) and dynamic compliance (C) to methacholine challenge were evaluated 24 h following the last OVA challenge as previously reported (39). Briefly, mice were anesthetized with 0.12-0.15 ml 1% pentobarbital sodium intraperitoneally (22, 40). After the mice were fully anesthetized, a cannula was subsequently inserted into the trachea, and the mice were connected to the flexiVent system (Scireq). Subsequently, the mice were mechanically ventilated at a rate of 150 breaths/min, a tidal volume of 5 mL/kg, and a positive-end expiratory pressure of 3 cm H_2O (35). They were initially challenged with saline followed by challenge with increasing concentrations of methacholine (0, 5, 10, and 20 mg/ml; Sigma–Aldrich; Merck KGaA) for 10 sec at each dose. R and C were calculated as percentage increases over baseline (saline challenge).

2.5 Enzyme-linked immunosorbent assay

Mice were euthanized by cervical vertebrae dislocation immediately after lung function measurement (41). Right-lung lavage was performed with 2 ml PBS, and bronchoalveolar lavage fluid (BALF) was collected and centrifuged at 4°C and 80xg for 10 min. The concentrations of IL-4 (SEA077Mu), IL-5 (SEA078Mu), IL-13 (SEA060Mu) and TGF-β1 (SEA124Mu) in the BALF were determined using ELISA kits (Cloud-Clone, Wuhan, China) according to the manufacturer's protocol.

2.6 Histological analysis

The left lungs of mice were fixed in 4% paraformaldehyde at room temperature for 24 h (42). Then, the lung tissues were embedded in paraffin and cut into 5-μm-thick sections. Inflammatory infiltration and airway wall thickness were evaluated by hematoxylin and eosin (H&E) staining. Collagen deposition within the mouse airway wall was assessed by Masson's trichrome staining (Masson). To assess goblet cell proliferation in the airway wall, the sections were stained with periodic acid-Schiff stain (PAS) (35).

Before staining, serial 5-μm-thick sections were dewaxed in xylene and rehydrated through a series of decreasing concentrations of ethanol (43). Sections were placed in sodium citrate (pH 6.0, G1201-1 L, Servicebio, Wuhan, China), boiled for 10 minutes, and cooled to room temperature for antigen retrieval. The appropriate amount of endogenous peroxidase blocker was added to the sample, which was incubated at room temperature in the dark for 10 min

10.3389/fimmu.2023.1167605

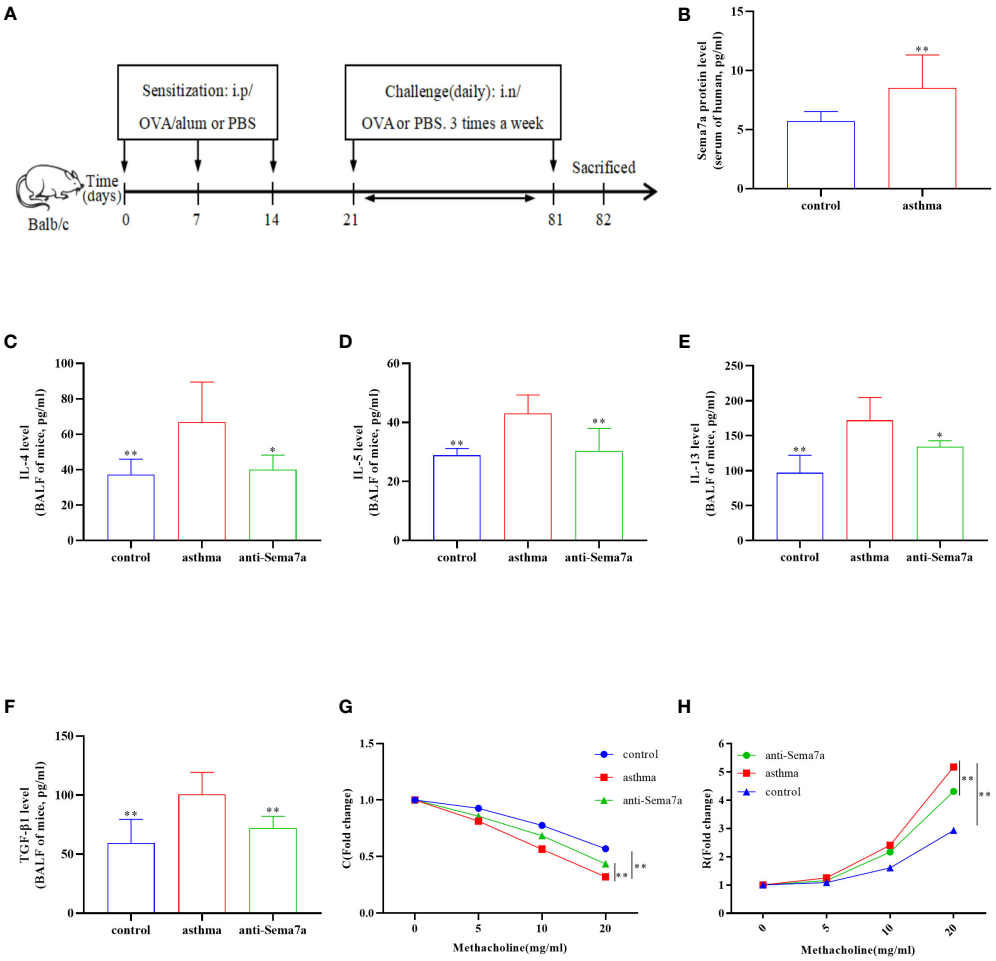

FIGURE 1
Airway inflammation and AHR in an OVA-challenged mouse model. **(A)** The establishment of chronic asthma mouse model; **(B)** The level of Sema7a in serum of patients with asthma was higher than that in serum of healthy subjects. **(C)** The asthma group had higher IL-4 levels in the BALF than the control group and the anti-Sema7a group had lower IL-4 levels than the asthma group. **(D)** The asthma group had higher IL-5 levels in the BALF than the control group and the anti-Sema7a group had lower IL-4 levels than the asthma group. **(E)** The asthma group had higher IL-13 levels in the BALF than the control group and the anti-Sema7a group had lower IL-4 levels than the asthma group. **(F)** The asthma group had higher TGF-B 1 levels in the BALF than the control group and the anti-Sema7a group had lower IL-4 levels than the asthma group. **(G)** It does not reveal significant differences among the three groups of baseline airway responsiveness (at 0 mg/ml methacholine); Stimulated by acetylcholine, the C was significantly descended in asthma group compared with control group, while enhanced in anti-Sema7a group compared with asthma group. **(H)** Stimulated by acetylcholine, the R was significantly enhanced in asthma group compared with control group, while descended in anti-Sema7a group compared with asthma group. Data represent means ± SD. *P < 0.05, **P < 0.01.

and then rinsed with PBS. The sections were treated with goat serum (SP-9001, Zhongshan, Beijing, China) at room temperature for 15 min to block nonspecific binding and incubated overnight at 4°C with rabbit polyclonal antibody against Sema7a (1:400, bs-2702R, Bioss, Beijing, China) diluted in PBS. After washing in PBS three times (5 min each time), the sections were incubated with anti-rabbit IgG antibody conjugated to horseradish peroxidase (HRP) (SP-9001, Zhongshan, Beijing, China). Next, DAB chromogen solution was added to the slide for 5 min at room temperature, washed extensively with PBS, and counterstained with hematoxylin for 20 s. Finally, slices were dehydrated with a gradient alcohol series, cleared in xylene and sealed with neutral gum. All sections were observed using a BX51 microscopic imaging system (Olympus Corporation, Japan).

2.7 Cell culture

The human bronchial epithelial cell line (16HBECs) was obtained from Fuheng Biology (Shanghai, China) and cultured in keratinocyte culture medium (KM) and penicillin–streptomycin. 16HBECs were treated with different concentrations of TGF-β1 (2.5, 5 and 10 ng/ml) for 12 h, 24 h or 48 h with or without pretreatment with integrin-β1 blockers (GLPG0187) (2 μm, 5 μm,

10 μm) for 1 h. The cells were harvested for the following experiments.

2.8 Cell proliferation assay

Cells were detached from the 25 cm3 cell-culture flask with 0.25% trypsin-EDTA (1×) (25200-056, Gibco, Thermo Scientific), and they were counted and suspended at a density of 5×10^5/ml in KM culture medium. Then, cells were seeded onto 96-well plates at a density of 2000 cells/well for 24 h and subsequently incubated with KM culture medium containing various dilutions of TGF-β1 and integrin-β1 (0 ng/ml TGF-β1 + 0 μm GLPG0187, 5 ng/ml TGF-β1 + 0 μm GLPG0187, 5 ng/ml TGF-β1 + 2 μm GLPG0187, 5 ng/ml TGF-β1 + 5 μm GLPG0187, 5 ng/ml TGF-β1 + 10 μm GLPG0187) at 37°C in a 5% CO_2 humidified atmosphere for 12, 24, 48 and 72 h. Following incubation for the indicated times, 10 μl Cell Counting Kit-8 (CCK-8) solution was added to each well and incubated for 2 h at 37°C with 5% CO_2 to examine the effect of integrin-β1 on 16HBECs proliferation. Cell proliferation was determined by measuring the absorbance at 450 nm using a microplate spectrophotometer.

2.9 Reverse transcription–quantitative PCR

Total RNA in mouse lung tissues was extracted using an RNA Isolation Kit (RC101, Vazyme, Nanjing, China) according to the manufacturer's instructions. First-strand cDNA was generated from 1 μg of total RNA using an RT SuperMix RT kit (R323, Vazyme, Nanjing, China) to prime the reverse transcription reaction according to the manufacturer's protocol. Gene expression was determined by SYBR Real-Time PCR Master Mix (Q711, Vazyme, Biotechnology). The primer pairs were synthesized by Takara (Table 1). Target mRNA levels were determined using the quantification cycle (Cq) values normalized against the expression of GAPDH. Gene expression was calculated using the $2^{-\Delta\Delta cq}$ method (44).

2.10 Western blot analysis

The tissue and cell proteins were extracted by using RIPA buffer, phenylmethanesulfonyl fluoride (PMSF), and phosphatase inhibitors. Protein concentration was determined with a protein assay kit (P0012; Beyotime Biotechnology, Shanghai, China) according to the protocol described previously (43). The samples were separated by 7.5-10% sodium dodecyl sulfate–polyacrylamide gel electrophoresis (SDS–PAGE), and the bands were electrotransferred to a 0.45 mm polyvinylidene fluoride (PVDF) membrane. After blocking with 5% skim milk, the membrane was incubated at 4°C overnight with rat monoclonal antibody for Sema7a (1:500, MAB2068, R&D Systems), rabbit monoclonal antibody for integrin-β1 (1:2,000, ab179471, Abcam), mouse monoclonal antibody for E-cadherin (1:1,000, ab231303, Abcam), rabbit monoclonal antibody for fibronectin (1:1,000, ab268020, Abcam), α-SMA (1:10,000, ab124964, Abcam), focal-adhesion kinase (FAK) (1:500, SAB4502495, Sigma), extracellular-signal-regulated kinase1/2 (ERK1/2) (1:20,000, M5670, Sigma), p-FAK (1:1000, ab81298, Abcam), and p-ERK1/2 (1:1000, SAB4301578, Sigma). The secondary antibody was incubated at room temperature for 1 h and washed with PBS three times. An enhanced chemiluminescence detection system was used to detect target proteins, with β-tubulin as the loading control. All data were analyzed by ImageJ Software (version 10.4, Tree Star Inc.).

TABLE 1 Primer sequences for the target genes.

Target gene	Primer sequence (5′→3′)
Mice Sema7a forward	TACCAGGGTCTATGGCGTTTTC
Mice Sema7a reverse	GCCCATGTGGTAGCCTTTGA
Mice Integrin-β1 forward	GGGTATTT GTGAATGTGGTGCTT
Mice Integrin-β1 reverse	TTTGGTGAGATTGAAGTGGGAGC
Mice GAPDH forward	AGAAACCTGCCAAGTATGATGACA
Mice GAPDH reverse	GGAAGAGTGGGAGTTGCTGTTG

2.11 Statistical analysis

All data are expressed as the means ± standard deviations (SD). The results were analyzed using GraphPad Prism 8 software. Pairwise comparisons were performed using Student's t test, and comparisons among multiple groups were conducted using one-way analysis of variance. Values of $P < 0.05$ indicated statistical significance.

3 Results

3.1 Expression of Sema7a in serum was enhanced significantly in asthmatic patients

Previous studies have found that Sema7a is expressed on airway eosinophils and plays an important role in immunoglobulin-E (IgE)-mediated airway inflammation (45, 46). Therefore, we examined whether Sema7a expression in serum differs between allergic asthmatic individuals and healthy individuals. As shown in Figure 1B, the level of Sema7a in patients with asthma was significantly higher than that in healthy subjects (Figure 1B; $P < 0.01$). These findings suggest that Sema7a is likely implicated in the development of allergic asthma.

3.2 Expression of Sema7a and integrin-β1 in lung tissue was obviously increased in OVA-treated mice

Sema7a is preferentially expressed on activated T cells, eosinophils, and thymocytes (47–49). The Sema7a gene is

moderately expressed in the heart, lung, and pancreas in mice. Sema7a can mediate macrophage and dendritic cell migration and tumor lymphatic metastasis through integrin-β1 receptors (50). We asked whether the expression status of Sema7a and integrin-β1 protein is different between PBS-treated mice and OVA-treated mice. To this aim, we established a chronic asthmatic mouse model. As shown in Figures 2A, D, Sema7a and integrin-β1 were both expressed in lung tissue in mice. Sema7a and integrin-β1 expression were significantly higher than those of the control group (Figures 2B, C, E, F; $P < 0.01$). Although Sema7a expression was observed in bronchial epithelial cells of both asthmatic and control mice, immunohistochemical analyses revealed that the expression of Sema7a in asthmatic epithelial cells was significantly higher than that in the control group (Figures 2G–I; $P < 0.01$). These findings indicate that Sema7a is likely involved in the pathogenesis of allergic asthma.

3.3 AHR and AR were alleviated by Sema7a blockade in a chronic asthmatic model

AR is one of the key features of asthma and has an essential role in disease progression (51), which often correlates with the severity of clinical disease (52, 53). AR is regarded as an important factor contributing to AHR and irreversible airflow limitation (54–56). In the present study, the association between Sema7a and AHR and AR was subsequently probed. As illustrated in Figures 1G, H, there were no significant differences among the three groups of baseline airway responsiveness (at 0 mg/ml methacholine) (Figures 1G, H; $P > 0.05$). Stimulated by acetylcholine, R was significantly enhanced and C was decreased in the asthma group compared with the control group (Figures 1G, H; $P < 0.01$), while R was significantly decreased and C was enhanced in the anti-Sema7a group mice compared with the asthma group mice (Figures 1G, H; $P < 0.01$). In addition, the ELISA results showed that the levels of these inflammatory factor cytokines in serum were significantly decreased in anti-Sema7a group mice compared with the OVA-challenged group (Figures 1C–F; $P < 0.05$). At 200× objectives with H&E staining, the accumulation of airway inflammatory factors, turbulence of bronchial epithelial cells, stenosis of the bronchial cavity, and thickening of the airway wall were observed in OVA-challenged mice. All of the abovementioned pathological changes were alleviated by preadministration of anti-Sema7a, as shown in Figure 3. These findings clearly suggest that Sema7a and integrin-β1 play a role in the process of AR in a mouse model of allergic asthma.

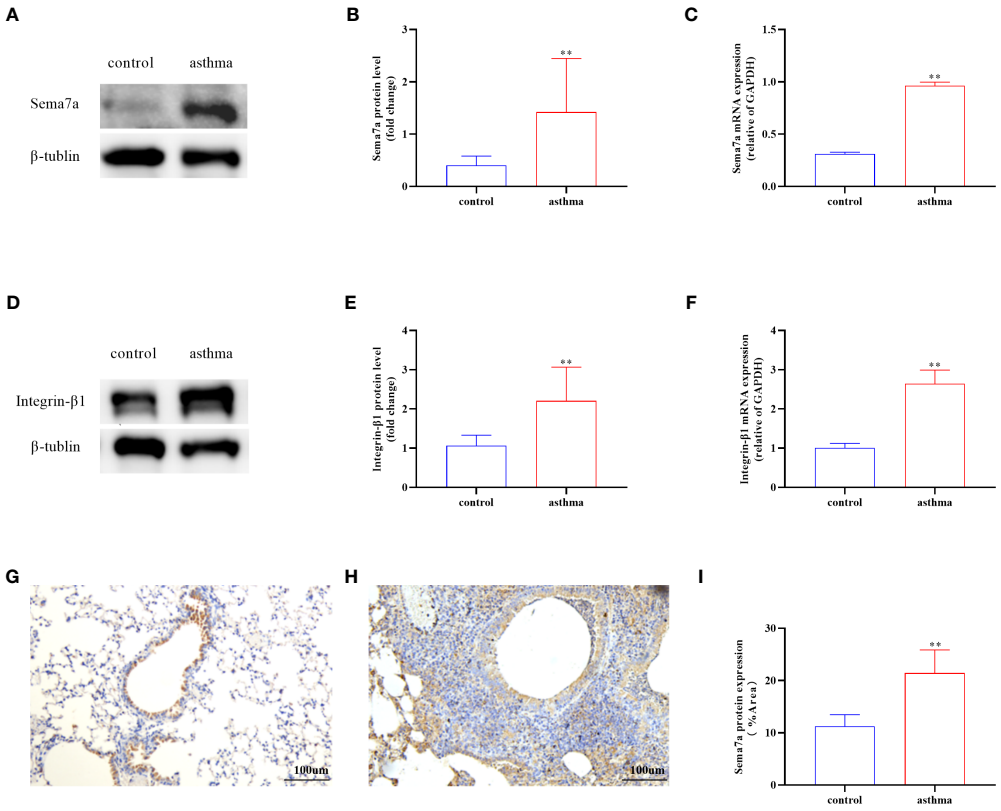

FIGURE 2
Protein and mRNA expression in lung tissues of Sema7a and Integrin-β1 in each group. **(A, B)** The level of Sema7a protein in lung tissue of asthma group was higher than control group. **(C)** The level of Sema7a mRNA in lung tissue of asthma group was higher than control group. **(D, E)** The level of Integrin-β1 protein in lung tissue of asthma group was higher than control group. **(F)** The level of Integrin-β1 mRNA in lung tissue of asthma group was higher than control group. **(G–I)** Immunohistochemical analyses revealed that the expression of Sema7a in asthmatic epithelial cells was significantly higher than that in the control group. Data represent means ± SD.**P < 0.01.

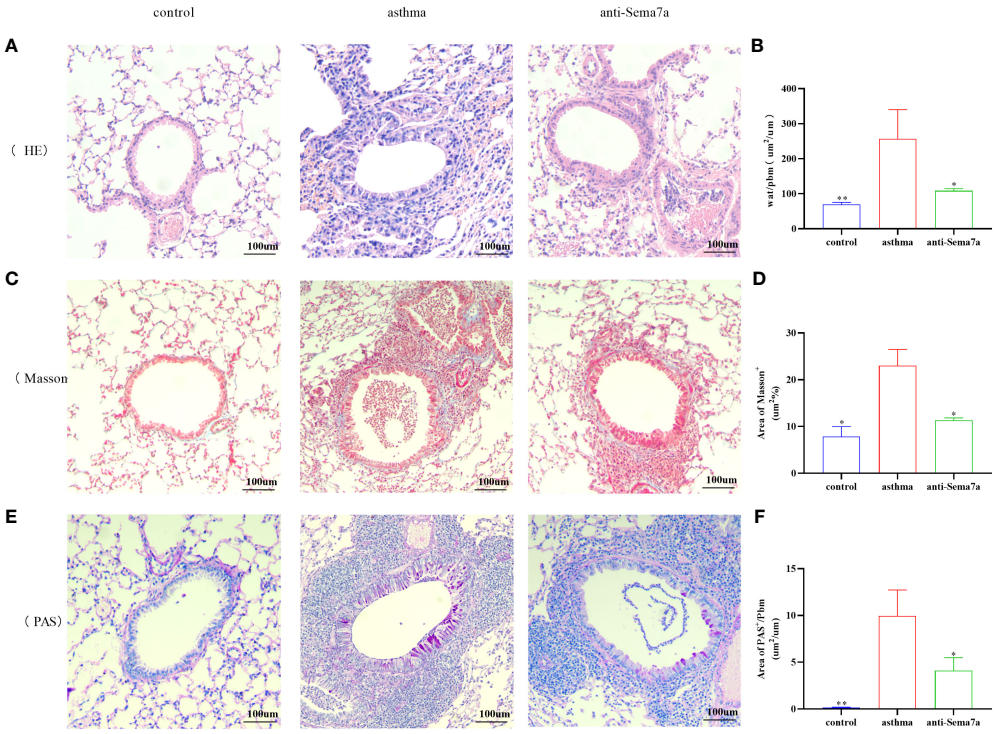

FIGURE 3
Histological examination of lung tissue was performed 24 h after the final OVA challenge. Lung tissues were fixed, sectioned at 5 um thickness, and stained with hematoxylin-eosin (HE), periodic acid-Schiff (PAS), and Masson stain. **(A, B)** Quantified results of airway wall thickness (Wat) analyzed by Image-Pro® Plus 6.0 software. **(C, D)** Quantified results of airway wall thickness (Wat) analyzed by Image-Pro® Plus 6.0 software. **(E, F)** Quantitative analysis of collagen deposition by Image-Pro® Plus 6.0 software. Data represent means ± SD. *P < 0.05, **P < 0.01.

3.4 Sema7a and integrin-β1 were induced by TGF-β1 in 16HBECs

The loss of airway epithelial integrity and EMT during AR contributes significantly to asthma pathogenesis (26, 29, 57). To elucidate whether the effects of Sema7a on AR were linked to EMT, 16HBECs were treated with 5 ng/ml TGF-β1, which markedly induced EMT in 16HBECs (Figures 4A, B) (58). A previous study reported that Sema7a and its receptor Integrin-β1 contributed to vascular endothelial cell injury and the pathophysiology of atherosclerosis (21, 22, 59). To determine the functional role of Integrin-β1 in the EMT of 16HBECs treated with TGF-β1, the protein expression levels of EMT-related proteins were analyzed using western blotting. As shown in Figures 4C–E, compared with the control group, TGF-β1 significantly upregulated the expression of Integrin-β1, α-SMA, and fibronectin but downregulated E-cadherin ($P < 0.01$). Therefore, TGF-β1-induced Sema7a and Integrin-β1 expression may play a critical role in promoting a mesenchymal phenotype.

3.5 TGF-β1-induced EMT could be reduced by GLPG0187 in 16HBECs

Integrins are heterodimeric receptors that serve to elicit a series of signal transduction events and sense the extracellular environment that participates in the control of cell cycle progression and apoptosis (α, β) (60). As a member of the integrin subfamily, Integrin-β1 is expressed on T lymphocytes, epithelial cells, and fibroblasts (61–63). The integrin-β1 blocking antibody GLPG0187 was used to detect the interaction between Sema7a and integrin-β1. 16HBECs were treated with different concentrations of GLPG0187 before TGF-β1 treatment to identify the function of Sem7a in EMT in asthma. As shown in Figures 4C, E, GLPG0187 significantly increased the expression of E-cadherin and decreased the expression of mesenchymal markers like fibronectin and α-SMA ($P < 0.01$). Additionally, CCK-8 was conducted and showed that proliferation in TGF-β1+ GLPG0187 cells was significantly lower (Figures 4F; $P < 0.01$). Taken together, these findings suggest that Sema7a may promote EMT through Integrin-β1 in 16HBECs.

3.6 Sema7a may aggravate EMT through the FAK/ERK1/2 signaling pathway in 16HBECs

FAK/ERK1/2 acts as a downstream signal pathway of the Sema7a-integrin-β1 axis, which mediates vascular endothelial dysfunction and tumor metastasis (21, 64). To further characterize the mechanism underlying the promotion of 16HBEC proliferation and migration by Sema7a, the expression

10.3389/fimmu.2023.1167605

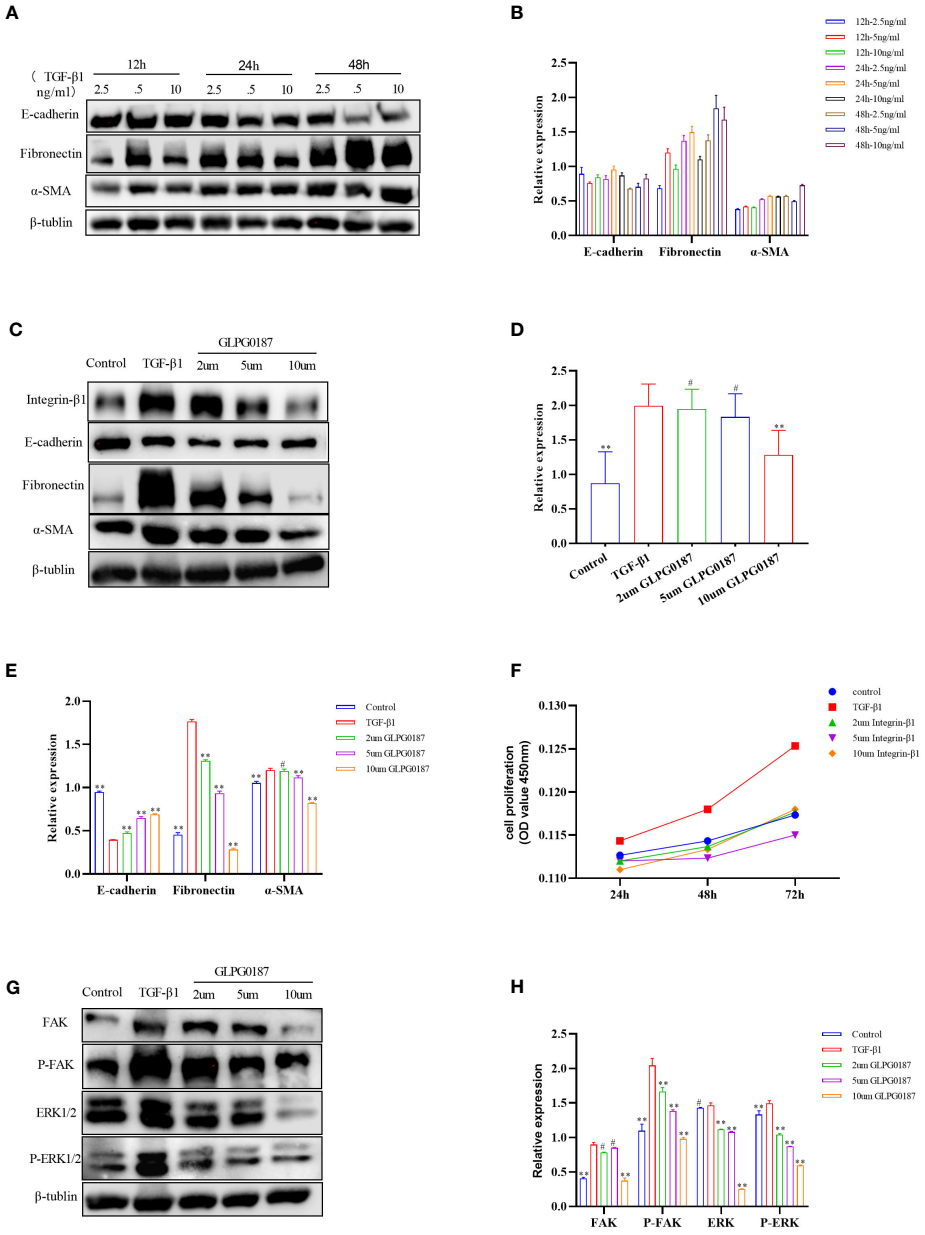

FIGURE 4
(A, B) 5ng/ml of TGF B 1 could induce obvious EMT changes in 16HBE cells. **(C–E)** TGF-β1 upregulated the expression of Integrin-β1, along with the upregulation of a-SMA and fibronectin, but downregulated E-cadherin compared with the control group; GLPG0187 significantly increased the expression of the Integrin-β1, E-cadherin and decreased that of the mesenchymal markers, fibronectin, a-SMA in a concentration-dependent manner. **(F)** GLPG0187 can reduce the 16HBE cells proliferation rate induced by TGF-β1. **(G, H)** TGF-B1 significantly upregulated the expression of the FAK, P-FAK, ERK and P-ERK, while the GLPG0187 can reduce the expression of the above signaling pathway indicators, **P < 0.01, #P>0.05.

levels of FAK, ERK, P-FAK and P-ERK1/2 were assessed using western blotting analysis. As shown in Figures 4G, H, GLPG0187 decreased phosphorylated FAK and ERK1/2 levels, suggesting that attenuation of FAK and the ERK1/2 pathway was caused by downregulation of cell surface integrin-β1 ($P < 0.01$). The molecular investigation indicates that Sema7A may promote TGF-β1-mediated EMT, cell migration and proliferation by activating Integrin-β1 and its downstream FAK and ERK1/2 signaling pathways.

4 Discussion

This work extends our current understanding of the mechanisms regulating EMT, provides new insights into the role of Sema7a cytokines in bronchial asthma with respect to AR, and strengthens the basis for the Sema7a-integrin-β1 axis in the treatment of human allergic asthmatic EMT and fibrotic diseases. First, we found that the levels of Sema7a in the serum of asthmatic patients were increased (Figure 1B). Second, Sema7a was

overexpressed in airway and lung tissue in asthmatic mice and promoted airway EMT, which was blocked by an integrin receptor antagonist, GLPG0187. To the best of our knowledge, this is the first study to assess the effect of Sema7a on bronchial epithelial cells in chronic asthma. Finally, GLPG0187 alleviated chronic airway inflammation and AR mainly through the FAK and ERK signaling pathways.

Sema7a is a membrane–associated GPI–linked protein that is mainly expressed on the surface of eosinophils and can also be present in the form of secretion (46, 65, 66). Because eosinophils play an important role in the transmission of airway allergic diseases such as asthma, we hypothesize that Sema7a may be a critical cytokine in the development of allergic airway diseases in asthma (67). First, our study identified, for the first time, the expression of Sema7a in serum and found these to be enhanced in asthma patients (Figure 1B; $P < 0.01$). These results are consistent with those of Esnault et al. who found elevated Sema7a levels in asthma patients (45). Previous studies have shown that TGF-β1 is mainly produced by eosinophils accumulated in the peribronchial and perivascular lesions (68). Asthma is characterized by subepithelial fibrosis, and ample evidence exists that eosinophils have a significant pathologic role in promoting airways fibrosis. In a murine fibrosis model, TGF-β1 has been reported to induce the expression of Sema7a in the murine lung (69). One study showed that Sema7a expression is stimulated by TGF-β1 in the murine lung, with Sema7a being a critical regulator of tissue remodeling in TGF-β1-induced pulmonary fibrosis (70). Thus, we speculate that sema7a may promote chronic airway inflammation and AR in asthma. Gan et al. also supported our hypothesis and found that TGF-β1 stimulates fibrocyte accumulation via a Sema7a–dependent, integrin-β1–dependent pathway (65). Our research showed that Sema7a and its receptor integrin-β1 were overexpressed in lung tissue in OVA-treated mice (Figures 2A–F; $P < 0.01$); treatment with anti-Sema7a was effective in alleviating AR in the model of chronic asthma. This has been confirmed in the study of Nobuaki Mizutani and Takeshi Nabe (46), in which treatment with anti-sema7a antibody suppressed subepithelial fibrosis in the lungs of Ig-E-sensitized mice. These results suggest that Sema7a is involved in the development of AR by activating its receptor integrin-β1 in asthma.

Epithelium damage and deficiency have been reported to result in EMT, which is considered to be intricately involved in AR and is the main cause of fixed airflow limitations that occur during asthma attacks (26, 71). In contrast, inhibition of the EMT process can alleviate AR in asthma. The increased expression of Sema7a in epithelial cells is closely related to the severity of atherosclerosis (21), and Sema7a has been shown to not only exacerbate inflammation but also promote fibrosis that is associated with EMT (70, 72); in an animal model, the expression of Sema7a in lung tissue was dependent on TGF-β1 (73). The present study supported the findings of the above investigations: integrin-β1 was overexpressed in TGF-β1-stimulated 16HBECs (Figures 4C, D, $P < 0.01$); GLPG0187 reduced the expression of integrin-β1 and attenuated the HBEC proliferation and EMT changes induced by TGF-β1 (Figures 4C–E, $P < 0.01$). However, the TGF-β1 present in the fetal bovine serum used in the cell culture medium in Stephane Esnault and Elizabeth A. Kelly study does not appear to increase sema7a on eosinophils (74). The inconsistent results of the above studies may be due to the different cell lines. Furthermore, it has been reported that not only integrin-β1 but also Sema7a together with its receptor, plexin C1, regulates cell migration. For instance, the sema7a interaction with plexin C1 expressed on dendritic cells is known to impair their migration (75). However, the interaction between plexin C1 and Sema7a was not further studied in our study; whether Sema7a can inhibit cell migration or EMT by activating plexin C1 remains to be studied. In summary, our results further confirmed the role of the Sema7a-integrin-β1 signaling axis in AR and suggested that it promotes airway EMT and is involved in the pathogenesis of asthmatic AR. Epithelial fibrosis is also an important pathological feature of airway remodeling in asthma. Thus, Sema7a and its integrin-β1 receptor may be potential therapeutic targets for allergic asthma.

The molecular investigation indicated that Sema7a-integrin-β1 and its downstream FAK and ERK1/2 signaling pathways promote nonvascular endothelial growth factor (VEGF) A/vascular endothelial growth factor receptor (VEGFR) 2-mediated cell migration and angiogenesis (23), and FAK/ERK1/2 is involved in T-cell-mediated inflammatory responses (20). Previous studies have shown that Sema7a is not only related to the inflammatory immune response but also regulates axon growth via the mitogen-activated protein kinase (MAPK) signaling pathway (73, 76). ERK constitutes one branch of the MAPK pathway responsible for the invasion of cancer cells by primarily breaking down the extracellular matrix (ECM) (77). A study showed that blockage of integrin-β1 or inhibition of FAK, mitogen-activated protein kinase (MEK) 1/2, or NF-κB significantly reduced the expression of cell adhesion molecules and THP-1 monocyte adhesion in Sema7a-overexpressing human umbilical venous endothelial cells (21). In summary, Sema7a may be involved in asthma airway EMT through the FAK/ERK1/2 signaling pathway. To gain insight into the mechanisms underlying the observed effects of Sema7a, we examined several proteins in the TGF-β1/FAK/ERK/1/2 signaling pathway and identified whether GLPG0187 can affect the kinase activity of FAK and its downstream targets. We analyzed the phosphorylation levels of FAK and ERK1/2 by performing western blotting. Interestingly, the levels of phosphorylated FAK and phosphorylated ERK1/2 were decreased in GLPG0187-pretreated cells (Figures 4G, H, $P < 0.01$), suggesting the involvement of FAK/ERK1/2 phosphorylation in the early stage of AR activation.

In conclusion, the present study demonstrated that Sema7a may contribute to asthma AR pathology by affecting HBEC function and airway EMT. GLPG0187 significantly increased the expression of E-cadherin and decreased that of the mesenchymal markers fibronectin and α-SMA in a concentration-dependent manner. These findings may explain the underlying mechanisms of the loss of airway epithelial integrity in OVA-induced asthma by promoting the phosphorylation of FAK and ERK. Collectively, these findings may provide insight into the multifaceted role of Sema7a in chronic asthma. With further studies, Sema7a or

integrin-β1 is expected to be used as an immunotherapeutic treatment target for asthma.

Epithelial fibrosis is also an important pathological feature of airway remodeling in asthma. Thus, Sema7a and its integrin-β1 receptor may be potential therapeutic targets for allergic asthma.

Data availability statement

The original contributions presented in the study are included in the article/Supplementary Material. Further inquiries can be directed to the corresponding author.

Ethics statement

The studies involving human participants were reviewed and approved by Medical Ethics Committee of the First Affiliated Hospital of Shandong First Medical University. The patients/participants provided their written informed consent to participate in this study. The animal study was reviewed and approved by Medical Ethics Committee of the First Affiliated Hospital of Shandong First Medical University. Written informed consent was obtained from the owners for the participation of their animals in this study.

Author contributions

DL, HP, and FS contributed to the conception and design of the present research. FS and ZG performed the experiments and analyzed the data. HP, YJ, XL, and AZ wrote and revised the manuscript. DL reviewed the article. All authors have read and approved the final version of the manuscript.

Funding

This work was supported by the Collaborative Innovation Center for Intelligent Molecules with Multi effects and Nanomedicine (No. 2019-01), Shandong Province, China; Shandong Provincial Natural Science Foundation (ZR2021LSW015) and Jinan Clinical Medicine Research Program for Respiratory disease (No. 202132002). The funders did not play a role in the design of the study, the collection and analysis of the data, or the decision to prepare and publish this manuscript.

Conflict of interest

The authors declare that the research was conducted in the absence of any commercial or financial relationships that could be construed as a potential conflict of interest.

Publisher's note

Supplementary material

The Supplementary Material for this article can be found online at: https://www.frontiersin.org/articles/10.3389/fimmu.2023.1167605/full#supplementary-material

References

1. Movassagh H, Koussih L, Shan L, Gounni AS. The regulatory role of semaphorin 3E in allergic asthma. *Int J Biochem Cell Biol* (2019) 106:68–73. doi: 10.1016/j.biocel.2018.11.006

2. Kardas G, Daszynska-Kardas A, Marynowski M, Brząkalska O, Kuna P, Panek M, et al. Role of platelet-derived growth factor (PDGF) in asthma as an immunoregulatory factor mediating airway remodeling and possible pharmacological target. *Front Pharmacol* (2020) 11:47. doi: 10.3389/fphar.2020.00047

3. Global, regional, and national incidence, prevalence, and years lived with disability for 328 diseases and injuries for 195 countries, 1990-2016: a systematic analysis for the Global Burden of Disease Study 2016. *Lancet (London England)* (2017) 390(10100):1211–59 . doi: 10.1016/S0140-6736(17)32154-2

4. Ricciardolo FL, Blasi F, Centanni S, Rogliani P. Therapeutic novelties of inhaled corticosteroids and bronchodilators in asthma. *Pulm Pharmacol Ther* (2015) 33:1–10. doi: 10.1016/j.pupt.2015.05.006

5. Jones TL, Neville DM, Chauhan AJ. Diagnosis and treatment of severe asthma: a phenotype-based approach. *Clin Med (London England)* (2018) 18(Suppl 2):s36–40. doi: 10.7861/clinmedicine.18-2-s36

6. Liu T, Liu Y, Miller M, Cao LZ, Zhao JP, Wu JX, et al. Autophagy plays a role in FSTL1-induced epithelial mesenchymal transition and airway remodeling in asthma. *Am J Physiol Lung Cell Mol Physiol* (2017) 313(1):L27–40. doi: 10.1152/ajplung.00510.2016

7. Tseliou E, Bakakos P, Kostikas K, Hillas G, Mantzouranis K, Emmanouil P, et al. Increased levels of angiopoietins 1 and 2 in sputum supernatant in severe refractory asthma. *Allergy* (2012) 67(3):396–402. doi: 10.1111/j.1398-9995.2011.02768.x

8. Bergeron C, Boulet LP. Structural changes in airway diseases: characteristics, mechanisms, consequences, and pharmacologic modulation. *Chest* (2006) 129 (4):1068–87. doi: 10.1378/chest.129.4.1068

9. Girodet PO, Ozier A, Bara I, Tunon de Lara J-M, Marthan R, Berger P, et al. Airway remodeling in asthma: new mechanisms and potential for pharmacological intervention. *Pharmacol Ther* (2011) 130(3):325–37. doi: 10.1016/j.pharmthera.2011.02.001

10. Zhang H, Yan HL, Li XY, Guo YN. TNFSF14, a novel target of miR-326, facilitates airway remodeling in airway smooth muscle cells via inducing extracellular matrix protein deposition and proliferation. *Kaohsiung J Med Sci* (2020) 36(7):508–14. doi: 10.1002/kjm2.12197

11. Kardas G, Kuna P, Panek M. Biological therapies of severe asthma and their possible effects on airway remodeling. *Front Immunol* (2020) 11:1134. doi: 10.3389/fimmu.2020.01134

12. McCracken JL, Veeranki SP, Ameredes BT, Calhoun WJ. Diagnosis and management of asthma in adults: A review. *Jama* (2017) 318(3):279–90. doi: 10.1001/jama.2017.8372

13. Hirota N, Martin JG. Mechanisms of airway remodeling. *Chest* (2013) 144 (3):1026–32. doi: 10.1378/chest.12-3073

14. Malmström K, Pelkonen AS, Mäkelä MJ. Remodeling, inflammation and airway responsiveness in early childhood asthma. *Curr Opin Allergy Clin Immunol* (2013) 13 (2):203–10. doi: 10.1097/ACI.0b013e32835e122c

15. Alto LT, Terman JR. Semaphorins and their signaling mechanisms. *Methods Mol Biol (Clifton N.J.)* (2017) 1493:1–25. doi: 10.1007/978-1-4939-6448-2_1

16. Wu X, Meng Y, Wang C, Yue Y, Dong CS, Xiong SD. Semaphorin7A aggravates coxsackievirusB3-induced viral myocarditis by increasing alpha1beta1-integrin macrophages and subsequent enhanced inflammatory response. *J Mol Cell Cardiol* (2018) 114:48–57. doi: 10.1016/j.yjmcc.2017.11.001

17. Püschel AW, Adams RH, Betz H. Murine semaphorin D/collapsin is a member of a diverse gene family and creates domains inhibitory for axonal extension. *Neuron* (1995) 14(5):941–8. doi: 10.1016/0896-6273(95)90332-1

18. Shapoori S, Mosayebi G, Ebrahimi Monfared M, Ghazavi A, Khansarinejad B, Farahani F, et al. Gene expression of semaphorin-3A, semaphorin-7A, neuropilin-1, plexin-C1, and beta1 integrin in treated-multiple sclerosis patients. *Neurol Res* (2020) 42(9):783–8. doi: 10.1080/01616412.2020.1774211

19. Elder AM, Tamburini BAJ, Crump LS, Black SA, Wessells VM, Schedin PJ, et al. Semaphorin 7A promotes macrophage-mediated lymphatic remodeling during postpartum mammary gland involution and in breast cancer. *Cancer Res* (2018) 78 (22):6473–85. doi: 10.1158/0008-5472.CAN-18-1642

20. Suzuki K, Okuno T, Yamamoto M, Pasterkamp RJ, Takegahara N, Takamatsu H, et al. Semaphorin 7A initiates T-cell-mediated inflammatory responses through alpha1beta1 integrin. *Nature* (2007) 446(7136):680–4. doi: 10.1038/nature05652

21. Hu S, Liu Y, You T, Heath J, Xu LR, Zheng XW, et al. Vascular semaphorin 7A upregulation by disturbed flow promotes atherosclerosis through endothelial β1 integrin. *Arterioscler Thromb Vasc Biol* (2018) 38(2):335–43. doi: 10.1161/ATVBAHA.117.310491

22. Hong L, Li F, Tang C, Li L, Sun LL, Li XQ, et al. Semaphorin 7A promotes endothelial to mesenchymal transition through ATF3 mediated TGF-β2/Smad signaling. *Cell Death Dis* (2020) 11(8):695. doi: 10.1038/s41419-020-02818-x

23. Hu S, Liu Y, You T, Zhu L. Semaphorin 7A promotes VEGFA/VEGFR2-mediated angiogenesis and intraplaque neovascularization in apoE(-/-) mice. *Front Physiol* (2018) 9:1718. doi: 10.3389/fphys.2018.01718

24. Zhang M, Yan X, Liu W, Sun R, Xie YH, Jin FG. Endothelial semaphorin 7A promotes seawater aspiration-induced acute lung injury through plexin C1 and β1 integrin. *Mol Med Rep* (2017) 16(4):4215–21. doi: 10.3892/mmr.2017.7097

25. Gai YP, Zhao HN, Zhao YN, Zhu BS, Yuan SS, Li S, et al. MiRNA-seq-based profiles of miRNAs in mulberry phloem sap provide insight into the pathogenic mechanisms of mulberry yellow dwarf disease. *Sci Rep* (2018) 8(1):812. doi: 10.1038/s41598-018-19210-7

26. Sun Z, Ji N, Ma Q, Zhu RR, Chen ZQ, Wang ZX, et al. Epithelial-mesenchymal transition in asthma airway remodeling is regulated by the IL-33/CD146 axis. *Front Immunol* (2020) 11:1598. doi: 10.3389/fimmu.2020.01598

27. Wang T, Zhou Q, Shang Y. MiRNA-451a inhibits airway remodeling by targeting Cadherin 11 in an allergic asthma model of neonatal mice. *Int Immunopharmacol* (2020) 83:106440. doi: 10.1016/j.intimp.2020.106440

28. Xiao W, Tang H, Wu M, Liao YY, Li K, Li L, et al. Ozone oil promotes wound healing by increasing the migration of fibroblasts *via* PI3K/Akt/mTOR signaling pathway. *Biosci Rep* (2017) 37(6):BSR20170658. doi: 10.1042/BSR20170658

29. Fan Q, Jian Y. MiR-203a-3p regulates TGF-beta1-induced epithelial-mesenchymal transition (EMT) in asthma by regulating Smad3 pathway through SIX1. *Biosci Rep* (2020) 40(2):BSR20192645. doi: 10.1042/BSR20192645

30. Zou Y, Song W, Zhou L, Mao YX, Hong W. House dust mite induces Sonic hedgehog signaling that mediates epithelialmesenchymal transition in human bronchial epithelial cells. *Mol Med Rep* (2019) 20(5):4674–82. doi: 10.3892/mmr.2019.10707

31. Charbonneau M, Lavoie RR, Lauzier A, Harper K, McDonald PP, Dubois CM. Platelet-derived growth factor receptor activation promotes the prodestructive invadosome-forming phenotype of synoviocytes from patients with rheumatoid arthritis. *J Immunol* (2016) 196(8):3264–75. doi: 10.4049/jimmunol.1500502

32. Hackett TL, Warner SM, Stefanowicz D, Haheen F, Pechkovsky DV, Murray LA, et al. Induction of epithelial-mesenchymal transition in primary airway epithelial cells from patients with asthma by transforming growth factor-beta1. *Am J Respir Crit Care Med* (2009) 180(2):122–33. doi: 10.1164/rccm.200811-1730OC

33. Liu TJ, Guo JL, Wang HK, Xu X. Semaphorin-7A contributes to growth, migration and invasion of oral tongue squamous cell carcinoma through TGF-β-mediated EMT signaling pathway. *Eur Rev Med Pharmacol Sci* (2018) 22(4):1035–43. doi: 10.26355/eurrev_201802_14386

34. Reddel HK, Bacharier LB, Bateman ED, Brightling CE, Brusselle GG, Buhl R, et al. Global Initiative for Asthma Strategy 2021: executive summary and rationale for key changes. *Eur Respir J* (2022) 59(1):2102730. doi: 10.1183/13993003.02730-2021

35. Lu D, Lu J, Ji X, Ji YB, Zhang ZW, Peng HY, et al. IL–27 suppresses airway inflammation, hyperresponsiveness and remodeling via the STAT1 and STAT3 pathways in mice with allergic asthma. *Int J Mol Med* (2020) 46(2):641–52. doi: 10.3892/ijmm.2020.4622

36. National Research Council Committee for the Update of the Guide for the C, Use of Laboratory A. The National Academies Collection: Reports funded by National Institutes of Health. *Guide for the care and use of laboratory animals*. Washington (DC: National Academies Press (US (2011).

37. Cao L, Liu F, Liu Y, Liu T, Wu JX, Zhao JP, et al. TSLP promotes asthmatic airway remodeling *via* p38-STAT3 signaling pathway in human lung fibroblast. *Exp Lung Res* (2018) 44(6):288–301. doi: 10.1080/01902148.2018.1536175

38. Overmyer KA, Thonusin C, Qi NR, Burant CF, Evans CR. Impact of anesthesia and euthanasia on metabolomics of mammalian tissues: studies in a C57BL/6J mouse model. *PloS One* (2015) 10(2):e0117232. doi: 10.1371/journal.pone.0117232

39. Hoymann HG. Lung function measurements in rodents in safety pharmacology studies. *Front Pharmacol* (2012) 3:156. doi: 10.3389/fphar.2012.00156

40. Kim SR, Park HJ, Lee KB, Kim HJ, Jeong JS, Cho SH, et al. Epithelial PI3K-delta promotes house dust mite-induced allergic asthma in NLRP3 inflammasome-dependent and -independent manners. *Allergy Asthma Immunol Res* (2020) 12 (2):338–58. doi: 10.4168/aair.2020.12.2.338

41. Liu J, Yin J. Immunotherapy with recombinant alt a 1 suppresses allergic asthma and influences T follicular cells and regulatory B cells in mice. *Front Immunol* (2021) 12:747730. doi: 10.3389/fimmu.2021.747730

42. Zhang L, Lin J, Guo J, Sun WL, Pan L. Effects of 1, 25-(OH)2D3 on airway remodeling and airway epithelial cell apoptosis in a murine model of asthma. *Zhonghua yi xue za zhi* (2015) 95(48):3945–9. doi: 10.3760/cma.j.issn.0376-2491.2015.48.016

43. Zhang Y, Li S, Huang S, Cao LZ, Liu T, Zhao JP, et al. IL33/ST2 contributes to airway remodeling *via* p-JNK MAPK/STAT3 signaling pathway in OVA-induced allergic airway inflammation in mice. *Exp Lung Res* (2019) 45(3-4):65–75. doi: 10.1080/01902148.2019.1611972

44. Livak KJ, Schmittgen TD. Analysis of relative gene expression data using real-time quantitative PCR and the 2(-Delta Delta C(T)) Method. *Methods* (2001) 25 (4):402–8. doi: 10.1006/meth.2001.1262

45. Esnault S, Kelly EA, Johansson MW, Liu LY, Han ST, Akhtar M, et al. Semaphorin 7A is expressed on airway eosinophils and upregulated by IL-5 family cytokines. *Clin Immunol (Orlando Fla.)* (2014) 150(1):90–100. doi: 10.1016/j.clim.2013.11.009

46. Mizutani N, Nabe T, Yoshino S. Semaphorin 7A plays a critical role in IgE-mediated airway inflammation in mice. *Eur J Pharmacol* (2015) 764:149–56. doi: 10.1016/j.ejphar.2015.07.004

47. Yamada A, Kubo K, Takeshita T, Harashima N, Kawano K, Mine T, et al. Molecular cloning of a glycosylphosphatidylinositol-anchored molecule CDw108. *J Immunol* (1999) 162(7):4094–100. doi: 10.4049/jimmunol.162.7.4094

48. Mudad R, Rao N, Angelisova P, Horejsi V, Telen MJ. Evidence that CDw108 membrane protein bears the JMH blood group antigen. *Transfusion* (1995) 35(7):566–70. doi: 10.1046/j.1537-2995.1995.35795357878.x

49. Bobolis KA, Moulds JJ, Telen MJ. Isolation of the JMH antigen on a novel phosphatidylinositol-linked human membrane protein. *Blood* (1992) 79(6):1574–81. doi: 10.1182/blood.V79.6.1574.1574

50. Jiang J, Zhang F, Wan Y, Fang K, Yan ZD, Ren XL, et al. Semaphorins as potential immune therapeutic targets for cancer. *Front Oncol* (2022) 12:793805. doi: 10.3389/fonc.2022.793805

51. Hamid Q, Tulic M. Immunobiology of asthma. *Annu Rev Physiol* (2009) 71:489–507. doi: 10.1146/annurev.physiol.010908.163200

52. Li JJ, Wang W, Baines KJ, Bowden NA, Hansbro PM, Gibson PG, et al. IL-27/IFN-γ induce MyD88-dependent steroid-resistant airway hyperresponsiveness by inhibiting glucocorticoid signaling in macrophages. *J Immunol* (2010) 185(7):4401–9. doi: 10.4049/jimmunol.1001039

53. Meurs H, Gosens R, Zaagsma J. Airway hyperresponsiveness in asthma: lessons from *in vitro* model systems and animal models. *Eur Respir J* (2008) 32(2):487–502. doi: 10.1183/09031936.00023608

54. Fajt ML, Wenzel SE. Asthma phenotypes and the use of biologic medications in asthma and allergic disease: the next steps toward personalized care. *J Allergy Clin Immunol* (2015) 135(2):299–310. doi: 10.1016/j.jaci.2014.12.1871

55. Eifan AO, Orban NT, Jacobson MR, Durham SR. Severe persistent allergic rhinitis. Inflammation but no histologic features of structural upper airway remodeling. *Am J Respir Crit Care Med* (2015) 192(12):1431–9. doi: 10.1164/rccm.201502-0339OC

56. Tang X, Nian H, Li X, Yang Y, Wang XJ, Xu LP, et al. Effects of the combined extracts of Herba Epimedii and Fructus Ligustrilucidi on airway remodeling in the asthmatic rats with the treatment of budesonide. *BMC Complement Altern Med* (2017) 17(1):380. doi: 10.1186/s12906-017-1891-0

57. Bartis D, Mise N, Mahida RY, Eickelberg O, Thickett DR. Epithelial-mesenchymal transition in lung development and disease: does it exist and is it important? *Thorax* (2014) 69(8):760–5. doi: 10.1136/thoraxjnl-2013-204608

58. Liu F, Shang YX. Sirtuin 6 attenuates epithelial-mesenchymal transition by suppressing the TGF-beta1/Smad3 pathway and c-Jun in asthma models. *Int Immunopharmacol* (2020) 82:106333. doi: 10.1016/j.intimp.2020.106333

59. You T, Zhu Z, Zheng X, Zeng NM, Hu SH, Liu YF, et al. Serum semaphorin 7A is associated with the risk of acute atherothrombotic stroke. *J Cell Mol Med* (2019) 23 (4):2901–6. doi: 10.1111/jcmm.14186

60. Park CC, Zhang H, Pallavicini M, Gray JW, Baehner F, Park CJ, et al. Beta1 integrin inhibitory antibody induces apoptosis of breast cancer cells, inhibits growth, and distinguishes Malignant from normal phenotype in three dimensional cultures and in *vivo*. *Cancer Res* (2006) 66(3):1526–35. doi: 10.1158/0008-5472.CAN-05-3071

61. Ieda M, Tsuchihashi T, Ivey KN, Ross RS, Hong TT, Shaw RM, et al. Cardiac fibroblasts regulate myocardial proliferation through beta1 integrin signaling. *Dev Cell* (2009) 16(2):233–44. doi: 10.1016/j.devcel.2008.12.007

62. DeNucci CC, Pagán AJ, Mitchell JS, Shimizu Y. Control of alpha4beta7 integrin expression and CD4 T cell homing by the beta1 integrin subunit. *J Immunol* (2010) 184 (5):2458–67. doi: 10.4049/jimmunol.0902407

63. Ulanova M, Puttagunta L, Marcet-Palacios M, Duszyk M, Steinhoff U, Duta F, et al. Syk tyrosine kinase participates in beta1-integrin signaling and inflammatory responses in airway epithelial cells. *Am J Physiol Lung Cell Mol Physiol* (2005) 288(3): L497–507. doi: 10.1152/ajplung.00246.2004

64. Wang C, Zhang S, Liu J, Tian Y, Ma BY, Xu SR, et al. Secreted pyruvate kinase M2 promotes lung cancer metastasis through activating the integrin beta1/FAK signaling pathway. *Cell Rep* (2020) 30(6):1780–1797 e1786. doi: 10.1016/j.celrep.2020.01.037

65. Gan Y, Reilkoff R, Peng X, Russell T, Chen QS, Mathai SK, et al. Role of semaphorin 7a signaling in transforming growth factor beta1-induced lung fibrosis and scleroderma-related interstitial lung disease. *Arthritis Rheum* (2011) 63(8):2484–94. doi: 10.1002/art.30386

66. van Rijn A, Paulis L, te Riet J, Vasaturo A, Reinieren-Beeren I, Schaaf AVD, et al. Semaphorin 7A promotes chemokine-driven dendritic cell migration. *J Immunol* (2016) 196(1):459–68. doi: 10.4049/jimmunol.1403096

67. Tost J. Epigenetic plasticity of eosinophils and other immune cell subsets in childhood asthma. *Lancet Respir Med* (2018) 6(5):322–4. doi: 10.1016/S2213-2600(18) 30051-1

68. Lee YZ, Yap HM, Shaari K, Tham CL, Sulaiman MR, Israf AL. Blockade of eosinophil-induced bronchial epithelial-mesenchymal transition with a geranyl acetophenone in a coculture model. *Front Pharmacol* (2017) 8:837. doi: 10.3389/ fphar.2017.00837

69. Garcia-Areas R, Libreros S, Amat S, Keating P, Carrio R, Robinson P, et al. Semaphorin7A promotes tumor growth and exerts a pro-angiogenic effect in macrophages of mammary tumor-bearing mice. *Front Physiol* (2014) 5:17. doi: 10.3389/fphys.2014.00017

70. Kang HR, Lee CG, Homer RJ, Keating P, Carrio R, Robinson P, et al. Semaphorin 7A plays a critical role in TGF-beta1-induced pulmonary fibrosis. *J Exp Med* (2007) 204 (5):1083–93. doi: 10.1084/jem.20061273

71. Zhang X, Xie J, Sun H, Wei Q, Nong GM. miR−29a−3p regulates the epithelial −mesenchymal transition via the SPARC/ERK signaling pathway in human bronchial epithelial cells. *Int J Mol Med* (2021) 48(3):171. doi: 10.3892/ijmm.2021.5004

72. Roth JM, Köhler D, Schneider M, Granja TF, Rosenberger P. Semaphorin 7A aggravates pulmonary inflammation during lung injury. *PloS One* (2016) 11(1): e0146930. doi: 10.1371/journal.pone.0146930

73. Pasterkamp RJ, Peschon JJ, Spriggs MK, Kolodkin AL. Semaphorin 7A promotes axon outgrowth through integrins and MAPKs. *Nature* (2003) 424(6947):398–405. doi: 10.1038/nature01790

74. Esnault S, Kelly EA, Schwantes EA, Liu LY, DeLain LP, Hauer JA, et al. Identification of genes expressed by human airway eosinophils after an *in vivo* allergen challenge. *PloS One* (2013) 8(7):e67560. doi: 10.1371/journal.pone.0067560

75. Walzer T, Galibert L, Comeau MR, Smedt TD. Plexin C1 engagement on mouse dendritic cells by viral semaphorin A39R induces actin cytoskeleton rearrangement and inhibits integrin-mediated adhesion and chemokine-induced migration. *J Immunol* (2005) 174(1):51–9. doi: 10.4049/jimmunol.174.1.51

76. Yazdani U, Terman JR. The semaphorins. *Genome Biol* (2006) 7(3):211. doi: 10.1186/gb-2006-7-3-211

77. Jayalakshmi J, Vanisree AJ. Naringenin sensitizes resistant C6 glioma cells with a repressive impact on the migrating ability. *Ann Neurosci* (2020) 27(3-4):114–23. doi: 10.1177/0972753120950057

Frontiers in Immunology

Explores novel approaches and diagnoses to treat immune disorders.

The official journal of the International Union of Immunological Societies (IUIS) and the most cited in its field, leading the way for research across basic, translational and clinical immunology.

Discover the latest Research Topics

See more →

Frontiers

Avenue du Tribunal-Fédéral 34
1005 Lausanne, Switzerland
frontiersin.org

Contact us

+41 (0)21 510 17 00
frontiersin.org/about/contact